National Library
of Canada

Canadian Theses Service

Ottawa, Canada
K1A 0N4

Bibliothèque nationale
du Canada

Services des thèses canadiennes

CANADIAN THESES

THÈSES CANADIENNES

NOTICE

The quality of this microfiche is heavily dependent upon the quality of the original thesis submitted for microfilming. Every effort has been made to ensure the highest quality of reproduction possible.

If pages are missing, contact the university which granted the degree.

Some pages may have indistinct print especially if the original pages were typed with a poor typewriter ribbon or if the university sent us an inferior photocopy.

Previously copyrighted materials (journal articles, published tests, etc.) are not filmed.

Reproduction in full or in part of this film is governed by the Canadian Copyright Act, R.S.C. 1970, c. C-30.

AVIS

La qualité de cette microfiche dépend grandement de la qualité de la thèse soumise au microfilmage. Nous avons tout fait pour assurer une qualité supérieure de reproduction.

S'il manque des pages, veuillez communiquer avec l'université qui a conféré le grade.

La qualité d'impression de certaines pages peut laisser à désirer, surtout si les pages originales ont été dactylographiées à l'aide d'un ruban usé ou si l'université nous a fait parvenir une photocopie de qualité inférieure.

Les documents qui font déjà l'objet d'un droit d'auteur (articles de revue, examens publiés, etc.) ne sont pas microfilmés.

La reproduction, même partielle, de ce microfilm est soumise à la Loi canadienne sur le droit d'auteur, SRC 1970, c. C-30.

THIS DISSERTATION
HAS BEEN MICROFILMED
EXACTLY AS RECEIVED

LA THÈSE A ÉTÉ
MICROFILMÉE TELLE QUE
NOUS L'AVONS REÇUE

NL-339 (r.86/06)

Canada

THE UNIVERSITY OF ALBERTA

ANALYTICAL MODELLING OF TRANSIENT FLOW TO WELLS IN COMPLEX AQUIFER SYSTEMS: CHARACTERIZATION AND PRODUCTIVITY OF THESE SYSTEMS

by

©

CLAUDE M. SAUVEPLANE

A THESIS
SUBMITTED TO THE FACULTY OF GRADUATE STUDIES AND
RESEARCH IN PARTIAL FULFILMENT OF THE REQUIREMENTS FOR
THE DEGREE OF DOCTOR OF PHILOSOPHY
IN WATER RESOURCES (DEPARTMENT OF CIVIL ENGINEERING)

EDMONTON, ALBERTA
SPRING, 1987

Permission has been granted to the National Library of Canada to microfilm this thesis and to lend or sell copies of the film.

The author (copyright owner) has reserved other publication rights, and neither the thesis nor extensive extracts from it may be printed or otherwise reproduced without his/her written permission.

L'autorisation a été accordée à la Bibliothèque nationale du Canada de microfilmer cette thèse et de prêter ou de vendre des exemplaires du film.

L'auteur (titulaire du droit d'auteur) se réserve les autres droits de publication; ni la thèse ni de longs extraits de celle-ci ne doivent être imprimés ou autrement reproduits sans son autorisation écrite.

ISBN 0-315-37667-8

THE UNIVERSITY OF ALBERTA

RELEASE FORM

NAME OF AUTHOR: Claude M. Sauveplane

TITLE OF THESIS: Analytical Modelling of Transient Flow to Wells in Complex Aquifer Systems: Characterization and Productivity of These Systems

DEGREE: Water Resources (Civil Engineering)

YEAR THIS DEGREE GRANTED: 1987

Permission is hereby granted to THE UNIVERSITY OF ALBERTA LIBRARY to reproduce single copies of this thesis and to lend or sell such copies for private, scholarly or scientific research purposes only.

The author reserves other publication rights, and neither the thesis nor extensive extracts from it may be printed or otherwise reproduced without the author's written permission.

(Student's signature)

7708 - 110 Street, Edmonton, Alberta T6G 1G1
(Student's permanent address)

Date: 1987-04-15

THE UNIVERSITY OF ALBERTA

FACULTY OF GRADUATE STUDIES AND RESEARCH

The undersigned certify that they have read, and recommend to the Faculty of Graduate Studies and Research, for acceptance, a thesis entitled:

ANALYTICAL MODELLING OF TRANSIENT FLOW
TO WELLS IN COMPLEX AQUIFER SYSTEMS:
CHARACTERIZATION AND PRODUCTIVITY OF THESE SYSTEMS.

submitted by CLAUDE M. SAUVEPLANE
in partial fulfilment of the requirements for the degree of Doctor of Philosophy.

....

....

....

Frank W. Schwartz
....
Supervisors

....
T.N. NARASIMHAN Jan. 30, 1987
External Examiner

Date 1987-04-15

Ce qui est simple est toujours faux.
Ce qui ne l'est pas est inutilisable!

(What is simple is always in error.
What is not simple is unusable!)

Paul Valery

To Nancy and Alexander

ABSTRACT

The ideal assumptions of the Theis analytical model are rarely met in practice because of the common occurrence of complex aquifer systems. This work considers radial flow to fully penetrating wells for systems whose large-scale heterogeneities comprise (1) interlayer cross-flow with vertical leakage through aquitards; (2) confined aquifers naturally and uniformly fractured ("dual-porosity" models); (3) interlayer cross-flow between aquifers of different flow properties in perfect hydraulic contact; (4) radial heterogeneities; (5) viscoelastic and confined aquifers; and (6) combined - linear and post-linear - flow regime for confined aquifers.

The originality of this work is three-fold:

1. a consistent derivation and formulation of the solutions in the dimensionless Laplace space is presented together with efficient techniques of evaluation of the solutions by analytical and numerical inversion of the Laplace dimensionless transforms;
2. a detailed study of asymptotic behaviors is conducted reasoning in the dimensionless Laplace space; detailed analyses of the model sensitivity to the depending dimensionless parameters are also carried out, thus increasing the understanding of each system; the behavioral similarity of different systems is demonstrated;
3. practical recommendations are made for the use of these models in aquifer test analysis and a standard method of evaluating aquifer and well productivities is proposed.

Two important highlights of this study are (1) a new method of evaluation of the solutions for the three-aquifer system and (2) new solutions for the case of combined flow regime in confined aquifers. The proposed methods facilitate the use of complex analytical models for both the inverse problem (characterization of aquifer systems) and the direct problem (predictions of responses to various stimuli). They constitute the necessary footwork for the preparation of an expert system aimed at semi-automated type-curve analysis of aquifer and well tests.

ACKNOWLEDGEMENTS

I would like to express my sincere appreciation to those who have helped me complete this dissertation, especially:

- Professor Verschuren of the Department of Civil Engineering, and Professor Toth of the Department of Geology, University of Alberta, who have been the principle advisors of this work;
- Professor Farouq Ali of the Department of Petroleum Engineering, University of Alberta for reviewing this dissertation and for helping me to realize that hydrogeologists and reservoir engineers have a common and very similar problem when they evaluate groundwater and hydrocarbon resources;
- Professor Narasimhan of the Department of Earth Sciences, University of California (Berkeley) who kindly accepted to sit on the Reviewing Committee of this dissertation;
- Professor Schwartz of the Department of Geology of the University of Alberta, who kindly accepted to review this study;
- Professor Israel of the Department of Physics, University of Alberta for the great insight he provided on the use of integral transforms for the solution of partial differential equations;

- Dr. E.A. Babcock, Dr. J.A. Boon and Dr. Brian Hitchon of the Alberta Research Council for their material (and moral) assistance.
- Mrs. Kathie Skogg, Basin Analysis Group, Alberta Research Council, who has done fantastic work in typing this manuscript;

I dedicate this work to my wife, Nancy, and to my son, Alexander, who have shown invaluable support (and patience) during these last three years.

TABLE OF CONTENTS

Page

Abstract v
Acknowledgements vii
Main notations xix
Introduction 1

1. CONCEPTUAL APPROACH 4
1.1 Quantitative Aspects of the Evaluation of Groundwater Resources 4
1.2 The Governing Equation 10
1.2.1 The Assumptions 10
1.2.2 The Structural Parameters for Flow in an Aquifer System - Levels of Heterogeneity 13
1.3 Definition of Complex Aquifer Systems 18

2. MATHEMATICAL METHODS OF SOLUTION FOR ANALYTICAL FLOW MODELS 19
2.1 Some Fundamental Solutions of the Diffusion Equation 19
2.2 Integral Transforms 22
2.3 A Formal Method of Solution 23

3. APPROXIMATE INVERSION OF LAPLACE TRANSFORMS 26
3.1 Approximate Laplace Inversion Using Analytical Formulae 27
3.2 Numerical Inversion of Laplace Transforms 35
3.2.1 Use of Gaussian Quadrature Formulae 35
3.2.2 Use of Fourier Series 37
3.2.3 The "Probabilistic" Approach 38
3.2.4 The Use of Numerical Inverters of Laplace Transforms 39

4. ANALYTICAL AND SEMI-ANALYTICAL MODELS FOR COMPLEX AQUIFER SYSTEMS 47
4.1 Infinite Leaky Aquifer Systems 49
4.1.1 Study of the Two-Aquifer System 54
4.1.2 Study of the Three-Aquifer System 70
4.2 Uniformly Fractured and Confined Infinite Aquifer Systems 90
4.2.1 Geometry and Flow Parameters in Dual Porosity Systems 94
4.2.2 The Dual Porosity Line Source Solutions 97
4.2.2.1 The "Pioneer Work" in the Soviet Union 98
4.2.2.2 Selected Line-Source Solutions for Dual Porosity Systems 103
4.2.3 Discussion Concerning the Dual Porosity Systems 106
4.2.3.1 Validity of the Pseudo-Steady-State Assumption for Interporosity Flow 108
4.2.3.2 Comparison of Transient Interporosity Flow Type Curves 125
4.3 Multilayered Aquifer Systems 143
4.4 Radially Composite and Confined Aquifer Systems 147
4.5 Combined Flow Regime in Confined Aquifers 156
4.6 Viscoelastic and Confined Aquifers 159

5. ANALYTICAL MODELS FOR SINGLE-WELL TESTING OF COMPLEX AQUIFER SYSTEMS 164

6. AQUIFER AND WELL PRODUCTIVITIES OF COMPLEX SYSTEMS 168

CONCLUSIONS 172

REFERENCES 178

APPENDIX A: Derivation of the diffusion equation 193

APPENDIX B: Integral transforms for radial flow problems 204

APPENDIX C: Leaky aquifer systems 210

APPENDIX D: Dual porosity system 230

APPENDIX E: Two-layered system 259

APPENDIX F: Radially composite systems 275

APPENDIX G: Combined flow regime 285

LIST OF TABLES

Table 1: Accuracy of analytical inverters for a double-porosity model 34
Table 2: Comparison of numerical values for dimensionless drawdowns in two- and three-aquifer systems 75

LIST OF ILLUSTRATIONS

Page

Figure 1. Levels of heterogeneity in a porous medium: A. common case; B. periodically stratified 17

Figure 2. A schematic method for deriving analytical solutions to radial flow problems 25

Figure 3. Theis solution: percent error using approximate analytical inverters of Laplace transform 32

Figure 4. Theis solution: per ten thousand error with approximate numerical inverters of Laplace transform 40

Figure 5. Dual porosity model (slabs). Comparison of exactly inverted solutions: percent error between results of Sauveplane (1984a) and Streltsova-Adams (1978) for various values of the dimensionless radius 42

Figure 6. Dual porosity model (slabs). Per ten thousand error with Stehfest inverter. The comparison is with the results of Sauveplane (1984a) 44

Figure 7. Two-aquifer model. Error with Stehfest inverter when $\beta=0.01$, $r/B=0.1$. The comparison is with Neuman and Witherspoon (1969) results (continuous lines) for the pumped aquifer (s_{D_1}), the unpumped aquifer (s_{D_2}) and at mid-point of the aquitard (s'_D). The discrete points are obtained with Stehfest inverter 56

Figure 8. Parametric analysis for the two-aquifer model: influence of $a=(T_1/T_2)^{1/2}$ when $b=(S'/S_1)^{1/2}=\sqrt{10}$, $c=(S_2/S_1)^{1/2}=\sqrt{3}$ and $r_D=r/H'(T'/T_1)^{1/2}=1$ 58

Figure 9. Parametric analysis for the two-aquifer model: influence of $b=(S'/S_1)^{1/2}$ when $a=\sqrt{2}$, $c=\sqrt{3}$ and $r_D=1$ 62

Figure 10. Parametric analysis for the two-aquifer model: influence of $c=(S_2/S_1)^{1/2}$ when $a=\sqrt{2}$, $b=\sqrt{10}$ and $r_D=1$ 64

Figure 11. Parametric analysis for the two-aquifer model: influence of $r_D=r/H'(T'/T_1)^{1/2}$ when $a=\sqrt{2}$, $b=\sqrt{10}$ and $c=\sqrt{3}$ 66

Figure 12a. Parametric analysis for the three-aquifer model: influence of $r_{D_1}=r_{D_2}$ when $a_1=a_2=3.0$, $b_1=b_2=10.0$ and $c_1=c_2=1.0$ 77

Figure 12b. Parametric analysis for the three-aquifer model: influence of $r_{D_1}=r_{D_2}$ when $a_1=3.0$, $a_2=c_2=0.5$, $b_2=1.3$ and $b_1=c_1=1.5$ 78

Figure 12c. Parametric analysis for the three-aquifer model: influence of $r_{D_1}=r_{D_2}$ when $a_1=1.0$, $a_2=b_1=1.5$, $b_2=1.3$, $c_1=2.0$ and $c_2=1.5$ 79

Figure 13. Parametric analysis for the three-aquifer model: influence of $c_1=c_2=c$ when $r_{D_1}=r_{D_2}=1.0$, $b_1=b_2=10.0$, $a_1=a_2=1.0$ 82

Figure 14. Parametric analysis for the three-aquifer model: influence of $b_1=b_2$ when $a_1=a_2=1.0$, $r_{D_1}=r_{D_2}=1.0$ and $c_1=c_2=1.0$ 83

Figure 15a. Fracture drawdown type curves for the Barenblatt et al. model of a dual porosity and confined aquifer system. The dimensionless radius varies between 10^{-3} and 1 99

Figure 15b. Matrix block drawdown type curves for the Barenblatt et al. model of a dual porosity and confined aquifer system. The dimensionless radius varies between 10^{-3} and 1 100

Figure 16a. Comparison of type curves for fracture drawdown when the interporosity flow is assumed to be pseudo-steady-state and unsteady for the "slab" configuration of the fracture network and for b=100 and 1000. The dimensionless radius is 0.1 114

Figure 16b. Comparison of type curves for fracture drawdown when the interporosity flow is assumed to be pseudo-steady-state and unsteady for the "cylinder" configuration of the fracture network and for b=100 and 1000. The dimensionless radius is 0.1 116

Figure 16c. Comparison of type curves for fracture drawdown when the interporosity flow is assumed to be pseudo-steady-state and unsteady for the "sphere" configuration of the fracture network and for b=100 and 1000. The dimensionless radius is 0.1 117

Figure 16d. Comparison of type curves for fracture drawdown when the interporosity flow is assumed to be pseudo-steady-state and unsteady for the "sphere" configuration, a dimensionless fracture skin of 0.01 and for b=100 and 1000. The dimensionless radius is 0.1 118

Figure 17a. Comparison of type curves for matrix block drawdown when the interporosity flow is assumed to be pseudo-steady-state and unsteady for the "slab" configuration of the fracture network and for $b=100$ and 1000. The dimensionless radius is 0.1 and $z_D=0.5$ 121

Figure 17b. Comparison of type curves for matrix block drawdown when the interporosity flow is assumed to be pseudo-steady-state and unsteady for the "cylinder" configuration of the fracture network and for $b=100$ and 1000. The dimensionless radius is 0.1 and $\rho_D=0.5$ 122

Figure 17c. Comparison of type curves for matrix block drawdown when the interporosity flow is assumed to be pseudo-steady-state and unsteady for the "sphere" configuration of the fracture network and for $b=100$ and 1000. The dimensionless radius is 0.1 and $\rho_D=0.5$ 123

Figure 17d. Comparison of type curves for matrix block drawdown when the interporosity flow is assumed to be pseudo-steady-state and unsteady for the "sphere" configuration, a dimensionless fracture skin of 0.01 and for $b=100$ and 1000. The dimensionless radius is 0.1 and $\rho_D=0.5$ 124

Figure 18a. Comparison of type curves for fracture drawdown when the interporosity flow is unsteady for various configurations of the fracture network and when b=100 and r_D=0.01 127

Figure 18b. Comparison of type curves for fracture drawdown when the interporosity flow is unsteady, for various configurations of the fracture network when b=1000 and r_D=0.1 128

Figure 18c. Comparison of type curves for fracture drawdown when the interporosity flow is unsteady and for various configurations of the fracture network and when r_D=0.1 and b=1000 129

Figure 18d. Comparison of type curves for fracture drawdown when the interporosity flow is unsteady and for various configurations of the fracture network and when r_D=0.01 and b=1000 130

Figure 19a. Comparison of type curves for matrix block drawdown when the interporosity flow is unsteady and for various configurations of the fracture network and when r_D=0.1 and b=100 132

Figure 19b. Comparison of type curves for matrix block drawdown when the interporosity flow is unsteady and for various configurations of the fracture network and when r_D=0.1 and b=1000 133

Figure 19c. Comparison of type curves for matrix block drawdown when the interporosity flow is unsteady and for various configurations of the fracture network when r_D=0.1 and b=1000 134

Figure 19d. Comparison of type curves for matrix block drawdown when the interporosity flow is unsteady and for various configurations of the fracture network when and r_D=0.01 and b=1000 135

Figure 20a. Comparison of type curves for fracture drawdown when the interporosity flow is unsteady for the "sphere" configuration of fracture network and high values of depending parameters 137

Figure 20b. Comparison of type curves for matrix block drawdown when the interporosity flow is unsteady and for high values of the depending parameters 138

Figure 21. Asymptotes to the fracture drawdown type curves for unsteady interporosity flow and "slab" geometry of the fracture network 139

Figure 22a. Radially composite and confined aquifer: type curves for drawdown in the inner region for values of the dimensionless radius (r/R) 150

Figure 22b. Radially composite and confined aquifer: type curves for drawdown in inner region for different values of $a=(K_1/K_2)^{1/2}$ 151

Figure 23a. Radially composite and confined aquifer: type curves for drawdown in outer region when a=0.5 and $b=(S_{s_2}/S_{s_1})^{1/2}=3$ 152

Figure 23b. Radially composite and confined aquifer: type curves for drawdown in outer region when r_D=1.5 and b=3 153

Figure 24. Radially composite aquifer: type curve for s'_{D_1} on a semi-log scale for ab=0.1, 0.8 and 10 155

Figure 25a. Type curves for the composite flow regime in a confined aquifer: (b_D is defined in equation G10 of Appendix G) 158

Figure 25b. Semi-log type curves for the derivative of the dimensionless drawdown of composite flow regime in a confined aquifer: (b_D is defined in equation G10 of Appendix G) 160

Figure 25c. Semi-log type curves for dimensionless drawdowns of composite flow regime in a confined aquifer: detail of the "crossing" point with the type curve for linear flow (Theis) (b_D is defined in equation G10 of Appendix G) 161

MAIN (CONVENTIONAL) NOTATIONS*

h_o = uniform initial hydraulic head [L]

r = radial distance from a point in the aquifer system to the operating well [L]

t = time elapsed after application of a constant rate perturbation [T]

Q = constant rate of perturbation of the system (positive for a withdrawal, negative for an injection) $[L^3T^{-1}]$

h = hydraulic head at r and t caused by the perturbation Q [L]

s = drawdown $[h_o-h(r,t)]$ or build-up $[h(r,t)-h_o]$ [L]

H = thickness of the mobilized aquifer [L]

H' or b' = aquitard thickness in leaky systems [L]

ℓ = characteristic block size in dual porosity systems [L]

K = hydraulic conductivity $[LT^{-1}]$ (see definition in Appendix A)

S_s = specific storage $[L^{-1}]$ (see definition in Appendix A)

$T=KH$ = transmissivity $[L^2T^{-1}]$

$S=S_sH$ = storativity or storage coefficient [dimensionless]

α = hydraulic diffusivity $[L^2T^{-1}]$ (see definition in Appendix A)

k = intrinsic permeability $[L^2]$

ρ = density of liquid $[ML^{-3}]$

μ = dynamic viscosity of liquid $[ML^{-1}T^{-1}]$

n = porosity (dimensionless)

c = vertical compressibility of granular skeleton $[M^{-1}LT^2]$

z = vertical coordinate [L]

p = pore pressure $[ML^{-1}T^{-2}]$

β = liquid compressibility $[M^{-1}LT^2]$

U or V = specific discharge or Darcy fictitious velocity $[LT^{-1}]$

$s_D=4\pi KHs/Q$ = dimensionless drawdown (or build-up)

$t_D=Kt/S_sr^2$ = dimensionless time

---

* This list is incomplete; the specific notations used for different analytical models are defined in the appendices at the time of their first appearance. The SI units are used for any numerical application; g is the gravity acceleration = 9.806 m/s^2; π = 3.14159...; γ = Euler's constant = 0.5772156...

INTRODUCTION

Analytical flow models occupy a central role in the areas of groundwater resource and hydrocarbon resource evaluation and as such are of great interest to hydrogeologists and reservoir engineers. One may identify two major reasons to this: (1) these models are traditionally used in aquifer and well test interpretation which is an attempt to solve the inverse problem, i.e. to characterize the flow properties of an unknown system on the basis of its known response(s) to a given stimulus and (2) they are more recently used to validate the results of numerical simulators and generally, for predictive purposes in lieu of or conjunctively with simulators once the system has been characterized. With respect to the first important problem of characterization of a system, two major technological advances now permit conducting a much more accurate analysis than in the past: the advent of fast computers, together with the development of more realistic flow models has greatly enhanced our theoretical base for test interpretation and the introduction of precision gauges, continuous downhole recording has vastly improved the quality of the response data available for analysis. There is still a "psychological" barrier to the "routine" utilization of both types of analytical models and measurement techniques in practice; this is understandable in the first instance when one considers the mathematical complexity of the real space solutions obtained for most of the recently proposed models. One major objective of this work is to make the analytical models more "user friendly" by reasoning on the simpler dimensionless Laplace space solutions that are inverted with analytical formulae and numerical procedures. Specifically, we have subdivided this work into six chapters for the study of complex aquifer systems:

1. a conceptual approach defines modern evaluation of groundwater resources, the terminology used in this study and recalls the intrinsic assumptions made in the derivation of the governing diffusion equation;
2. a description of the mathematical techniques available for the solution of analytical flow models using essentially integral transforms;
3. an evaluation of the methods that permit easier inversions of Laplace space solutions;
4. a longer chapter devoted to the study of specific analytical flow models (line-source solutions only) for complex aquifer systems;
5. an indication of how these solutions can easily be transformed for single-well test analysis including wellbore storage and skin effect;
6. a proposed method of defining and evaluating aquifer and well productivities for aquifer systems.

For the reader who is not especially interested in the necessary mathematical developments and proofs, we present the great majority of these in 7 appendices each referring to a given class of flow problems and including derivation of the solutions, study of asymptotic behaviors and details about the computing codes prepared to evaluate the solutions. Only a few selected equations are present in the main text. Most of the notations used are defined at the level of their first appearance and are essentially consistant throughout the report: this avoids a cumbersome reference to a lengthy notation list. In addition, a list of the conventional symbols used is presented at the end of the main text. The SI system is used. Finally, we have tried as much as possible to present the illustrating figures together with the text where they are discussed.

1. CONCEPTUAL APPROACH

"A system is any structure, device or process, real or abstract which relates for a given time step, an input, cause or impulse (of matter, energy or information) to an output, effect or response (of matter, energy or information)."

(Anonymous)

1.1 Quantitative Aspects of the Evaluation of Groundwater Resources

In this study, we are interested in the evaluation of exploitable groundwater resources and thus of aquifer systems. The "systemic" approach is used for convenience in an effort of unification and clarification of the terminology and of the concepts. For centuries, men have empirically learned how to find and exploit groundwater. The concept of groundwater resource is historically recent; it started from the observations that wells may experience decreasing pumping rates with time and that interference effects - on springs, rivers or between wells - could be detrimental. The early conclusion was that aquifers can be over exploited and lead to the concept of maximum withdrawals or "safe yield". With the increase of groundwater exploitation, this concept was progressively replaced by the one of management of an exploitable resource: its evaluation is necessary to arrive at an optimal use defined by comparing the offer to the present or projected demands. However, groundwater is both a renewable (assimilated to a "flux") and a nonrenewable (assimilated to a "reserve") resource and it is very difficult to exploit part of the flux without affecting - locally and temporarily - the reserve. In any case, it is a finite resource. The determination of an optimal use for that resource becomes particularly crucial when the cumulative demands become superior or equal to the offer.

The problem cannot be treated at the local scale of the well productivities, but requires a global approach at the scale of the aquifer system. Such an evaluation of the system is physically inseparable from the projected actions upon it: their magnitude, volume of influence and duration. It is further inseparable from a series of nonhydrogeological constraints (economical, ecological, judicial...). One may define an aquifer system as a natural and continuous flow domain that converts a variable impulse (input) into a variable response (output). Both impulse and response can be local or regional, sudden or sustained. The propagation of the response is controlled by the natural boundaries and by the hydraulic properties of the system. In more physical terms, an aquifer system is a three-dimensional flow domain characterized by structural parameters that govern its conductive and capacitive functions and by initial and boundary conditions. Impulse variations of these conditions are converted into flux and reserve responses. This conversion defines the hydrodynamic behaviour of the system.

The structure of an aquifer system is a more or less simplified hydrogeological translation of its more or less complex geology, that is, both its geometry and its partition in relatively homogeneous blocks that are interconnected. The constitution and the delineation of a saturated aquifer system is based on three hydrogeological components: the aquifers, the aquitards and the aquicludes. These three groups are traditionally classified on the basis of structural and hydrodynamic criteria. These criteria can be descriptive: a continuous or discontinuous aquifer; an unconfined, semi-confined or confined aquifer; a storative or nonstorative aquitard. They can be more quantitative on the basis of the variability and range of the structural flow parameters (hydraulic conductivity, transmissivity, storativity and diffusivity) and this will be further discussed.

They can relate to the main form of the flow (dimensionality and direction) and to the main flow regime; for instance, in a confined aquifer, the flow is essentially bidimensional, steady or unsteady, while leakage through aquitards is commonly assumed to be unidimensional and vertical. Finally, they may refer to the main functions of the system in terms of conductivity, capacity and propagation of influence; depending on its transmissivity, an aquifer may be a good conductor of low capacity with a large propagative function (large diffusivity). The term "capacity" is used here as dependent on both the storativity and the volume. For example, an aquiclude has a zero conductivity, zero capacity and zero propagation of influence. For a given flow problem, the system may be physically composed of various hydrogeological components, especially in the case where leakage cannot be neglected; and from a resource evaluation viewpoint, these composite systems are still an "aquifer system".

A flow model is a logical and usually simplified representation of the physical reality of an aquifer system. The descriptive analysis of the system comprises gathering and interpretation of all the pertinent hydrogeological information required as an input to reach that level of conceptualization. The models are of three types: empirical, physical and mathematical. In the first case, the transfer function between impulse and response is not analysed, as in the "black box" approach. The physical models are either a prototype constructed in a laboratory or an analogic model based on the macroscopic similitude, for instance between Darcy's law and Ohm's law. In the mathematical approach, an abstract formulation of the perceived phenomena and processes involved in the relationship impulse/response is attempted. The base of that formulation is either stochastic or deterministic. The latter postulates a causal relationship between impulse and response transcribed mathematically by a set of governing, initial and boundary equations. The derivation of the governing equations will be further discussed, mainly from the point of view of the physical assumptions that are implied in this conceptualization. They are traditionally obtained in a differential form, but Narasimhan and Witherspoon (1977) and Herrera et al. (1973) presented an integrodifferential form. In this work, we are only interested in mathematical modelling of flow problems based on differential equations resulting from the deterministic approach. With respect to our definitions, one could restrict mathematical modelling to a well-defined set of equations that describe the system, without including the search of the solution. The obtaining of a solution is, however, the usual objective of a groundwater evaluation process and the concept of mathematical modelling can be expanded to integrate this aspect. With that respect, we define an analytical model as a mathematical model for which an exact solution can be found. It is thus restricted to a limited number of systems that are sufficiently simple to allow the mathematical treatment. Even so, additional assumptions may have to be made between the complete formulation of the mathematical model and the solution. A numerical model or simulator is a tool that solves numerically the problem and permits an approximate solution for the more complicated cases. Both efforts - analytical and numerical - are not excluding each other, as too commonly believed: validation of results of a simulator can often be partially or totally made when analytical methods are adequately considered. A simulator is used to verify the adequacy of the model vis-a-vis the aquifer system (calibration) and further to simulate the system response to impulses that may be unique, spatially distributed and variable in time. Theoretically, both functions of a simulator can be performed equally when an analytical model is available.

A semi-analytical model is one for which an analytical solution exists, but requires numerical and approximate techniques for its evaluation. Calculations for both simulators and semi-analytical models necessitate the use of fast and powerful computers; more recently, codes are being developed for the treatment of some of these problems on microcomputers. This study is restricted to analytical and semi-analytical groundwater flow models. Specifically, it is focusing on the transient response of aquifer systems when the impulse is a withdrawal or an injection at a single well location. When the impulses are spatially distributed, the cumulative response can be obtained by the principle of superposition of individual responses.

The considered class of flow models can play an invaluable role - often underestimated - in the analysis of impulse/response relationships of aquifer systems. This role is traditionally limited to the interpretative description of the aquifer system by aquifer and well testing. Their usage could be advantageously expanded for some predictive problems *in lieu of* or *conjunctively with* usually expensive simulators. In the first case, one might be only interested by an approximate evaluation of the responses that can be accommodated with the simplified assumptions required by the analytical model or one is facing an insufficient level of information to prepare a simulator with enough confidence. In the second instance, these models can be used as a control of the validity and even accuracy of the simulator. Two complementary reasons can be invoked to explain the under utilization of analytical and semi-analytical flow models:

1. the multitude of these models and the mathematical complexity of most of the solutions when the aquifer systems are not ideally simple. The practitioner has difficulty in remaining current with the profusion of published models and encounters the problem of their evaluation;
2. a great enthusiasm has been experienced since the beginning of the 1970s for complex models requiring sophisticated computer codes and more and more powerful computers. This enthusiasm has been and remains legitimate but, in the meantime, an important number of practitioners have lost ground with new developments occurring with analytical and semi-analytical models. These are often disregarded as inefficient predictive tools because they are incapable of accounting for the natural complexity of the systems.

This study has the modest ambition to correct some of these common and somehow preconceived ideas on the basis of three main arguments: the complexity of the aquifer systems is often overlooked when compared to the dimensions of the flow problem; the sought answers cannot usually be based on a sufficient level of hydrogeological information to justify sophisticated and costly simulators; the practitioners are not sufficiently aware of all the existing analytical models and that these solutions can be expeditiously applied to a variety of aquifer systems.

1.2 The Governing Equation

While developing and using an analytical model, one is usually focusing on the various assumptions involved in the particular configuration of the idealized aquifer system. The assumptions inherent to the obtention of the governing equation - the diffusion equation - are not often remembered and restated.

In Appendix A, we present a derivation of the diffusion equation that is slightly different from the classical work of Jacob (1950) and de Wiest (1969) that one may find in many textbooks. The objective is to emphasize the various physical assumptions introduced at each step of the mathematical development. At the same time, we introduce the difficult question of change of scale that will be discussed in the next section, together with the concept of degree of heterogeneity of the aquifer systems.

1.2.1 The Assumptions

The differential form of the diffusion equation obtained as equation A21 supposes:

1. that the flow is isothermal and involves small pressure gradients; the fluid viscosity is assumed constant;
2. that the considered volume of saturated porous medium is statistically homogeneous;
3. that the granular skeleton is only compressed (or decompressed) elastically in the vertical direction. Verruijt (1969) uses Biot's theory to investigate the implications of lateral elastic deformations; for the class of flow problems considered here, assumption 3 is supposed to be a good enough approximation;
4. that the total stress on the considered elemental volume is constant and is the sum of the pore pressure and of the intergranular effective stress (no "arch effect");
5. that the volume of solid grains remains constant due to a smaller compressibility of the material itself,
6. that the flow is slow (inertia forces are negligible);
7. that the external (friction fluid/fluid) forces of viscosity are negligible when compared to the internal ones (friction fluid/grains) and derive from a potential;
8. that the pressure gradient is negligible in the vertical direction;
9. that Darcy's experimental law is applicable, that is, mainly that the fictitious velocity in a statistically homogeneous porous medium derives from a potential;
10. that Darcy's law applies equally to transient conditions.

For simplicity, equation A21 is derived for a macroscopically isotropic and confined homogeneous medium. In the general case, the partial differential equation ceases to be linear (in particular, for an unconfined aquifer):

$$\Delta(\bar{K}.h) = S_s(\partial h/\partial t) \tag{1}$$

In the particular case of a homogeneous but anisotropic confined medium, the matrix of the hydraulic conductivity tensor reduces to the diagonal (principal) components K_{xx}, K_{yy} and K_{zz} when the axis of coordinates coincide with the three main directions of permeability so that equation 1 can be written as:

$$K_{xx} \frac{\partial^2 h}{\partial x^2} + K_{yy} \frac{\partial^2 h}{\partial y^2} + K_{zz} \frac{\partial^2 h}{\partial z^2} = S_s \frac{\partial h}{\partial t} \tag{2}$$

The presented forms of the diffusion equation A21, 1 and 2 admit an infinity of solutions; its derivation constitutes the first aspect of mathematical modelling of an aquifer system. The solution becomes unique when a set of initial and boundary conditions and eventually source or sink terms are added to these forms of the governing equation. This second aspect of mathematical modelling transforms an undetermined problem into a well-defined initial boundary-value problem (IBVP) and requires additional and specific assumptions about the particular configuration of the modelled system, as we shall see in further developments. The phase of analytical modelling strictly starts when an exact solution is mathematically sought for the resulting system of equations obtained for the IBVP at hand.

Steady-state problems imply that the dependent variable (here hydraulic head) is only a function of the spatial coordinates and is independent of time. This reduces the governing equations 1 or 2 to a right-hand term of zero; also the IBVP becomes a BVP since the initial conditions do not have to be considered in the mathematical formulation.

The Laplace equation is then the particular governing equation written as follows for the isotropic case:

$$K \Delta h = 0 \tag{3}$$

1.2.2. The Structural Parameters for Flow in an Aquifer System - Levels of Heterogeneity

In the preceding derivation of the governing diffusion equation, the basic assumption was to consider a macroscopically homogeneous volume of porous medium for which a statistically global flow velocity could be defined as deriving from a potential. In hydrogeology[1], the conventionally used flow parameters have been defined as a combination of intrinsic parameters of the fluid and the rock material. These definitions render the form of equation A21 relatively simple. These parameters can be directly measured in the field (aquifer and well testing) or indirectly estimated from laboratory measurements of permeability, porosity, rock compressibility (on cores) and of fluid density, compressibility and dynamic viscosity. Literature values for permeability and porosity of different rock materials can be found in Davis (1969). In all cases, one may question what is actually measured. The basic level of heterogeneity and anisotropy is at the scale of the pores and grains. At this level, the hydrodynamic equations of Navier and Poisson are valid, but no solution can be found because of the unknown and very complex boundary conditions. Hence, the concept of a statistically homogeneous equivalent volume (representative elemental volume) is introduced; this volume is sufficiently large to annul the microscopic heterogeneity but sufficiently small to justify a macroscopically quasi-uniform flow (U and gradp constants). In fact, because of the linearity of Navier's equations, the proportionality between U and gradp was previsible as long as the existence and uniqueness of the solution is demonstrated for a given set of boundary conditions. What is more surprising with Darcy's law is the macroscopic homogeneity of the permeability, i.e. two volumes of the same porous medium with nonidentical grain and pore configuration (form and dimensions) can have the same permeability. This type of homogeneity is statistical by nature.

---

[1] In petroleum engineering, the continuous (dependent variable) is the pore pressure $[ML^{-1} T^{-2}]$ and the flow parameters for slightly compressible fluids are the permeability, the viscosity, the porosity and the total compressibility. The "normalization" in the derivation of the continuity equation is with respect to the pore volume; it follows that the total compressibility C_T is the sum of the fluid compressibility and of the pore volume compressibility.
If one defines the specific storage as $\rho g n C_T$, the ratio $k/\mu n C_T$ is the same as K/S_s and is also called the hydraulic diffusivity $[L^2 T^{-1}]$. The diffusivity equation for oil is the same as equation A21 where p replaces h. It follows that the analytical models that will be considered here are valid for liquid monophasic flow, that is essentially for oil, in reservoir engineering. Gas being far more compressible than oil or water, some assumptions leading to equation A21 cannot be validated and the diffusion equation becomes more complex: influence of Klinkenberg effect, adsorption/desorption on the pores, different equation of state (Kucuk and Sawyer, 1980).

In his theoretical work, Matheron (1967) uses geostatistical considerations to demonstrate the conservation of the energy and further Darcy's law when operating the microscopic to macroscopic change of scale. Matheron (op.cit.) demonstrates that for pores of dimensions less than 1 mm, the representative elemental volume has dimensions of 1 to 10 cm, and that in such a volume, the flow is quasi-uniform (U and gradp vary slowly at the scale of the pores). The change of scale operator is not mathematically the spatial average but the better defined concept of probabilistic expectation; however, physically, the meaning is the same because, by ergodicity, the expectation is the limit of the spatial average taken over larger and larger volumes.

In groundwater resource evaluations, a second level of heterogeneity is of interest; it concerns the change of scale between the rather localized parameters - as measured, for instance, in-situ by aquifer and well testing - and the equivalent parameters that can be used at the scale on an entire aquifer system or at least at the level of blocks or elements in a simulator. In a stratified medium, one can use the arithmetic and harmonic averages for flow parallel and perpendicular, respectively, to the strata. In the case of randomly distributed localized parameters, Matheron (op.cit.) showed that in two dimensions, the equivalent permeability is the geometric average of the localizedpermeabilities when these are log-normally distributed and the flow is quasi-uniform; with the same conditions but with a three-dimensional flow, the equivalent permeability is located at 2/3 of the distance between the harmonic and the arithmetic averages. Although generally comprised between the harmonic and the arithmetic averages, the same demonstration in the case of radial and transient flow conditions becomes very complicated. Darcy's law is shown to be applicable at this superior (or "megascopic") level of heterogeneity, using equivalent permeabilities.

Delhomme (1984) recognizes the important contribution of the geostatistical approach, but stresses the importance of coupling it as much as possible with the available geological information on the structure of the aquifer systems. K. Hubbert (1956) had already illustrated the problem encountered with the definition of an elementary representative volume; he considers the two following diagrams

(Figure 1) for porosity n inside a small sphere of radius r centred on a considered point of the porous medium.

The diagram (A) is classical: if $r > r_2$, the porosity is influenced by outside regions and does not have a stable local value. If $r < r_1$, on the contrary, the sphere is too small to allow an averaging effect and the local porosity acknowledges important fluctuations (at the limit, when $r \to 0$, the porosity can be either 0 or 1). For certain types of porous media, the range (r_1, r_2) presents a relative stability so that it is advantageous to choose r (or the size of the elemental volume) within that interval. However, one may find porous media for which this range does not exist or (diagram (B)) where various ranges of stability exist for the porosity; this diagram illustrates the case of a stratified medium that is approximately repeated periodically; the first range (r_1, r_2) corresponds to a detailed description of such a medium that respects the scale of the strata; the second range (r_3, r_4) refers to a coarser definition of the medium where the scale is superior to the thickness of the strata; the second type of porosity might be sufficient to describe the local porosity of an aquifer system. But why choose a sphere and not a parallelepiped or an ellipsoid? Further, if the chosen porosity needs to be differentiated, (as we did in Appendix A), the sphere diameter should be infinitely large when compared to the pore dimensions, which are not themselves well defined.

We shall assume in all the following developments that the measured parameters represent roughly the macroscopic level and need to be statistically considered as "regionalized" variables for a global or partial characterization at the scale of an aquifer system. It follows

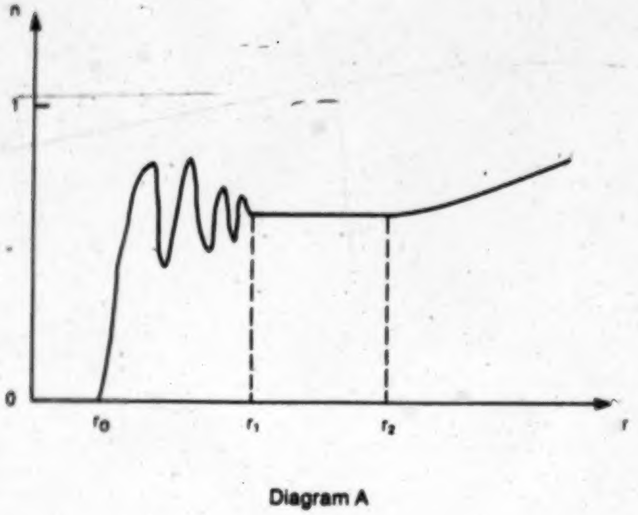

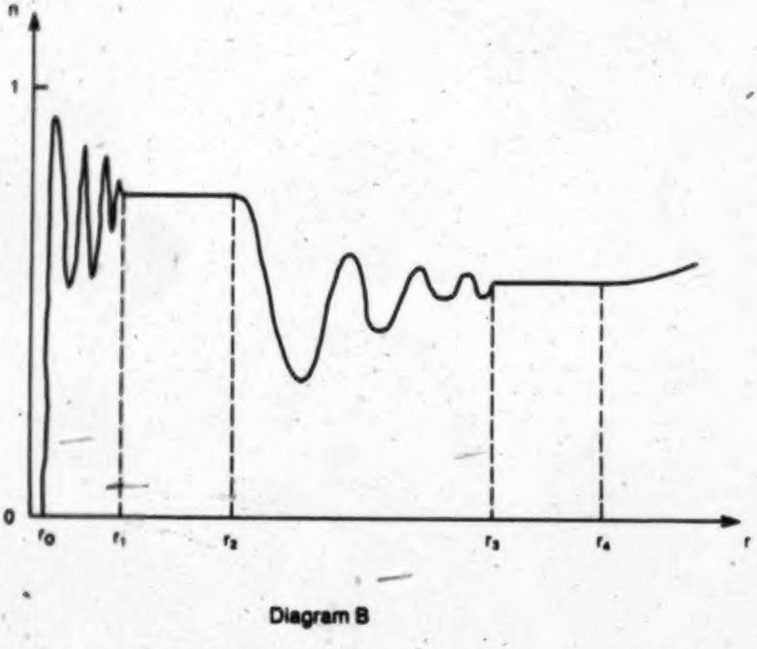

Figure 1. Levels of heterogeneity in a porous medium: A. common case; B. periodically stratified

that only in the ideal case of isotropy and homogeneity on a regional scale, should the parameters used for predictive purposes be identical to the localized values, accessible by measurements.

1.3 Definition of Complex Aquifer Systems

Because we are only interested in the transient flow to wells and by the analytical flow models that may represent this category of problems, we further limit the scope of this study to the case of complex aquifer systems. The complexity may arise from the dimensionality (2-D or 3-D) and the regime (radial, linear, spherical or a conjunction of these) of the flow as well as from the nature of the boundary conditions (finite boundaries of various types, leakage, uniform fracturation). The homogeneity at the local scale is assumed in all instances and we thus prefer the term of "complex" to the term of "heterogeneous", often used.

All the assumptions used in obtaining the governing equation will remain valid for all the models considered and will not be repeated. Perhaps a better definition of a complex system could be one of a transient system that does not satisfy at least one of the assumptions of the Theis model that is derived in Appendix B together with its list of specific assumptions. The Theis solution is also known as the exponential integral solution or in petroleum engineering as the "infinite-acting" solution. Most of the specific concepts contained in the title of this work - except the one of productivity that will only be defined towards the end for reasons that will then be clear - have been defined and discussed. We are now going to consider the mathematical "tools" at our disposal for solving analytical flow models.

2. MATHEMATICAL METHODS OF SOLUTION FOR ANALYTICAL FLOW MODELS

2.1 Some Fundamental Solutions of the Diffusion Equation

Let us consider the diffusion equation derived in Appendix A (equation A21):

$$\alpha \Delta h = \partial h / \partial t$$

In cartesian coordinates and three dimensions, this equation is satisfied by:

$$h = \frac{Q}{8(\pi\alpha t)^{3/2}} \quad \exp -[(x-x')^2 + (y-y')^2 + (z-z')^2]/4\alpha t \tag{3}$$

When $t \rightarrow 0$, $h \rightarrow 0$ at all points except (x', y', z') where it becomes infinite.

When $t > 0$, $\int_{-\infty}^{+\infty}\int_{-\infty}^{+\infty}\int_{-\infty}^{+\infty} h \, dxdydz = Q$

because each of the integrals of the form:

$$1/[2(\pi\alpha t)^{1/2}] \int_{-\infty}^{+\infty} [-\frac{(x-x')^2}{4\alpha t}] \, dx' \text{ is unity.}$$

The solution 3 is the hydraulic head due to an instantaneous point source of strength Q at (x',y',z') for $t=0$ with a flux QS_s instantaneously generated at that point.

Let $Q=qdx'dy'$ and consider the integral $\int_{-\infty}^{+\infty} hdz'$ with h given by 3. Back-substituting $qdx'dy'$ by Q, we obtain:

$$h = \frac{Q}{4\pi\alpha t} \exp (- [(x-x')^2 + (y-y')^2]/4\alpha t) \tag{4}$$

which satisfies equation A21 in two dimensions.

The hydraulic head of equation 4 is due to an instantaneous line source at (x',y') and t=0 of strength Q per unit length (of strength q). Similar reasoning would lead to:

$$h = \frac{Q}{2(\pi at)^{1/2}} \exp[-(x-x')^2/4at] \qquad (5)$$

by integrating equation 3 with regard to both y' and z' from $-\infty$ to $+\infty$ and back substituting Q for qdx'. From this point of view, the one-dimensional solution of equation 5 can be viewed as the hydraulic head due to an instantaneous plane source at x' and t=0 of strength Q per unit area (of strength q').

Of greater interest in the following developments is the case of cylindrical symmetry for two-dimensional flow. If (r,θ) is the cylindrical coordinate system, the Laplacian of h is:

$[(\partial^2/\partial r^2) + (1/r)(\partial/\partial r)]$. The point (x',y') is now defined by (r',θ').

Let us integrate $\left[(qr'dr'd\theta')/(4\pi at)\right] \exp \left[-(r^2+r'^2-2rr'\cos\theta)/4at\right]$ with regard to θ' from 0 to 2π. We obtain:

$$h = \frac{qr'dr'}{4\pi at} \exp-(r^2+r'^2)/4at \int_0^{2\pi} \exp[(\frac{rr'}{2at})\cos\theta']d\theta'$$

or

$$h = \frac{qr'dr'}{2at} \exp\left[-(r^2+r'^2)/4at\right] I_0(\frac{rr'}{2at})$$

and writing $Q = 2\pi r'qdr'$:

$$h = \frac{Q}{4\pi at} \exp\left[-(r^2+r'^2)/4at\right] I_0(\frac{rr'}{2at}) \qquad (6)$$

where I_0 is the modified Bessel function of zero order. From equation 6, when $t \rightarrow 0$, $h \rightarrow 0$ at all points except at $r=r'$ where it becomes infinite. When $t > 0$, it can be shown that $2\pi\int_0^\infty hrdr = Q$ using Weber's first integral:

$$\int_0^\infty \exp(-a^2u^2)\, J_0(bu)udu = 1/(2a^2)\, \exp(-b^2/4a^2)$$

where J_0 is the Bessel function of zero order.

We can thus regard equation 6 as the hydraulic head due to a flux QS_s per unit length instantaneously generated on the surface of the cylinder $r=r'$ at $t=0$.

Finally, with spherical polar coordinates $[\Delta = (\partial^2/\partial r^2)+(2/r)(\partial/\partial r)]$ and for the case of spherical symmetry, we would obtain with the same reasoning:

$$h = \frac{Q}{8\pi rr'(\pi\alpha t)^{1/2}}\left(\exp[-(r-r')^2/4\alpha t] - \exp[-(r+r')^2/4\alpha t]\right) \qquad (7)$$

where $h \to 0$ when $t \to 0$ at all points except on the sphere $r=r'$ where it becomes infinite. Also:

$$4\pi\int_0^\infty h\, r^2dr = Q \text{ when } t > 0$$

and equation 7 can be regarded as the hydraulic head due to a flux QS_s instantaneously generated on the surface of the sphere $r=r'$ at $t=0$. Equations 3, 4, 5, 6 and 7 represent fundamental solutions of the diffusion equation for unsteady flow through porous media. These solutions are in the form of source functions (or influence functions). Besides its physical interest, the method provides very fast solutions as shown in Appendix B for the simple case of the Theis model. However, for more complex IBVP, the difficulty is to find the corresponding source (or Green's) function. For the complex aquifer systems, the general method of solution of transient flow problems involves the use of integral transforms. However, the method of separation of variables presented in Javandel (1982) may offer some interesting possibilities. Also, for steady-state problems, a very powerful tool for complex boundary conditions is the method of conformal transformation.

2.2 Integral Transforms

A general definition of integral transforms can be formulated by the following. Let us consider a known function K(u,v) of two variables u and v and the integral:

$$f(u) = \int_a^b F(v)\ K(u,v)\ dv \qquad (8)$$

If the integral is convergent, then f(u) is called the integral transform of the function F(v) by the kernel K(u,v). The function F(v) is defined for positive values of v.

The particular integral transforms useful in transient groundwater flow problems are:

- the infinite Laplace transformation

$$L[F(t)]=f(p)=\int_0^\infty \exp(-pt)F(t)dt \qquad (9)$$

- the infinite Hankel transformation of zero order:

$$H[G(r)]=g(a)=\int_0^\infty r\ J_0(ar)G(r)dr \qquad (10)$$

- the finite Fourier cosine and sine transformations:

$$\text{cosine}\ F_c[H(z)]=h_c(n)=\int_0^b H(z)\ \cos[(n\pi z)/b]dz \quad o < z < b \qquad (11)$$

$$\text{sine}\ F_s[H(z)=h_s(n)=\int_0^a H(z)\ \sin[(n\pi z)/a]dzo < z < a \qquad (12)$$

The variables p, a and n are called the transform variables. The various kernels of the transforms are easily identified in equations 9, 10, 11 and 12. The useful properties of these transformations for solving IBVP involving the diffusion equation are summarized in Appendix B which also presents the derivation of the Theis solution as an example of use of integral transforms and source functions.

2.3 A Formal Method of Solution

Analytical solutions for flow problems around wells can be found in a formalized manner using integral transforms. The proposed method is suggested by the simple examples given in Appendix B (sections 3-2 and 3-3) and by the nature of the usual initial and boundary conditions (of Neumann and Dirichlet type, only).

The independent variables are the radial distance r, the time t and the vertical elevation z usually measured from the base of the system. The latter is only considered here when aquitard responses are involved or for the case of layered aquifers with cross-flow. These variables have the following common limits: t varies from 0+ to a finite value (that can be large); r tends either towards 0+ (infinitesimal well radius) or has a finite lower bound (real or equivalent well radius) while its upper bound is either finite (circular systems) or infinite; z has either a zero or finite lower bound and a finite upper bound. For a constant rate of production (or injection), the inner boundary condition is an imposed flux, meanwhile the outer boundary condition is usually an imposed potential or hydraulic head. The initial condition is usually a horizontal piezometric (or water-table) surface (imposed hydraulic head). Figure 2 represents the schematic approach that can be devised in these conditions. In this scheme, the symbols H^{-1} and L^{-1} represent the inverse transformations. The advantages of using integral transforms are self-explanatory by the left part of Figure 2. The operation H^{-1} is not usually difficult because the image solution is an algebraic equation that can be put in a form suitable for application of the equation B14 of Appendix B. The result of H^{-1} is a closed form expression of the image solution $\bar{s}(r,z,p)$. The problematic operation is L^{-1}, necessary to obtain the original solution. In simple cases (section 3-2 of Appendix B), this inversion can be made from tables of Laplace transforms. In most of the cases considered in this work, this is not possible and two options are left: either use equation B10 that will produce - after lengthy developments based on complex variable theory and sometimes delicate evaluations of contour integrals - an original solution in a closed form, or have recourse to approximate methods of the Laplace inversion. Such methods will be discussed in depth in the following chapter because they constitute the main thrust of this work.

Although the approach of Figure 1 will be quite general in the next developments, it might be convenient to replace the Hankel transform by a finite Fourier transform, especially for problems in which at least two of the boundaries are parallel and separated by a finite distance. The cosine transform is useful when imposed fluxes are given on these boundaries; the sine transform is preferred for imposed heads on these parallel boundaries. The inversion formulae for both transforms involve Fourier series and the subsequent Laplace inversions might suffer of this particular feature.

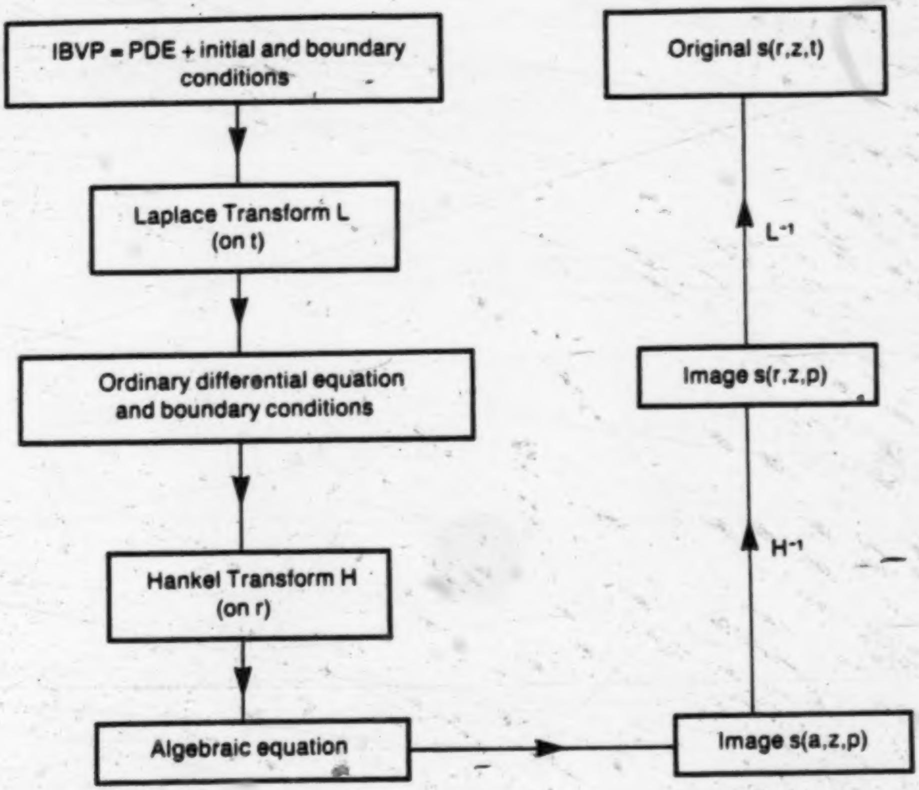
IBVP = PDE + initial and boundary conditions
Laplace Transform L (on t)
Ordinary differential equation and boundary conditions
Hankel Transform H (on r)
Algebraic equation
Image s(a,z,p)
H⁻¹
Image s(r,z,p)
L⁻¹
Original s(r,z,t)

Figure 2. A schematic method for deriving analytical solutions to radial flow problems

3. APPROXIMATE INVERSION OF LAPLACE TRANSFORMS

When the flow problem is such that the Laplace transform does not possess a simple inverse, the general inversion integral (B10) must be used. It leads to an infinite integral or an infinite series (or sometimes both) that are difficult to handle from a computational standpoint because they are expressed in terms of oscillating Bessel functions. This difficulty is a major disadvantage of analytical models for complex aquifer systems. A classical method evaluates the original solutions with numerical techniques of integration (great attention has to be devoted to the stability of the results for certain time domain and/or values of depending parameters). The results may remain uncertain and are computer expensive. Another classical way to go around the difficulty is to limit the evaluation of the original solution to its asymptotic behaviour for small values of time (p is large) and for large values of time (p is small); but frequently, the times of interest lie somewhere between these two extremes. The recourse to approximate inversion techniques - although less conventional - deserves particular attention. The idea is to evaluate the original solution from the Laplace space either directly through (approximate) numerical algorithms or indirectly with analytical (approximate) formulae. In the latter case, a similar closed form can be obtained that is easier to evaluate than the exact original solution. In the former case, numerical values are evaluated at discrete values of time without that intermediate real space expression.

As pointed out by Bellman et al. (1966), the problem of approximately inverting Laplace transform solutions does not admit a universal solution because of the unbounded character of the Laplace transform. A small variation (and error) in the image solution may generate a great variation (and error) for the original function.

When no control can be exercised from the knowledge of the exact original solution, an uncertainty remains about the accuracy of the results which may vary greatly from one technique to another. The difficulty is to select the most suited method to a given problem. More confidence can be sought by having an insight on the limitations of each method in general and when applied to a particular image function. Also, one may use a combination of different methods and compare the results. In the following, we briefly describe the mathematical foundations of available techniques with the objective to know their limitations when applied to flow problems.

3.1 Approximate Laplace Inversion Using Analytical Formulae

Most of the formulae have been derived for stress analysis of viscoelastic problems. Let us consider the definition of the Laplace transformation (equation 9 or B1); it can be written as:

$$f(p) = \int_0^\infty \frac{F(t)}{t} [t\exp(-pt)]dt \qquad (13)$$

As was pointed out by ter Haar (1951), the function in brackets[2] is similar to Dirac delta function and may be approximated by:

$$t\exp(-pt) = [\delta(t-t_0)/p^2] \qquad (14)$$

where the factor p^2 is introduced for normalization purposes.

---

[2] called the "intensity function"

Equation 13 becomes:

$$p^2 f(p) = \int_0^\infty \frac{F(t)}{t} \delta(t-t_0)\, dt \qquad (15)$$

Applying the sifting integral property of the Dirac function[3] yields:

$$p^2 f(p) = [F(t)/t]_{t=to}$$

Locating the delta function at a point t_0 where the intensity function has a maximum, say $t_0 = 1/p$, yields:

$$F(t) = [pf(p)]_{p=1/t} \qquad (16)$$

Equation 16 is the ter Haar approximation formula.

Rather than using the maximum of the intensity function for the location of the delta function, Schapery (1961) uses the centroid of the intensity function on a logarithmic scale which is the point where $pt = 0.5$ and writes:

$$F(t) = [pf(p)]_{p\ =\ 1/(2t)} \qquad (17)$$

Equation 17, the Schapery approximation formula, is limited (mainly) to problems where pf(p) is a quasi-linear function of lnp; lnp is the natural logarithm of p.

---

[3] This property can be easily demonstrated and it is stated as:

$$\int_0^\infty x(t)\delta(t-\tau)dt = x(\tau) \quad \tau > 0$$

where $\delta(t-\tau)$ is zero for $t \neq \tau$ and is the limit when Δt tends towards 0 of $1/\Delta t$. for $t = \tau$.

More precisely, equation 17 is applicable to problems where f(p) is such that:

$\frac{d[pf(p)]}{d(\ln p)}$ varies slowly with lnp.

The centroid of the intensity function on a logarithmic scale is more precisely located at $pt = \gamma$ where $\gamma = 0.5772...$is Euler's constant, so that equation 17 can be rewritten as:

$$F(f) = [pf(p)]_{p=\gamma/t} \tag{18}$$

We shall refer to equation 18 as the Modified Schapery approximation formula. The restrictions on f(p) for equation 17 are of course the same for equation 18.

Widder (1946) differentiates equation 9 n times with respect to p and uses the same sifting property of the Dirac function to propose:

$$F(t) = \lim_{n\to\infty} \left\{\frac{(-1)^n p^{n+1}}{n!} \frac{d^n[f(p)]}{dp^n}\right\}_{p=n/t} \tag{19}$$

Alfrey's (1944) formula is a particular case of equation 19 when n=1. The use of equation 19 for n=1 or n>1 requires derivatives of successively higher orders for f(p). This is best achieved by numerical differentiation techniques (3-, 5-, 7-point formulae). Doing so, Cost (1964) found that, for relatively well behaved functions f(p), the accuracy of these numerical techniques decreases sharply beyond the third order. For some line-source flow problems, the function $p^n f(p)$ is of the form $K_0[u(p)]$ where u(p) is a function of p and analytical differentiation can be achieved in principle to higher orders. However, for the functions tested, little improvement has been obtained with equation 19 beyond the first order (n=1).

Sauveplane (1984) discussed the use of equation 17 for evaluating three groundwater flow model solutions; he concluded that the Schapery formulae is a valid approximation for intermediate and long times; it is of simple use and a plot of pf(p) versus lnp is recommended to determine its range of linearity with respect to the Laplace variable p. An evaluation of the real time domain of validity can then be done by replacing p with 1/t in the range for p. Sternberg (1969) was the first to propose application of equation 17 to groundwater flow problems; Corapcioglu and Brutsaert (1977) used the technique for studying subsidence due to pumping with a viscoelastic aquifer model.

To assess the relative merits of formulae 16, 17, 18 and 19 with n=1, we apply them to the Theis solution that can be precisely computed. Using the linear property (equation B8) of the Laplace transformation, equation B19 becomes simply:

$$sD(p') = 2K_0[(p')^{1/2}]/p' \tag{20}$$

where $s_D(t_D) = \frac{4\pi KHs(r,t)}{Q}$ is the dimensionless drawdown and p' is the Laplace variable with respect to the dimensionless time $t_D=(\alpha t)/r^2$. Successive applications of equations 16 to 19 to the equation 20 yields: With the ter Harr formula 16:

$$s_D = 2K_0[(t_D)^{-1/2}] \tag{21}$$

With the Schapery formula 17:

$$s_D = 2K_0[(2t_D)^{-1/2}] \qquad (22)$$

With the Modified Schapery formula 18:

$$s_D = 2K_0[(\gamma/t_D)^{1/2}] \qquad (23)$$

Finally, with the Alfrey formula (equation 19 for n=1), letting $(t_D)^{-1/2} = x$, we have:

$$s_D = \left[-p'^2 \frac{ds_D}{dp'}\right]_{p'=1/t_D} = 2K_0(x) + xK_1(x) \qquad (24)$$

The results obtained with equations 21 to 24 for the usual range of t_D $[10^{-1}, 10^6]$ are compared to the values given by $s_D = E_1[(4t_D)^{-1}]$ which is the exact Theis solution in the form of percent error for each value of t_D. These percent errors are plotted versus t_D on a semi-log scale on Figure 3. Figure 3 illustrates that the best estimates of s_D are provided by the Modified Schapery formula over the largest range of t_D. An acceptable accuracy less than 10 percent error is given by equation 23 for $t_D > 2$; beyond $t_D = 10$, equation 23 reproduces quasi-perfectly the exact solution (between 0 and 1 percent error). Figure 3 also shows that for the Theis model, the ter Harr formula systematically overestimates the solution with less than 10 percent error for $t_D > 100$ only. The results obtained with equation 22 are close to those obtained with equation 23; however, a less-than-10 percent-error is only obtained for $t_D > 5$ and, even then, the absolute values of the percent errors are slightly higher than with equation 23.

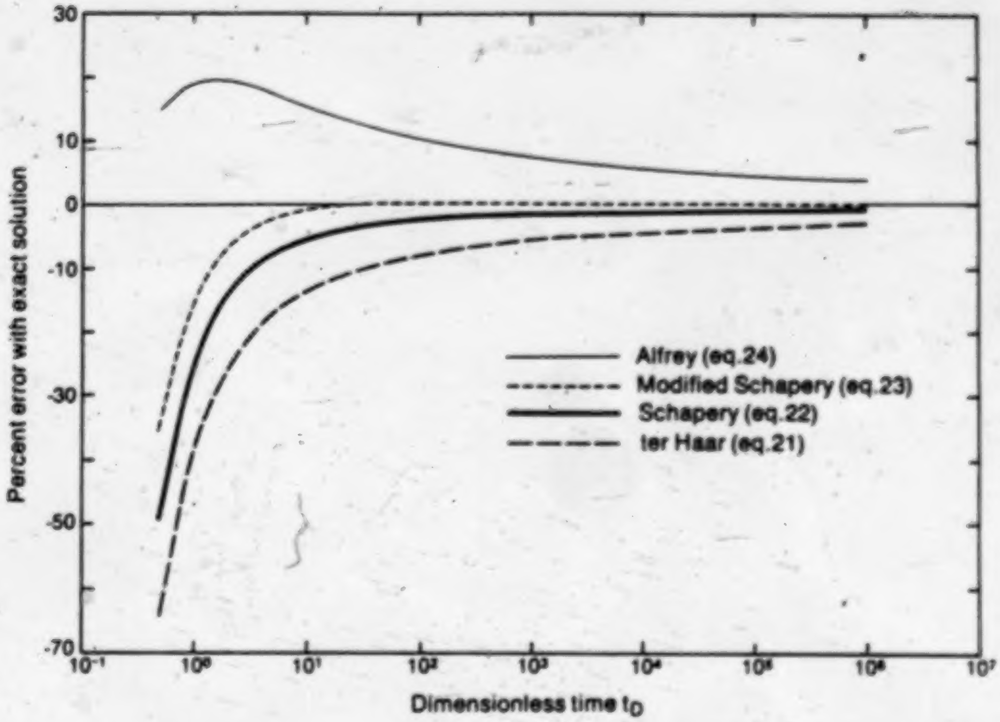

Figure 3. Theis solution: percent error using approximate analytical inverters of Laplace transform

Alfrey's formula 24 is the most approximative one for low values of t_D. No significant improvement could be noticed by using the formula of Widder for $n=2$ (second order derivative in equation 19). It appears that the location of the Dirac function plays a significant role in the accuracy of the results.

For the Theis solution, the most successful analytical inverter is definitely the Modified Schapery formula of equation 18.

Another test of the accuracy of the Schapery and Modified Schapery analytical inverters was made with the dual porosity model of Boulton and Streltsova (1977a). The model will be discussed in more detail in further sections. The comparison is with our results for the exactly inverted solution (Sauveplane, 1984a). Using previous notations, the dimensionless Laplace solution can be written as follows:

$$\overline{s_D} = 2K_0[u(p')] \quad \text{where } u(p') = \left[p' + \frac{r_D}{\eta} p' \tanh\left(\frac{\sqrt{p'}}{r_D \eta}\right)\right]^{1/2} \qquad (25)$$

Formulae 17 and 18 were applied to equation 25 for t_D varying between 1 and 10,000, for $\eta = 10$ and for $r_D = 0.01$, 0.1, 0.5, 2 and 5. Typical results are illustrated by Table 1 for $r_D = 0.01$ and 2. Again, formula 18 gave slightly better results than formula 17. Better than 10 percent accuracy was achieved with equation 18 for $t_D > 5$ and $r_D = 0.01$, 0.1 and 0.5 but only for $t_D > 100$ when $r_D = 2$ and 5. The sensitivity to the depending parameter η was not analysed. When t_D is large, that is $p' \to 0$, $u(p') = [p'(1+1/\eta^2)]^{1/2}$ and equation 25 represents a shifted Theis solution, independent of r_D. This asymptotic (long-time) behaviour is not valid at least until $t_D = 10^6$ with the numerical values used for r_D and η. So that equation 8 provided accurate results for s_D for an

Table 1 : Accuracy of analytical inverters for a dual porosity model (slab)

RD=0.01

TD1	SD1			
	(1)	(2)	(3)	(4)
1.0	0.215	0.468517	0.408555	0.121
2.0	-	0.823412	0.741337	0.235
5.0	1.197	1.43625	1.33124	0.534
10.0	1.779	1.97841	1.86194	0.928
20.0	-	2.56225	2.43888	1.470
50.0	3.243	3.36558	3.23858	2.296
100.0	-	3.97850	3.85182	2.930
1000.0	5.871	5.91843	5.80465	4.922
10000.0	7.549	7.57643	7.48193	6.600

RD=2.00

TD1	SD1			
	(1)	(2)	(3)	(4)
1.0	-	0.0505014	0.0424563	-
2.0	0.0503	0.109529	0.0939564	0.022
5.0	0.1427	0.272014	0.237759	0.078
10.0	0.2863	0.496123	0.441142	0.221
20.0	0.5582	0.827697	0.750036	0.493
50.0	1.1576	1.42340	1.31959	1.093
100.0	1.7403	1.96825	1.85006	1.675
1000.0	3.9436	4.08337	3.94422	3.878
10000.0	6.2363	6.35591	6.21294	6.178

(1) "Exact" inversion for dimensionless fracture drawdown when S2=10.S1 as per C.M.Sauveplane(1984a)

(2) Same with Schapery analytical inverter (equation 17)

(3) Same with Modified Schapery inverter (equation 18)

(4) Same as per "exact"inversion calculations of Streltsova-Adams(1978)

intermediate range of t_D. This could not be achieved with the asymptotic solution. For both tests, computations have been performed on a VAX/VMS 780 with a specially written double-precision FORTRAN program which uses the International Mathematical and Statistical Libraries (IMSL) subroutines to obtain the values of the functions E_1, K_o and K_1.

For transient flow problems it is recommended not to use "blindly" the analytical formulae of equations 16 to 19. These methods are attractive by their simplicity: with tables of functions E_1, K_o and K_1, the computations can be done with a hand-calculator. We have shown that the inverse Laplace transformations can be sensitive to very slight changes in the form of these approximate analytical inverters (compare the difference between equations 17 and 18!). Although the modified Schapery formula 18 seems to give the best results for the two problems tested, it might not be true for other problems; the limitations of each method should be thoroughly understood: they are, at best, intermediate to long-time approximations.

3.2 Numerical Inversion of Laplace Transforms

3.2.1 Use of Gaussian Quadrature Formulae

Using the inversion formula B10, Piessens (1971) demonstrates that, if f(p) is the Laplace transform of F(t), then:

$$F(t) = t^{m-1} \sum_{k=1}^{n} [A_k (\frac{u_k}{t})^m f(\frac{u_k}{t})] \qquad (26)$$

where m is a real (positive) variable chosen so that:

$$p^m f(p) = \sum_{k=0}^{\infty} a_k p^{-k}.$$

The transformation of the Bromwich's integral in equation B10 by the approximate form of equation 26 becomes operational if m and both coefficients A_k and u_k (that depends on m and n) can be evaluated. From the theory of Gaussian quadrature formulae, it can be shown that the abscissae u_k and the weights A_k can be determined using orthogonal polynomials. Specifically, the abscissae u_k are the zeros of $Pn,m(p^{-1})$ and the weights A_k are given by:

$$A_k = (-1)^{n-1} \frac{(n-1)!}{\Gamma(n-m-1)n\ u_k^2} \left[\frac{2n + m-2}{Pn-1,m(u_k^{-1}}\right]^2 \tag{27}$$

The polynomial $P_{n,m}(x)$ are in fact special cases of the generalized Bessel polynomials that can also be expressed in terms of the confluent hypergeometric functions. The function $\Gamma(x)$ is the gamma function. Zeros of $P_{n,m}(p^{-1})$ are found with an iterative numerical procedure (Newton-Raphson, for example).

Piessens (op.cit.) claims that this algorithm presents the advantage of being applicable to cases where the image functions have a branch point at infinity.

Other quadrature formulae based on Legendre, Chebycheff and Laguerre polynomials (Cost, 1963) - which are all orthogonal polynomials - give unsatisfactory results when f(p) has a branch point at infinity.

3.2.2 Use of Fourier Series

Durbin (1974) proposes a Fourier series approximation for the inverse Laplace transform. If $\hat{F}(t)$ is the estimated value of F(t), the formula is:

$$\hat{F}(t) = \frac{e^{at}}{T}\left\{\frac{\mathrm{Re}[f(a)]}{2} + \sum_{k=1}^{\infty}\mathrm{Re}[f(a+\frac{ik\pi}{T})]\cos(\frac{k\pi t}{T}) - \sum_{k=1}^{\infty}\mathrm{Im}[f(a+\frac{ik\pi}{T})\sin\frac{k\pi t}{T}]\right\} \quad (28)$$

The discretization error can be expressed by:

$$F(t) - \hat{F}(t) = \sum_{n=1}^{\infty}\exp(-2naT)f(2nT+t) \quad (29)$$

Application of equation 28 supposes that F(t) is piecewise continuous and of exponential order, i.e. it exists a real number c such that f(p) is an analytic function for Re(p)>c; c is called the abscissa of convergence of f(p). The parameters a and T in equations 28 and 29 can be chosen freely, but their values affect strongly the discretization error. For instance, one may use T=16t and a=c+2/t to minimize the discretization error.

Crump (1976) has written the subroutine FLINV (suggested by IMSL) as a direct application of these equations and principles; in addition, he accelerates the convergence of the infinite series in equation 28 with the ε-algorithm (Wynn, 1958) in order to fit a requested accuracy, whenever possible. We will use here the "Crump inverter".

Note that in equation 28, f(p) is considered as a complex function of a complex variable p that is to be evaluated separately by a user-supplied subroutine in Crump's algorithm.

3.2.3 The "Probabilistic" Approach

Gaver (1966) studied the expectation of F(t) with respect to the probability density:

$$y_n(a,t) = a\frac{2n!}{n!(n-1)!}[1-\exp(-at)]^n \exp(-nat) \text{ for } a>0$$

Based on the properties of y_n, he derived the following expression:

$$F(t) = \frac{\ln 2}{t}\sum_{i=1}^{n} Vi\ f(\frac{\ln 2}{t}i) \qquad (30)$$

where $V_i = (-1)^{i+n/2} \sum_{k=(\frac{i+1}{2})}^{a} \frac{k^{1+n/2}\ 2k!}{(\frac{n}{2}-k)!k!(k-1)!(i-k)!(2k-i)!}$

and $a = \min(i,\frac{n}{2})$ and n is even.

It is worth noting that f(p), the Laplace transform of F(t), is assumed to be a real function of a real variable p.

Stehfest (1970) wrote a subroutine LINV for computer use of equation 30, and tested LINV satisfactorily on 50 Laplace transforms. LINV was translated from ALGOL into FORTRAN for use in this work. We will refer to that procedure as the "Stehfest inverter". Stehfest noted that F(t) estimated by equation 30 does not become more accurate as n increases: due to the unbounded character of the Laplace transformation, when n increases, the V_i becomes greater and greater generating worse and worse rounding errors. The array V_i needs to be calculated only once if several uses of LINV are to be done with the same value of n. Stehfest suggests n=10 or at most n=18. We obtain also good results for n=8.

3.2.4 The Use of Numerical Inverters of Laplace Transforms

The Stehfest inverter is elegant and fast; it provides usually sufficient accuracy for transient flow problems. Hence, its popularity in reservoir engineering and more recently in hydrogeology (Moench and Ogata, 1983). It also presents the advantage of operating with real functions and real variables, which avoids the difficulty of evaluating Bessel and other functions of complex variables. In general, however, the Laplace transform variable p and the image function f(p) are complex.

Usually, numerical inverters provide good accuracy over the entire practical range of dimensionless time, but this may depend on the values of the depending parameters of the complex aquifer systems. Because for these systems, published values of the numerical calculations of the exactly inverted solutions are rarely available, a case by case check against these results is not possible. Even though these results are accessible, one may question their accuracy for some values of the depending parameters as we will see for the double-porosity model; this follows the difficulty of numerically integrating oscillating Bessel functions of the type J_0, J_1 and Y_0. Within their time domain of validity, asymptotic (exact) solutions are usually easier to calculate and these results can be compared with those of the numerical inverters. As suggested by Stehfest (op.cit.) it is prudent to compare results of at least two numerical inverters, for instance the Stehfest and the Crump inverter. This was done for the simple Theis solution and the results are illustrated on Figure 4, where the relative error with respect to the exponential integral are no longer expressed in percent, but in per ten thousand. For the Crump inverter, a FORTRAN algorithm

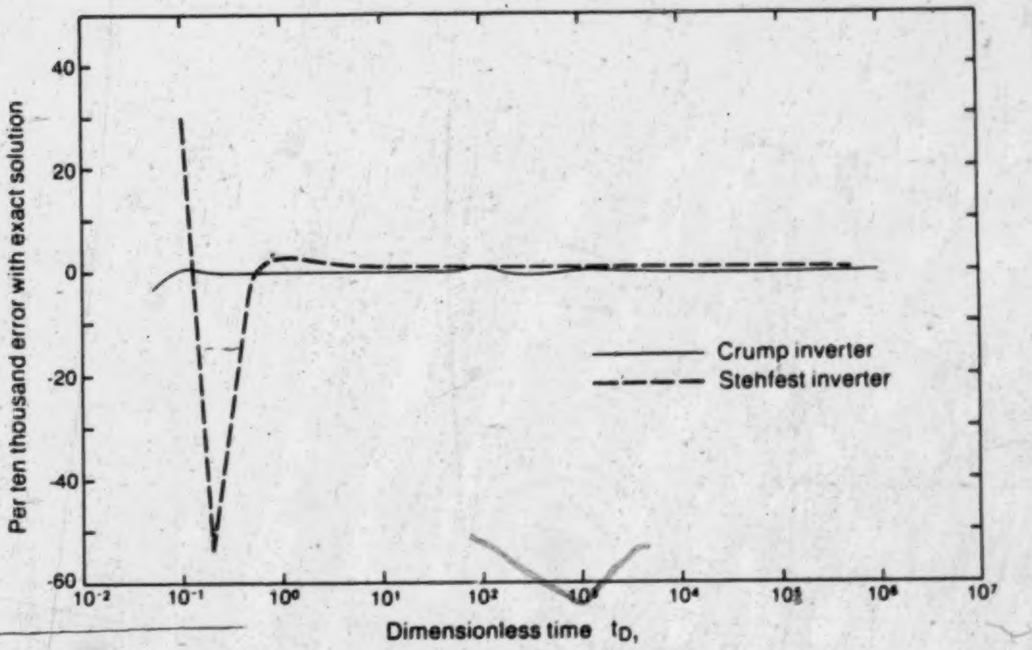

Figure 4. Theis solution: per ten thousand error with approximate numerical inverters of Laplace transform

developed by Burrell (1974) is used to evaluate $\exp(x)K_0(z)$ where z is the complex variable and x is its real part; this algorithm is very efficient, but unfortunately not available in the IMSL library. Figure 4 shows that for the usual range of t_D, that is 0.05 to 10^6, the accuracy of the Crump inverter for the Theis solution varies between 10^{-6} and 3.7×10^{-4}. In the same range, relative error with the Stehfest inverter varies between 36 percent (at $t_D=0.05$) and 6.6×10^{-5} with an accuracy better than 3×10^{-4} as long as $t_D>0.5$.

These results are impressive when compared to the ones obtained with the analytical inverters; however, one should keep in mind that they have been obtained with a powerful digital computer, which was not indispensible with the analytical inverters. In these calculations, the number of iterations for the Crump inverter was 900 for 6 arithmetic digits of requested accuracy. We used n=8 for the Stehfest inverter. Both calculations were done in double-precision with specially written FORTRAN codes.

Before describing the performance of the Stehfest and Crump inverters for the double-porosity model described by equation 25, we compare on Figure 5 the difference between two sets of results for the exactly inverted solution of this model - the references are the calculations made by Sauveplane (1984a) and the compared values of s_{D_1} are from Streltsova-Adams (1978, Table VI) for $S_2=10S_1$. Our computations use an adaptive Simpson's rule technique (precision 10^{-4}) meanwhile the method used to calculate the second set of results is unknown. Figure 5 illustrates that for $r_D=0.1$ and 0.5, the agreement between the two sets of results is acceptable (within 10 percent error) when $t_{D_1}>1$. This is only true for $t_{D_1}>20$ when $r_D=2$ and 5 and it is never the case when

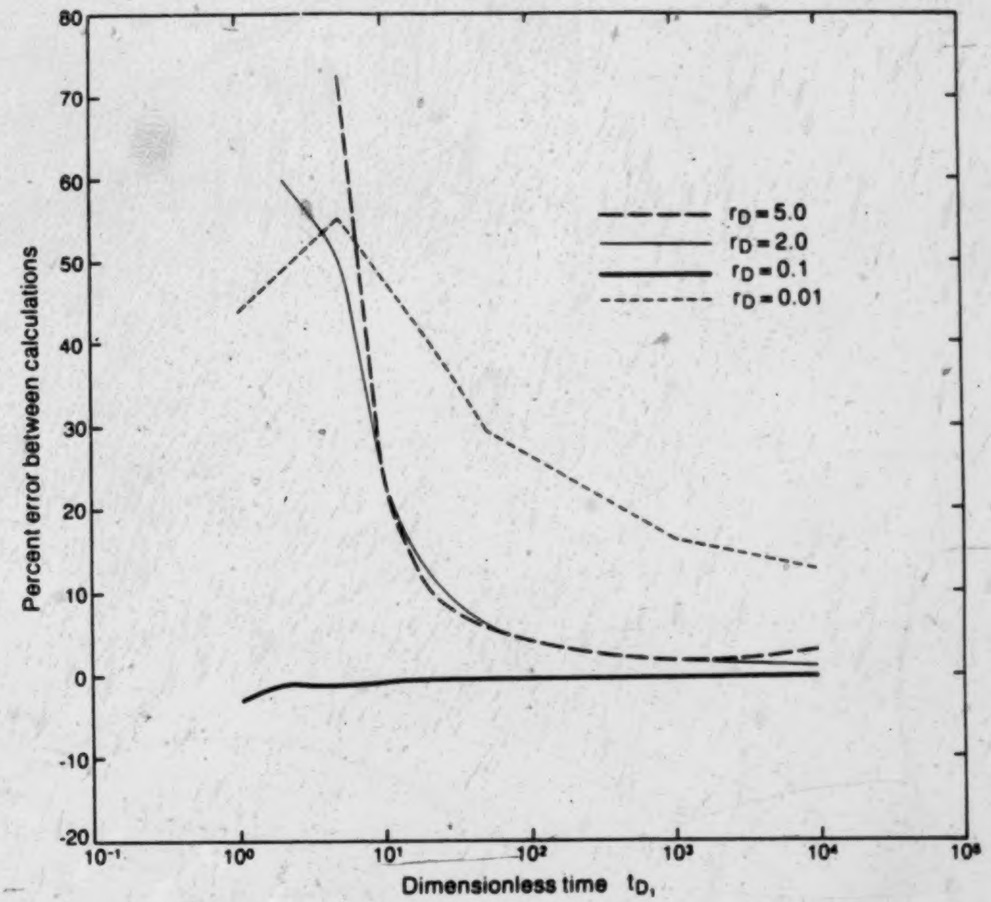

Figure 5. Dual porosity model (slabs). Comparison of exactly inverted solutions: percent error between results of Sauveplane (1984a) and Streltsova-Adams (1978) for various values of the dimensionless radius

r_D=0.01. Recalling the real space solution of this model (equation 63 of Streltsova-Adams, 1978) written with the notations of equation 25 as:

$$s_{D_1} = 2\int_0^\infty x' J_o(r_D x') \left[\sum_{m=1}^{\infty} \Psi_m\right] dx' \qquad (31)$$

where $\psi_m = \dfrac{1-\exp(-\beta^2_m r_D{}^2 t_{D_1}/\eta)}{\beta^2_m/\eta+\beta_m/2(\tan\beta_m+\beta_m\sec^2\beta_m)}$

and β_m is the positive root of $\beta^2_m/\eta+\beta_m\tan\beta_m=x'^2$, it is not astonishing that the computation of s_{D_1} is not straightforward, especially for small values of r_D and t_{D_1}. We apply the Stehfest algorithm to equation 25 and compare the results with the calculations of Sauveplane (op.cit.); this comparison is illustrated on Figure 6 where the relative error is in per ten-thousand.

Figure 6 shows that, in the interval 1 to 10,000 for t_{D_1}, the overall results of the inverter are within 0.6 percent accuracy when r_D varies between 0.01 and 5. The relative error is of the order of 10^{-3} or less for t_D greater than 10 and all r_D. It is only for $t_D<5$ that this error becomes a fraction of one percent. A similar plot for the same conditions but comparing this time with the Crump inverter results would show all the data on the zero line and was not produced. This test permits drawing of two conclusions:

1. it suggests that our 1983 calculations of this double-porosity model are correct;
2. the numerical inverters can be used with a sufficient degree of confidence for complex aquifer systems; an impressive accuracy can be obtained with the Crump inverter but the Stehfest inverter of easier use is probably sufficient for the cases when it can be applied.

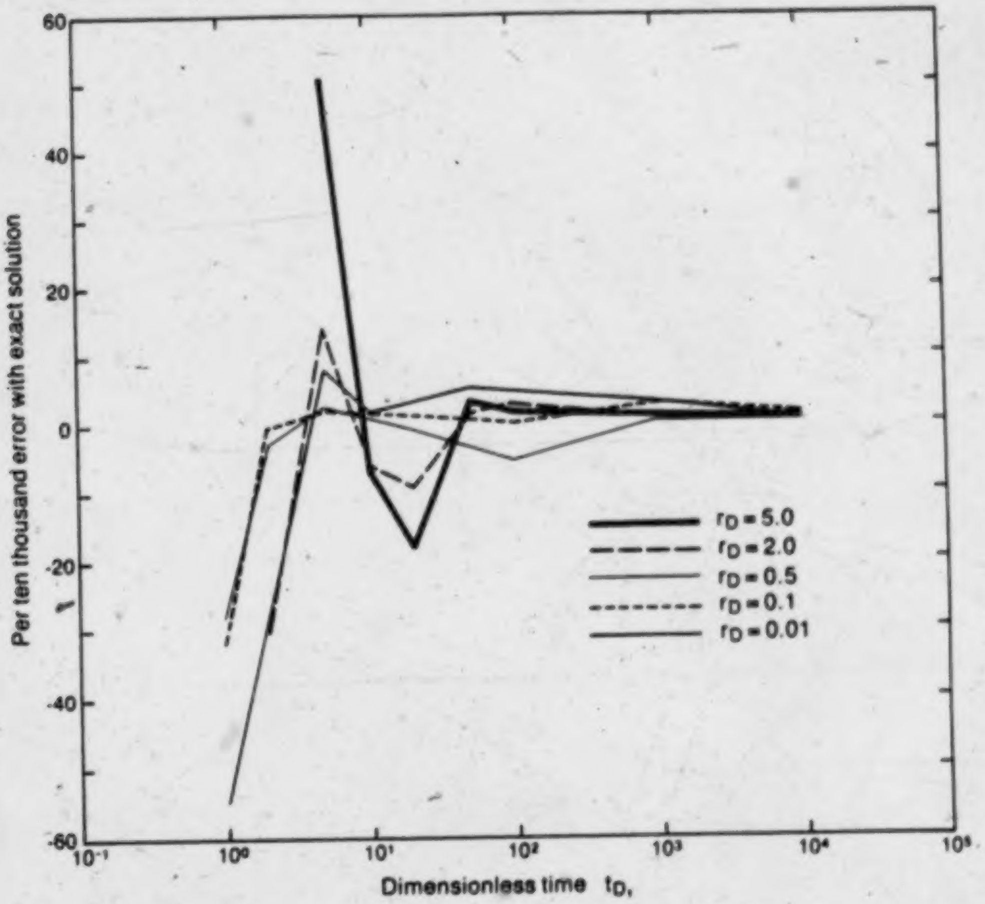

Figure 6. Dual porosity model (slabs). Per ten thousand error with Stehfest inverter. The comparison is with the results of Sauveplane (1984a)

For this study, we have performed the calculations of the solutions with either the Stehfest or the Crump inverters and, therefore, cannot comment on the use of Gaussian quadrature formulae such as equation 26 for numerical inversion of Laplace transform solutions. Javandel and Witherspoon (1980) have used - apparently with success - Bellman et al. (op.cit.) formula that involves ~~shifted Legendre po~~lynomials for the evaluation of the solution in the case of partial penetration in a two-layer aquifer. That solution in the Laplace space was already in the form of an infinite integral involving the J_0 function and was not, therefore, a good candidate for application of Stehfest or Crump inverters.

We may summarize this chapter with the following conclusions and recommendations:

1. Approximate inversion methods of Laplace transform solutions provide a powerful technique of evaluating the solutions of complex flow models. The technique avoids tedious mathematical developments attached to the exact inversion of the Laplace space solutions. Even when real space solutions have been obtained in closed form, their evaluation is best achieved with the proposed technique: when $r_D=0.01$, the computation of one value of s_{D_1} with the real space solution of equation 31 can take up to 1 hour CPU time! computation of the type curve $r_D=0.01$ (values of s_{D_1} for a range of some 20 values of t_{D_1}) is done in a few seconds CPU time on a VAX/VMS 780 computer with the Stehfest algorithm. Slightly more time is needed with the Crump inverter which works in the complex plane, but provides a greater accuracy.
2. Although numerical inversion methods are more accurate by at least two orders of magnitude, analytical formulae (especially the

Modified Schapery formula of equation 18) may provide a good estimate of intermediate to long-time solutions. They can be implemented without a powerful computer. Depending on the problem and on the degree of accuracy required, they may represent an interesting alternative because they can cover wider ranges of time than the classical asymptotic solutions.

3. These techniques should not be used "blindly"; tests with exactly inverted solutions are recommended whenever possible; if not, the comparison between results provided by two or three methods may provide some insight into the behaviour of a particular inversion technique and help choosing the most appropriate method for a given problem and accuracy requirement. The comparison may be for results obtained with the Modified Schapery technique, the Stehfest and Crump inverters. However, in some cases that will be discussed later, only one of these three methods is applicable. If the Laplace transform solutions do not have the form of well-behaved functions or are too difficult to evaluate, then the recourse to Gaussian quadrature formulae based on orthogonal polynomials may represent the only alternative.

4. ANALYTICAL AND SEMI-ANALYTICAL MODELS FOR COMPLEX AQUIFER SYSTEMS

The first three chapters are a brief overview of the theoretical and practical concepts and methods that are now going to be applied to analytical flow models for complex aquifer systems. It is our contention that the majority of practising engineers may be confused by the profusion of existing analytical models for complex systems and that there is first a need to present an overview of their specificity and domains of validity (assumptions and boundary conditions considered). The second and probably more important aspect is to make these existing models "user friendly" by proposing methods for type curve evaluation. Both aspects are strongly related and will not be separated. The term "user friendly" is borrowed from the jargon of software analysts precisely because the proposed methods are best implemented on computers. For complex aquifer systems, the difficulty to evaluate real space analytical solutions render their use problematic when (legitimate) sensitivity analyses are to be conducted; such sensitivity analyses can be, for example, necessary for a satisfactory type curve matching in aquifer and well test interpretation or for predictive purposes once the structural parameters have been locally or regionally estimated. The accuracy of both the flow parameters and the predictions can be greatly improved if the engineer has access to an adequate analytical model and can perform this type of sensitivity analysis with it.

We shall distinguish line-sink(-source) solutions, where the well radius is assumed to be negligible (or infinitesimal) compared to the distance to the point of observation in the system, from the cylindrical (-sink-source) solutions where this assumption is not valid and the well radius is not neglected. The first series of solutions are useful for aquifer (or interference) test analysis and for regional predictions of well-induced transient flow processes once the structural parameters are known. The second type apply to well test analysis and prediction of local impacts. In practice, the first category is applicable to hydrogeological investigations (except for slug test interpretation) and the second to reservoir engineering ones.

Also, for convenience, we shall limit the scope to cases where the operated well fully penetrates the aquifer systems. The categories of considered problems are also limited to complex systems where the mobilized aquifer is:

1. semi-confined and part of a multilayered system where leakage is not negligible and influences the transient flow towards or from the well (the assumption of perfect confinement is not valid),
2. confined, uniformly fractured and can be modelled with the dual-porosity concept,
3. confined and consisting of two contiguous layers of different properties that are both fully tapped by the well (two-layer model with and without crossflow),
4. confined and presents a radial discontinuity of flow properties.

We also present a (new) analytical solution for non-Darcian radial flow based on Forchheimer law and applicable to very coarse confined aquifers (fluid=water) as well as a set of the type curves for viscoelastic and confined aquifers.

4.1 Infinite Leaky Aquifer Systems

Following the pioneer work of Hantush (1949, 1956), of Hantush and Jacob (1955) and Boulton (1954), much has been published about the concept of leakage and apparented "delayed yield" from storage in semi-confining beds. Hantush (1964) suggests that the induced or natural flow through these beds can be considered as vertical when the ratio of the horizontal hydraulic conductivity K_h, of the supposedly homogeneous aquifer to the vertical hydraulic conductivity K' of the semi-confining layer is greater than 500. With finite-element modelling, Neuman and Witherspoon (1969) have shown that this lower bound of the assumption could be decreased to 100 without creating significant errors, except in the immediate vicinity of the operated well. The semi-confining beds are usually silty, argillaceous or shaly sediments for which K' varies between 10^{-6} and 10^{-12} m/s (Davis, 1969; Schoeller, 1962). Because exploitable aquifers have K_h comprised between 10^{-4} and 10^{-1} m/s, the condition required for vertical leakage is thus commonly verified in nature and its corollary (horizontal flow in the mobilized aquifer) can be considered as valid in most situations.

Although leakage through semi-confining beds is commonly observed and accounted for by hydrogeologists, it is usually neglected by reservoir engineers who consider the caprock of the producing zone as strictly impervious. Single-layer theories for transient flow (Theis, 1935; Muskat, 1946) predict that any exploitation of an aquifer that is not recharged will be followed by a continuous and unavoidable pore pressure depression. The following simple calculations are showing that it may not be true when simplistic leakage is considered.

Let us assume a non-capacitive aquitard whose function is only to vertically transmit fluxes as a consequence of hydraulic head (or pressure) difference between the two permeable layers it separates. The upper aquifer is drained with negligible change of hydraulic head. If a depletion Δh has been created between the aquifers (following for instance, exploitation of the lower unit), we seek a relationship between Δh and the time necessary to compensate for Δh by vertical leakage. Writing Darcy's law and performing the balance of fluxes, we find:

$$S\frac{d(\Delta h)}{dt} = K'\Delta h/b'$$

yielding after integration:

$$\frac{\Delta h}{h_o} = \exp(-K't/Sb') \qquad (32)$$

where S is the storativity of the exploited aquifer and b' is the aquitard thickness. Assuming $K' = 10^{-8}$ m/s, $S = 10^{-4}$ and $b' = 50$ m, $\Delta h/h_o = 0.01$ after 27 days. If $K' = 10^{-9}$ m/s and 10^{-10} m/s, the time is

270 and 2700 days, respectively. A 50 m thick caprock of 10^{-10} m/s (0.01 md equivalent) is a serious hydrodynamic barrier; it still allows important pressure transfers because the areas of contact are very large. This can be further illustrated with the balance of fluxes; we obtain:

$$\frac{K'}{K_h} = \frac{bb'}{a\Delta h}\,\frac{dh}{dl} \tag{33}$$

where a is the side of a supposedly square system and dh/dl is the natural horizontal gradient in the aquifer. Assuming that Δh is the natural hydraulic head difference between upper and lower aquifers, equation 33 simply traduces that the horizontal and vertical fluxes (by leakage) are equal. For $a=100$ km, $b=b'=50$ m, $dh/dl=2\times10^{-3}$ and $\Delta h=10$ m, we obtain $K'/Kh=5\times10^{-6}$. A 10 m natural depletion between aquifers in a sedimentary basin is not uncommon.

In deriving equation 32, we have, for simplicity, made two reductive assumptions: (1) the aquitard storativity is negligible and (2) an induced depletion in the exploited aquifer was not followed by a depletion of the drained (upper) aquifer. The finer material that constitutes aquitards is generally more compressible and may have a higher porosity than the aquifer itself; it follows that ~~its~~ storativity S' can be higher by an order of magnitude than S, so that there is no physical reason to neglect S'. To assume no depletion of the drained unit means that this unit can be recharged while the lower unit is exploited; this is not usually the case so that the two assumptions, although practical to give orders of magnitude, are not generally valid. The early work of Hantush and Jacob (1955) is based on these two assumptions: it is commonly known as the "r/B" model where B is defined as the coefficient of leakage

$B = \left(\frac{KHb'}{K'}\right)^{1/2} [L]$. This model characterized by flattening type-curves reflecting long-time steady-state conditions has been intensively used by hydrogeologists. The aquifer is assumed isotropic and of infinite lateral extent. Later, Hantush (1960) published a model that accounts for storage in the aquitard and based on the dimensionless parameter $\beta = r/4H(K'S'_s/KS_s)^{1/2}$ but still neglects drawdown in the upper aquifer (we refer to it as the "β" model). Neuman and Witherspoon (1969) were the first ones to our knowledge to present an analytical model that accounts for both effects. However, to make the problem tractable they assume that the vertical gradients in the unexploited aquifer units are negligible which, in other words, postulates a uniform drawdown (or build-up) in these units throughout their thicknesses. These units are thus relatively thin.

The flow in the i^{th} aquifer of a multiple aquifer system of infinite extent underlain by the j^{th} aquitard and overlain by the $j+1^{th}$ aquitard can be described by the following IBVP (the aquifer i is pumped with constant rate Q):

$$\left.\begin{array}{ll}
\multicolumn{2}{l}{\Delta s_i + \frac{K'_{j+1}}{T_i} \left.\frac{\partial s'_{j+1}}{\partial z}\right|_{z_{i,j+1}} - \frac{K'_j}{T_i} \left.\frac{\partial s'_j}{\partial z}\right|_{z_{i,j}} = \frac{1}{\alpha_i} \frac{\partial s_i}{\partial t}} \\
s_i(r,z,o) = 0 & \text{initial condition} \\
s_i(\infty,z,t) = 0 & \text{(outer boundary condition)} \\
\multicolumn{2}{l}{\lim_{r \to 0} \left[2\pi K_i H_i r \frac{\partial s_i}{\partial r}\right] = -Q_i \text{ (inner boundary condition)}}
\end{array}\right\} \quad (34)$$

where the notation $z_{i,j}$ refers to the interface between units i and j. The quantity $s_i(r,z,t)$ refers to a drawdown of hydraulic head or pore pressure[4]. The one-dimensional flow in the j^{th} aquitard is solved simultaneously to obtain the interface source terms of the governing equation in 34:

$$\frac{\partial^2 s'_j}{\partial z^2} = \frac{1}{\alpha_j} \frac{\partial s'_j}{\partial t}$$

$$s'_j(r,z,o) = 0 \text{ initial condition} \tag{35}$$

$$s'_j(r,z_{i,j},t) = s_i(r,z_{i,j},t)$$

Each unit is in addition assumed to be horizontal, homogeneous, isotropic of uniform thickness and of infinite extent with constant specific storage. Neuman and Witherspoon (1969) have solved the system (equations 34 and 35) for the two-aquifer system: a lower aquifer 1, being pumped or injected under radial flow conditions, is overlain by an intervening aquitard and an upper aquifer 2 which is not tapped by the well. Zero flow boundaries are present at the top and the base of the system. They also proposed a solution for the three-aquifer system where 3 aquifers are separated by two aquitards. In both cases, the solutions are obtained in the real space after a successive use of

---

[4] it could be a build-up (of hydraulic head or pore pressure) in the case of injection; in that case, s changes sign; the interface terms in the governing equation 34 change sign and that equation is unchanged. The sign of Q_i in the inner boundary condition (equation 34) changes sign; therefore the overall solution of equations 34 and 35 is the same as for the pumping case.

Laplace transform (on the time) and infinite zero-Hankel transform (on the radial distance r) and inversion with equation B10 in the real space. The resulting solutions for the two-aquifer system have been evaluated in the real space with the Zonneveld-Adams-Moulton numerical procedure of integration. The solutions for the three-aquifer system has not been evaluated to date.

4.1.1 Study of the Two-Aquifer System

In Appendix C, we propose a revised formulation of Neuman and Witherspoon results in the Laplace space that in our opinion is more amenable for a sensitivity analysis of four different dimensionless parameters besides the dimensionless time. These Laplace solutions are then written in terms of dimensionless Laplace space variables that are used as input functions for the Stehfest inverter. The resulting code computes directly five dimensionless drawdowns s_{D_1}, s'_D at $z_D=0.2$, 0.5 and 0.8 in the aquitard and s_{D_2} in an average CPU time of about 25 sec on a VAX 780 computer.

Accuracy and Comparison with Neuman and Witherspoon Notations

The correspondence between our dimensionless parameters (Appendix C) and the notations β_{ij} and r/B_{ij} of Neuman and Witherspoon can be easily established as follows:

$$\frac{r}{B_{11}} = r\sqrt{\frac{K'}{T_1H'}} = \frac{r}{H'}\sqrt{\frac{T'}{T_1}} = r_D$$

$$\beta_{11} = \frac{r}{4H_1}\left(\frac{K'S'_s}{K_1S_{s1}}\right)^{1/2} = \frac{r_Db}{4} \text{ since } b = \left(\frac{S'}{S_1}\right)^{1/2}$$

$$\beta_{21} = \frac{r}{4H_2}\left(\frac{K'S'_s}{K_2S_{s2}}\right)^{1/2} = \frac{abr_D}{4c} \text{ since } a = \left(\frac{T_1}{T_2}\right)^{1/2} \text{ and } c = \left(\frac{S_2}{S_1}\right)^{1/2}$$

$$\frac{r}{B_{21}} = r\sqrt{\frac{K'}{T_2H'}} = \frac{r}{H'}\sqrt{\frac{T'}{T_2}} = \frac{r}{H'}\sqrt{\frac{T'}{T_1}}\sqrt{\frac{T_1}{T_2}} = ar_D$$

Figure 7 illustrates the accuracy of the Stehfest inverter applied to the equation C2 when $r/B_{11} = r/B_{21} = 0.1$ and $\beta_{11} = \beta_{21} = 0.01$, that is for $a=1$, $r_D=0.1$, $b=0.4$ and $c=1$. The continuous line represents the exact solution as computed by Neuman and Witherspoon. The discrete points represent the results obtained with the Stehfest inverter. The agreement is excellent for all the range of dimensionless time.

Sensitivity Analysis

The coefficients a, b, c, and r_D have been defined so that they relate to structural flow parameters of not more than two units at the time - which was also true for the β_{ij} and r/B_{ij} - but, in addition, they concern either transmissivities (a and r_D) or storativities (b and c). Only r_D has some reference to geometric information that is the ratio between the radial distance r and the aquitard thickness H'; because these parameters are usually of the same order of magnitude (and are usually known), the impact of this ratio is minimal for sensitivity analysis.

We vary one of the four parameters at the time with the values 0.01, 0.1, 1 and 10 and the other three remain constant and always the same. The chosen constant values are realistic: $a= 2$, $b= 10$, $c= 3$ and $r_D=1$ or $T_1=2T_2$, $S'=10S_1$, $S_2=3S_1$ and $T'=T_1$ (assuming $r=H'$). The results for s_{D_1}, s'_D at $z_D=0.5$ and s_{D_2} and for the successively varied values of a, b, c and r_D are illustrated on Figures 8 to 11, respectively.

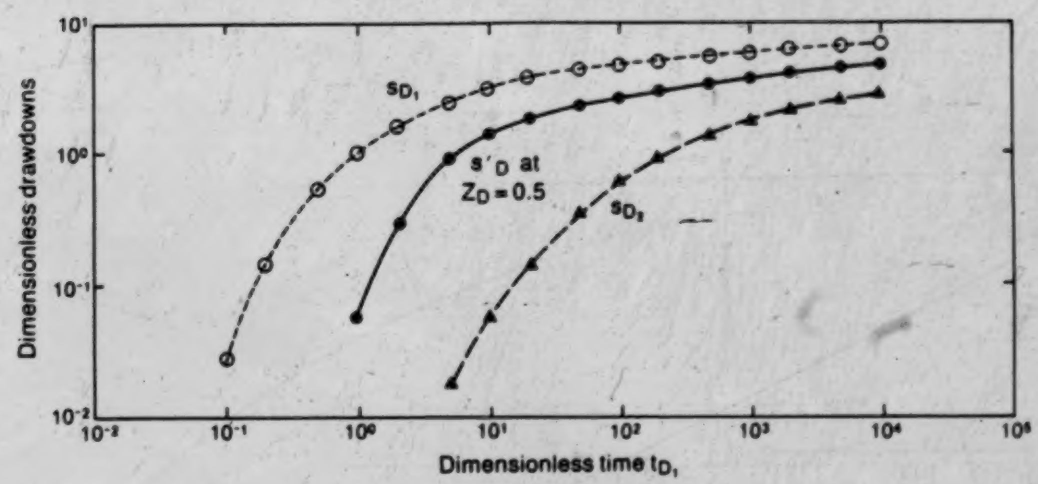

Figure 7. Two-aquifer model. Error with Stehfest inverter when β=0.01, r/B=0.1. The comparison is with Neuman and Witherspoon (1969) results (continuous lines) for the pumped aquifer (s_{D_1}), the unpumped aquifer (s_{D_2}) and at mid-point of the aquitard (s'_D). The discrete points are obtained with Stehfest inverter

Figure 8 illustrates the influence on the dimensionless drawdowns of the ratio T_1/T_2 (that is of a). This ratio increases from 10^{-4} (a=0.01) to 100 (a=10) and for the drawdowns in the pumped aquifer and at mid-point in the aquitard the curves are generally shifted upwards at intermediate and long-times and they are confunded at early times. The early-time behaviour represents, in fact, the "β" solution of Hantush as discussed in Appendix C (see equation C6). However, at early times, the type curves for the unpumped aquifer are separated for the given values. This could not be deduced from the asymptotic solutions. The drawdown increase at intermediate and long times when a increases corresponds physically to the fact that the upper (drained) aquifer becomes less and less transmissive and provides less and less leakage to the pumped aquifer. One interesting peculiarity, however, is the fact that for intermediate times (t_{D_1} comprised between 5 and 200), the type curve a=1 is, in fact, located above the type curve a=10. In that range of dimensionless times, the "equal" aquifer case that corresponds (in part) to a=1 ($T_1=T_2$) represents an "upper envelope" for the type curves. This role is amplified in the unpumped aquifer where the phenomenon starts for $t_{D_1}<1$. Because at long times, the type curve a=10 will be located above the type curve a=1, the former shows an inflexion in the intermediate time range for s_{D_1} and s'_D. This inflexion at about $t_{D_1}=20$ for a=10 reflects the time at which the influence of the upper aquifer on s_{D_1} starts to be dominant; beyond that flexure and up to the crossing point with the type curve a=1, the drawdown s_{D_1} increases sharply, in a quasi-linear fashion (this could be wrongly interpreted at a lateral boundary effect on an aquifer test). The "composite" intermediate regime described for s_{D_1} when a>1 is also clear for s'_D. The ranges of

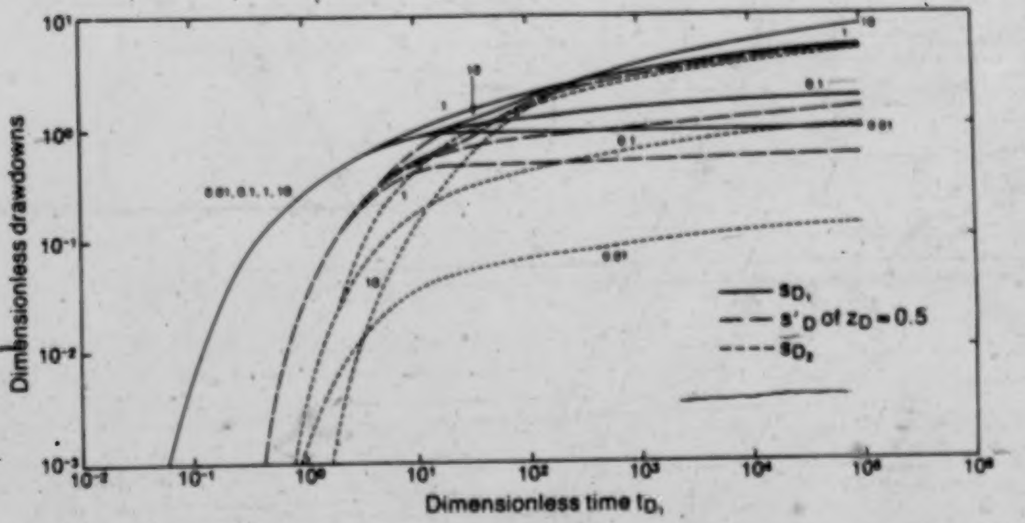

Figure 8. Parametric analysis for the two-aquifer model: influence of $a=(T_1/T_2)^{1/2}$ when $b=(S'/S_1)^{1/2}=\sqrt{10}$, $c=(S_2/S_1)^{1/2}=\sqrt{3}$ and $r_D=r/H'(T'/T_1)^{1/2}=1$

dimensionless times given above are of course specific to the numerical values assigned to b, c, and r_D, but we could observe the same peculiarity when b, c and r_D have different values. The trends remain the same. Drawdown stabilization is only clear for a=0.01 at long times (T_2 is four orders of magnitude greater than T_1).

When b varies between 0.1 and 10, S' varies between $10^{-2}S_1$ and $100S_1$; the case b=0.01 is not realistic and not illustrated on Figure 9. When b increases, the three sets of type curves are now shifted downward with a smaller difference between b=0.1 and 1 than for b varying from 1 to 10. As in Figure 8, all the curves are located below the Theis type curve of any value of dimensionless time.

At early times, s_{D_1} is asymptotically represented by the Hantush "β" solution as shown in Appendix C; because that solution depends on b, the type curves for different values of b are separated. For example, when b=10, early-times coincidence with the "β" solution is expected when

$$t_{D_1} < \left(\frac{b}{3r_D}\right)^2 = 11$$

when $t_{D_1}=10$, the function H of equation C6 is 0.35 and the value obtained for s_{D_1} is 0.346; at $t_{D_1}=20$, the corresponding values are 0.6 and 0.5, respectively. It can be deduced that at all times, the type curves are located below the Theis solution which is above the "β" solution. Beyond

$$t_{D_1} = \left(\frac{b}{3r_D}\right)^2$$

the type curves remain located below the "β" solution.

At long-times, there is no tendancy towards a steady-state regime mainly because T_2 is too small (only half of T_1 with the chosen value for a). The interesting feature is that the type curves for s_{D_1} and s_{D_2} apparently "converge" towards a single type curve for b=0.1 and 1. A similar "convergence" is also clear when b=10 and the "unique" type curve will remain below the previous one when t_{D_1} increases: in the case b=0.1 and 1, the "convergence" starts at $t_{D_1}=20$, but only at $t_{D_1}=200$ when b=10. This behaviour for the three drawdowns could have been predicted from consideration of equations C9 a[illegible] C10. Because a and c are close to 1, the considered system can be approximated by an "equal" two-aquifer system for which asymptotic solutions at large values of time are given by C9 and C10. Using the usual approximation for the function W(u,r/B) when $u=1/4t_{D_1}$ is small, it can be seen that for a given r_D both s_{D_1} and s_{D_2} will tend towards a solution of the exponential integral type that will mainly depend on the values of the "shifting" factor γ_1 which is solely a function of b.

Specifically, at large times, we may approximate further equations C9 and C10 as follows:

$$\text{when } t_{D_1} > 5\gamma_1 \qquad s_{D_1} = \ln\left(\frac{3}{2}\sqrt{\frac{t_{D_1}}{\gamma_1}}\right) + K_o\left(\sqrt{2}r_D\right)$$

$$s_{D_2} = \ln\left(\frac{3}{2}\sqrt{\frac{t_{D_1}}{\gamma_1}}\right) - Ko\left(\sqrt{2}r_D\right) \qquad (37)$$

$$(s'_D)_{z_D = 0.5} = \ln\left(\frac{3}{2}\sqrt{\frac{t_{D_1}}{\gamma_1}}\right)$$

Equation 37 shows that we might have $s_{D_1}=s_{D_2}=s'_D$ when the argument of the function K_o is such that its value is negligible with regard to ln( ). This happens only when $r_D > 3.5$. For $r_D < 3.5$ (usual case in practice), the type curves are not confounded but simply displaced by a value that depends only on r_D. In the case of Figure 9, $r_D=1$ and $K_0(\sqrt{2}r_D)=0.2392$; the "convergence" to a single type curve is only apparent and enhanced by the use of a log scale. For instance at $t_{D_1}=1000$ when $b=1$, we have from equation 37 $s_{D_1}=3.896$, $s'_D=3.657$ and $s_{D_2}=3.417$; the exact values obtained from equations C3 and C4 are 3,927, 3.727 and 3.527, respectively. So that equation 37 approximates the long-time drawdowns within 3% error, which is acceptable if one considers that we are not exactly dealing with an "equal" aquifer system. When $b=0.1$ and still for $t_{D_1}=1000$ and $r_D=1$, we find from equation 37, $s_{D_1}=4.096$, $s'_D=3.857$, $s_{D_2}=3.618$ and the three type curves are still separated. Now, when $r_D=5$ $b=1$ and $t_{D_1}=1000$, K_0 $(\sqrt{2}r_D)=3.94\times10^{-4}$ and $s_{D_1}=s_{D_2}=s'_D=3.657$; the exact value from equations C3 and C4 is 3.761.

We just have shown that, at long-times, the two-aquifer system may behave as an equivalent homogeneous system as long as the properties of the pumped and unpumped aquifers are about the same and the properties of the intervening aquitard are such that:

$$\frac{K'}{T_1} > \frac{49H'}{4r^2} \text{ with } S' < S_1$$

For example, a system composed of a 10 m thick aquitard with $K'=10^{-6}$ m/s overlaying and aquifer of transmissivity 10^{-3} m²/s would behave at long times as a homogeneous system at a radial distance superior or equal to 350 m if the transmissivity of the upper aquifer is of the order of 10^{-3} m²/s. When these conditions are met, equation C9 shows that the storativity of the equivalent homogeneous system is $(S_1+S'/2)$.

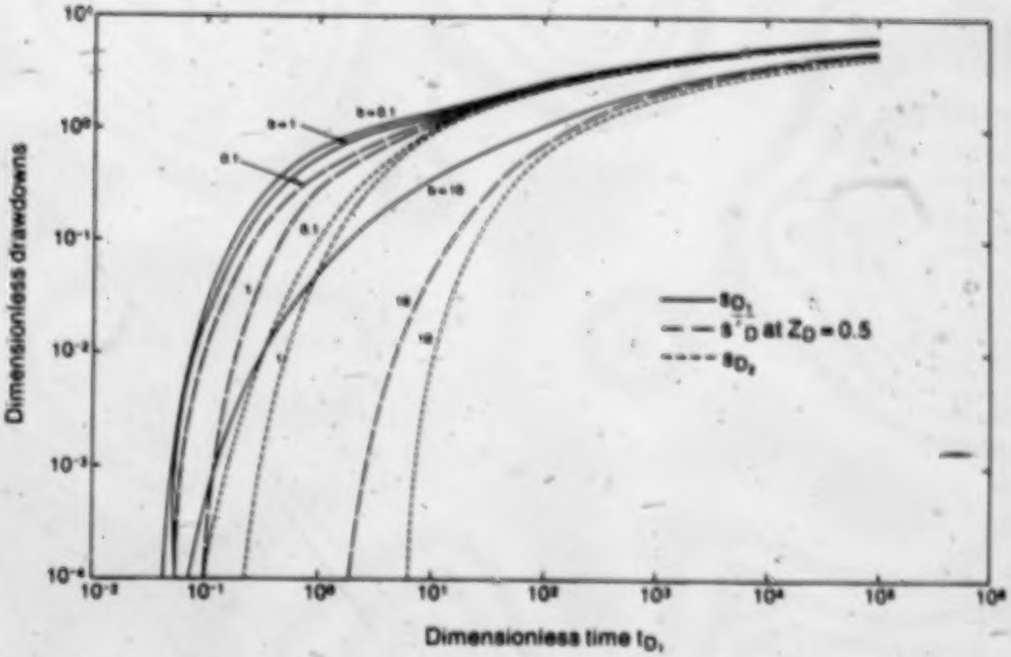

Figure 9. Parametric analysis for the two-aquifer model: influence of $b=(S'/S_1)^{1/2}$ when $a=\sqrt{2}$, $c=\sqrt{3}$ and $r_D=1$

Figure 9 also illustrates that the differences between s_{D_1}, s'_D and s_{D_2} are more pronounced at early and intermediate times when b=10 than when b<1. In physical terms, this means that proportionally less drawdown than otherwise will be observed in the three units when the aquitard storativity is higher than the storativity of the pumped aquifer, which is common sense.

Figure 10 shows the influence of the ratio of storativities of the two aquifers when this ratio varies from 10^{-4} (c=0.001) to 100 (c=10). When c<1, the influence of c on s_{D_1} is minimal: a single type curve is obtained at all times. Also, in that case, the curves for s'_D are confounded outside the short time range $2<t_{D_1}<100$. For s_{D_2}, they are all confounded when $t_{D_1}>20$.

At intermediate times, an inflexion (non horizontal) is observed for s_{D_1} and s'_D when c=10 but is not noticeable for s_{D_2}. This intermediate time regime occurs between $t_{D_1}=2$ and $t_{D_1}=500$, with an inflexion point at about $t_{D_1}\approx 5$. It is interpreted (as in Figure 8) as the point at which the influence of the unpumped aquifer comes into effect. This influence is traduced on Figure 10 by less drawdown in the two lower units because of the relatively high storativity of the upper unit. The resulting S-shaped type curves are characteristic of a "delayed yield" phenomenon; in our case, a pseudo-stabilization with horizontal inflexion is not noticeable. Physically, when S_2 is substantially greater than S_1, the rates of drawdown increase in the pumped aquifer and the aquitard are "slowed down" when water starts being released from storage in the drained aquifer. An important difference with Boulton's theory, however, is that, unlike the aquitard-aquifer system, delayed yield for a two-aquifer system is not observed in the exploited aquifer because of

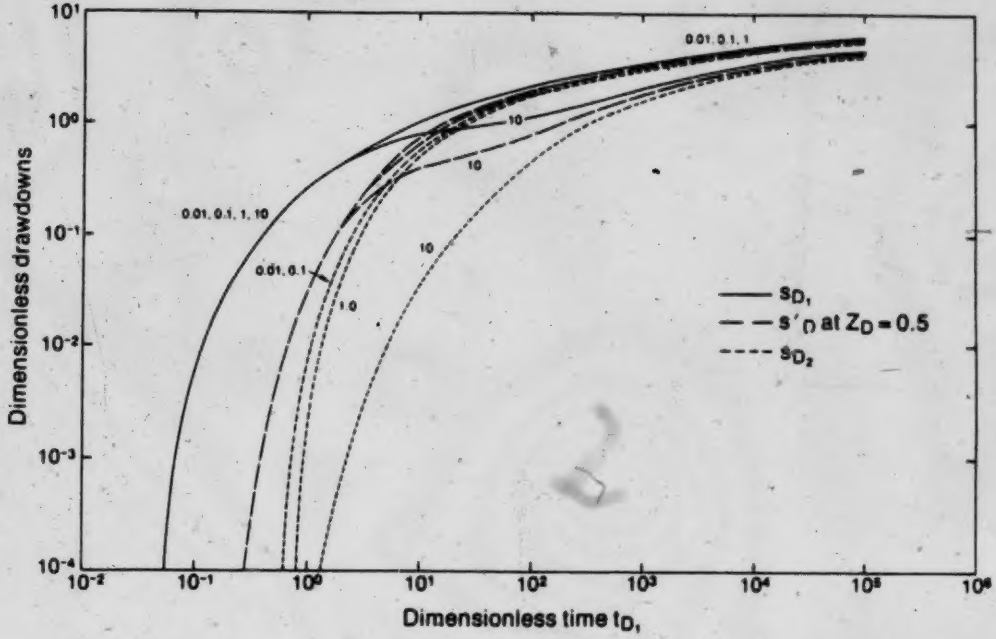

Figure 10. Parametric analysis for the two-aquifer model: influence of $c=(S_2/S_1)^{1/2}$ when $a=\sqrt{2}$, $b=\sqrt{10}$ and $r_D=1$

a progressive release from storage in the aquitard (unapparent on Figure 9 for all values of b) but only when the ratios T_1/T_2 and S_2/S_1 become large: it thus depends on the relative properties of the two aquifers. The phenomenon is more pronounced when S_2/S_1 is large than when T_1/T_2 is large (compare curves for a=10 and c=10 on Figures 8 and 10).

The "dimensionless radius" r_D is a function of the geometric ratio r/H' (usually known in interference testing) and of the ratio of the vertical transmissivity of the aquitard to the one of the exploited aquifer. As illustrated on Figure 11, when $r_D=0.01$, the two aquifer system behaves as a single (confined) aquifer at early times: the type curve for s_{D_1} is located below the Theis curve with a departure of less than 3% up to $t_{D_1}=2$ and less than 5% up to $t_{D_1}=50$. The difference continuously increases beyond $t_{D_1}=50$ to reach 25% at $t_{D_1}=100,000$. The curve $r_D=0.1$ is noticeably separated for s_{D_1} from the case $r_D=0.01$ when $t_{D_1}>1$. Increasing r_D, the converse is true, that is large separation of the curves $r_D=1$ and $r_D=10$ at early times (up to $t_{D_1}=10$) and progressive merging of the curves beyond. Overall s_{D_1} decreases when r_D increases, which is physically obvious. When the transmissive (vertical) capacity of the aquitard decreases, the drawdowns s'_D and s_{D_2} are decreasing: at small values of r_D these two units exhibit only late time responses; however, these responses are rapidly merging with the ones corresponding to higher values of r_D. Figure 11 illustrates the largest horizontal span for the aquitard and upper aquifer responses.

At very long times, a similar trend as described for Figures 9 and 10 is noticed and this can be interpreted along the lines of equations C9, C10 and 37.

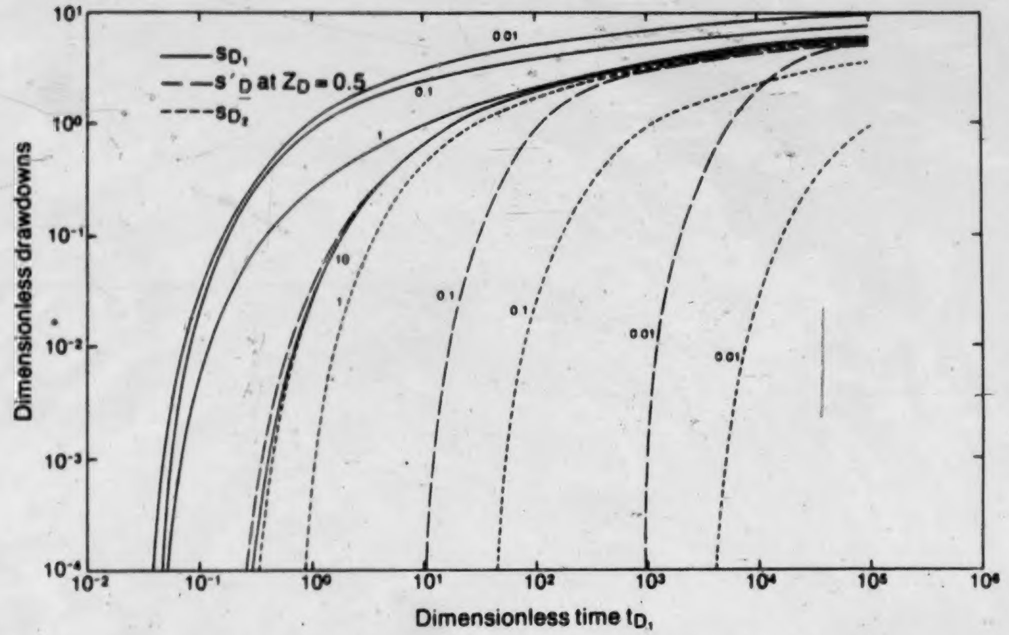

Figure 11. Parametric analysis for the two-aquifer model: influence of $r_D=r/H'(T'/T_1)^{1/2}$ when $a=\sqrt{2}$, $b=\sqrt{10}$ and $c=\sqrt{3}$

Finally, it is interesting to note that beyond $t_{D_1}=1000$, the curves in Figures 9 and 10 are strictly overlapping each other as if, beyond that time, the system did not "recognize" whether it responds to the influence of b or c. Moreover, beyond that same time, the curves $r_D=1$ and $r_D=10$ in the pumped aquifer and the aquitard are nearly merged (Figure 11) at an intermediate position between the "merged" curves of Figures 9 and 10, that is for b(or c)<1 and b(or c)=10. These features are all attributed to the close to unity values chosen for a and c which render our analysis similar to the "equal" two-aquifer case for which long times asymptotic solutions are expressed by equations C9, C10 and 37.

Comparison with Neuman and Witherspoon Results

For the two aquifer system, Neuman and Witherspoon (1969) compared the analytical approach - limited to thin upper aquifers and large ratios of K_1/K' and K_2/K' - with the results of a finite element simulator that covers a wider range of field situations. So doing, they pointed out an important limitation of the simulator which "does not enable representation of dimensionless drawdowns in the form of a small (5) number of parameters as with the analytical approach". Because the forms of these dimensionless parameters cannot be used as input in the simulator, all the thirteen basic variables (time, hydraulic conductivities, porosities, compressibilities and thicknesses) have to be combined. These authors have also studied the asymptotic behaviours of the exactly inverted solutions and found that as long as:

$$t_{D_1} < \frac{1.6\beta_{11}^{\,2}}{(r/B_{11})^2} = 0.1\left(\frac{b}{r_D}\right)^2 \tag{38}$$

the drawdown s_{D_1} is independent of a and c, that is of the properties of the umpumped aquifer. Reasoning in the Laplace dimensionless space, we have shown in Appendix C that equation C6 (Hantush "β" solution) is applicable up to $t_{D_1}=0.11\ (b/r_D)^2$ which is similar to equation 38. Both time domains are shown to be valid on Figures 8 and 10. However, these figures show that the predicted upper bound can be expanded to $0.2(b/r_D)^2$, that is, with our numerical values, up to $t_{D_1}=2$ and not $t_{D_1}=1$ as 38 would predict. It can also be verified on the same figures that this expanded upper bound for t_{D_1} is valid for the drawdown in the aquitard that remains independent of a and c up to $t_{D_1}=2$.

Another conclusion of Neuman and Witherspoon was that both horizontal and vertical spreads between the type curves for s_{D_1}, s'_D and s_{D_2} are directly proportional to the ratio $\beta_{11}/r/B_{11}$, that is b/4, with our notations. Figure 9 testifies that when b increases, the spread between s_{D_1}, s'_D and s_{D_2} increases. However, Figure 11 shows that when b is maintained constant and r_D varies, a more significant spread is observed in the sense of reduced spread for increased r_D: for $r_D=10$, the three curves for s_{D_1}, s'_D and s_{D_2} are practically confounded; at small values of r_D (either H' large or T'/T_1 small), the spread is the most pronounced. This "refinement" was possible because we were able to separate in our analysis the storative from the transmissive properties of the units. These were lumped in the parameters β_{ij} of Neuman and Witherspoon.

We have also shown that for large values of a and c, delayed yield phenomena from the upper aquifer could occur at intermediate values of dimensionless time. This result is not apparent in Neuman and Witherspoon's work.

Reasoning in the Laplace space, we easily obtained the Hantush "r/B" solution as a special case when a=0 (or T_2 infinite) and showed that the steady-state long-time regime is not apparent beyond a=0.01; this invalidates the application of Hantush "r/B" solution to the two-aquifer system in most of the field cases (where T_1/T_2 is usually greater than 1). In fact, we showed that, in the most general case, the long-time behaviour of the drawdowns depends on the four parameters a, b, c and r_D so that there are no unique branches. Only in the situation where a and c are close to 1, does the long-time behaviour follow an asymptotic solution that becomes unique and solely dependent on b when $r_D>3.5$. Physically, this latter condition implies a thin aquitard and a large radial distance even when K' is relatively high (10^{-6} m/s). With $r_D>3.5$, the unique long-time asymptotic behaviour does not follow the Hantush "r/B" solution, including when b=0. The failure of that solution to describe the long-time behaviour of a two-aquifer system is also discussed by Neuman and Witherspoon although not with the same insight. In practice, we find useful the solutions proposed for the "equal" two-aquifer system because the condition a=c=1 is often verified (similar depositional environment and compaction history of the two aquifers).

Finally, besides providing an analysis that covers a wider range of the 4 depending dimensionless parameters than Neuman and Witherspoon did (their results were mostly limited to the equal aquifer case $\beta_{ij}=r/B_{ij}$), we are proposing a fast and accurate method of computing the solutions of the two-aquifer system. The application of this method for aquifer test analysis will be discussed in a further section.

4.1.2 Study of the Three-Aquifer System

The model proposed by Neuman and Witherspoon is merely an extension upward of the two-aquifer system; aquifer 2 (unpumped) in the two-aquifer case is now overlain by another aquitard and a third aquifer (unpumped) with a no-flow boundary at the top and bottom of the five layers. The assumptions for the aquifers and the aquitard remain the same.

The IBVP is well defined by a system of 5 governing equations and attached boundary and initial conditions that describe the flow in the 3 aquifers and in the two aquitards. The method of solution is along the lines of Figure 2.

In Appendix C (section 2), we transform the Laplace space solutions of Neuman and Witherspoon into the dimensionless Laplace space using a set of 11 dimensionless depending parameters which group the 5 geometric and the 10 structural parameters along the same principles as for the two-aquifer case. We now have 5 dimensionless drawdowns s_{D_1}, s_{D_2} and s_{D_3} for the aquifers and s'_{D_1} and s'_{D_2} for the aquitards and one dimensionless time t_{D_1} that refers to the lower aquifer being exploited.[5] The dimensionless Laplace space solutions with p' referring to t_{D_1} can be written as follows for the case when the lower aquifer is exploited:

---

[5] Neuman and Witherspoon give also the Laplace space solutions when the intermediate aquifer is exploited. For simplicity, we will not consider this case here, except briefly in Appendix C where we show how it reduces to Hantush (1960) model. However, given the similarity of the Laplace space solutions, a similar method of evaluation can be easily inferred from Appendix C for this case also.

$$\left.\begin{aligned}
\overline{s_{D_1}} &= \frac{1}{p'}\left[M_1N_1K_o(\sqrt{-Z_3}) + M_2N_2K_o(\sqrt{-Z_2}) + M_3N_3K_o(\sqrt{-Z_1})\right] \\
\overline{s_{D_2}} &= \frac{B_2}{p'}\left[M_1(A_3+Z_3)K_o(\sqrt{-Z_3})+M_2(A_3+Z_2)K_o(\sqrt{-Z_2})+M_3(A_3+Z_1)K_o(\sqrt{-Z_1})\right] \\
\overline{s_{D_3}} &= \frac{B_2B_4}{p'}\left[M_1K_o(\sqrt{-Z_3})+M_2(\sqrt{-Z_2})+M_3K_o(\sqrt{-Z_1})\right] \\
\overline{s'_{D_1}} &= P_1\overline{s_{D_2}} + P_2\,\overline{s_{D_1}} \\
\overline{s'_{D_2}} &= Q_1\overline{s_{D_3}} + Q_2\overline{s_{D_2}}
\end{aligned}\right\}\quad (39)$$

In equations 39, Z_1, Z_2 and Z_3 are the roots of the cubic equation:

$$Z^3 + mZ^2 + qZ + n = 0 \qquad (40)$$

where $m = A_1+A_2+A_3$, $q = A_1A_3+A_2A_3+A_1A_2-B_1B_2-B_3B_4$ and

$$n = A_1A_2A_3-A_1B_3B_4-A_3B_1B_2$$

and we have:

$$M_1 = \frac{2}{(Z_1-Z_3)(Z_2-Z_3)},\quad M_2 = \frac{2}{(Z_2-Z_3)(Z_2-Z_1)},\quad M_3 = \frac{2}{(Z_3-Z_1)(Z_2-Z_1)}$$

$$N_1 = A_2A_3-B_3B_4+(A_2+A_3)Z_3+Z_3^2$$

$$N_2 = A_2A_3-B_3B_4+(A_2+A_3)Z_2+Z_2^2$$

$$N_3 = A_2A_3-B_3B_4+(A_2+A_3)Z_1+Z_1^2$$

$$P_1 = \sinh(z_{D_1}\phi_1)/\sinh(\phi_1)$$

$$P_2 = \sinh[(1-z_{D_1})\phi_1]/\sinh(\phi_1)$$

$$Q_1 = \sinh\,[(z_{D_2}-h_D)\phi_2]/\sinh(\phi_2)$$

$$Q_2 = \sinh\,[(1+h_D-z_{D_2})\phi_2]/\sinh(\phi_2)$$

$$A_1 = p'+r_{D_1}{}^2\phi_1\coth(\phi_1) \qquad \phi_1 = b_1\sqrt{p'}/r_{D_1}$$

$$A_2 = a_1c_1p'+a_1r_{D_1}{}^2\phi_1\coth(\phi_1)+a_1r_{D_2}{}^2\phi_2\coth(\phi_2) \qquad \phi_2 = b_2\sqrt{p'}/r_{D_2}$$

$$A_3 = a_2c_2p'+a_2r_{D_2}{}^2\phi_2\coth(\phi_2)$$

$$B_1 = r_{D_1}{}^2\phi_1/\sinh(\phi_1)$$

$$B_2 = a_1B_1$$

$$B_3 = a_1r_{D_2}{}^2\phi_2/\sinh(\phi_2)$$

$$B_4 = a_2B_3$$

and the dimensionless depending parameters are:

$$a_1 = \frac{T_1}{T_2} \quad a_2 = \frac{T_1}{T_3} \quad b_1 = \left(\frac{S'_1}{S_1}\right)^{1/2} \quad b_2 = \left(\frac{S'_2}{S_1}\right)^{1/2} \quad c_1 = \frac{S_2}{S_1} \quad c_2 = \frac{S_3}{S_1}$$

$$r_{D_1} = \frac{r}{H'_1}\left(\frac{T'_1}{T_1}\right)^{1/2},\; r_{D_2} = \frac{r}{H'_2}\left(\frac{T'_2}{T_1}\right)^{1/2} \quad z_{D_1} = \frac{z}{H'_1} \quad z_{D_2} = \frac{z}{H'_2} \text{ and}$$

$$h_D = \frac{H_2+H'_1}{H'_2}$$

where as before the transmissivities are represented by the letter T, the storatitivies by the letter S, the thicknesses by the letter H. The notation r refers to the radial distance from the well and z is the elevation above the base of the lower aquitard. The subscript 1 refers to the lower aquifer (pumped), subscripts 2 and 3 are for the intermediate and upper aquifers, respectively. The notation ($'_1$) refers to the lower aquitard and the notation ($'_2$) to the upper aquitard. The solutions in equation 39 have been programmed in the code 3AQF for numerical inversion of the Laplace transforms for the dimensionless drawdowns s_{D_1}, s_{D_2} and s_{D_3} in the aquifers only. This code written in FORTRAN is further detailed in Appendix C. Given the simplicity of the expressions P_1, P_2, Q_1 and Q_2, the computations of s'_{D_1} and s'_{D_2} in the aquitards can be easily performed once the aquifer drawdowns are known.

Numerical inversions of the dimensionless Laplace space solutions of equation 39 are performed with the Crump inverter because these solutions cannot generally be treated as real procedures (the roots of 40 can be complex). The Bessel functions $K_0(z)$ for complex arguments are evaluated with the code BESK01 of Burrell (op. cit.) and the roots of 40 are obtained with the code ZCPOLY (Jenkins and Straub, 1972) that calculates the zeros of a complex polynomial.

Neuman and Witherspoon (op. cit.) do not provide - understandably - numerical results for the exactly inverted solutions they obtained for the three-aquifer system. To our knowledge, there is no indication to date that these solutions have been evaluated. Needless to say that this is a very difficult task, if at all possible. Therefore, our numerical results cannot be checked for accuracy with the results of the exactly inverted solutions. An alternative method would be to develop a finite element simulator of the system as done for the two-aquifer system by Neuman and Witherspoon (op. cit.) or to use the simulator of Chorley and Frind (1978). A third possibility would be to develop a simulator based on the memory and response functions as proposed by Herrera et al. (1980) who use an integro-differential formulation[6]. Such a modelling effort is beyond the stated scope of the present work. Besides the fact that the numerical results look reasonable (see Figures 12 to 14), we may test the code for the special case when the three-aquifer system reduces to the two-aquifer system which obviously implies $r_{D_2}=a_2=0$ and $b_2=a_2=0$ (see the details for the mathematical proof of this "reduction" in Appendix C). Table 2 best illustrates this comparison for the case $a_1=2$, $c_1=3$, $b_1=10$ and $r_{D_1}=1$.

Perfect coincidence is obtained for s_{D_1} and s_{D_2} when the comparison is made for the series of results (1) and (2). Small but noticeable differences are, however, experienced if the comparison of (2) is made with (3) where s_{D_1} and s_{D_2} for the two-aquifer system are calculated with the Stehfest inverter. The missing values in (2) for $t_{D_1}>20{,}000$ are discussed in the next section related to the sensitivity analysis for the three-aquifer system.

---

[6] In his paper on the "exact aquitard response functions" for application in the numerical solution of integro-differential equations characterizing the two-aquifer system, Frind (1979) proposes three discrete stages for the aquitard response: a first period where water is only released from storage in the aquitard ("uncoupled" aquifers), a second period where the unpumped aquifer starts to respond and to contribute to the general flow to the well ("coupled" system) and a third period where a steady-state regime has been established through the aquitard. Examination of Figures 8 to 11 which have been established for a realistic and wide range of depending parameters demonstrates the general unsteady response of the intervening aquitard, even at large dimensionless times (at best the late-time regime could be qualified as "pseudo-steady state"). The drawdown stabilization in the aquitard is only apparent on Figure 8 when the transmissivity of the unpumped aquifer is 10,000 times the one of the pumped aquifer!

Table 2.
Comparison of numerical values for dimensionless drawdowns in two- and three-aquifer systems.

t_{D_1}	Two-aquifer (Crump inverter) (1)		"Reduced" Three-aquifer (2)		Two-aquifer (Stehfest inverter) (3)	
	s_{D_1}	s_{D_2}	s_{D_1}	s_{D_2}	s_{D_1}	s_{D_2}
0.1	0.41306E-03	0.71487E-31	0.41306E-03	0.71487E-31	0.40125E-03	-
0.2	0.33931E-02	0.10032E-21	0.33931E-02	0.10032E-21	0.33902E-02	-
0.5	0.20213E-01	0.17305E-13	0.20213E-01	0.17305E-13	0.20233E-01	-
1.0	0.51548E-01	0.14581E-09	0.51548E-01	0.14581E-09	0.51571E-01	-
2.0	0.1061	0.17574E-07	0.10614	0.17574E-07	0.10616	0.29341E-04
5.0	0.2221	0.11564E-03	0.11106	0.11564E-03	0.22207	0.52944E-04
10.0	0.3461	0.64542E-02	0.34611	0.64542E-02	0.34617	0.58995E-02
20.0	0.5029	0.63098E-01	0.50293	0.63098E-01	0.50200	0.61507E-01
50.0	0.7783	0.32752	0.77832	0.32752	0.77479	0.30651
100.0	1.0772	0.66849	1.07717	0.66849	1.05796	0.61175
200.0	1.4481	1.07722	1.44808	1.07722	1.39753	0.97159
500.0	2.0016	1.66059	2.00159	1.66059	1.89323	1.48259
1000.0	2.4442	2.11444	2.44420	2.11444	2.28528	1.88036
2000.0	2.8965	2.57260	2.89650	2.57260	2.68426	2.28231
5000.0	3.5012	3.18117	3.50118	3.18117	3.21673	2.81662
10000.0	3.9619	3.64229	3.96188	3.64229	3.62133	3.22183
20000.0	4.4232	4.10446	-	-	4.02663	3.62744
50000.0	5.0333	4.71509	-	-	4.56292	4.16392
100000.0	5.4949	5.17684	-	-	4.96879	4.56986

Sensitivity Analysis

Equations 39 state that $s_{D_1}(t_{D_1})$, $s_{D_2}(t_{D_1})$ and $s_{D_3}(t_{D_1})$ are functions of eight dimensionless parameters that are expressed in terms of ratios of equivalent flow properties for the five units of the three-aquifer system.

An analysis as complete as for the two-aquifer system is not feasible within the scope of this work because of the shear amount of possible combinations between the twofold number of parameters. To simplify, two parameters that have the same meaning - for example a_1 and a_2 - are varied with a unique value at the time meanwhile the other set of parameters are maintained constant. Because the parameter r_D was found for the two-aquifer system to create the greatest spreads of the type curves, a particular attention has been given to its influence on a three-aquifer system (Figures 12a, 12b and 12c). As already mentioned, the aquitard responses are not considered. Let us call aquifer 1, the lower aquifer which is being pumped and aquifer 2 and 3 the intermediate and upper aquifers, respectively. Similarly, aquitard 1 is the aquitard that directly overlies aquifer 1 and aquitard 2 overlies aquifer 2.

The Figures 12 illustrate the influence of the parameters r_{D_1} and r_{D_2}. On Figure 12a, both parameters take successively the values 0.01, 0.1 and 1 meanwhile the aquifer 1 is three times more transmissive than the other 2 aquifers ($a_1=a_2=3$) and the three aquifers have the same storativities ($c_1=c_2=1$). The storativities of the two aquitards are 100 times greater than the storativity of aquifer 1 ($b_1=b_2=10$). Dimensionless drawdowns in aquifer 1, s_{D_1}, show a decrease when the r_D's increase, which is normal because r_{D_1} and r_{D_2} are proportional to the

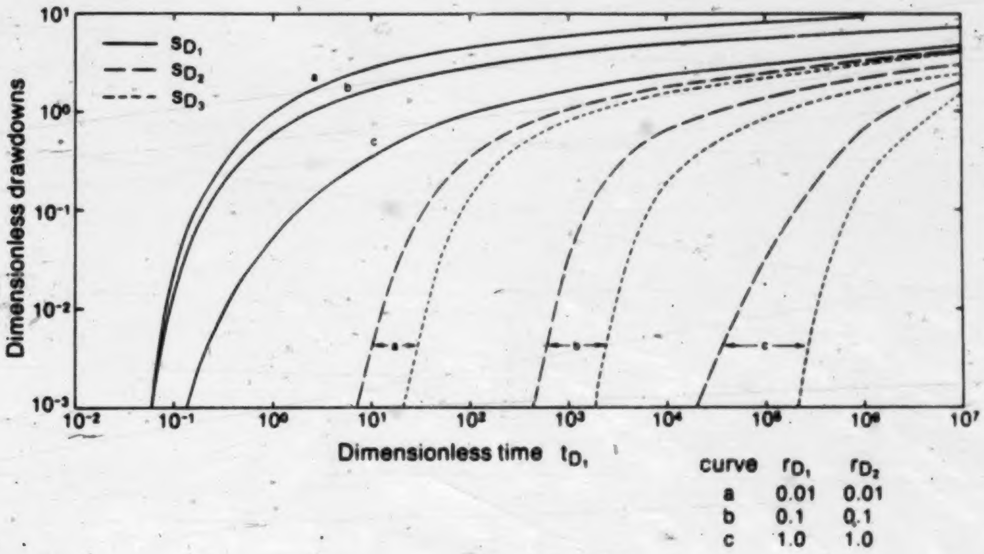

Figure 12a. Parametric analysis for the three-aquifer model: influence of $r_{D_1}=r_{D_2}$ when $a_1=a_2=3.0$, $b_1=b_2=10.0$ and $c_1=c_2=1.0$

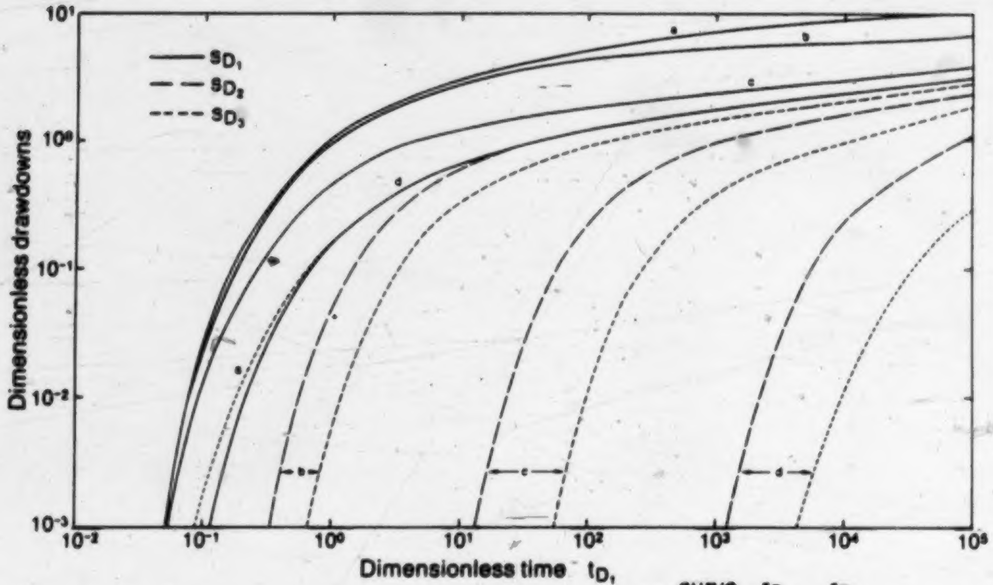

curve	r_{D_1}	r_{D_2}
a	0.01	0.01
b	0.1	0.1
c	1.0	1.0
d	10.0	10.0

Figure 12b. Parametric analysis for the three-aquifer model: influence of $r_{D_1}=r_{D_2}$ when $a_1=3.0$, $a_2=c_2=0.5$, $b_2=1.3$ and $b_1=c_1=1.5$

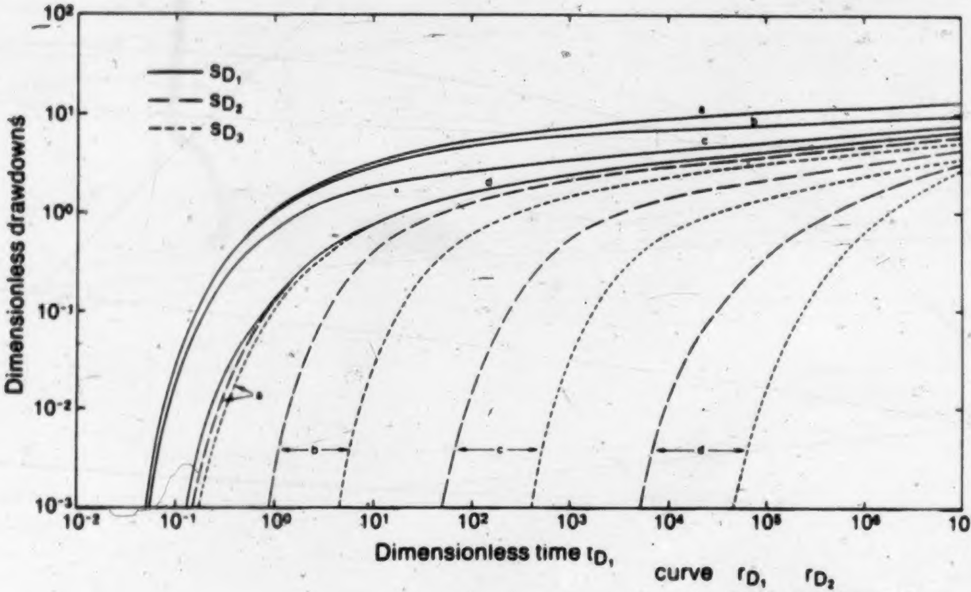

curve	r_{D_1}	r_{D_2}
a	0.005	0.003
b	0.05	0.03
c	0.5	0.3
d	5.0	3.0

Figure 12c. Parametric analysis for the three-aquifer model: influence of $r_{D_1}=r_{D_2}$ when $a_1=1.0$, $a_2=b_1=1.5$, $b_2=1.3$, $c_1=2.0$ and $c_2=1.5$

square root of T' and T'' respectively; the vertical spread is smaller at early times when the r_{D_s} vary from 0.01 to 0.1 than when they vary from 0.1 to 1; at late times, say after t_{D_1}=100, the vertical spreads are fairly constant between the three type curves. Greater and smaller vertical spreads are shown at early and late times, respectively, for the drawdowns in the aquifers 2 and 3; for early times, the greater the r_D's, the later will be the beginning of the responses in the unpumped aquifers; once these aquifers have been mobilized, they tend to exhibit a similar response at intermediate times (r_D=0.01) and at late times (r_D=0.1 and 1). All these features can be easily explained for the chosen set of parameters characterizing Figure 12a. The important aspect is that the three aquifers become "fully coupled" with parallel drawdown behaviours at late times.

On Figure 12b, we have reduced both the transmissivity (a_1=1 and a_2=0.5) and the storativity (c_1=1.5 and c_2=0.5) constrasts between the aquifers. Similarly, the contrast of aquitard storativities is lowered, but the same for both aquitards (b_1=b_2=1.5); as expected, the responses in the unpumped aquifers occur earlier and there is an earlier tendency for the late time curves to reach the "pseudo-steady" state regime with a parallel behaviour when the r_Ds increase. This feature, however, is not present in the pumped aquifer which exhibit at late time non-constant vertical spread when the r_Ds increase and relatively closer early time responses than in the case of Figure 12a. In other words, the shape of the drawdown curves varies more for the pumped aquifer than for the two other unpumped aquifers when r_D increases and the system has tighter and more different constrasts between the remaining parameters.

These features are even more emphasized on Figure 12c where the non-varied parameters have affected values between 1 and 2 as follows:

aquifers 2 and 3 have equal and 1.5 times smaller transmissivities, respectively, than aquifer 1, but they are twice and 1.5 times more storative. The aquitard storativities are such that $b_1=1.5$ and $b_2=1.3$ and the r_Ds are taking different values for each set of type curves.

It should be emphasized that because T' and T'' are usually much smaller than T_1, the cases r_{D_1} and r_{D_2} greater or equal to 1 have to correspond to thin aquitards (H' and H'' are small) in order to maintain reasonable values to the radial distance r. For example, if $T'=T''=10^{-4}T_1$ and $r_{D_1}=r_{D_2}=1$, we must have H'=H''=1m to keep r=100 m.

Figure 13 shows the influence of c_1 and c_2 in the four cases when these two parameters take simultaneously the values of 0.1, 1, 5 and 10 and the remaining constant parameters are all equal to 1. Three features are illustrated by this figure: (1) for a given aquifer, the type curves are practically confounded for all values of the coefficients c showing no sensitivity to the storativity ratios between aquifers for the drawdowns in each unit; (2) there is little vertical spread at late times for the drawdowns in the three aquifers; (3) there is a more important influence of the storativity ratios between the three aquifers on the time at which responses will start in the unpumped units (horizontal spread at early times).

Figure 14 illustrates a different early times behaviour for the unpumped aquifers and for the five cases when the storativity ratio of the aquitards with respect to S_1 are varied between 1 and 100. The same constant parameters as in Figure 13 are used. The main feature is that the early time type curves are all separated for each aquifer with a lag time between the responses of pumped and unpumped aquifers which is proportional to the values of the bs: the smaller b, the smaller the

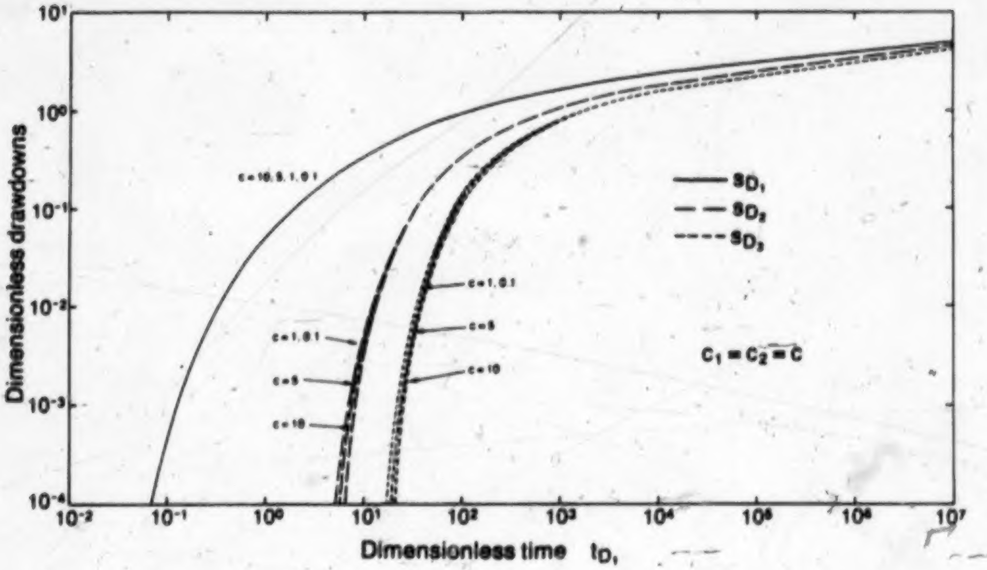

Figure 13. Parametric analysis for the three-aquifer model: influence of $c_1=c_2=c$ when $r_{D_1}=r_{D_2}=1.0$, $b_1=b_2=10.0$, $a_1=a_2=1.0$

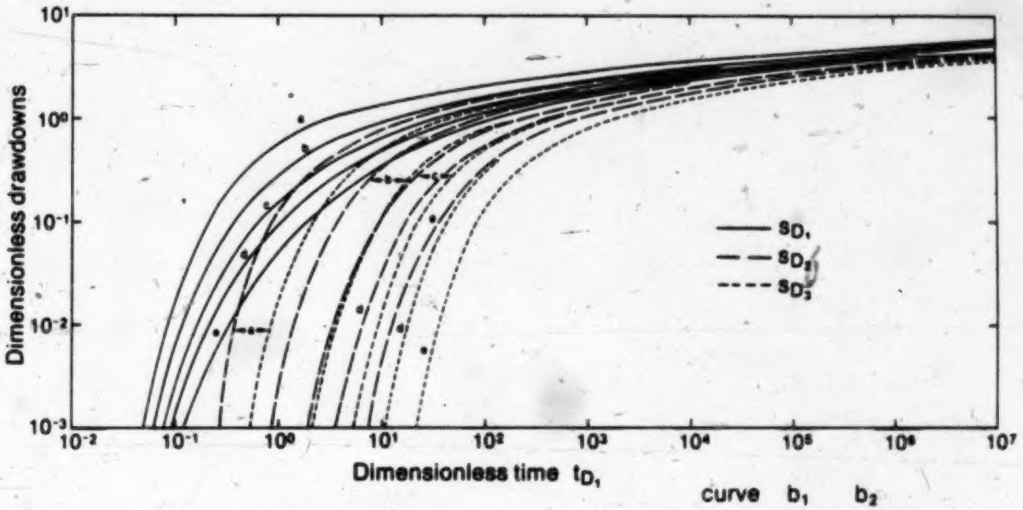

curve	b_1	b_2
a	1.0	1.0
b	3.0	3.0
c	5.0	5.0
d	7.0	7.0
e	10.0	10.0

Figure 14. Parametric analysis for the three-aquifer model: influence of $b_1=b_2$ when $a_1=a_2=1.0$, $r_{D_1}=r_{D_2}=1.0$ and $c_1=c_2=1.0$

early horizontal spread. The vertical "merging" of the curves at late times is similar to the one of Figure 13.

While performing the calculations to appreciate the influence of a_1 and a_2, that is of the ratio between the transmissivity of the pumped aquifer to the ones of the unpumped aquifers, we have experienced numerical instabilities of the code 3AQF at large values of dimensionless time and for a_1 and a_2 greater than 1. It appeared for the first time when we were trying to calculate the three dimensionless drawdowns at $a_1=a_2=5$ setting all the other parameters at a value of 1: abnormally high values of drawdown are obtained for t_{D_1} greater than 10,000. The code was first carefully checked for errors in the mathematical developments, without success.

The second thought was that the values given to the parameters b and r_D were not realistic: too low b and too high r_D meanwhile field situations may occur easily with a_1 and a_2 greater than 1.

Setting $b_1=b_2=10$ and $r_{D_1}=r_{D_2}=0.01$, it was found that still the entire domain of dimensionless times could not be satisfactorily calculated especially for s_{D_2} and s_{D_3} even when a_1 and a_2 are as low as 1.5. However, reasonable values for the drawdowns could be obtained at greater t_{D_1} than with the original set of values for the depending parameters. These trials gave the idea that the problem could be inherent to the intrinsic nature of the solutions. Specifically, when t_{D_1} is large, p' is inversely small. Using the first two terms only of the series expansions for the functions zcoth(z) and z/sinh(z) which are $1+z^2/3$ and $1-z^2/6$ (Abramovitz and Stegun, 1970, p. 85) respectively, where z has the form $b_i\sqrt{p'}/r_{Di}$ (i=1,2), we could not remove the numerical instabilities. The final attempt was to examine the complex values obtained for the three Laplace space solutions; they are just as reasonable as those obtained in the domain of numerical stability for dimensionless time. For the threshold value of dimensionless time where instable results are obtained for the drawdowns, it was observed that the number of iterations executed by the inverter code in applying the Durbin formula for the desired accuracy was sharply increased, denoting instability in the inverter itself and not in the calculation of the Laplace space solutions. Because there was little we could do at this stage of investigation (the inverter code is an IMSL subroutine) without going much beyond the scope of this work, it was decided to "live with the problem". The code 3AQF as written is, nevertheless, satisfactory for a very wide range of depending parameters (instability occurring only when a_1 and a_2 are greater than 1) and dimensionless times.

To assess a wide range influence of a_1 and a_2 greater than 1 on the dimensionless drawdowns, calculations were conducted for $r_{D_1}=r_{D_2}=0.01$ and $r_{D_1}=r_{D_2}=0.1$. In both cases, $b_1=b_2=20$ and $c_1=c_2=1$. The values for a_1 and a_2 were 0.05, 0.5, 1, 5, 10 and 50 in the first case and 0.5, 5 and 10 in the second case. With this set of depending parameters, it was found (1) that the drawdowns in the pumped aquifer are following a unique type curve for any pair of a_1 and a_2 and for both cases, and (2) that the drawdowns in the two unpumped aquifers are negligible at least up to $t_{D_1}=5000$ in the first case and up to $t_{D_1}=50$ in the second case. In the first case, the unique type curve for the pumped aquifer is almost coincident with the Theis type curve; in the second case where both r_{D_1} and r_{D_2} are tenfold, this curve is only shifted downward by a small amount. Although the chosen set of values is realistic, it probably represents a combination of flow parameters that one may qualify as "critical" to reflect the fact that the three-aquifer system may in these conditions respond as a more simple system (a simple confined aquifer in the first case).

Discussion and conclusions for the infinite leaky aquifer systems

A detailed analysis - mathematical and "behavioural" - has been conducted for the most complex analytical models derived for infinite leaky aquifer systems. Although based on the original work of Neuman and Witherspoon, mathematical developments have been extended to obtain dimensionless Laplace space solutions, simpler asymptotic and special case solutions by reasoning in the Laplace space and, most importantly, efficient computational codes for the evaluation of the solutions. In particular, the solutions for the three-aquifer system have been evaluated for the first time. This last result has far-reaching implications for aquifer (or interference) test analyses and so does the discussion on the behaviour of such systems which is based on a complete analysis of the sensitivity of the responses to the depending parameters.

One obvious direction of research (beyond this work) would be the coupling of our evaluation codes with least square fit (Saleem, 1970) or non-linear programming (Rosa and Horne, 1983) methods. The objective is to prepare an automatic procedure for analysing observation well responses of complex leaky systems.

In principle, there is no theoretical obstacle in developing an analytical model for the "four-aquifer" system: the pioneer work of Neuman and Witherspoon indicates the general method of derivation for the Laplace space solutions and the present work proposes efficient techniques for the evaluation of the solutions. However, such an effort is not worthwhile for two main reasons:

1. it is easy to deduce from our results that the real lag-time necessary to obtain a response in the third (upper aquifer) of the three-aquifer system is usually important and thus rarely compatible with the current economics of aquifer testing (even assuming that the cost of drilling and equipment of observation wells at three different levels is not prohibitive!); this situation would be even worse for a "four-aquifer" system;
2. such a system would depend on 12 reduced parameters, that is a very large number of possible combinations between their numerical values, rendering the use of such a model practically impossible in the interpretation of aquifer tests.

Our work clearly demonstrates three important points:

1. that the chances of observing steady-state regimes for the response of a multiple-aquifer system with impervious upper and lower boundaries are very limited in the pumped aquifers and virtually nil in the unpumped aquifers; this seriously questions the possible use of steady-state semi-analytical models for aquifer test analysis in such systems[7] (as proposed by Hemker, 1984);
2. that the aquitard storativity (parameters b in the two aquifer system and b_1 and b_2 for the three-aquifer system) has an important impact on the various drawdown responses and cannot be as such neglected. Again, this brings about reservations on the use of the unsteady semi-analytical model proposed by Hemker (1985) for aquifer test analysis of multiple-aquifer systems;

---

[7] This point is further evidenced in Sauveplane et al. (1986) where the analytical solutions for the two-aquifer system are compared favourably with the results of a finite-element simulator (FE3DGW) to predict the long-term impact of injection in a sedimentary block, evaluate the "strength" of aquitards for confinement and select the most suitable aquifer. This is an example of the predictive use of analytical models.

3. that the assumptions of zero drawdown in the unpumped aquifers is not generally valid even in the small time domain of aquifer testing and, therefore, the use of Hantush type curves should be discontinued, including those that account for aquitard storativity ("modified" theory).

It is beyond the scope of this work to propose a clearly defined and exemplified strategy for the design and interpretation of aquifer tests in infinite leaky systems. Moreover, data for observation well responses in aquitard and unpumped aquifers are rarely available even when such measurements are both technically and economically feasible. This arises from a short-sighted attitude of the practitioners who tend to prefer the repetition of an operation of different levels (drilling and testing) rather than obtaining the maximum information in a single operation. With that respect, one may deplore the poor use of the two-aquifer model in practice; this is, in part, due to inertia and traditions (the Hantush type curves are "popular") but also because of the difficulty generally sensed in evaluating specific type curves with this model. Hopefully, this contribution will help correct such misconceptions.

A natural method for analysing aquifer test results in two and three-aquifer systems is to utilize a step-by-step procedure based on successive approximations. Such a technique utilizes, at best, the asymptotic results of Appendix C for the time domain and the advantages of the codes TWOAQF and 3AQF for an efficient and accurate type-curve evaluation at each step of the procedure. To be more specific on the mechanics of this general approach, let us consider a three-aquifer system for which observation well responses are available for the five intervening units, the lower aquifer being pumped at a constant rate. It is assumed that modern techniques of water level measurement during aquifer tests have been used so that very early time responses could be measured. The main idea is to apply successively and as pumping time increases, the Theis model, the two-aquifer model and finally, the three-aquifer model with reasonable initial guesses of the flow parameters for each unit that are further refined by type curve matching on a limited number of type curves (computed in virtually no time with the numerical inverters). The initial guess and the restrictions on the type curves to consider are based on a single log-log scale plot of all the responses and on the results of the sensitivity analysis presented before. Ideally, the number of iterations will be reduced if the five responses are available at two different radial locations of the system and greater confidence in the final values of the 10 flow parameters to evaluate can be achieved (uniqueness of the solution of the inverse problem).

This method postulates a progressive vertical propagation of influence: at the very beginning of the test, the drawdowns in the pumper aquifer are mainly caused by the withdrawal of water released from storage in that unit; then a contribution of aquitard 1 will be followed by a reaction of aquifer 2 and so on until the third aquifer starts to contribute; however, until the second aquitard manifests a response, the system can be analysed with the two-aquifer model. Also, at the beginning of an aquitard response, the parameters r_D and z_D have no influence on the drawdowns: the aquitard behaves as if its thickness were infinite since no discernable pressure transient has reached the overlying unpumped aquifer. This approach uses, at best, the physics and the mathematics of the phenomena to progressively evaluate over discrete time domains the various flow parameters. The final "check" consists of matching the entire responses for each unit with the set of type curves obtained with the code 3AQF by the stepwise evaluation of the depending parameters.

This method can be tedious if conducted manually; it could be automatized (with a minimum of human intervention) through the development of an expert system that would use an automatic matching procedure, as already mentioned, and be controlled by visual displays. Because the key algorithms have now been developed, there is, in principle, no major obstacle in pursuing research in that direction. This, clearly, was not an objective of this work. An accurate characterization of the flow (natural or induced) through aquitards for multiple-aquifer systems is still a challenge in modern hydrogeology with a vast range of potential applications. The method proposed here is based on adequately conducted aquifer tests and on the use of analytical models for their interpretation; it has probably some future, if one wants to consider the very common occurrence of such systems in nature.

4.2 Uniformly Fractured and Confined Infinite Aquifer Systems

At an exploration level, hydrogeologists and petroleum geologists have access to a great variety of formation evaluation techniques: quantitative core analysis and outcrop studies, integrated analysis of a suite of geophysical well logs, in situ observations in wells with Bore

Hole Television Viewers (BHTV), thin section studies, anomalies detectable on seismic profiles etc. The conjunctive use of these methods is pertinent to characterise fractured aquifers (and hydrocarbon reservoirs). Natural fracturation can explain the existence of relatively good productivities in low permeability rocks, as confirmed by the production history of such formations. Knebel and Rodriguez-Eraso published in 1956 eloquent statistics: 41% of the 236 major oil fields that contained 82.5% of the world's reserves known at that date were developed in naturally fractured formations; this proportion has probably increased since.

Hydrogeologists working in "hard rock" environments (volcanic, metamorphic and granitic rocks) have evidenced the possibility of matching limited water-supply demands by wells intersecting fractures, especially in arid and semi-arid regions; extensive chalk aquifers are exploited in England and France; other examples can be found in Western Canada and in the United States (for example, coal and shale aquifers). Reservoir engineers are familiar with techniques of hydraulic fracturing that are applied to the development of tight reservoirs which are poorly or non-fractured in natural conditions.

In geotechnical engineering, groundwater flow in fractured rocks is of paramount importance for the stability of dams and for the construction of tunnels and mine galleries.

These facts explain why the description and characterization of flow in fractured formations have received much attention in the last two decades. Significant progress has been achieved around two main conceptual ideas:

1. neglecting the flow through the intergranular pores of the rock matrix, various authors - mostly with a geotechnical engineering background - have developed deterministic models whereby the flow through the fractures is simulated by a network of pipes or horizontal plates; individual fractures are characterized by their location, orientation, opening, roughness, friction coefficient, etc. and the flow in either laminar or turbulent depending on the Reynolds number. A network of fractures is the sum of these specific hydraulic behaviours and the resulting medium cannot be generally treated as a continuum; however, statistical techniques may be used to spatially average the nature of the fracturation when it is sufficiently dense and measured (Snow, 1968). Also, Louis (1969, 1975) defines a directional hydraulic conductivity for a system of fractures and uses the velocity potential to solve steady-state flow problems;
2. the other approach assumes continuity and statistically homogeneous rock and fluid properties. This "continualized" approach is based on the physical assumption that "the rock matrix 'feeds' its fluid into the highly permeable fractures" (Muskat, 1946). In more precise terms, the idea is that the matrix blocks, although separated by fractures, are in contact on surfaces which transmit the effective stress. Deformation of matrix blocks are followed by deformation of the fracture walls (i.e. change of the fracture width or fracture porosity); fracture deformations are obstructed (or supported) by the water pressure acting on its walls. Under an abrupt change of stress conditions - e.g. withdrawals or injections by wells - a part of the deformation takes place at the price of a

change of fracture porosity; the other (major) part is the result of compression - or expansion - of the matrix blocks. In principle, the liquid squeezed out of the blocks penetrates into the fractures and reverse; these transfers ("interporosity" flow) are simultaneous since the two systems are collocated. Assuming further that the fracture network is dense enough to introduce the concept of statistically average properties, the governing equations for flow in this dual porosity medium can be derived, as done in Appendix D. This derivation, although classical (Barenblatt et al., 1960; Romm, 1966) permits a precise definition of the flow parameters involved in the description of a dual porosity system; it is also shown that in the particular case when the block permeability can be neglected (purely fractured medium), the problems can, in principle, be treated with equivalent anisotropic homogeneous models. The "continualized" theory is at the same time realistic (the exact geometry of a fractured network is generally unknown) and "tractable" in terms of analytical solutions for transient flow problems common to hydrogeology and reservoir engineering; it is widely used with a reasonable degree of success in both disciplines. The remaining part of this chapter focuses on analytical models based on the dual porosity concept. The classical solutions for the equivalent anisotropic homogeneous models are not discussed here; the reader is referred to the works of Prats (1972) and Asfari and Witherspoon (1973) for the meaning of equivalent anisotropy in a regular pattern of fractures and to the transient solutions proposed by Papadopulos (1965), Hantush and Thomas (1966) and Saad (1967). When the producing well intersects a single vertical or horizontal fracture of finite extent in an otherwise anisotropic medium, Gringarten and Witherspoon (1972) have derived analytical solutions for radial flow to the fracture using source functions; these solutions are of particular interest when aquifer testing is used to evaluate the effects of hydraulic fracturing. The case of linear flow to a well intersecting a vertical fracture of finite length in an isotropic aquifer with linear flow to the fracture is considered by Sen (1986).

We have derived in Appendix D the system of governing equations for transient flow problems in dual porosity systems (Equation D4). To obtain line-source solutions of practical use in aquifer test analysis it is further required a mathematical description of the interporosity flow that generally depends upon the geometry of the fractured network.

4.2.1 Geometry and Flow Parameters in Dual Porosity Systems

The permeability and porosity of the fractures k_1 and $\bar{n}_1$ defined in Appendix D are related to their mean block size ℓ of the matrix and to the mean aperture w of the fracture. Both geometrical factors are not well defined by direct observation, but can be evaluated indirectly for different geometric schemes encountered in practice from the values of k_1 and $\bar{n}_1$ determined by aquifer testing. Another advantage of considering such relationships is to give a possible control on the validity of the analytical model used for interpretation, given that ℓ is generally comprised between 1 cm abd 100 m and w between 1 μ and

1 cm. The following relationships are valid for idealized block shapes such as the ones used in the analytical models.

Consider a parallelepipedic block (ℓ_1, ℓ_2, ℓ_3) surrounded on all its faces by a fracture system of average width w/2. By definition of $\bar{n}_1$ (see Appendix D1), we have:

$$\overline{n_1} = \frac{(\ell_1+1)\ (\ell_2+w)\ (\ell_3+w)-\ell_1\ell_2\ell_3}{(\ell_1+w)(\ell_2+w)(\ell_3+w)} \approx w\left(\frac{1}{\ell_1} + \frac{1}{\ell_2} + \frac{1}{\ell_3}\right) \qquad (41)$$

since w is much smaller than ℓ_1, ℓ_2 or ℓ_3.

Similarly, consider laminar flow in a planar fracture of width w over and underlain by a block of side (ℓ_1,ℓ_2). Assuming that the flow is parallel to the fracture planes, Poiseuille's equation gives:

$$q_1 = \frac{w^3\ell_1}{12\mu}\,\rho g\,\frac{\Delta h}{\ell_2}$$

where q_1 is the flow rate and Δh the hydraulic head drop. For n successive fractures across a section A:

$$q_n = nq_1$$

Darcy's law states that:

$$q = \frac{Ak_1\rho g}{\mu}\,\frac{\Delta h}{\ell_2}$$

The similitude $q \equiv q_n$, implies:

$$k_1 \equiv \frac{n}{A}\,\frac{w^3\ell_1}{12}$$

Defining f as the total fracture length per unit cross-section, we have:

$$f = \frac{n\ell_1}{A} \quad [L^{-1}]$$

and the general relationship:

$$k_1 = f\,\frac{w^3}{12} \qquad (42)$$

Equations 41 and 42 can now be applied to the idealized configurations used for studying transient flow towards wells in dual porosity aquifer systems. The aquifer is confined and uniformly fractured over a large lateral volume around the well; this volume is assumed to be infinite at the scale of the flow problem.

- for horizontal slabs of matrix separated by regularly spaced and parallel fracture planes: the matrix size ℓ is the thickness of the slabs. Letting ℓ_2 and ℓ_3 become infinite in equation 41 and since $f=1/\ell (n=1)$, we have:

  $$\left.\begin{aligned} \overline{n_1} &= w/\ell \\ k_1 &= w^3/12\ell \end{aligned}\right| \qquad (43)$$

  which represent the two equations necessary to evaluate the average dimensions of the network, if $\bar{n}_1$ and k_1 are known from aquifer test analysis;

- for a series of regularly spaced match sticks generated by two orthogonal sets of vertical fractures (n=2) in which the flow is essentially horizontal (perpendicular to the axis of the match sticks):

  $$\left.\begin{aligned} \overline{n_1} &= 2w/D \\ k_1 &= (1/12)(w^3/D) \end{aligned}\right| \qquad (44)$$

where D is the size of a match stick; note that this configuration can be approximated by vertical cylinders of radius D/2.

- for a set of equal cubes obtained with three sets of regularly spaced and orthogonal fractures with flow parallel to a fracture plane

$$\left.\begin{aligned} \overline{n_1} &= 3w/d \\ k_1 &= (1/6)(w^3/d) \end{aligned}\right| \qquad (45)$$

where d is the size of the cubes; note that this configuration can be approximated by spheres of radius d/2.

4.2.2 The dual porosity line source solutions

The governing equations are presented in part 3.1 of Appendix D together with the meaning of the basic parameters. In dual porosity systems, we have $K_1 >> K_2$ by several orders of magnitude. Despite a fracture compressibility higher than the one of the matrix blocks (about one order of magnitude), $S_{s_2} > S_{s_1}$ because of the low volume occupied by the fractures δ_1 is small compared to δ_2 and also n_1 is smaller than n_2, yielding $\overline{n_1} < \overline{n_2}$. Therefore, for the diffusivities, $\alpha_1 >> \alpha_2$. Also, the ratio $b = S_{s_2}/S_{s_1}$ is usually greater than unity, meanwhile the dimensionless radius r_D is smaller than unity.

4.2.2.1. The "pioneer work" in the Soviet Union

The system of partial differential equations D3 was first solved by Barenblatt et al. (1960). In part 3.2 of Appendix D, we present a method of solution based on the authors' assumptions; their original work has not been translated into English (at least to our knowledge) and has created some controversies. It is not sure that our method is exactly the same as the original one, but we obtain the correct answer for the fracture drawdown (see Gringarten, 1982); the block drawdown solution is at the centre of the controversy, but its Laplace space expression could not be found for control in the North American literature.

Barenblatt et al. (op.cit.) neglect the term $[S_{s_1}(\partial s_1/\partial t)]$ in front of the interporosity flow source term in provenance of the blocks; this practically confers the fractures a transmissive role only; the second assumption consists of neglecting the term $(-K_2\Delta s_2)$ which practically implies "pseudo-steady-state" interporosity flow.

With these assumptions, we obtain the dimensionless Laplace solutions for the drawdowns in the fractures and in the blocks. The type curves are straight lines on a log-log scale for both drawdowns (see Figures 15a and 15b), except at late times where they are asymptotic to the Theis solution. The type curves are calculated by numerical inversion of the Laplace space solutions using the Stehfest algorithm. On both figures, at intermediate times, the fracture type curves tend towards a Theis type curve when r_D is large (greater or equal to unity): this equivalent homogeneous behaviour can be explained by the fact that when r_D is large, K_1 is small and, therefore, the

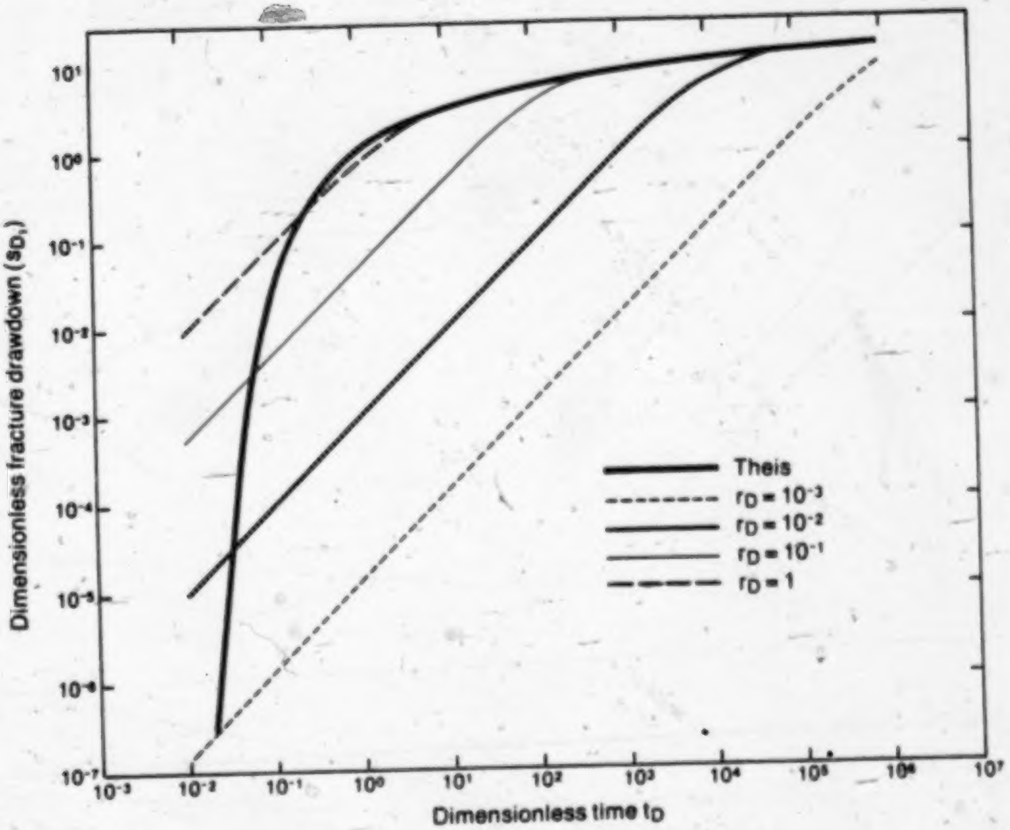

Figure 15a. Fracture drawdown type curves for the Barenblatt et al. model of a dual porosity and confined aquifer system. The dimensionless radius varies between 10^{-3} and 1

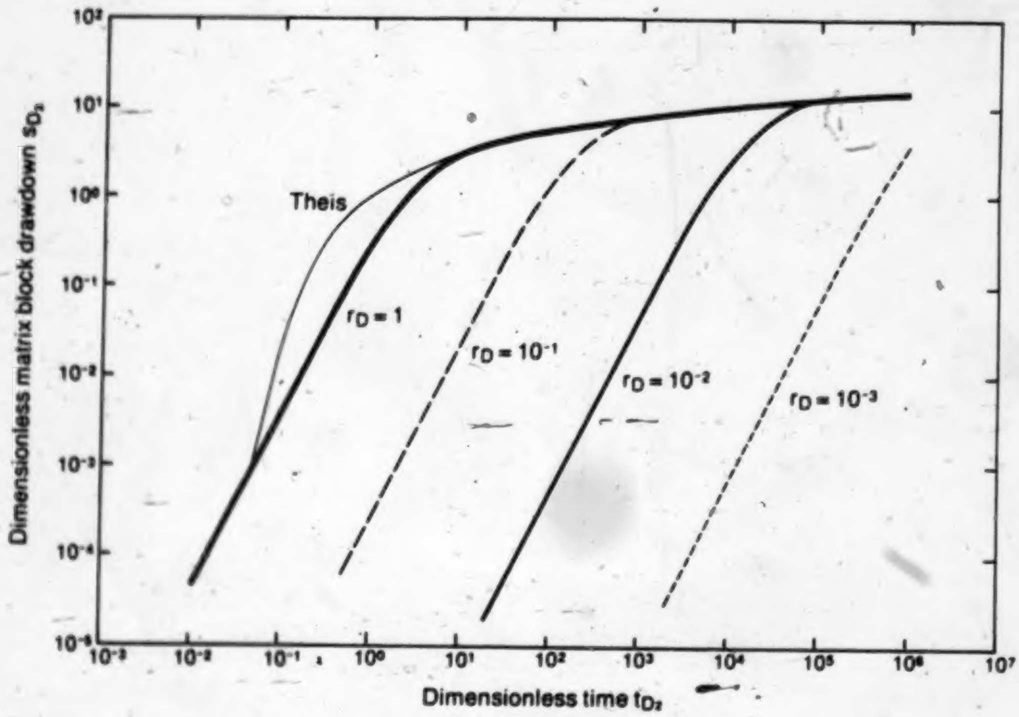

Figure 15b. Matrix block drawdown type curves for the Barenblatt et al. model of a dual porosity and confined aquifer system. The dimensionless radius varies between 10^{-3} and 1

fracture system does not play a significant role. The same is of course true for the block drawdown - at high values of r_D, K_2 is large and the aquifer responds as a homogeneous one with the dominant K_2.

Because the type curves are parallel to each other on a log-log scale and for a usually important range of dimensionless times, it is not recommended to use them for matching observation well responses. Semi-log plots of the type curves ~~do not~~ present this inconvenience; however, with semi-log plots of type curves the practical range for the dimensionless drawdowns becomes limited to values greater than unity and the early time match of the field data is imprecise. This is a lesser inconvenience because early time behaviour is atypical for any value of r_D.

The derived solution for the block drawdown (see equation D13 of Appendix D) is not interchangeable with the one for fracture drawdown; this is clear when comparing the two expressoins for $\overline{s_{D_1}}$ and $\overline{s_{D_2}}$; it is also illustrated on the Figures 15a and 15b: for r_D=0.1 and a common t_D=1, we have s_{D_1}=0.06 and s_{D_2}=0.003. A debate occurred in the Russian literature about what was the correct solution for each drawdown; the original result for the fracture drawdown was later qualified of solution for the matrix drawdown. This was apparently clarified in Romm (1966), but the same confusion perpetuated in the English literature (Streltsova, 1976 and Streltsova-Adams, 1978). Gringarten (1982) tries to explain this confusion by stating that the same PDE (our equation D6) is solved with two different inner boundary consitions and, therefore, should produce two drawdown solutions that are interchangeable. We showed that this is not the case and there is only one inner boundary condition (our D10) for s_1, simply because the well is not assumed to produce directly from the blocks; s_2 is simply deduced from the well-posed problem for s_1. In Streltsova-Adams (op.cit.), the interporosity flow parameter "α" has no dimension in her equation 2, has a dimension [1/LT] in equations 3 and 4 and further a dimension [1/T] in equation 14, without any apparent justification for the differences. In Appendix D, we have defined a "block shape factor" m of dimension $[L^{-2}]$ that is the same as the unambiguous parameter α in Warren and Root (1963).

In principle, a satisfactory match of observed data with the Barenblatt et al., type curves provides the fracture conductivity K_1 (ordinate of matching points), the matrix block specific storage S_{s_2} (abscissa of matching point) and the product (mK_2) of the matrix block from the value of r_D of the matched type curve. With two observation well responses, then both m and K_2 can be theoretically evaluated. We have already recommended to work with semi-log scales, but another possible technique is to use the type curves of ds_D/dt_D that can be evaluated from D13 by numerically inverting $p'\overline{s_{D_i}}$ (i=1,2) (see the B3 property of Laplace transforms in Appendix B), then the derivative $\partial s/\partial t$ of the observation well response is approximated by $\Delta s/\Delta t$ and plotted at the same scale to provide possibly a more accurate determination of the parameters than the classical matching procedure with the s_D type curves.

Three practical limitations of the Barenblatt et al. model are directly related to the nature of the assumptions:

1. an unclear relationship to the geometry of the fracture network: the model is virtually applicable to any fracture pattern;
2. the fracture specific storage is practically neglected;
3. the interporosity flow between blocks and fractures is pseudo-steady-state.

Historically, it has the merit of being the first analytical model for dual porosity fractured aquifers; however, unlike its pendant for the homogeneous systems, the Theis solution, it has not received a great deal of consideration in the western world, probably because, only three years later, Warren and Root (op.cit.) published in English, a solution that is less suffering of the limitations 1 and 2 identified above. This work acknowledged a great popularity until the mid 1970s when de Swaan (1976) published an article that has taken care of the limitation 3. However, the Warren and Root solutions are still commonly used.

4.2.2.2 Selected line-source solutions for dual porosity systems

The fine work of de Swaan (1976) represented a major step in the solution of the governing equations for dual porosity systems. However, like his colleagues, Warren and Root, he gave only late time asymptotic solutions for fracture drawdown. Variations on the de Swaan "theme" have been presented by various authors - sometimes presented as "new" solutions - with different parameters; they are all reducing to de Swaan's solutions after careful inspection. To date, there are only five useful analytical models for dual porosity systems:

- the Warren and Root solutions for pseudo-steady-state interporosity flow and adjustable geometry of the fracture network;
- the de Swaan solutions for transient interporosity flow with one (infinite horizontal slabs) and three (blocks idealized as spheres or cubes) - dimensional fracture networks;

- the Kucuk and Sawyer (1980) solutions for transient interporosity flow and two-dimensional (blocks idealized as cylinders or match-sticks) fracture network;
- the Moench (1984) solutions for transient interporosity flow with fracture skin applied to slab-shaped and sphere-shaped blocks; flow across the skin is assumed to be pseudo-steady-state.

As also suggested by Moench (1984), all these solutions can be written in a unified and convenient form in the Laplace dimensionless space:

$$\left.\begin{aligned} \overline{s_{D_1}} &= 2K_0\left\{[p'+u(p')]^{1/2}\right\} \\ \overline{s_{D_2}} &= v(p')\overline{s_{D_1}} \end{aligned}\right\} \qquad (46)$$

where u(p') and v(p') are different functions derived with our notations in section 3 of Appendix D. The depending parameters are $b=S_{s_2}/S_{s_1}$ and $r_D=r/\ell(K_2/K_1)^{1/2}$ where ℓ is the characteristic length for matrix blocks.

In the Moench's solutions, the fracture skin is treated in the same way as the skin around a well-bore: flow through the skin is assumed to be pseudo-steady-state and the skin has a negligible specific storage. It is clear that if the transient flow through a storative skin was to be considered, we would deal with "triple-porosity" systems and three constitutive partial differential equations; such systems are probably of interest in certain types of carbonate aquifers where three overlapping porosities can be identified. The mathematical difficulty to find analytical solutions for such flow problems explains probably why they have not yet been published. However, the same principles presented in this chapter and in Appendix D could be applied in the derivation of solutions for "triple-porosity" systems.

Based on equation 46 and the respective functions u(p') and v(p'), two computer codes have been written to compare the relative merits of the various models when r_D, b and the fracture skin dimensionless parameter f_{s_D} have each a given value. These codes DUPCOMP(F or M) where F and M stand for fracture and matrix block dimensionless drawdowns, respectively, are written in arithmetic double precision and FORTRAN language. In addition, specific codes have been written for each individual model.

Consideration of the significance of N in equation D17 for the pseudo-steady-state solutions implies that in practice it is only meaningful to compare these solutions on a one by one basis with the corresponding transient solutions for which the block geometry is identical. The comparisons are illustrated, for a common and typical set: r_D=0.1 and b=100, 1000, on Figures 16a (assuming horizontal slabs (N=12) and no fracture skin), Figure 16b (assuming cylindrical blocks (N=32) and no fracture skin), Figure 16c (assuming spherical blocks (N=60) and no fracture skin) and on Figure 16d (assuming spherical blocks and $f_{s_D}=10^{-2}$). This value for f_{s_D} corresponds for example to a skin thickness of 0.1 mm, a block size of 1 m and a ratio K_2/K' of 100 where K' is the skin conductivity, all of which are realistic values. The four plots of Figure 16 correspond to s_{D_1}, the dimensionless fracture drawdown. The same numerical values and assumptions are used to generate the four plots of Figure 17 for dimensionless drawdown s_{D_2} in the blocks. These figures will be discussed later.

4.2.3 Discussion concerning the dual porosity systems

To conduct detailed sensitivity analyses to b, r_D and f_{s_D} for the five considered models would be a task beyond the scope of the present work; however, it should be mentioned that such an effort, although tedious, is perfectly feasible with the formulations of equation 46 and the use of numerical inverters. We have, in fact, conducted a few calculations of s_{D_1} and s_{D_2} varying b, r_D and f_{s_D} one at a time. These calculations are not reported here, but lead to the conclusion that a thorough sensitivity analysis is not necessary because:

1. the shape of the type curves for both drawdowns in the transient interporosity flow case with no fracture skin are not significantly different from each other over the entire time domain; the study of one of the three models for $f_{s_D}=0$ gives a good enough idea of the behaviour of the two others. When f_{s_D} is not zero and greater than 0.1, there is little difference between the transient cases for slabs and spheres and the corresponding pseudo-steady-state case with $f_{s_D}=0$ (Moench, 1984). When f_{s_D} is less than 0.1, the behaviours are similar to the transient cases with $f_{s_D}=0$.
2. we demonstrate in Appendix D the identity of the type curves for fracture drawdown in the case of pseudo-steady-state interporosity flow to the ones of an unconfined aquifer with delayed yield; these type curves are classical and characterized by the following features:

   - an early response following a Theis solution as if b=0 (medium 1 or fracture reacts independently of medium 2, or blocks as if $S_{s_2}=0$),

- a transition period with a horizontal pseudo stabilization and an inflexion point; the width of the transition period is proportional to b,
- a late response that follows a shifted Theis solution [by (1+b)].

The proofs of both early and late behaviours are given in Appendix D.

3. we also demonstrate in Appendix D the exact identity of the type curves for fracture drawdown in slab-shaped blocks and transient interporosity flow with the type curves of an aquitard-aquifer system with no source bed above the aquitard. We also show that the early time response is asymptotic to a function H, different from the Theis solution, meanwhile the late time behaviour is the same as for the pseudo-steady-state case. During the "transition" period, these type curves do not exhibit a clear pseudo-stabilization and inflexion point.

For these three series of reasons, we choose to focus the discussion on two important questions of practical interest. The first question is whether or not the Warren and Root model - although not satisfactory theoretically: there is no sound base to assume a pseudo-steady-state interporosity flow - gives in practice good enough results when compared to those of the more realistic transient cases; a subsidiary to this first question is the presence or absence of two parallel straight lines at early and at late times for semi-log plots of dual porosity responses. The second question is concerned with the accessibility of information for the fracture network geometry on the sole basis of aquifer test analysis, given that in most instances, this general geometry is unknown when a test is conducted. This problem is related to the use of transient solutions that can incorporate the fracture network geometry; a subsidiary to the second question will be: with little or no geological information, is it possible to differentiate leaky systems from dual porosity fractured systems on the basis of response to pumping (or injection) only?

4.2.3.1 Validity of the pseudo-steady-state assumption for interporosity flow

Let us first consider the subsidiary to the first question:

- Semi-log analysis of aquifer tests with the Warren and Root model

By semi-log analysis, we understand the Jacob (or Horner) analysis that do not require type-curve matching. It is thus different from type curve matching on semi-log coordinates. The foundations of both Jacob and Horner methods are based on the following asymptotic behaviour of the exponential integral function:

$$\text{for } t_{D_1} > 25,\ E_1(1/4t_{D_1}) \approx \ln[4t_{D_1}/\exp\gamma) \qquad (47)$$

where $\exp\gamma = 1.781 \ldots$ and γ is the Euler constant.

When this approximation is valid, a plot of s_{D_1} versus $\log(t_{D_1})$ (or of s_1 versus log t) for both early and late fracture drawdowns and for systems following the assumptions of the Warren and Root model should be as straight lines; moreover, these straight lines should be parallel and translated by the quantity (1+b) as shown in Appendix D, section 3.1.

In reservoir engineering, a debate about the occurrence of both straight lines was started by Odeh (1965) who, on the basis of well test responses, argued that the first straight line was generally occulted by well bore effects. Odeh gave an example of a test where the specific behaviour of a dual porosity system was not different from that of a homogeneous system (presence of the late time straight line only) suggesting that for tests of sufficient duration, it was not really possible to use the specific dual porosity model of Warren and Root. A similar argument is often used by hydrogeologists to justify their use of the Theis solution for interpretation of aquifer tests in complex aquifer systems. Besides the fact that the use of specific line-source solutions can provide important and often unique information about the aquifer, a counter argument is clearly: how long should a test be to provide a clear definition of a late time homogeneous behaviour? Also, with the Warren and Root assumptions, a semi-log plot of the transition period provides equally a straight line: therefore, how sure can one be that the test data are reflecting the late equivalent homogeneous response? if it is not the case, the results of the interpretation will be obviously erroneous (the slopes of transition period and late time behaviour are roughly in the ratio 1 to 2). In general, "forcing" a semi-log interpretation on test data for fractured aquifers even when the reductive assumptions of pseudo-steady-state interporosity flow can be justified is a risky operation that should be definitely discouraged: one does not usually know what is being measured and interpreted. Let us examine this issue more carefully. Returning to equation 47 and considering observation well responses (well bore effects negligible) for aquifers that can be analysed with the Warren and Root model, we can easily argue that the early semi-log straight line may not be present for fracture drawdowns. The argument goes as follows. At early times, when p' is large, equation D17 (Warren and Root model) suggests that $u(p') \sim N r_D^2$ and $p' + u(p') \sim p'$ which leads to the Theis solution in the real space. Let us consider, for example, the slab-shaped block case: N=12, to be valid the first approximation implies that $r_D^2/bp' < 10^{-2}(1/N) = 8.3 \times 10^{-4}$ of the order of $t_{D_1} < 8.3 \times 10^{-4}(b/r_D^2)$; the second approximation for the argument of the Bessel function is more restrictive since it implies $t_{D_1} < 8.33 \times 10^{-4}/r_D^2$ (b is usually greater than 10). This last condition on t_{D_1} gives the time domain for which the early time behaviour is asymptotic to a Theis curve in most practical situations. The agreement with the time condition of 47 $t_{D_1} > 25$ is only obtained for $r_D < 5 \times 10^{-3}$, that is, only for low to very low values of r_D (the usual range of r_D is 10^{-3}-10^{-1}). This situation is even worse when N=32 (cylinder-shaped blocks) and N=60 (sphere-shaped blocks). Therefore, the obtention of early-time semi-log straight-line is the rare exception for aquifer test (where one cannot invoke the presence of perturbing well bore effects). In that sense, Odeh's argument for early time is considerably strengthened. This demonstration is also valid for early time response of block drawdown, that is for s_{D_2} since the asymptote is obtained with the same conditions on t_{D_1}.

Consider now, the late time asymptotic behaviour. Equation D17 suggests that when p' is small, $u(p')=v(p')$ bp' from which both drawdowns can be approximated by the shifted Theis solution (i.e. a shifted semi-log straight line). This implies that for both s_{D_1} and s_{D_2}:

$p'/Nr_D^2 < 10^{-2}/b$ of the order of $t_{D_1} > 100b/Nr_D^2$

Compatibility with the condition t_{D_1} in equation 47 written for the shifted Theis solution by (1+b) indicates that a late semi-log straight line will be obtained when the following conditions for t_{D_1} are simultaneously verified:

$t_{D_1} > 100b/Nr_D^2$ and $t_{D_1} > 25(1+b)$

The first condition means that for given b and r_D the lower N, the greater will be the condition for t_{D_1} and the slab-shaped configuration is again a "worst case" scenario for the minimum value of t_{D_1} at which a late semi-log straight line will be observed. Let then N be equal to 12. Because in most instances r_D will be less than 1 and b greater than 10, we may write b=1+b and separate the conditions on t_{D_1} as follows:

$$\left.\begin{array}{l} \text{if } r_D > I/\sqrt{3} \text{ the condition is } t_{D_1} > 25(1+b) \\ \text{if } r_D < 1/\sqrt{3} \text{ the condition is } t_{D_1} > 100b/Nr_D^2 \end{array}\right| \quad (48)$$

No doubt that the second case will be the most frequent with test data. With the numerical values of Appendix D: $r_D=0.1$, $b=100$, the condition on t_{D_1} for slab-shaped blocks is:

$t_{D_1} > 8.3\times10^4$

If, moreover, $r=10$ m, $K_1=0.1$ m/s and $S_{s_1}=5\times10^{-5}$ m^{-1}, a minimum duration of aquifer testing of 1.2 hours would be required to fulfill this worst case scenario; if $K=0.01$ m/s, this minimum time is only 12 hours. In conclusion, the likelihood of observing a semi-log straight line is greater at late times than at early times, although nothing is warranted especially at low values of r_D: if $r_D=0.001$, the minimum testing time becomes 500 days! for $K_1=0.1$ m/s.

Consequences of the rare occurrence of early time straight-line disqualifies the semi-log interpretation method to determine a first value of b (both lines have to be present and their vertical displacement Δs yields $b=10^{-\Delta s/m}$ where m is the common slope of the lines). Late time semi-log interpretation alone will provide (1+b) and K_1 but no individual values for K_2, S_{s_2} and S_{s_1}. An error on the determination of K_1 occurs if a straight line is "forced" through the transition period rather than through the late time behaviour of the observation well response when this last portion of the response is missing.

Theoretical analogy suggests that the assumption of pseudo-steady-state interporosity flow between blocks and fractures has the same physical meaning than when this assumption is applied to flow through an aquitard separating a pumped and an unpumped aquifer. We have amply discussed this aspect while studying the two-aquifer system and concluded after sensitivity analysis that the storative function of aquitards ought to be considered in the great majority of cases. A priori, thus, only transient interporosity flow models should be used for analysing dual porosity aquifer systems. To check the degree of approximation introduced by the pseudo-steady-state assumption and. therefore, the validity of the (widely used) Warren and Root model, we examine the plots of Figures 16 (a, b, c, d) for fracture drawdown and of Figures 17 (a, b, c, d) for block drawdown. On these two series of log-log plots, we compare for common matrix block geometries the type curves assuming pseudo-steady (referred to as WRM) to those of the transient interporosity flow models (referred to as TIFM). All these plots are produced for $r_D=0.1$ and b=100 and b=1000. Two values of b have been chosen because we are particularly interested by the impact of S_{s_2}. The numerical values given for t_{D_1} in the following are of course specific to these examples.

- Comparison of fracture drawdowns

In the case of slabs (N=12 and Figure 16a), the WRM transition periods are characterized by a "flat S" shape that is not apparent on TIFM curves. This difference is general for any TIFM geometry. Also, the WRM curves for b=100 and b=1000 are confunded up to $t_{D_1}=100$ and then get separated, the curve b=1000 remaining flat (pseudo-stabilization) for a longer period (and located below) the curve b=100.

In the absence of pseudo-stabilization of the drawdowns with the TIFM curves, more drawdown is predicted at early time by the WRM curve up to the crossing point (up to $t_{D_1}=50$ for b=100 and up to

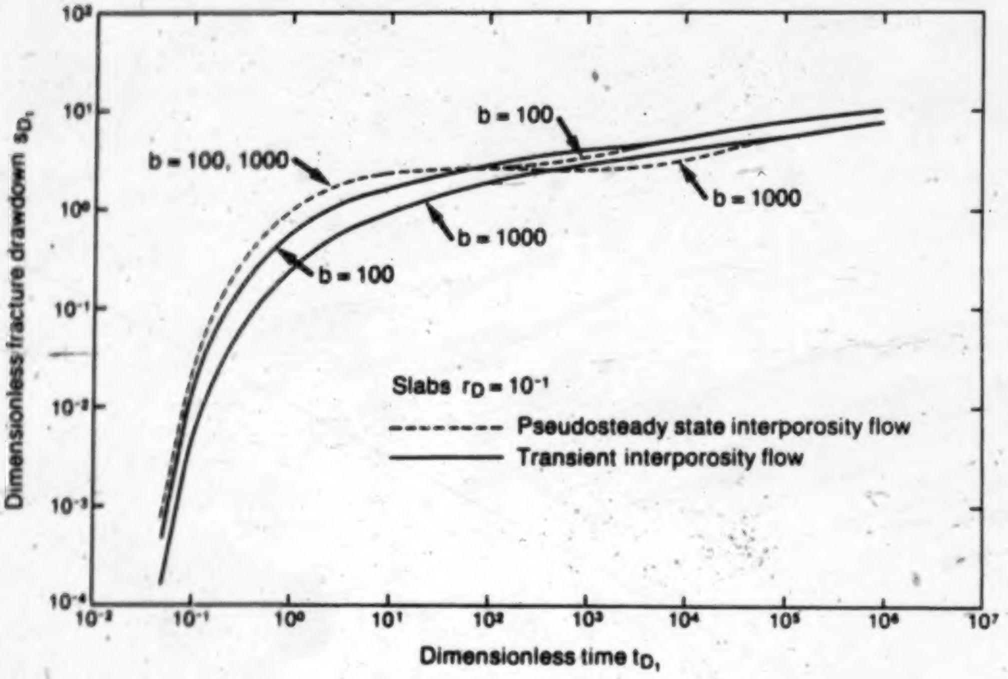

Figure 16a. Comparison of type curves for fracture drawdown when the interporosity flow is assumed to be pseudo-steady-state and unsteady for the "slab" configuration of the fracture network and for b=100 and 1000. The dimensionless radius is 0.1

r_{D_1}=500 for b=1000). Beyond these times, the reverse is true because the TIFM curves do not follow a "transition" period. Finally at t_{D_1}=10,000 (b=100) and at t_{D_1}=50,000 (b=1000), the WRM and TIFM merge into one shifted Theis solution: only then are the models really equivalent.

In the absence of fracture skin, figures 16b (N=32) and 16c (N=60) show the same features but the early time (up to the "crossing" point for a given b) difference between WRM curves and TIFM curves will be slightly more pronounced: for example at t_{D_1}=1 and b=1000, there is about one order of magnitude difference between the WRM and TIFM curves. The abscissa of the crossing point is slightly shifted to the left: for example, when b=100, it is at t_{D1}=25 for cylinders and at t_{D_1}=20 for spheres.

Figure 16d illustrates the case of spheres with fracture skin for the TIFM curves; a low value fs_D=0.01 for the fracture skin has been chosen intentionally to show a "minimum" trend: up to t_{D_1}=0.2, the WRM and TIFM curves are, this time, practically confunded and the degree of separation up to the "crossing" point is reduced when compared to the preceeding cases. Also for b=100, the "transition" period for the TIFM curve shows a practically constant slope up to the "merging" point; but, for b=1000, a slight inflexion of the TIFM occurs; this inflexion, unlike the corresponding WRM curve, is not horizontal. Beyond the "crossing" point that occurs earlier than on Figure 16c (skin=0) the difference between WRM and TIFM curves is practically the same as on Figure 16c and the "merging" point is at the values for t_{D_1} as in the case where the skin is zero.

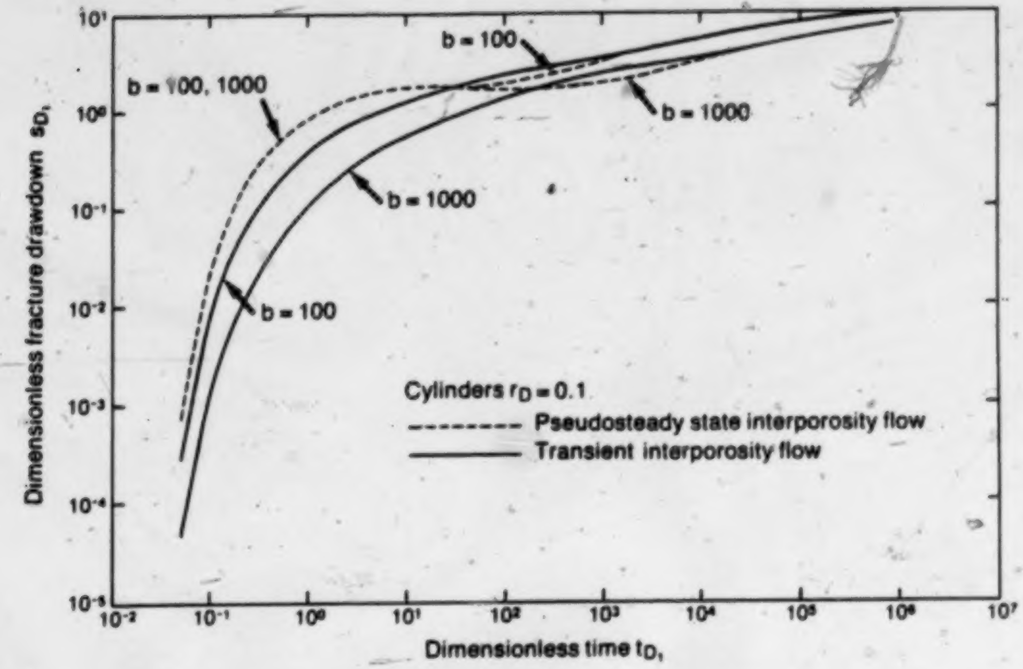

Figure 16b. Comparison of type curves for fracture drawdown when the interporosity flow is assumed to be pseudo-steady-state and unsteady for the "cylinder" configuration of the fracture network and for b=100 and 1000. The dimensionless radius is 0.1

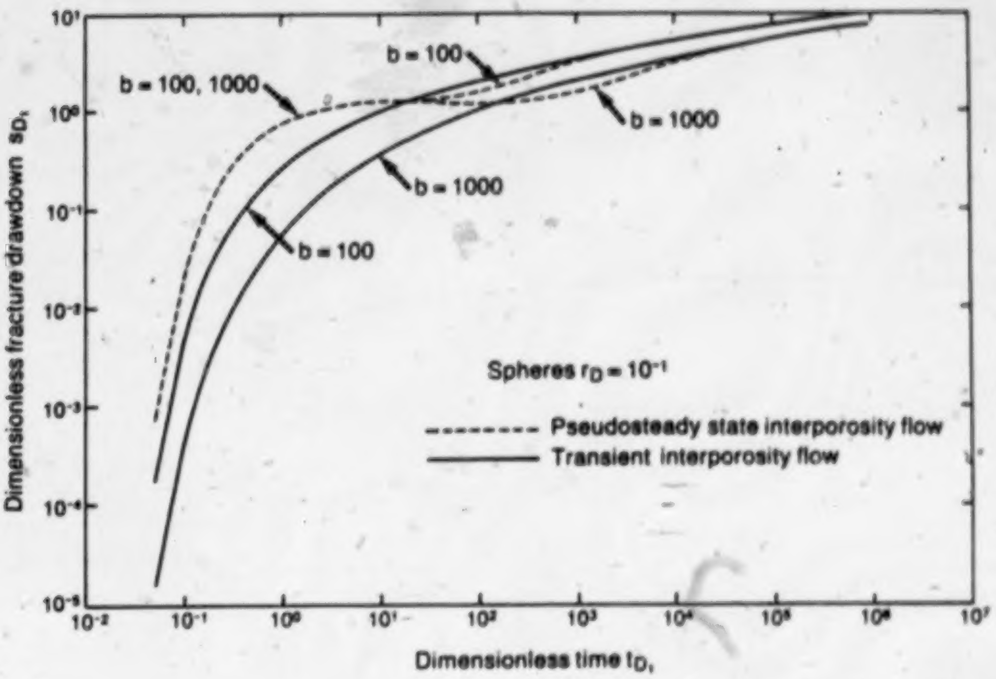

Figure 16c. Comparison of type curves for fracture drawdown when the interporosity flow is assumed to be pseudo-steady-state and unsteady for the "sphere" configuration of the fracture network and for b=100 and 1000. The dimensionless radius is 0.1

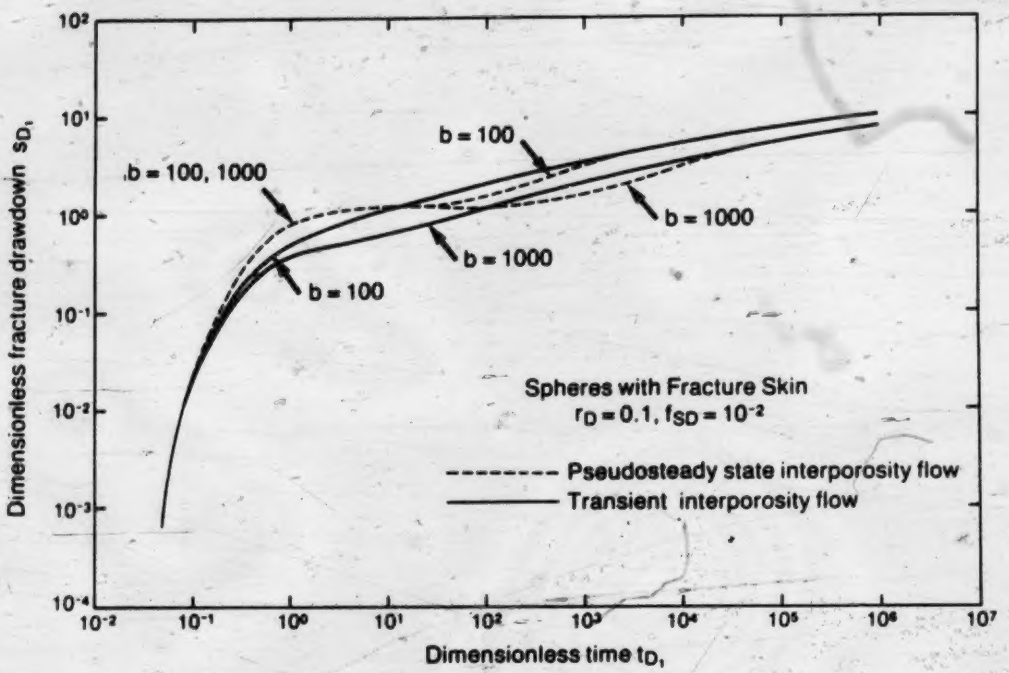

Figure 16d. Comparison of type curves for fracture drawdown when the interporosity flow is assumed to be pseudo-steady-state and unsteady for the "sphere" configuration, a dimensionless fracture skin of 0.01 and for b=100 and 1000. The dimensionless radius is 0.1

In summary, the four figures 16 which have been prepared for strictly comparable conditions of fracture drawdown are instructive of the three following points of practical interest:

1. WRM overestimates drawdowns at early times up to the "crossing"[8] point; during this period, the greatest error can be expected from a matching process with WRM type-curves rather than with the (more adequate) TIFM type curves;
2. this same error can still be significant between the "crossing" point and the "merging" point; the abscissa t_{D_1} of that point corresponds to the late time asymptotic solution (shifted Theis by (1+b)) common to WRM and TIFM; beyond that point, the analysis should provide the same results whether it is conducted with the WRM or the (more adequate) TIFM;
3. at all times, the error can be significantly reduced if the dual porosity aquifer is affected by fracture skin: the greater will be the dimensionless skin for a given set of b and r_D, the smaller will be the error; this point will be further discussed.

The error will affect mostly the determination of K_1, the fracture hydraulic conductivity.

---

[8] The reader will easily establish that the value of t_D for the crossing point is obtained by solving for p' in the dimensionless Laplace space:

$$[u(p')]_{WRM} = [u(p')]_{TIFM}$$

and doing $t_{D1} = 1/p_o'$ where p'_o is the convenient root of these (transcendantal) equations.

- Comparison of drawdown in the blocks

Examination of the Figures 17a, 17b, 17c and 17d which correspond exactly to the conditions of the Figures 16a, 16b, 16c and 16d, respectively, indicates basically the same features for block and fracture drawdowns. However, the WRM curves are widely separated from the TIFM curves at early times (one or more cycle log of dimensionless time). Also, for a given b, there is no "crossing" point of the WRM and of the TIFM curves: TIFM block drawdowns are constantly less or equal to WRM block drawdowns. Equivalence occurs at late time and at slightly higher values of t_{D_1} than with the fracture drawdowns ($t_{D_1} > 10^4$ in our example). For the TIFM curves, an increase of b displaces them to the right: the greater S_{s_2}, the lesser are the block drawdowns. A different behaviour of the TIFM curves can be observed (Figure 17d) at early time for the case when fracture skin is present and this is probably not caused by numerical instability as in Figure 17a; we shall discuss this in more detail later, on plots that are more convincing than 17d.

In general, the shape of the curves for WRM and TIFM are so different that interpretation errors should not occur by using WRM type curves rather than the TIFM ones. In the absence of geological evidence of fracturing, the TIFM drawdowns could be (wrongly) analysed with a Theis solution.

From this analysis, we conclude that the assumption of pseudo-steady-state interporosity flow overestimates early fracture drawdowns, but can yield acceptable results with type curve matching of late time

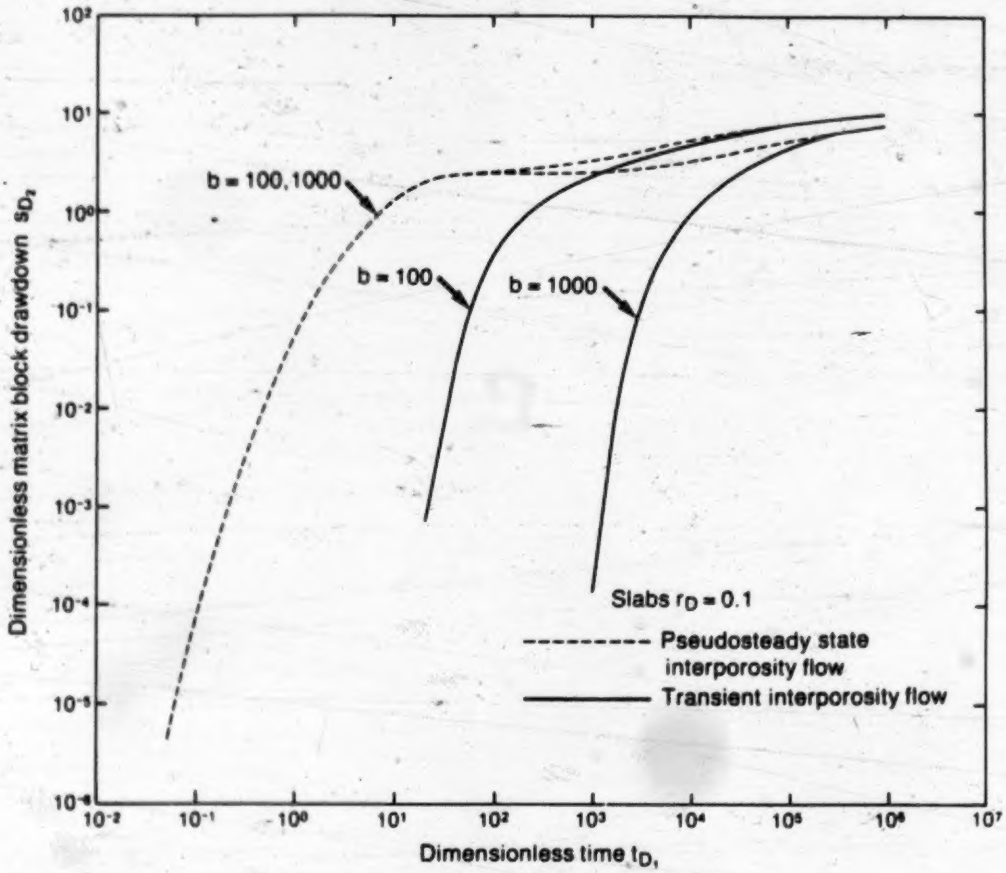

Figure 17a. Comparison of type curves for matrix block drawdown when the interporosity flow is assumed to be pseudo-steady-state and unsteady for the "slab" configuration of the fracture network and for b=100 and 1000. The dimensionless radius is 0.1 and z_D=0.5

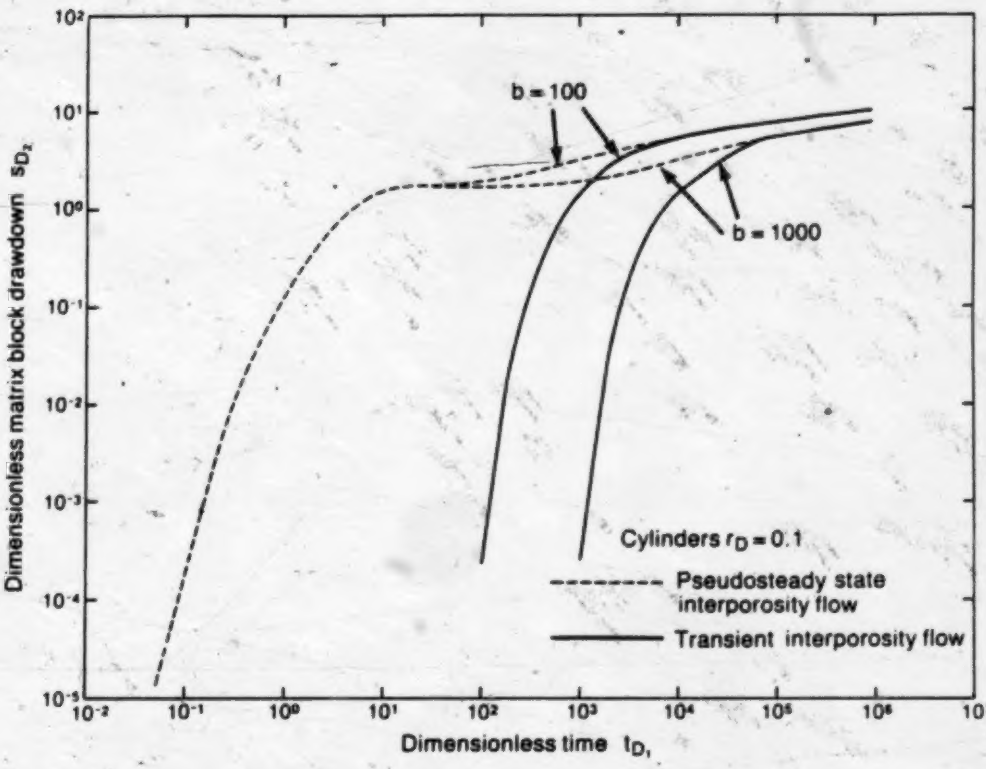

Figure 17b. Comparison of type curves for matrix block drawdown when the interporosity flow is assumed to be pseudo-steady-state and unsteady for the "cylinder" configuration of the fracture network and for b=100 and 1000. The dimensionless radius is 0.1 and $\rho_D=0.5$

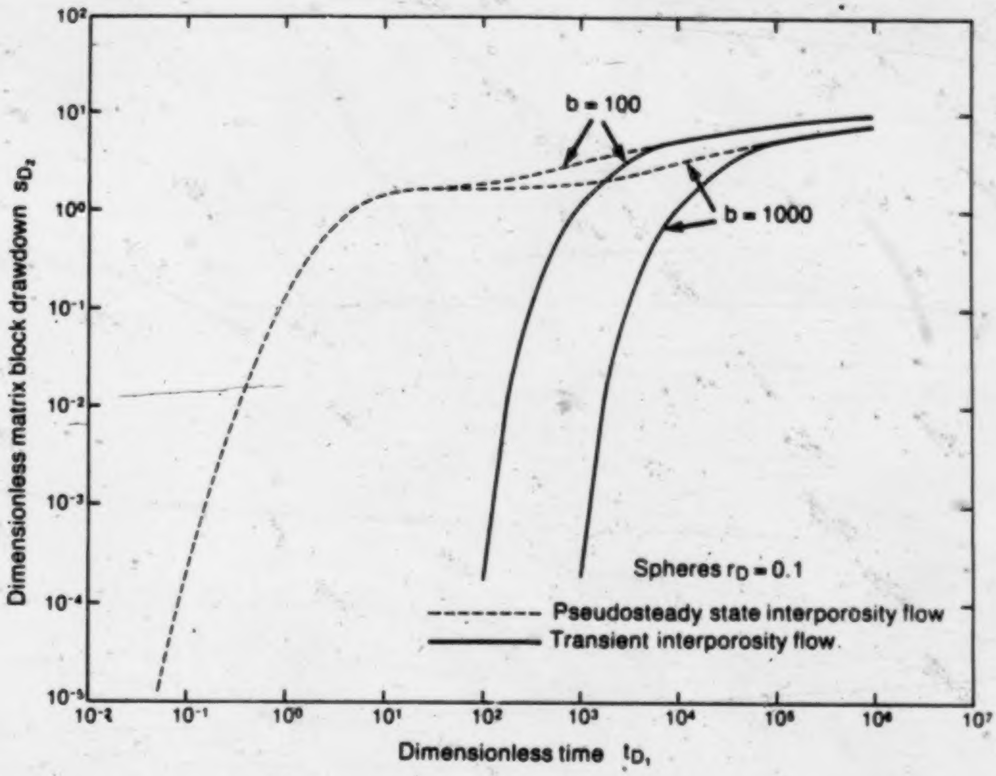

Figure 17c. Comparison of type curves for matrix block drawdown when the interporosity flow is assumed to be pseudo-steady-state and unsteady for the "sphere" configuration of the fracture network and for b=100 and 1000. The dimensionless radius is 0.1 and ρ_D=0.5

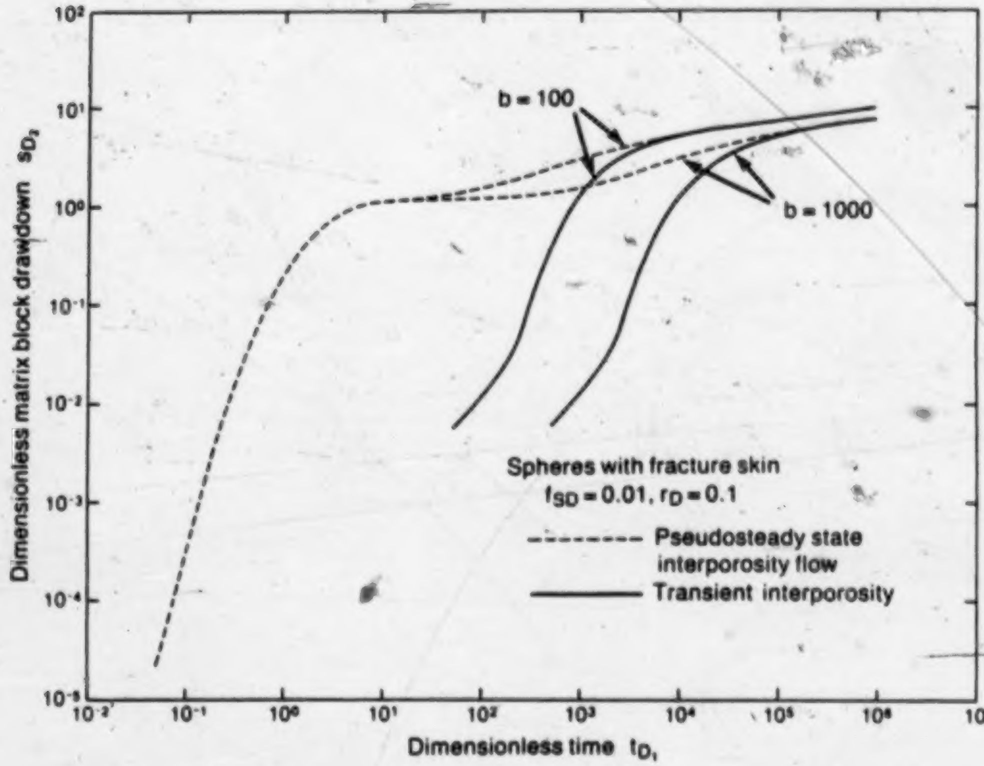

Figure 17d. Comparison of type curves for matrix block drawdown when the interporosity flow is assumed to be pseudo-steady-state and unsteady for the "sphere" configuration, a dimensionless fracture skin of 0.01 and for b=100 and 1000. The dimensionless radius is 0.1 and ρ_D=0.5

data; the analysis of block drawdown is likely to introduce errors at all times. This has greater implication in hydrogeology where the line source solutions discussed in this chapter are currently used for aquifer test analysis. It is often very difficult to complete observation wells in the same "porosity" system as the producing well, and it happens commonly that, unlike the producing well, an observation well will record the response of the blocks rather than the one of the fractures. Data for fracture drawdown in other observation wells are a good control that this is, in fact, happening and the final values for all the flow parameters should be consistent. If the given response is unique or if the other responses are similar, it is highly recommended: (1) to use block drawdown type curves to analyse these data, and (2) to use interpretative models with transient interporosity flow. In all cases, Jacob or Horner analysis based on the pseudo-steady-state assumption should be discouraged.

4.2.3.2 Comparison of transient interporosity flow type curves

It has been suggested (Moench, 1984) that there is little difference for the various TIFM between fracture drawdown type curves. However, this point has not been thoroughly analysed. What about the TIFM block drawdown type curves? This "second" question deserves closer examination because it is commonly believed that the use of TIFM could give an important insight on the fracture network geometry; obviously if all type curves are hardly separated and have the same shape for a given type of response (fracture and/or block), then the value of the information concerning the system geoemtry that can be expected from aquifer testing becomes questionable, an interpretation with a "slab" model giving practically the same result as one with a "cylinder" or a "sphere" model.

Comparison of fracture drawdowns for transient interporosity flow models

On each of the Figures 18a, 18b, 18c and 18d, we compare the type curves of the TIFM for the fracture drawdowns, for typical values of r_D, b and fs_D. The comparison is for type curve related to one-dimensional ("slab"); two-dimensional ("cylinder") and three-dimensional ("cube or sphere") fracture network geometries.

The four figures show the same type curve for the "slab" and "cylinder" geometry for b=100 (Figure 18a) and b=1000 (Figure 18b and 18c) as well as for r_D=0.1 (Figure 18a) and r_D=0.01 (Figure 18d).

Comparing the four figures also shows that for r_D=0.1, the "sphere" type curve stays below the "slab-cylinder" one and the distance between the two is proporational to b (compare Figures 18a and 18b). However, when r_D is divided by 10 (Figure 18d), this curve becomes very close to the "slab-cylinder" one even for a high value of b.

For a given ratio S_{s_2}/S_{s_1}, all other factors being equal, the lower K_2/K_1 is, the closer the responses will be with the three geometries. For a given K_2/K_1 and all other factors being equal, the greater is S_{s_2}/S_{s_1}, the more separated the "sphere" type curve will be from the "slab-cylinder" one. However, because of the similarity of shapes of the two curves, it will be prudent to conclude about the geometry by analysing the data with both type curves and compare the four results with the results of core analysis: if $\overline{n_1}$ and $\overline{n_2}$, the porosities, are

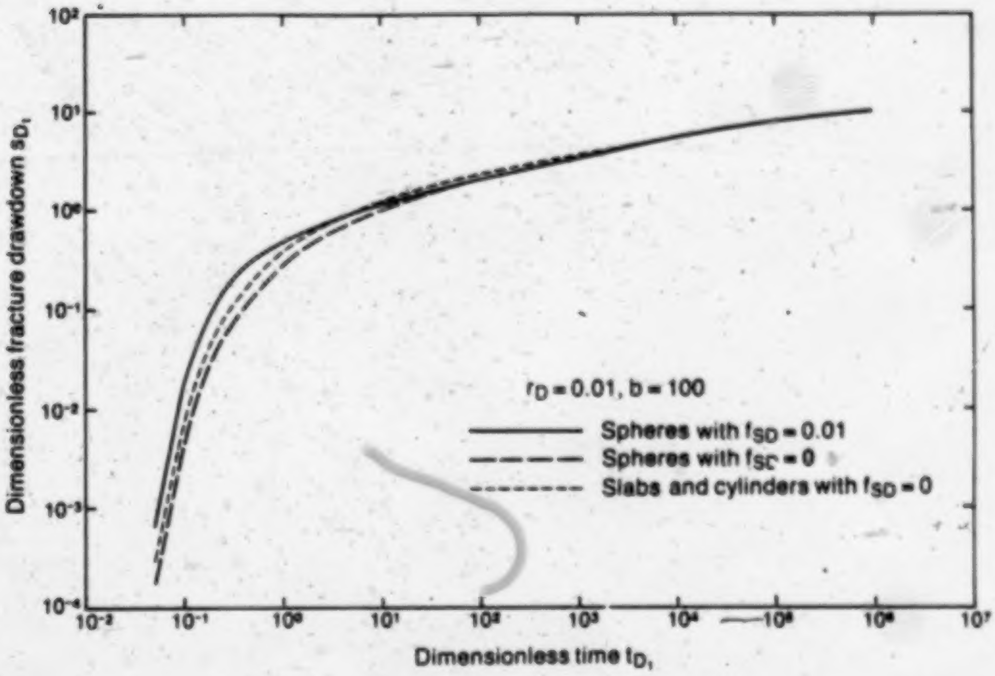

Figure 18a. Comparison of type curves for fracture drawdown when the interporosity flow is unsteady for various configurations of the fracture network and when $b=100$ and $r_D=0.01$

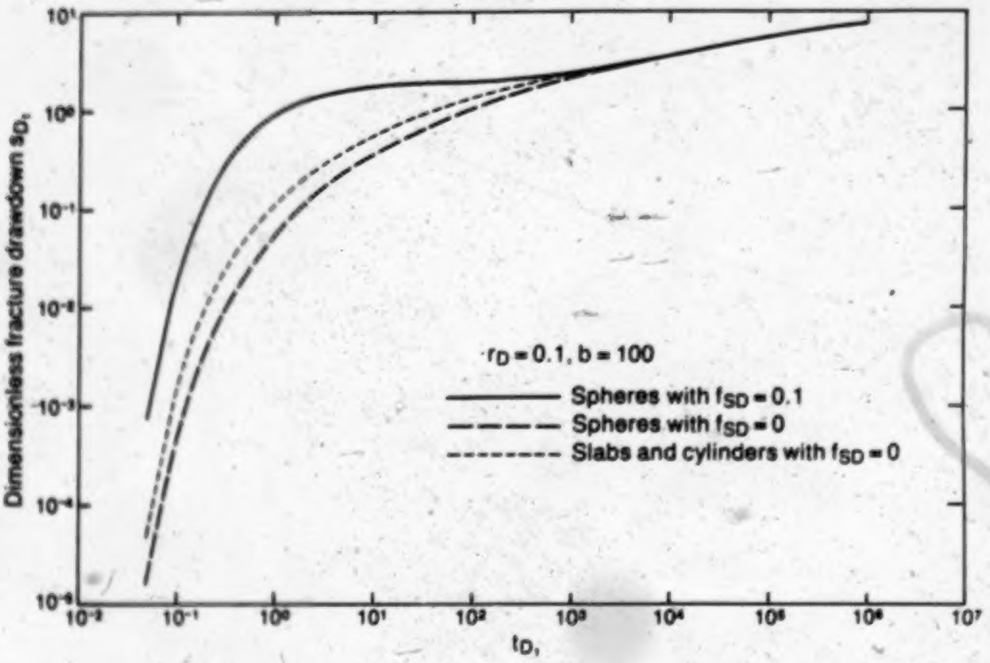

Figure 18b. Comparison of type curves for fracture drawdown when the interporosity flow is unsteady, for various configurations of the fracture network when b=1000 and r_D=0.1

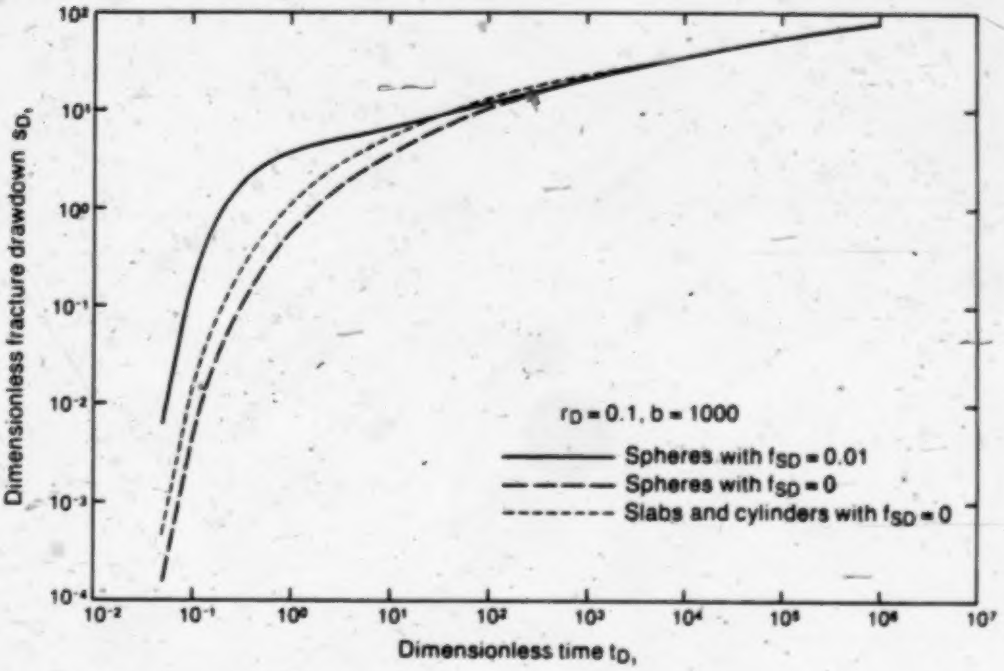

Figure 18c. Comparison of type curves for fracture drawdown when the interporosity flow is unsteady and for various configurations of the fracture network and when r_D=0.1 and b=1000

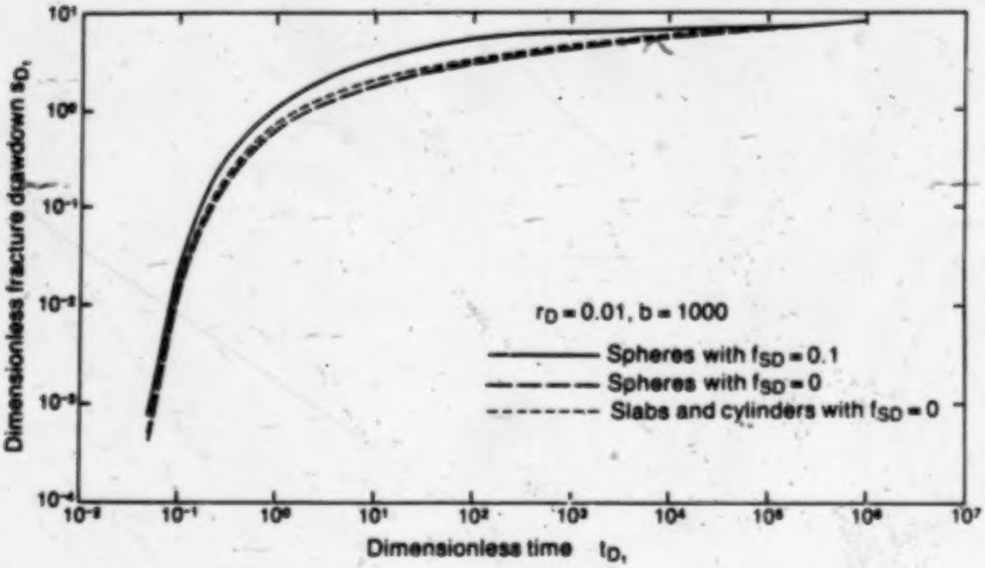

Figure 18d. Comparison of type curves for fracture drawdown when the interporosity flow is unsteady and for various configurations of the fracture network and when r_D=0.01 and b=1000

known, it may be possible to evaluate S_{s_2} and S_{s_1} and to check which of the two interpretations presents the closest agreement. However, the results of the analysis with both type curves may yield values of S_{s_1} and S_{s_2} that are so close that this method may not work. The only hope then would be to have other observation well responses that could be matched uniquely with either the "slab-cylinder" or with the "sphere" type curve. The four figures show that even a low fracture skin (Figure 18a) displaces upward the fracture drawdown type curves and that this displacement increases when b increases (compare Figure 18a, b=100 to Figure 18c, b=1000). For a tenfold value of f_{s_D} (Figure 18b), the effect of fracture skin can be clearly recognized by the same upward displacement of the type curve and by the apparition of a pseudo-stabilization period (similarity with the WRM type curves). Comparison of Figures 18b and 18d indicate that for a given b and f_{s_D}, the reduction of r_D by a factor of 10 will prolongate the accession to the pseudo-stabilized regime.

Comparison of block drawdowns for transient interporosity flow models

The four Figures 19a, 19b, 19c and 19d correspond to the block drawdown type curves s_{D_2} (t_{D_1}) when the values of b, r_D and f_{s_D} are respectively the same as on the four Figures 18. The block response lags behind the fracture response by at least one cycle log of dimensionless time; when r_D is 0.01, this difference goes up to four cycle logs of t_{D_1}; this lag time between noticeable drawdowns in both the fracture and the block system is inversely proportional to K_2 (to r_D) and proportional to S_{s_2} (to b), as expected. The drawdowns in the

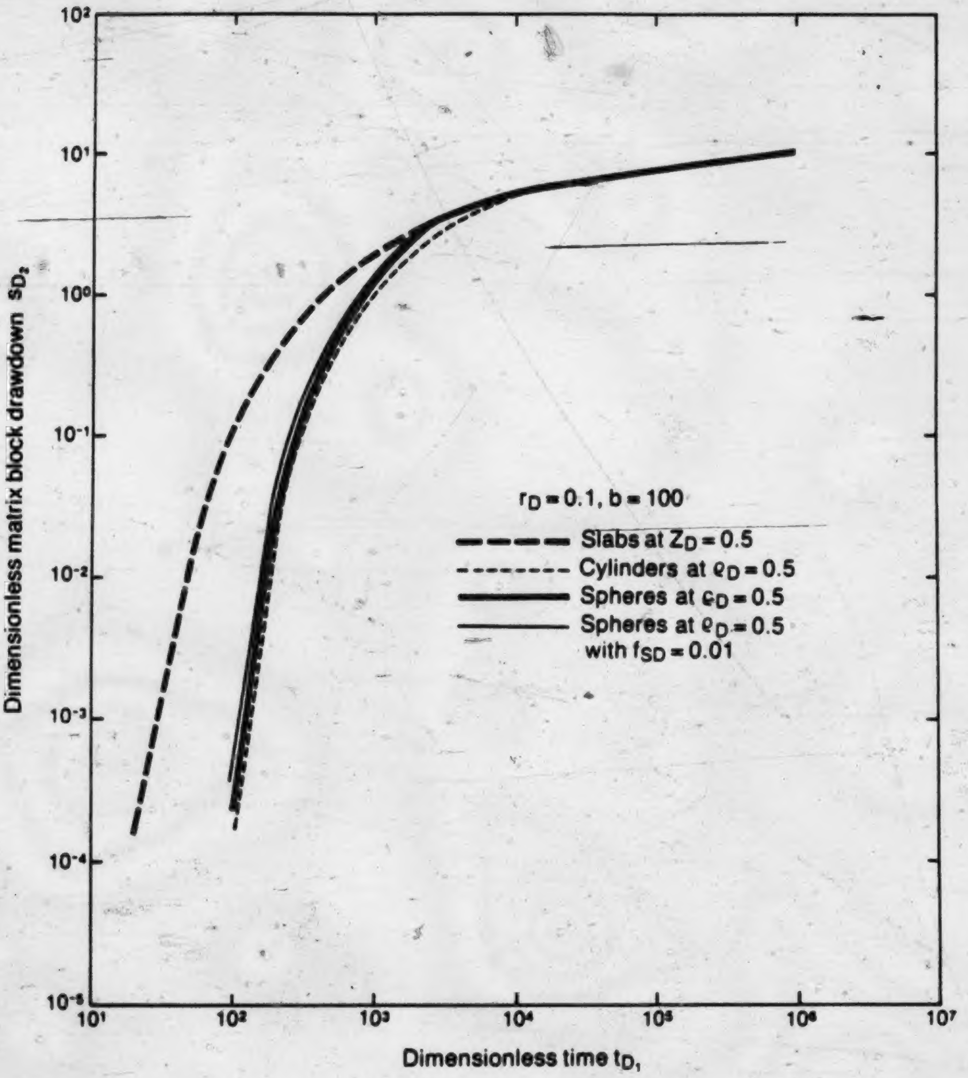

Figure 19a. Comparison of type curves for matrix block drawdown when the interporosity flow is unsteady and for various configurations of the fracture network and when r_D=0.1 and b=100

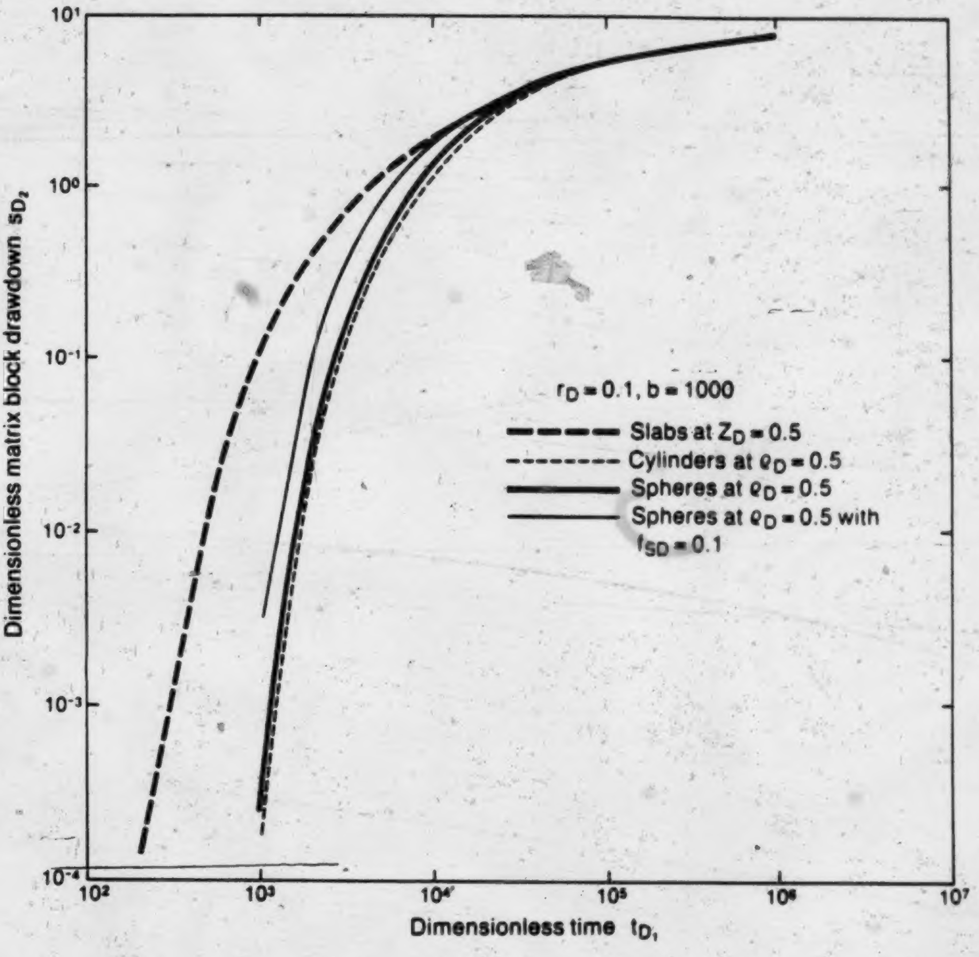

Figure 19b. Comparison of type curves for matrix block drawdown when the interporosity flow is unsteady and for various configurations of the fracture network and when r_D=0.1 and b=1000

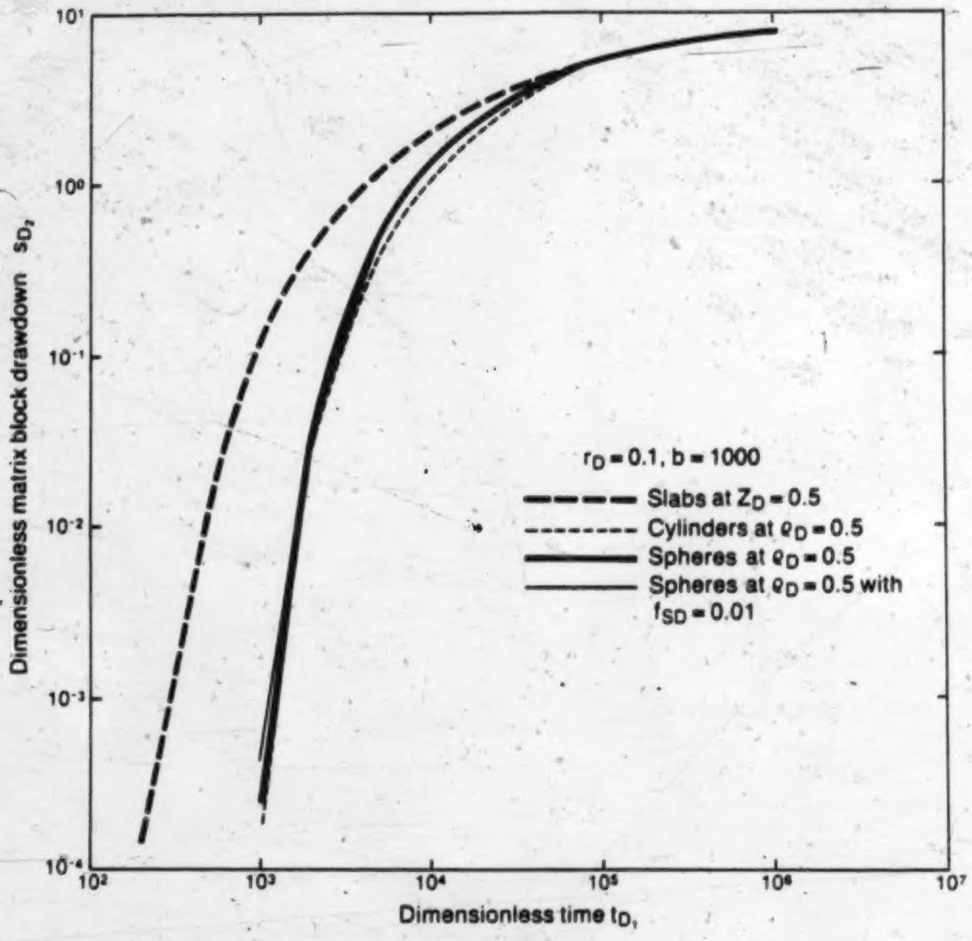

Figure 19c. Comparison of type curves for matrix block drawdown when the interporosity flow is unsteady and for various configurations of the fracture network when r_D=0.1 and b=1000

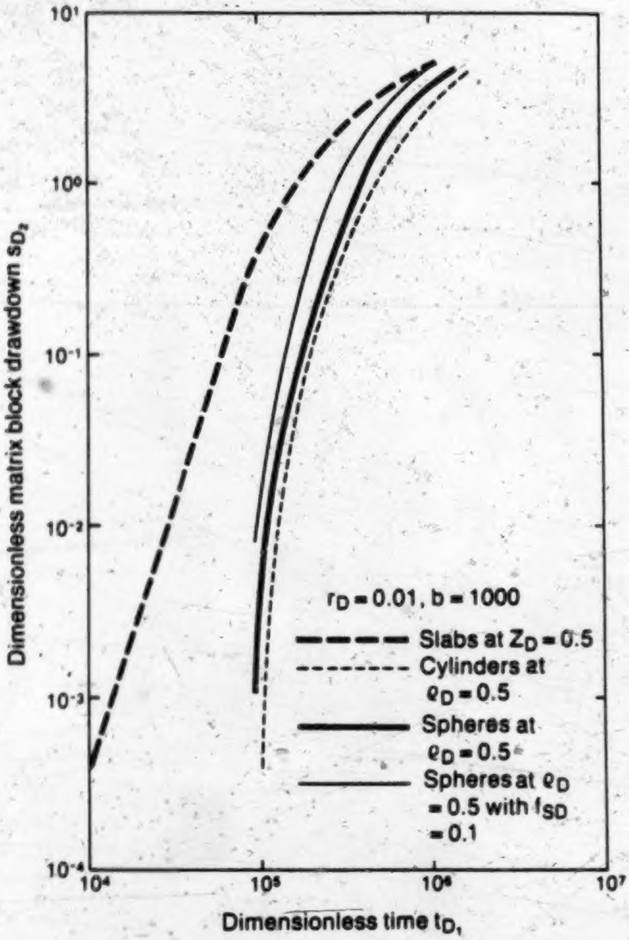

Figure 19d. Comparison of type curves for matrix block drawdown when the interporosity flow is unsteady and for various configurations of the fracture network when and r_D=0.01 and b=1000

"slab" case occur earlier and all the type curves for the values of b and r_D considered are separated from the three other cases under study. This earlier contribution of the matrix rock with one-dimensional fracture network can be hypothesized as characteristic of the block response in a "slab" system. Unfortunately, the "sphere" and "cylinder" type curves remain very close to each other and will be difficult to identify from observation well responses. All the type curves have a similar shape indicating a continuous drawdown increase. The "merging" point time is usually above $t_{D_1}=10^6$ on Figure 19d where r_D is the smallest. Fracture skin has practically no influence for $f_{s_D}=0.01$ (Figures 19a and 19c), the type curves for $f_{s_D}=0.1$ are steeper and suggest a possible distinction with the "sphere" case and no fracture skin (Figures 19b and 19d).

Behaviour at higher values of the dimensionless parameters

Figure 20a (fracture drawdown) and 20b (block drawdown) are for the cases of "high" values of the dimensionless parameters: $r_D=1$, b=1000 and $f_{s_D}=1$. These plots have been prepared to show the marked difference of the type curves for (high) fracture skin which shows a WRM behaviour and, therefore, can be clearly recognized on observation ~~well responses~~.

Asymptotic Solutions

Figure 21 illustrates the agreement between the type curve for fracture drawdown in the case of the "slab" configuration and the asymptotic solutions proposed in Appendix D.

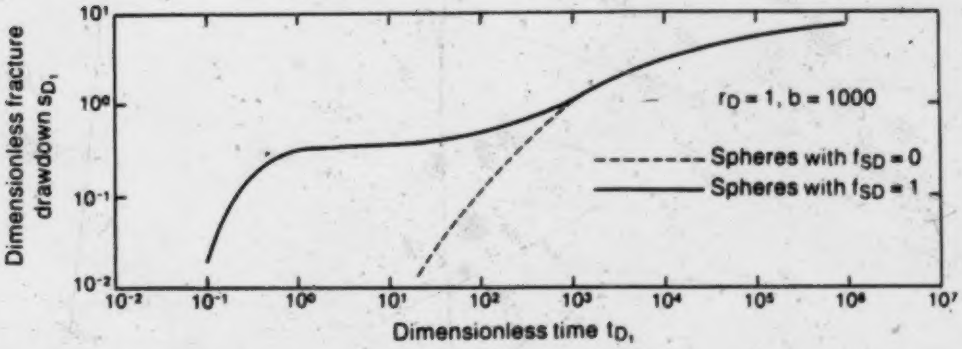

Figure 20a. Comparison of type curves for fracture drawdown when the interporosity flow is unsteady for the "sphere" configuration of fracture network and high values of depending parameters

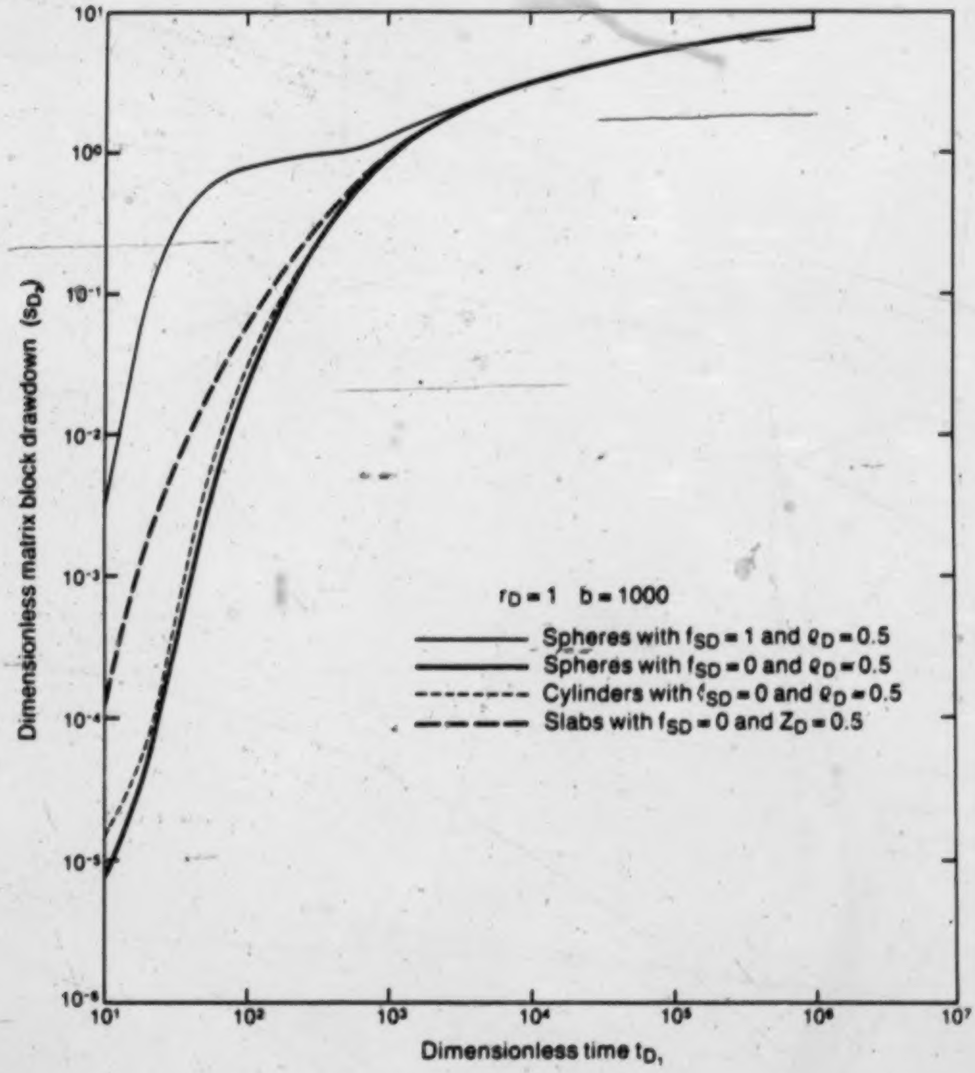

Figure 20b. Comparison of type curves for matrix block drawdown when the interporosity flow is unsteady and for high values of the depending parameters

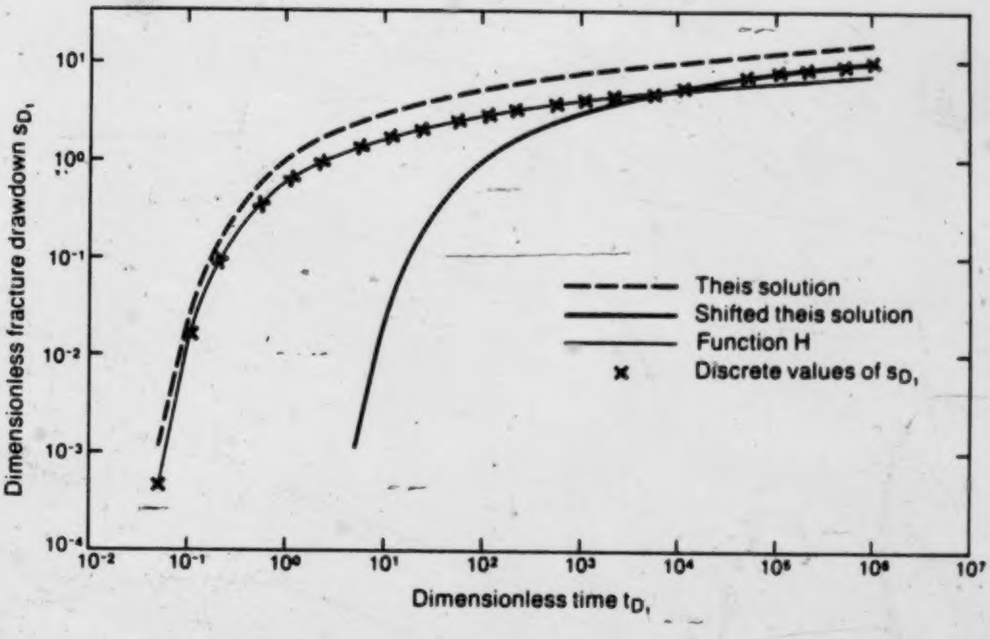

Figure 21. Asymptotes to the fracture drawdown type curves for unsteady interporosity flow and "slab" geometry of the fracture network

Consequences for aquifer test analysis

/The simplicity of producing type curves by use of numerical inverters or approximate inversion formulae[9] to perform the inverse Laplace transformation of the solutions suggests that the inaccurate semi-log interpretation should be replaced by type curve analysis for the analysis of dual porosity systems.

Streltsova (1982) discusses the implication of considering pseudo-steady-state interporosity flow for leaky systems; mutatis mutandis and because there is a great similitude in the behaviour and solutions of both systems, the same could be developed for dual porosity systems. Specifically, the pseudo-steady-state assumption implies an instant flow adjustment at any point within the matrix block. Consequently, the matrix block influence on the fracture drawdown is delayed compared to the case of transient interporosity flow. This explains why the fracture drawdowns show a pseudo-stabilization period with the pseudo-steady-state assumption (similar to the "delayed yield" of unconfined aquifers). If the blocks are compressible, there is no physical reason to justify this delay and the flow from matrix block to fracture should be on the transient mode. Note again that with the methods presented in this work, there is no practical reason to prefer the pseudo-steady-state assumption on the grounds that the solutions are more complicated; moreover, the real space analytical solution given by Kazemi et al. (op.cit.) seems to be only slightly simpler to evaluate than the "slab" real space solution given in Streltsova-Adams (op.cit.). Both are very easy to evaluate reasoning in the Laplace space. The controversy raised by Odeh (op.cit.) can be clearly resolved from this study. Schematizing: the interporosity flow is transient and there is no transition period in the fracture drawdowns; therefore, no parallel slopes at early and late time on semi-log plots; if an "S" shape curve is obtained on an observation well response, one should invoke fracture skin rather than pseudo-steady-state interporosity flow.

---

[9] The use of the Schapery's technique is described in detail for the "slab" configuration in Sauveplane (1984b)

To illustrate further this point, we present on Figure 21 the type curve for fracture drawdown in a "slab" configuration for r_D=0.1 and b=100 together with the asymptotes of early and late time evaluated after the developments of Appendix D. The type curve of the Theis solution is also plotted for comparison and shown to be clearly separated from the "slab" TIFM type curve; there is, therefore, no chance to see a semi-log straight line of early time. The "slab" TIFM type curve is in excellent agreement with the H function up to its merging with the Theis shifted solution (beyond t_{D_1}=5000; the predicted dimensionless time from Appendix D is $t_{D_1}=b/16r_D^2=625$, that is 8 times less!).

This leads us to the final (and crucial) question. If one accepts that only transient interporosity solutions should be used for analysing tests in dual porosity (fractured) aquifers, these solutions are of delicate use: not only different systems of fractures can lead to quasi-confunded type curves as discussed before, but these type curves do not have a fundamentally different shape than those of the leaky systems. In the absence of convincing geological evidence or shear lack of information, is it possible to resolve these ambiguities on the basis of aquifer test responses? The solution to this difficult problem is, like the type curves, not unique and there is probably no magic method. One can try and measure both fracture and block responses for a possible solution to the first ambiguity; that is when confusion with a leaky system is excluded. These measurements can be conducted either on the same observation well with two intervals open at different levels or, better, on two observation wells that are located at different but not too large distances from the pumping well (different r_D). It is of prime importance to record as many measurements as possible during the very early two responses, because these might be the key to conclude on the dominant geometry of the fracture network. Analysis of both responses after a "trial and error" procedure using initial guesses and preparing sets of possible type curves may lead to a solution that will incorporate all the details of both responses; the responses should have a marked difference in shape (Figures 18 and 19). We believe that the key is to consider both fracture and block responses to pumping. Gringarten (1982) reports an example of two observation well responses in a chalk aquifer that he interpreted with his solution for horizontal fracture in a homogeneous anisotropic aquifer; the shape of these two responses is similar to the ones of Figures 19 and we would have tried to analyse these data with block drawdown type curves for dual porosity systems. In the case of the second ambiguity, again the use of two observation wells at different levels may be the key in some situations. To obtain the same values for K_2 and K_1 after a satisfactory match of both responses with different r_D type curves permit an evaluation of ℓ, the characteristic dimension; in general, ℓ will have a good order of magnitude difference if it corresponds to a dual porosity fractured aquifer or a leaky aquitard-aquifer system (it would be the aquitard thickness in that case). One can also take advantage of the fact shown in Appendix D that type curves are only strictly the same for an aquitard-aquifer system and a "slab" configuration. Finally, the aquitard response in a leaky system is usually different from a block drawdown response, emphasizing the importance of trying to measure the response of either the block or the aquitard.

We conclude this chapter with an optimistic note: with the increasing level of resolution in modern formation evaluation techniques, it becomes perfectly reasonable to predict that hydrogeologists and/or reservoir engineers will soon be faced with the problem of finding analytical solutions for dual porosity (fractured) _and_ leaky systems: how about the uniformly fractured aquifer overlain by a leaky aquitard? We have already evoked that configuration as a "triple porosity" system; no analytical solution has been proposed to date. Bennett et al. (1985) have solved the problem of fractured wells producing layered and bounded reservoirs (with no cross flow); their model assumes a single fracture of finite extent. This is different than the above problem, but suggests that research is being originated in that direction.

4.3 Multilayered Aquifer Systems

Two important differences exist between these stratified systems and the two- and three-aquifer systems studied previously:

1. each individual aquifer is fully penetrated by the producing well that operates at a constant rate Q; the aquifers are thus simultaneously contributing to the formation of Q;

2. in the general case when cross-flow occurs between aquifers, their interfaces have a perfect hydraulic contact implying that the direction of cross-flow cannot be assumed to be strictly vertical as was the flow through the aquitards in the leaky systems; it can be viewed as if the aquitard thickness of the leaky systems were vanishing.

Such systems are of common occurrence in nature and have been studied mostly in petroleum literature. The existing mathematical models belong to two categories:

- "cross-flow" models as briefly described in 2 above;
- "no cross-flow" models for which it is assumed, for example, that an impervious layer of finite thickness separates two successive aquifers that are produced simultaneously; the formulation is the same if the thickness of this intervening layer is negligible with respect to the thicknesses of the aquifers themselves.

Each aquifer is supposed to fulfill the Theis assumptions, in that it is homogeneous, isotropic, horizontal and of constant thickness. The system can be uniformly bounded at a radial distance R (circular system) or of infinite lateral extension. The well radius can be finite or negligibly small. Mathematically, the cross-flow models present the additional complication that the drawdown in each aquifer is a function of the elevation of the considered point in the system. This is a direct consequence of the above-mentioned point 2. . Therefore, we study functions $s_i(r,z,t)$ where $i=1, n$ rather than $s_i(r,t)$ as it could be done with the leaky systems, or as it can be done for models with no cross-flow. Theoretically, there is no difficulty in defining the IBVP for a multilayered system of n aquifers; this is worthwhile for the models with no cross-flow where we have $s_1(r,t)$. It is a futile exercise for the cross-flow models given the level of complexity of the solutions already experienced when n=2 (two-layer system). Also, the cross-flow analytical models should account for vertical anisotropy of the stratified aquifers because that property governs the direction and amount of exchange between the units. This is not generally done because it introduces another level of mathematical difficulty in the derivation of the solutions which is not really needed as illustrated in Appendix E. When the problems are solved with simulators, it is desireable to consider anisotropy as long as this parameter is reasonably well quantified. In this study, we have restricted ourselves to the study in the dimensionless Laplace space of the two-layer aquifer system without anisotropy. Solutions for dimensionless drawdowns are presented in Appendix E for, successively:

- cross-flow model with finite inner and outer boundary conditions (equations E23 to E26), referred to as the "general case";
- cross-flow model with finite inner and infinite outer boundary conditions (equation E27);
- cross-flow model with infinitely small wellbore radius and infinite outer boundary conditions (equation E28);
- model with no cross-flow in the "general case" (equations E30), finite inner and infinite outer boundary conditions (equation E31) and finally the simple case where the wellbore radius is negligibly small and the aquifers are infinite (equation E32). In this latter case, real space solutions can be immediately derived (equation E32) and easily evaluated.

The full-time evaluation of the cross-flow solutions E26, E27 and E28 remains an open problem that, to date, has not received a satisfactory solution. The difficulty is essentially to evaluate the n roots of the transcendental (non-linear) system of equations E23. In this work, the approach has been to use the Newton-Raphson technique to solve this system. Unfortunately, this effort has not been successful because the method of solution depends on an initial guess of the roots; this initial guess is, of course, a function of the dimensionless Laplace variable p' which varies between zero and infinity. We found that for a given p', different initial guesses yield different values of the roots instead of a unique determination and the method does not work. It remains possible that other numerical algorithms might lead to satisfactory results, but this was not investigated.

The case with no cross-flow is also presented in terms of cylindrical-source (E30) and line-source solutions (E32). Equation E30 is presented in the dimensionless Laplace space and type curve solutions can be evaluated with numerical inverters without difficulty. Equation E32 can easily be converted into exponential integral solutions that do not require any further discussion; these are further compared with equations E34 and E35 to the equivalent homogeneous system. The formulation of the cross flow case as equation E36 permits to study the early time behaviour of the system and we show that as long as $t_{D_1} < 0.1/r_D^2$, cross-flow can be neglected; the late time behaviour cannot be easily derived.

With reductive assumptions: considering partial penetration in the upper unit and the lower aquifer of infinite thickness (Javandel and Witherspoon, 1980) or, on the contrary, assuming that it has a small thickness compared to upper aquifer thickness (Boulton and Streltsova, 1977b), analytical solutions have been proposed for a two-layer system with cross-flow. In both cases, the Laplace transforms are obtained under the form of integrals that are not easily implemented with the type of numerical inverters considered in this work. In the first article, numerical inversion is obtained by means of Legendre polynomials for a Gaussian quadrature technique. Boulton and Streltsova invert directly the Laplace-Hankel transform solutions in the real space, but do not give details on how they computed the type curves in the real space (the solutions are, of course, not simple). Gao Cheng-Tai (1984) presents a solution for a "semi-permeable wall" model that is reducible to equation E30, i.e. does not account for strict cross-flow. Pottier (1961) evaluates the series of equations E24 and E25 as inverted by Jacquard (op.cit.) in the real space to give pseudo-steady-state (late times) approximations for the solutions at the well.

This brief literature review and the equations of Appendix E may help the reader who is interested in trying to solve the "cross-flow problem", which is physically simple and of potential common occurrence in practice, but which is very complicated mathematically.

4.4 Radially Composite and Confined Aquifer Systems

These systems are characterized by a cylindrical inner flow domain of different properties (K and S_s) than an outer domain which is supposed to have an infinite extent. The system is confined and each region is homogeneous and isotropic with no vertical variation of the properties over the entire thickness. A fully penetrating well is located at the centre of the inner region and produced at a constant rate. A perfect hydraulic contact exists at the surface $r=R$ that separates the inner region from the outer region. The radius R of the inner region is supposed to be much greater than the wellbore radius so that the latter can be considered as infinitesimal. This problem is axisymmetrical and best treated with radial coordinates. It can be viewed as a case of radial discontinuity with cross flow rather than a case of vertical discontinuity that was considered in the previous chapter. Fortunately, the solutions $s_1(r,t)$ $(0<r<R)$ and $s_2(r,t)$ $(r>R)$ for the drawdowns in each region have a much simpler form, mostly because both s_1 and s_2 can be treated as independent of the vertical position z in the system. The derivation of these solutions are presented in Appendix F. The dimensionless drawdowns with respect to the respective dimensionless times are given by equations F7 and F8, for the inner region and by equation F9 for the outer region in the dimensionless Laplace space. They reduce to the solutions presented by W. Hurst (1981) in the special case when $S_{s_1}=S_{s_2}$ and are, therefore, more general. We also show that early time behaviours cannot be approximated by a simple solution that would be independent of the groups a, b and r_D. At late times, when t_{D_1} or $t_{D_2}>[(20ab)/r_D]^2$, both s_{D_1} and s_{D_2} can be approximated by a Theis solution.

Two computer codes RADHET1 for region 1 and RADHET2 for region 2 have been prepared to perform the type curve calculations using the Stehfest inverter. These codes calculate, respectively, s_{D_1} for $r_D<1$ and s_{D_2} for $r_D>1$ for various values of r_D and a given set of a and b. Calculations are performed in arithmetic double precision using the IMSL subroutines MMBSI0, MMBSI1, MMBSK0 and MMBSK1 that evaluate, respectively, $\exp(-x)\ I_0(x)$, $\exp(-x)\ I_1(x)$, $\exp(x)\ K_0(x)$ and $\exp(x)$

$K_1(x)$ in the dimensionless Laplace space for a wide range of x (i.e. of t_{D_1} or t_{D_2}). The codes are written in FORTRAN language.

Examples of the resulting type curves are shown on Figures 22a and 22b for $s_{D_1}(t_{D_1})$ and on Figures 23a and 23b for $s_{D_2}(t_{D_2})$. Figures 22a and 23a show the variations of s_{D_1} and s_{D_2} with r_D for a=0.5 ($K_2=4K_1$) and b=3 ($S_{s_2}=9S_{s_1}$). The Theis solution is plotted for comparison and late time asymptotic behaviour. Figure 23a illustrates that when $r_D>5$ ($r>5R$), the response in the outer region is practically a Theis solution, as if there was no radial discontinity for the chosen values of a and b; at smaller values of r_D, the departure with a Theis type curve is only perceptible at early and intermediate times and even then it is not pronounced. Figure 22a shows a more unexpected result: when the ratio of diffusivities α_1/α_2 is greater than 1 and for $0.8<r_D<1$, the drawdown in region 1 may actually decrease during a certain (intermediate) time interval. Such an effect is similar to the "Noordbergum" effect for leaky systems described by Verruijt (1969). To our knowledge, it is the first time that it is evidenced for radially composite systems. It means that the transition period - before the two regions are "fully coupled" - may well be characterized by a negative drawdown segment in the inner region that will be more and more pronounced when the point of observation gets closer to the radial discontinity; such an effect, however, is also observed when α_1/α_2 is less than 1. In practice, we usually have either $K_2>K_1$ and $S_{s_2}>S_{s_1}$, that is the specific storages follow an inverse trend of the hydraulic conductivities. When the hydraulic conductivity contrast is of the same order of magnitude as the specific storage contrast, i.e., $K_1/K_2=S_{s_2}/S_{s_1}$, then the product of these ratios which is α_1/α_2 can be

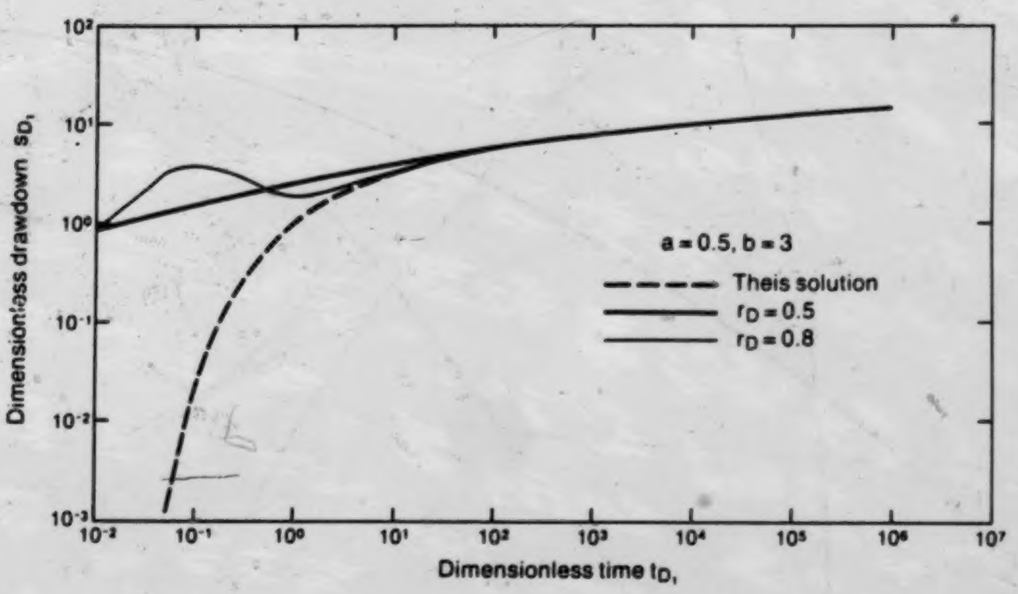

Figure 22a. Radially composite and confined aquifer: type curves for drawdown in the inner region for values of the dimensionless radius (r/R)

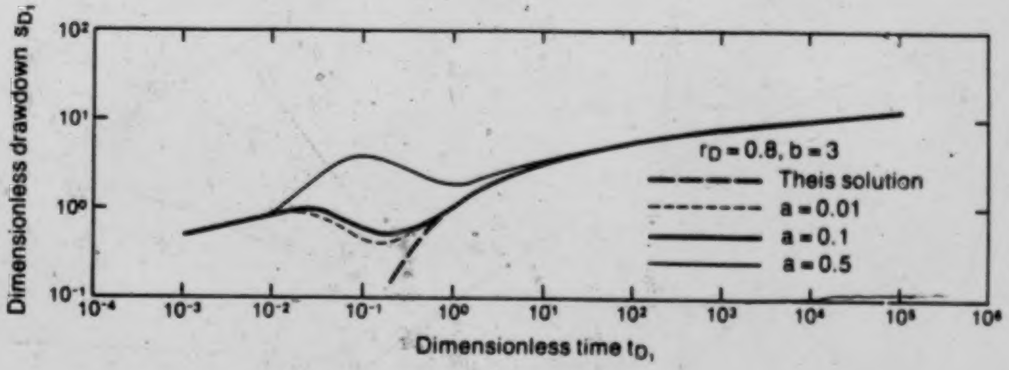

Figure 22b. Radially composite and confined aquifer: type curves for drawdown in inner region for different values of $a=(K_1/K_2)^{1/2}$

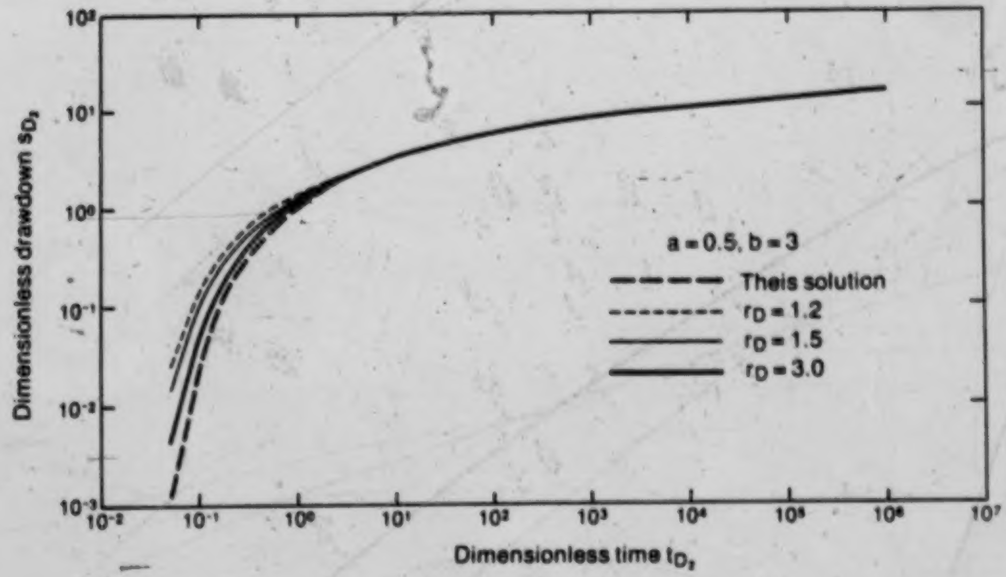

Figure 23a. Radially composite and confined aquifer: type curves for drawdown in outer region when a=0.5 and $b=(S_{s_2}/S_{s_1})^{1/2}=3$

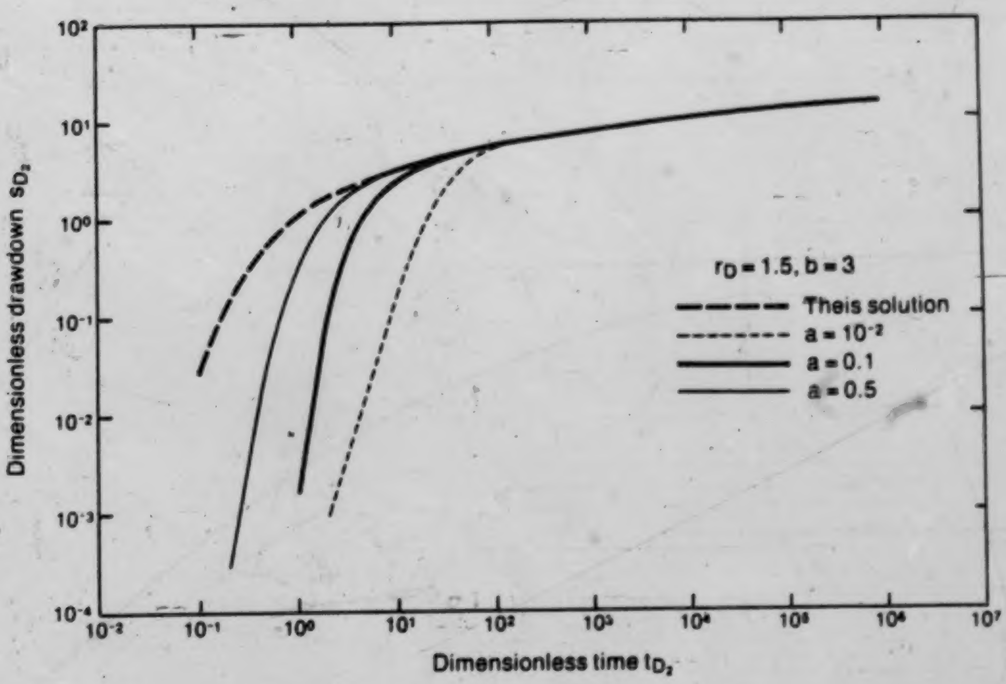

Figure 23b. Radially composite and confined aquifer: type curves for drawdown in outer region when r_D=1.5 and b=3

slightly above 1 or slightly less than 1. A common case, however, is $K_1/K_2<<1$ and $S_{s_2}/S_{s_1}>1$ yielding always $\alpha_1/\alpha_2<1$ and the particular effect on the drawdowns of region 1 will also be observed. In our particular example, we have $\alpha_1/\alpha_2=2.25$ which is not an unrealistic value. Figure 22b shows that for a given b and for r_D close to 1, the amplitude of the drawdown "hump" is proportional to a. The effect of a beyond the radial discontinuity is illustrated by Figure 23b that shows a shift to the left (towards the Theis solution) when a increases and for both r_D and b fixed, which is a normal trend.

The shape of the "hump" for certain type curves of the inner region suggests that the dimensionless drawdown goes through a maximum and later through a minimum, that is $s'_{D_1}=(ds_{D_1})/(dt_{D_1})$ should go through two zeros during the transition period. In the dimensionless Laplace space, it means that $p'_1 s_{D_1}$ should have two zeros within this time range. This is illustrated on Figure 24 where s'_{D_1} is plotted on semi-log coordinates versus t_{D_1} for $r_D=0.85$ and $ab=(\alpha_1/\alpha_2)^{1/2}=0.1$, 0.8 and 10. s'_{D_1} is computed with the Stehfest inverter applied to $p'_1 s_{D_1}$ with s_{D_1} given by equation F8. The first zero is not ambiguous: it is slightly displaced to the right (at increasing values of t_{D_1}) when ab is multiplied by 100. The abscissa of the second zero is not clear because s'_{D_1} tends asymptotically towards zero when t_{D_1} increases. This corresponds to a flat portion of the type curve $s_{D_1}(t_{D_1})$ rather than a clear minimum beyond the "hump" (Figure 22a).

Figure 24 presents another interest: type curves have been derived by Agarwal et al. (1970) for the case of a well of finite radius with wellbore storage ("annulus unloading") and skin effect producing at a constant rate from a confined aquifer of infinite extent. These authors

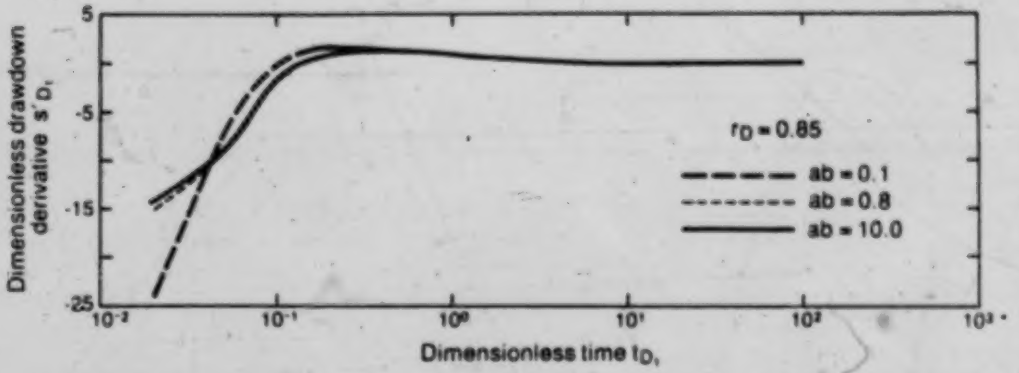

Figure 24. Radially composite aquifer: type curve for s'_{D_1} on a semi-log scale for ab=0.1, 0.8 and 10

assume that the flow through the skin annulus is pseudo-steady-state which postulates that the specific storage of the skin is negligible. This is the same as assuming that s'_{D_1} is constant at all times. The curve ab=0.1 of Figure 24 has been obtained for $a=10^{-2}$ ($K_1=10^{-4}K_2$) and $b=10$ ($S_{s_2}=100S_{s_1}$). These conditions are typical for a skin and similar to Agarwal et al. (op.cit.) conditions: and usual high contrast between the positive skin and the aquifer in terms of hydraulic conductivity and a small specific storage for the skin. Figure 24 (curve ab=0.1) testifies that the common assumption of pseudo-steady-state flow through the skin around a wellbore is at best valid beyond $t_{D_1}=2$, that is, it is an intermediate to late time assumption.

4.5 Combined Flow Regime in Confined Aquifers

Darcy's law is linear and postulates a proportionality between the seepage velocity v and the hydraulic gradient J. It corresponds to the usual conditions of laminar seepage at low velocities. However, at higher velocities such as those that can be expected when exploiting very permeable aquifers (coarse sand or gravel), the linear relationship ceases to be valid. This is supported by experimental evidence (Lindquist, 1933,; Thirriot, 1969). The flow regime ceases to be laminar and goes through a transition zone before reaching the turbulent conditions at very high velocities. In the transition zone, the role of inertia forces cannot be neglected as done in Appendix A when compared to the friction forces. Such flow regimes are often qualified of "post-linear" and may lead to a strictly turbulent regime if the velocity continues to increase. The formulation of Forchheimer (1924):

$$J = av + bv^2 \qquad (49)$$

has been shown to be in good agreement with theoretical results to characterize the combined or post-linear regimes of flow. Note that 49 reduces to Darcy's law with $a=1/K$ when $b=0$; for the case of a strict turbulent regime $J=bv^2$. It should be stressed, however, that 49 is only strictly valid within a certain range of velocity (or Reynolds number) when the coefficients a and b are constant and specific of the porous medium.

Coupling of 49 with the equations of state and continuity leads to a non-linear partial differential equation that governs the flow to the well. Solutions of IBVP in these conditions are usually based on approximations that linearize the governing equation (for instance Dupuit-Forchheimer assumption). In Appendix G, we propose a new method of solution based on the Boltzmann transformation for the simplest IBVP that considers a confined homogeneous and isotropic aquifer, a fully penetrating well produced at constant rate and of infinitesimal radius, and a post-linear flow regime. The non-linearity of the governing equations is preserved and the coefficients a and b are assumed to remain constant. The resulting line-source solution can be further evaluated without difficulty by using numerical integration.

Figure 25a is a log-log plot of s_D versus t_D for the numerical values of b_D used in generating the Table G1 of Appendix G. It is illustrated that up to a "crossing zone" defined by $4<t_D<6$, less drawdown is expected with $b_D>0$ than with $b_D=0$ (equivalent to the Theis solution for Darcy linear flow). The reverse is true beyond that "crossing zone": for instance, at $t_D=10^5$, the ratio $(s_D)b_D=10/(s_D)b_D=0$ is 7.8.

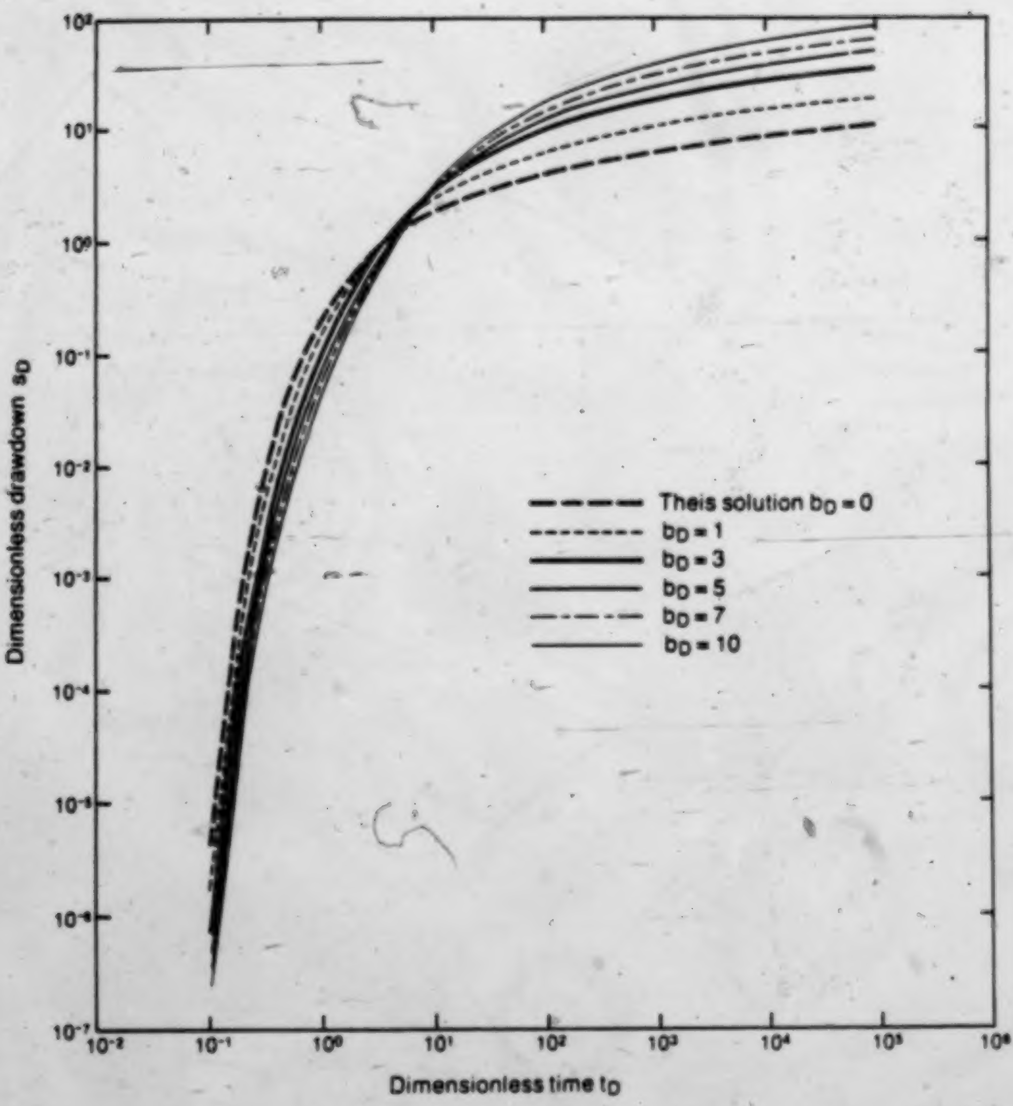

Figure 25a. Type curves for the composite flow regime in a confined aquifer: (b_D is defined in equation G10 of Appendix G)

Although the type curves are generally steeper than a Theis curve, they are very close to it and this may generate some inaccuracy in determining b_D with aquifer test analysis. Figure 25b is a semi-log plot of s'_D, the derivative of s_D with respect to t_D, versus t_D (t_D is on the log scale). Plotting at the same scale $\delta s/\delta t$ versus logt for the observation well response should provide an unambiguous determination of b_D since the "bell-shaped" curves are more separated and of more typical shape.

Figure 25c is a detailed semi-log plot of s_D versus log t_D for the crucial area referred earlier as the "crossing zone". The crossing abscissae between the curves $b_D=0$ and $b_D\neq0$ are shifted towards increasing t_D for increasing b_D. The ordinate of the "crossing" points show a smaller span (s_D comprised between 1 and 1.5).

4.6 Viscoelastic and Confined Aquifers

Brutsaert and Corapcioglu (1976) present an interesting line-source solution for viscoelastic aquifers. Viscoelastic models have been developed in soil mechanics to account for the secondary consolidation in fine-grained systems for which the classical elastic theory of Terzaghi (used in the derivation of the diffusion equation in Appendix A) is not satisfactory. This failure is, for example, exemplified in Lohman (1972) who shows that compaction of formations that contain, for example, lenses of clay and silty clay is more important than what could be predicted assuming a purely elastic granular skeleton.

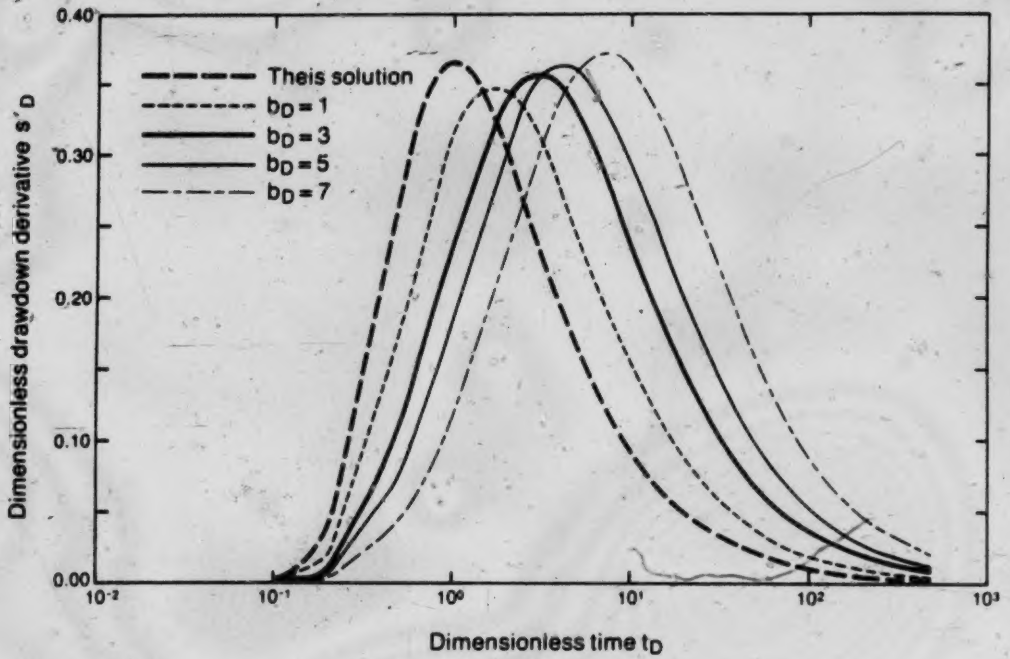

Figure 25b. Semi-log type curves for the derivative of the dimensionless drawdown of composite flow regime in a confined aquifer: (b_D is defined in equation G10 of Appendix G)

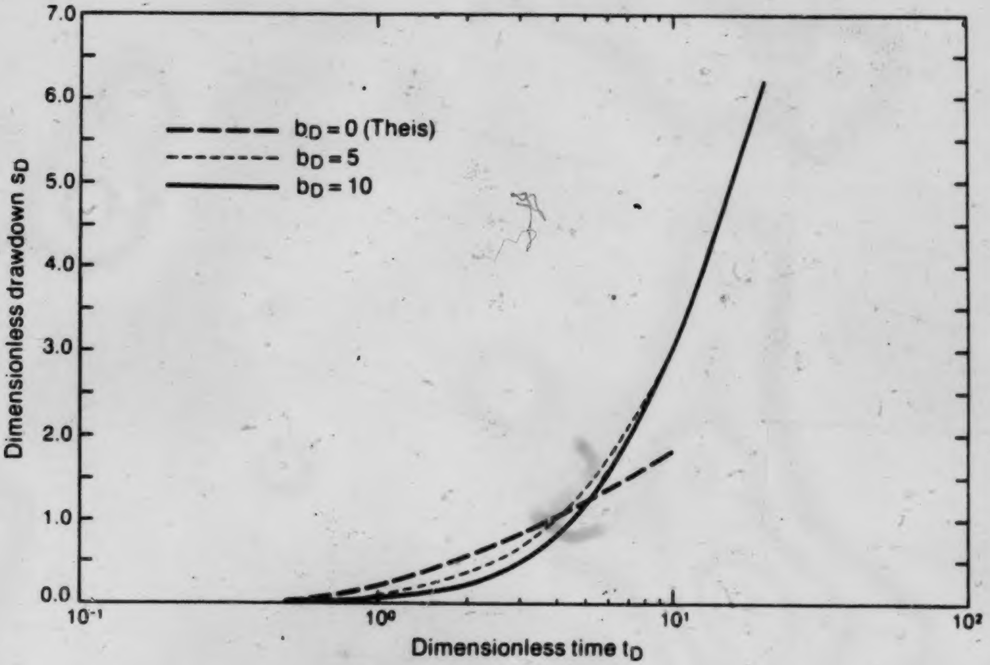

Figure 25c. Semi-log type curves for dimensionless drawdowns of composite flow regime in a confined aquifer: detail of the "crossing" point with the type curve for linear flow (Theis) (b_D is defined in equation G10 of Appendix G)

Brutsaert and Corapcioglu (op.cit.) assume no horizontal displacement of solid material and a constant total stress expressed as the sum of pore pressure and intergranular stress as done in Appendix A. However, their stress-strain relationship is following the work of Taylor and Merchant (1940) in one-dimension which postulates that:

1. the aquifer skeleton is equivalent to a Hookean spring in series with a Kelvin body or in parallel with a linear dashpot;
2. the secondary consolidation occurs simultaneously with the primary one and displacement is impeded by structural resistance to flow beside the usual friction forces.

With these conditions, the governing flow equation for drawdown in a viscoelastic aquifer is:

$$K\Delta s = S_s \frac{\partial s}{\partial t} + \frac{\rho g}{q''_1} \frac{\partial}{\partial t} \int_0^t s(\zeta)\exp\left[\frac{-(t-\zeta)}{\alpha_2 q''_1}\right] d\zeta \tag{50}$$

where q''_1 is the viscosity of dashpot of Kelvin element and α_2 is the coefficient of secondary compressibility.

When the same boundary conditions as for the Theis model are coupled with equation 50, the solution in the Laplace space is derived by Brutsaert and Corapcioglu (op.cit.) as:

$$\bar{s} = \frac{Q}{2\pi kHp} K_0 \left(\frac{p}{k}[S_s + \rho g/(q''_1 p + 1/\alpha_2)]^{1/2} r\right) \tag{51}$$

where p is the Laplace variable corresponding to the time t.

Transforming equation 51 in the dimensionless Laplace space defined by:

$$\overline{s_D} = \frac{4\pi KHs}{Q}, \quad b = \frac{S'_s}{S_s} = \frac{\rho g \alpha_2}{S_s}, \quad r_D = r(q''_1 \alpha_2 \alpha)^{1/2}, \quad L(t_D = \frac{\alpha t}{r^2}) = p'$$

we find:

$$s_D = 2K_0\ [p'+u(p')]^{1/2}/\ p'$$
$$u(p') = p'b/(1+p'/r_D^2) \qquad (52)$$

This solution is identical to the one for unconfined aquifers with delayed yield and to the Warren and Root solution for dual porosity system with pseudo-steady-state interporosity flow. What changes is the meaning of r_D and of b, but the same type curves are obtained for $s_D(t_D)$. In particular, if α_2=0, u(p')=0 and equation 52 reduces to a Theis solution. When, on the contrary, $r_D \to \infty$, we obtain a shifted Theis solution by (1+b); this case corresponds to $q''_1=0$ with α_2 different from zero. The reader is referred to the discussion of the Warren and Root model for additional information about the behaviour of this model. The program VISCEL has been written in double precision and FORTRAN to compute $s_D(t_D)$ for various r_D and a given b. Brutsaert and Coraciopglu (op,cit.) use the Schapery inversion formula to obtain the real space solutions.

This concludes our study of line-source solutions for analytical models of complex aquifer systems. To be complete, one should have considered the cases of laterally bounded systems; we give the solutions for circular aquifers with no flux and constant head boundaries (equations F10 and F11 of Appendix F) without studying in detail these important cases (especially the first one). The principle of superposition can be used to derive solutions for linear discontinuities, either single or multiple (square, rectangular aquifers, for example). In all instances, the solutions are really tractable for confined aquifers only.

5. ANALYTICAL MODELS FOR SINGLE-WELL TESTING OF COMPLEX AQUIFER SYSTEMS

In single-well testing, when the well is operated at a constant rate, it is generally necessary to account for the finite wellbore radius and the perturbing effects caused by wellbore storage and skin effect. The class of analytical solutions referring to these problems are the cylindrical-source solutions. It is beyond the scope of this study to consider these solutions for complex aquifer systems. The method of derivation is along the same techniques as for the line-source solutions with slight differences, however, that will be specified in the simplest case of a confined aquifer of infinite extent (Theis assumptions). For a well fully penetrating a "Theis" aquifer, one simply changes the inner boundary condition of equation B15.4 (Appendix B) to read:

$$\left.\frac{\partial s}{\partial r}\right|_{r=r_w} = -Q/2\pi KH = -q \qquad (53)$$

where r_w is the wellbore radius and wellbore storage and skin effect are neglected. This condition 53 renders the use of infinite zero Hankel transform unsuitable because we do not have the convenient equation:

$$\lim_{r \to 0} \left(\frac{\partial s}{\partial r}\right) = -q$$

when applying this second transformation. However, one usually obtains a Bessel partial differential equation in the Laplace space that can be solved as in Appendix D. Alternatively, a second transformation might be useful as proposed by Javandel (1982): the finite zero Hankel transform; one obtains with this technique Laplace space solutions in the form of series after inversion of this second transformation.

If we define the dimensionless groups:

$$s_{w_D} = \frac{4\pi KHs_w}{Q}, \quad t_D = \alpha t/r_w^2 \quad \text{and} \quad r_D = r/r_w$$

for a "Theis" aquifer where wellbore storage and skin effect are not negligible, the inner boundary conditions become in dimensionless form:

$$C_D \frac{ds_{w_D}}{dt_D} + \left[-\frac{\partial s_D}{\partial r_D}\right]_{r_D=1} = 1 \tag{54}$$

$$s_{w_D} = \left[s_D - S\left(\frac{\partial s_D}{\partial r_D}\right)\right]_{r_D=1} \tag{55}$$

where C_D is the dimensionless wellbore storage, S is the dimensionless skin factor and s_D is the dimensionless drawdown in the aquifer as defined for the line-source solutions. Usually, one solves the IBVP for s_D and then deduce s_{w_D} from it by considering these two conditions which introduce two new dimensionless parameters C_D and S to be determined from the interpretation of single-well tests. The dimensionless r_D is not a new parameter because the solutions can be considered as $s_{w_D}(t_D/r_D^2)$ in type curve analysis. The definition of C_D and S can be found in Earlougher (1977). Note that with equation 55 and this definition of S, the skin radius is assumed infinitely small and it is assumed that the additional drawdown created by the skin occurs under pseudo-steady-state flow conditions. For compressible skins of finite radius, we have discussed the validity of this assumption in section 4.4 of the previous chapter.

Considering equation 53 only, the cylindrical-line source solution for a "Theis" aquifer in the dimensionless Laplace space is:

$$\overline{s_D} = 2\, r_D K_o(\sqrt{p'})/p'\sqrt{p'}K_1(\sqrt{p'}/r_D) \tag{56}$$

where p' is the transform of $\alpha t/r_w{}^2$ and $r_D = r/r_w$. s_D is the aquifer dimensionless drawdown. For the case when both equations 54 and 55 are accounted for:

$$\overline{s_{w_D}} = \frac{2}{p'}\left\{\frac{K_o(\sqrt{p'}) + S\sqrt{p'}\,K_1(\sqrt{p'})}{\sqrt{p'}K_1(\sqrt{p'}) + C_D p'[K_o(\sqrt{p'}) + S\sqrt{p'}K_1(\sqrt{p'})]}\right\} \tag{57}$$

$\overline{s_{w_D}}$ is the well dimensionless drawdown and p' is the same as in 56.

Both solutions 56 and 57 are easily computed with the Stehfest numerical inverter.

For more complex aquifer systems, the reader is referred to existing literature. Specifically for the counterparts of the cases considered in this work for line-source solutions:

- solutions including equations 54 and 55 can be found in Mavor and Cinco (1979) for dual porosity systems; additional solutions are presented in Niko (1983) or Moench (1984);
- solutions for a two-layer system with and without cross-flow are presented in Appendix D for inclusion of equation 53; the case without cross-flow and including equation 54 only, is found in Wikramaratna (1984);
- solutions for a leaky system composed of one aquifer over- and under-lain by aquitards and including equations 54 and 55 are proposed by Moench (1985);

- to our knowledge, there is no existing solution that would include equations 53 and 54 and 55 for two-aquifer systems; although the obtention of Laplace space solutions is, in principle, possible, the practicality of such solutions may be questioned: it would include at least 6 dimensionless depending parameters!
- similarly there is no existing solutions for the case of viscoelastic systems that would include either of the inner boundary conditions; the same can be said about the case of combined flow regime since the line-source solutions are presented here for the first time.

The reader will easily verify that all of these existing solutions can be advantageously computed with the use of numerical (Stehfest) inverters. An important technology for single-well testing is the common use of slug-tests in hydrogeology and drillstem tests in reservoir engineering when the well is producing from low permeability zones and a constant pumping rate cannot be sustained during the duration of the test. For a "Theis" aquifer, solutions for slug test including wellbore storage are to be found in Cooper et al. (1967). For dual porosity systems, these have been extended by Barker and Black (1983) and the case of wellbore storage and skin effect is considered by Moench (1985). There are no solutions available for slug or drillstem tests in the case of the other complex systems considered in this study.

6. AQUIFER AND WELL PRODUCTIVITIES OF COMPLEX SYSTEMS

All the previous developments can be viewed as focusing towards this last chapter where we are presenting some methods to answer the crucial question in quantitative hydrogeology and reservoir engineering: what is the "safe" production (or injection) rate of a well tapping a system for which the geometry and the hydraulic properties are known to a certain degree? The system is confined or semi-confined, bounded or infinite. We define the aquifer (or the reservoir) productivity as a theoretical concept that may, however, have useful applications. Let us consider first the hydrogeological problem: an aquifer test has been conducted and analysed with all the precautions suggested in the previous chapters, The productivity of such a system is the theoretical rate that could be sustained over a given time period by an ideal well (no well loss, no skin effect, no wellbore storage) fully penetrating the selected component of that system for a given "available drawdown". We standardize the definition of the available drawdown as follows:

$$s_{av} = \frac{3}{4} h \tag{57}$$

where h is the distance between the piezometric head of the considered aquifer (at rest; t=0) and the top of that aquifer. The coefficient 3/4 represents a "security" to avoid the dewatering of the aquifer; it has also some connection with the position where a submerged pump would be best located if the aquifer were to be produced. Accepting these definitions and concepts, the aquifer productivity is defined by:

$$Q_{th} = 4\pi KH \frac{s_{av}}{s_D^*(t_D)} \tag{58}$$

where s_{av} is defined by 57 (and known) and $s_D^*(t_D)$ is a function that is computed making the following remarks. Recalling that t_D is of the form $\alpha t/r^2$, to evaluate t_D we need to normalize both r and t since α, the diffusivity, is known. We choose arbitrarily r=1m and give to t a flexible definition because it depends on the problem at hand. If one is only interested in the evaluation of a short-term productivity, then t may be 1 year or less; longer term productivities may be of the order of 10 to 25 years. The practitioner has to decide, but once t is defined, the productivity will refer to that period of exploitation. Then equation 58 is applied by using the particular function $s_D^*(t_D)$ used in the aquifer test interpretation, that is referring to the particular analytical model used and with the final set of hydraulic and geometric properties that have been obtained after aquifer test analysis. Note that the choice of r=1m will permit use of the most accurate r_D and thus the most adequate type curve in the family of type curves usually considered. The same for the other dimensionless groups a and b defined in this work for each model. Hence, the value of $s_D^*(t_D)$ can be accurately obtained by using the proper computer code presented in this study.

Although theoretical, the value of $(Qth)_t$ - the subscript t refers to the time period considered - can be very useful in decision-making for water resources management: it permits the comparison of aquifers between each other on a rational and homogeneous basis. For example, for a given system of large extension, one may map the various values of productivity that can be derived for the same time period by the proposed method and select the most suitable area for future developments on the basis of one single parameter $(Qth)_t$ that incorporates at best all the various hydraulic and geometric properties of the system.

This method is mostly limited to hydrogeological problems. In reservoir engineering, aquifer tests are not usually carried out for economical reasons related to the cost of drilling observation wells at great depths. Even when existing observation wells could be used, interference testing is not traditionally considered; however, Ramey (1982) suggests that this is likely to change in the comming years. With the usual technique of single-well tests, the determination of $s_D^*(t_D)$ is attached to a greater uncertainty because of early time perturbing effects. We have stressed the importance of the early time responses for a proper selection of the interpretative model for complex systems. Even when the wellbore storage and skin effect are considered, type curve analysis may remain ambiguous because of the "parallel" character of the type curves. Also, one may question the representativity of the hydraulic and geometric properties deduced from single-well test analysis. Hence, the proposed method for evaluating the reservoir productivity is less reliable in reservoir engineering when interference tests have not been conducted; this could also be extended when the produced fluid is compressible (gas).

The concept of well productivity may be deduced from the preceeding one although a more detailed analysis is necessary. One is now interested by the production of a real well that has been drilled, equipped and developed in a particular fashion and equation 58 has to be modified to account for additional well loss. We propose to solve by trial and error the following equation:

$$s_{av} = \frac{(Q_{th})}{4\pi KH} \; s_D^*(t_D) + \Delta s$$
$$\Delta s = A(Q_{th})_t + B(Q_{th})_t^n \qquad (59)$$

where the coefficient A refers to well loss due to partial penetration, flow through the well screen, skin effect and wellbore storage. The coefficients B and n are related to flow in the casing ($n=2$) and to all possible turbulent effects in the formation and in the gravel pack. The definition of s_{av} is generally given by 57 although in specific conditions, s_{av} may be imposed by technical and economical considerations. The determination of A, B and n can be determined through a combination of step-test and type curve analysis as proposed in Sauveplane (1982). The calculation of $s_D^*(t_D)$ usually requires data from aquifer tests and is the same as for the aquifer productivity. Several calculations conducted by the author show that $(Q_{th})_t$ determined with 58 can be up to an order of magnitude greater than $(Q_{th})_t$ obtained with 59. An overview discussion of the coefficients A, B and n can be found in Ramey (1982).

CONCLUSIONS

Detailed (partial) conclusions as well as practical recommendations are developed at the end of each section or chapter and we shall focus here on the main highlights and on possible avenues of research suggested by this study.

One may deplore that within the limited scope of this work aquifer test data have not been treated as examples of the use of the models and proposed techniques of analysis; although practical recommendations are made whenever appropriate, we recognize that our approach remains in that sense "theoretical". Also linear and spherical flow regimes have not been considered nor the case of aquifers bounded by single or multiple linear discontinuities; finally, the important case of partial penetration has not been treated. In the first three instances, solutions can be found in a straightforward fashion using integral transforms and the principle of superposition; in the last case, finite Fourier or Hankel transforms are more appropriate than the infinite Hankel transform proposed in Figure 2 and Laplace space solutions are in the form of infinite series. However, this last method may lead to untractable solutions in the general cases of multiple-aquifer, dual porosity, multilayered and radially composite systems considered here; reductive assumptions concerning the nature of leakage, interporosity flow and crossflow have to be made to obtain analytical solutions.

In spite of these well-recognized limitations, the major achievements of this research are:

1. A consistent and efficient method of deriving, formulating and calculating analytical solutions by means of integral transforms and approximate inversion of Laplace transforms; full time scale type

curves for complex aquifer systems are shown to be easily calculated with the help of numerical inverters and fast computers within very acceptable degrees of accuracy when these results are compared to more complicated calculations of real space solutions; the steps are: obtention of Laplace space solutions, transformation in the dimensionless Laplace space and type curve generation with appropriate computer codes. When a lesser degree of accuracy and intermediate to late time solutions are sufficient, analytical inverters may also be used with some precautions and the simple use of tables and hand calculators. It is clear that a useful area of research is the transfer of the numerical inverter capability to microcomputers; this does not appear to be an insurmountable task in software development; one may take advantage of the asymptotic solutions presented in this study over discrete time domains.

2. A detailed sensitivity analysis to flow parameters of the various components has been conducted with the help of 1 (above) for the two and three-aquifer systems which represent the most complex and analytical models for leaky systems (forms of the solutions and "realism" of the assumptions). It is shown that reductive assumptions used in simpler models have no realistic base over a wide range of depending parameters and that the use of these models should be encouraged together with the proposed methods of type curve evaluation; type curve evaluation could be done for the first time for the three-aquifer model for which the shape of the type curves do not differ significantly from the two-aquifer case; a step-by-step procedure is deduced for analysing test data in three-aquifer systems.

3. For dual porosity and uniformly fractured aquifers, it is first demonstrated that the s-shaped type curves obtained on log-log scales with the assumption of pseudo-steady-state interporosity flow are not typical of such systems and it is postulated that observed similar shapes of observation well responses are caused by the commonly occurring phenomenon of fracture skin combined with transient interporosity flow. Also, the use of more appropriate type curves accounting for transient interporosity flow is delicate for the interpretation of the major features of fracture network geometry from aquifer test data. In addition, semi-log analysis of responses should be discouraged as too unreliable.
4. An important limitation of 1 (above) and analytical or semi-analytical models is illustrated for the general case of cross-flow in a two-layered aquifer: dimensionless Laplace space solutions can be derived, but could not be evaluated. The reductive assumption of "no cross flow" does not present this difficulty. We present an important early time asymptotic solution for the cross flow case, i.e. that cross flow can be neglected within a defined time domain. Late time asymptotic solutions for that case have also been proposed by other authors, but the full time scale evaluation of this model remains an open problem.
5. Solutions are presented for both inner and outer regions of a radially composite aquifer; in the latter case, type curves are hardly departing from a Theis type curve for reasonable values of depending parameters. An interesting feature of drawdown reversal for the type curves of the inner region is evidenced for the first time in the subregion close to the radial discontinuity. This

peculiarity similar to the "Noordbergum effect" described by Verruijt for leaky systems may be advantageously used in the design of aquifer tests for a complete characterization of the radially composite aquifers.

6. It is shown that the similarity of type curves for the viscoelastic model, for the models of an unconfined aquifer with delayed yield and of a dual porosity system with the assumption of pseudo-steady-state interporosity flow is not mathematically a surprise.
7. The non-linear equations for a composite regime in highly permeable aquifer materials are solved by means of the Boltzmann transformation; these new solutions permit with aquifer tests conducted in such aquifers, evaluation of both coefficents a (linear regime) and b (post-linear regime) of the Forchheimer equation. The model is derived without any reductive assumptions aimed at a quasi-linearization of the problem, but the solution could only be obtained for the simplest case of the Theis assumptions for the aquifer. It is demonstrated that in this instance less drawdown than in the linear case (the Theis solution) occurs at early times, but considerably more drawdown can be expected at late times when b increases.
8. Reasoning in the Laplace space with approximate inverters opens a new area of test interpretations based on type curves referring to the time derivative of the drawdowns. This technique is found to be particularly useful for dual porosity systems, with transient interporosity flow and for the newly derived solution of an aquifer with composite flow regime.

9. Finally, a unifying definition and method of evaluation of aquifer and well productivities is proposed. It has the major advantage of being accurate and permitting rational comparisons between both aquifers and wells. It is, in fact, based on one of the many predictive capabilities of analytical models and require properly designed, conducted and interpreted aquifer and well tests.

We hope that this work will help to develop a new enthusiasm for the use of analytical models for both the characterization (with aquifer and well tests) and the predictive assessment of complex aquifer systems. With our general proposition of reasoning in the Laplace space (for reasonably well-behaved solutions), we believe that an important class of flow problems can be considered with more realistic assumptions and less limitations for type curve analysis. An equally important amount of information about these systems of common occurrence can be derived. A rational approach to the difficult task of model selection based on available information can be undertaken with a trial and error procedure aimed at verifying initial hypothesis about the system. This is made possible by the new capability of obtaining very quickly and accurately type curves for the considered models. With that respect, one may view this study as the necessary footwork towards the development of an "expert system" that would render semi-automatic the analysis of the responses of the complex aquifer systems (and a fortiori of simpler systems). Such software could greatly accelerate and ease the procedures of selecting a model and type curve matching with a given model; visual displays on a terminal screen at different stages of the process would constitute the necessary controls. Least square fitting and non-linear programming could be added as well-established techniques to the "intelligence" of the software system. A modular approach would be best suited. We think that this area of research is probably the most promising outcome of our study.

REFERENCES

Abramowitz, M. and Stegun, I.A. (1972): Handbook of mathematical functions; Tenth Printing, Dover Publications Inc., New York, pp.1045.

Agarwal, R.G., Al Hussainy, R. and Ramey, H.J., Jr. (1970): An investigation of well bore storage and skin effect in unsteady liquid flow, 1. Analytical Treatment, Soc. Pet. Eng. J., 10(3), p. 279

Alfrey, T. (1944): Non-homogeneous stress in viscoelastic media, Quart. Appl. Mech. 2, pp. 113-119.

Asfari, A. and Witherspoon, P.A. (1973): Numerical simulation of naturally fractured reservoirs, SPE 4290, Proc. of 3rd Numerical Simulation of Reservoir Performance, SPE of AIME, Houston, Texas, (January 10-12, 1973).

Barenblatt, G.I., Zheltov, I.P. and Kochina, N. (1960): Basic concepts in the theory of seepage of homogeneous liquids in fissured rocks, Prikl. Mat. Mekh. 24, pp. 852-864, in Russian.

Barker, J.A. and Black, J.H. (1983): Slug tests in fissured aquifers, Water Resour. Res. 19(6), pp.1558-1564.

Bellman, R., Kalaba, R.E. and Lockett, J.A., Jr. (1966): Numerical inversion of the Laplace transform, Elsevier, New York.

Bennett, C.O., Camacho, R.G., Reynolds, A.C. and Raghavan, R. (1985): Approximate solutions for fractured wells producing layered reservoirs, Soc. Pet. Eng. J., October, pp.729-742.

Boulton, N.S. (1954): Unsteady radial flow to a pumped well allowing for delayed yield from storage, Bull. IAHS, No. 37, pp. 472-477.

Boulton, N.S. (1963): Analysis of data from non-equilibrium pumping tests allowing for delayed yield from storage, Proc. of Inst. of Civil Engineering, 26(6693), pp.469-482.

Boulton, N.S. and Streltsova, T.D. (1977a): Unsteady flow to a pumped well in a fissured water-bearing formation, J. of Hydrology, 35, pp. 257-269.

Boulton, N.S. and Streltsova, T.D. (1977b): Unsteady flow to a pumped well in a two-layered water-bearing formation, J. of Hydrology, 35, pp. 256-256.

Brutsaert, W. and Corapcioglu, Y.M. (1976): Pumping of aquifer with viscoelastic properties, J. of Hydraulics Division ASCE, 102, HY11, November, pp. 1663-1675.

Burrell, K.H. (1974): Evaluation of the modified Bessel functions $K_0(z)$ and $K_1(z)$ for complex arguments, Algorithm 484, Comm. ACM, 17(9), September, pp. 524-526.

Carslaw, H.S. and Jaeger, J.C. (1959): Conduction of heat in solids, Oxford University Press, London, 2nd edition, 510 p.

Chorley, D.W. and Frind, E.O. (1978): An iterative quasi-three-dimensional finite element model for heterogeneous multiaquifer systems, Water Resources Research, 15, p. 943.

Cooper, H.H., Jr. (1966): The equation of groundwater flow in fixed and deforming coordinates, J. of Geophys. Res. 71(20).

Cooper, H.H., Jr., Bredehoeft, J.D. and Papadopulos, I.S. (1967): Response of a finite-diameter well to an instantaneous charge of water, Water Resources Research, 3(1), pp. 263-269.

Corapcioglu, Y.M. and Brutsaert, W. (1977): Viscoelastic aquifer model applied to subsidence due to pumping, Water Resources Research, 13(3), pp. 597-604.

Cost, T.L. (1963): Approximate Laplace transform inversion techniques in viscoelastic stress analysis, Rohm and Hass Co., Quart. Progr. Rept. on Eng. Res. Rept P63-13, July.

Cost, T.L. (1964): Approximate Laplace transform inversions in viscoelastic stress analysis, AIAA Journal, 2(12), pp. 2157-2166.

Crump, K.S. (1976): Numerical inversion of Laplace transforms using a Fourier series approximation, JACM, 23(1), January, pp. 89-96.

Darcy, H. (1856): Les fontaines publiques de la ville de Dijon, Victor Dalmont, Paris.

Davis, S.N. (1969): Porosity and permeability of natural materials, in Flow through Porous Media (R.J.M. de Wiest, editor), Academic Press, New York, pp. 54-90.

de Boor, C. (1971): CADRE: an algorithm for numerical quadrature, Math. Software (John R. Rice, editor), Academic Press, New York, chapter 7.

de Swaan, O.A. (1976): Analytical solutions for determining naturally fractured reservoir properties by well testing, Soc. Pet. Eng. J., June, pp. 117-122.

de Wiest, R.J.M. (1965): Geohydrology, Wiley, New York.

de Wiest, R.J.M. (1966): On the storage coefficient and the equations of groundwater flow, J. of Geophys. Res., 71, pp. 1117-1122.

de Wiest, R.J.M. (1969): Fundamental principles of groundwater flow, in Flow through Porous Media (R.J.M. de Wiest, editor), Academic Press, New York, pp. 1-52.

Delhomme, J.P. (1984): Distribution spatiale des permeabilites dans les milieux poreux souterrains: moyens d'etude et modelisation, Ann. des Mines, 5-6, May-June, pp. 113-126, in French.

Durbin, P. (1974): Numerical inversion of Laplace transforms: an efficient improvement of the Dubner and Abate's methods, Comp. J. 17, pp. 371-376.

Duvaut, G. (1961): Drainage des systems heterogenes, Revue IFP XVI, October, 10, pp. 1165-1181, in French.

Earlougher, R.C. (1977): Advances in well test analysis, 2nd printing, Monograph vol. 5, H.L. Doherty Series SPE of AIME, New York and Dallas, pp. 264.

Forchheimer, Ph. (1924): Hydraulik, Teubner, Leipzig and Berlin, pp. 566, in German.

Frind, E.O. (1979): Exact aquitard response functions for multiple aquifer mechanics, Adv. in Water Resour., 2, June, pp. 77-82.

Gao Cheng-Tai (1984): Single-phase fluid flow in a stratified porous medium with cross flow, Soc. Pet. Eng. J., February, pp. 97-106.

Gaver, D.P. (1966): Observing stochastic processes and approximate transform inversion, Oper. Res. 14(3), pp. 444-459.

Gringarten, A.C. (1982): Flow test evaluation of fractured reservoirs, in Recent Trends in Hydrogeology, GSA Special Paper 189, Boulder, Colorado, pp. 237-263.

Gringarten, A.C. and Witherspoon, P.A. (1972): A method of analyzing pumping test data from fractured aquifers, in Proc. Symposium on Percolation in Fissured Rocks ISRM, Stuttgart, 3, pp. B1-B9.

Hantush, M.S. (1949): Plain potential of groundwater with linear leakage, Trans. Am. Geophys. Union, 35, p. 917.

Hantush, M.S. (1956): Analysis of data from pumping tests in leaky aquifers, Trans. Am. Geophys. Union, 37, p. 702.

Hantush, M.S. (1960): Modification of the theory of leaky aquifers, J. of Geophys. Res., 65(11), pp. 3713-3725.

Hantush, M.S. (1964): Hydraulics of wells, Adv. in Hydrosciences 1, (V.T. Chow, editor), Academic Press, New York, pp. 281-432.

Hantush, M.S. and Jacob, C.E. (1956): Nonsteady radial flow in an infinite leaky aquifer, Trans. Am. Geophys. Union, 36, p. 95.

Hantush, M.S. and Thomas, R.G. (1966): A method for analyzing a drawdown test in anisotropic aquifers, Water Resour. Res. 2(2), pp. 281-285.

ter Haar, D. (1951): An easy approximate method of determining the relaxation spectrum of a viscoelastic material, J. of Polymer Sci., 6, p. 247.

Hemker, C.J. (1984): Steady groundwater flow in leaky multiple-aquifer systems, J. of Hydrology, 72, pp. 355-374.

Hemker, C.J. (1985): Transient well flow in leaky multiple-aquifer systems, J. of Hydrology, 81, pp. 111-126.

Herrera, I. and Rodarte, L. (1973): Integrodifferential equations for systems of leaky aquifers and applications. 1. The nature of approximate theories, Water Resour. Res., 9, p. 995.

Herrera, I., Hennart, J.P. and Yates, R. (1980): A critical discussion of numerical models for multiaquifer systems, Adv. in Water Resour. 3(4), pp. 159-163.

Hubbert King, M. (1956): Darcy's law and the field equations of the flow of underground fluids, J. of Pet. Techn., October, p. 222.

Hunter, D.B. (1964): The calculation of certain Bessel functions, Math. Comp. 18, pp. 123-128.

Hurst, W. (1981): Advances in Petroleum Engineering, PennWell Publishing Co., Tulsa, Oklahoma, p. 382.

Jacob, C.E. (1950): Flow of groundwater in Engineering Hydraulics, (H. Rouse, editor), John Wiley and Sons, New York, Chapter 5.

Jacquard, P. (1960): Etude mathematique du drainage d'un reservoir heterogene, Revue IFP, XV, 10, pp. 1384-1400 (in French).

Javandel, I. (1982): Analytical solutions in subsurface fluid flow, in Recent Trends in Hydrogeology, GSA Special Paper 189, Boulder, Colorado, pp. 223-235.

Javandel, I. and Witherspoon, P.A. (1980): A semi-analytical solution for partial penetration in two-layer aquifers, Water Resour. Res., 16(6), pp. 1099-1106.

Jenkins, M.A. and Traub, J.F. (1972): Zeros of a complex polynomial, CACM, 15(2), pp. 97-99.

Knebel, G.M. and Rodriguez-Eraso, G. (1956): Habitat of some oil, Bull. Am. Pet. Geol. 40(4), pp. 547-564.

Kazemi, H., Seth, M.S. and Thomas, G.W. (1969): The interpretation of interference tests in naturally fractured reservoirs with uniform fracture distribution, Soc. Pet. Eng. J., 4(4), pp. 463-472.

Kucuk, F. and Sawyer, W.K. (1980): Transient flow in naturally fractured reservoirs and its application to Devonian gas shales, Proc. 55th Fall Conf. SPE, Dallas, SPE9397, September.

Lindquist, E. (1933): On the flow of water through porous soil, Proc. 1st Congress of ICOLD, Stockholm.

Lohman, S.W. (1972): Groundwater hydraulics, US Geological Survey Prof. Paper 708, 70 pp.

Louis, C. (1969): A study of groundwater flow in jointed rock and its influence on the stability of rock masses, Imp. College, U. of London, Res. Rept. 10 on Rock Mechanics.

Louis, C. (1975): Introduction a l'hydraulique des roches, These de doctorat, Universite Paris VI, Paris (in French).

Matheron, G. (1967): Elements pour une theorie des milieux poreux, Masson, Paris (in French).

Mavor, M.J. and Cinco, H. (1979): Transient pressure behaviour of naturally fractured reservoirs, Proc. California Reg. Meeting SPE of AIME, Ventura, California, April.

Moench, A.F. and Ogata, A (1984): Analysis of constant discharge wells by numerical inversion of Laplace transform solutions, in Groundwater Hydraulics, Wat. Resour. Monograph Series No. 9, AGU editor, Washington, pp. 146-170.

Moench, A.F. (1984): Double-porosity models for a fissured groundwater reservoir with fracture skin, Water Resour. Res. 20(7), pp. 831-846.

Moench, A.F. (1985): Transient flow to a large-diameter well in an aquifer with storative semi-confining layers, Water Resour. Res. 21(8), pp. 1121-1131.

Mongan, C.E. (1985): Validity of Darcy's law under transient conditions, USGS Prof. Paper 1331, Washington, 16 pp.

Muskat, M. (1946): The flow of homogeneous fluids through porous media, J.W. Edwards Inc. editor, Ann Arbor, Michigan, First Edition, Second Printing, 763 pp.

Narasimham, T.N. and Kanehiro, B.Y. (1980): A note on the meaning of storage coefficient, Water Resour. Res., 16(2), pp. 423-429.

Narasimhan, T.N. and Witherspoon, P.A. (1969): Unified numerical model for saturated-unsaturated flow in deformable porous media, 1. Theory, Water Resour. Res. 13(3), pp. 657-664.

Neuman, S.P. and Witherspoon, P.A. (1969): Transient flow of groundwater to wells in multiple aquifer systems, Geotech. Eng. Publication 69-1, Dept. of Civil Eng., University of California (Berkeley), 182 pp.

Niko, H. (1983): Well test interpretation in heterogeneous reservoirs with skin and afterflow: some new theoretical solutions and general field experience, Proc. 58th SPE Conf. (SPE 11964), San Francisco, October.

Odeh, A.S. (1965): Unsteady state behaviour of naturally fractured reservoirs, Soc. of Pet. Eng. J., 17(3), p. 245.

Papadopulos, I.S. (1965): Nonsteady flow to a well in an infinite anisotropic aquifer, in Proc. IAH Dubrovnik Symp. on Hydrology of Fractured Rocks, 1, pp. 21-31.

Piessens, R. (1971): Gaussian quadrature formulae for the numerical integration of Bromwich's integral and the inversion of Laplace transforms, J. Eng. Math. 5(1), pp. 1-9.

Pottier, J. (1961): Modeles heterogenes avec communications, Revue IFP XVI, 10, October, pp. 1127-1146 (in French).

Prats, M. (1972): The influence of oriented arrays of thin impermeable shale lenses or highly conductive natural fractures on apparent permeability anisotropy, J. of Pet. Techn., 22(1), p. 97.

Ramey, H.J., Jr. (1982): Well loss function and the skin effect: a review, in Hydrogeology, GSA Special Paper 189, Boulder, Colorado, pp. 265-271.

Romm, E.S. (1966): Flow phenomena in fractured rocks, Moscow, Nedra (in Russian).

Rosa, A.J. and Horne, R.N. (1983): Automated type-curve matching in well test analysis using Laplace space determination of parameter gradients, Proc. 58th Conf. SPE of AIME (SPE 12131), San Francisco, pp. 1-15.

Saad, K.F. (1967): Determination of the vertical and horizontal permeabilities of fractured water-bearing formations, Bull. IAHS, 3, p. 22.

Sauveplane, C.M. (1982): Skin effect and well loss evaluation: a critical review of concepts and methods, Proc. of 2nd National IAH Conf., Winnipeg, February, pp. 99-107.

Sauveplane, C.M. (1984a): On the use of approximate analytical inversion of Laplace transform solutions for radial flow problems, Proc. Int. IAH Symp. on Groundwater Resour. Utilization and Contaminant Hydrogeology, Montreal, May, pp. 197-215.

Sauveplane, C.M. (1984b): Pumping test analysis in fractured aquifer formations, in Groundwater Hydraulics, Water Resour. Monograph Series No. 9, AGU editor, Washington, pp. 171-206.

Sauveplane, C.M., Bachu, S. and Hitchon, B. (1986): Comparison of analytical and numerical methods for evaluating cross-formational flow and selecting the preferred injection aquifer, Swan Hills, Alberta, Canada, in Proc. of Int. Symposium on Subsurface Injection of Liquid Wastes, New Orleans, pp. 485-508.

Schapery, R.A. (1961): Approximate methods of transform inversion for viscoelastic stress analysis, Proc. US Nat. Congress on Appl. Mech., 4th, pp. 1075-1085.

Scheidegger, A.E. (1963): The physics of flow through porous media, revised ed., Univ. of Toronto Press., 308 pp.

Schoeller, H. (1962): Les eaux souterraines, Masson, Paris, (in French).

Sen, Z. (1986): Aquifer test analysis in fractured rocks with linear flow pattern, Groundwater, 24(1), pp. 72-78.

Snow, D.T. (1968): Anisotropic permeability of fractured rocks, in Hydrology of flow through porous media (Muskat volume), R.J.M. de Wiest, editor, New York, Academic Press.

Stehfest, (1970): Algorithm 368: Numerical inversion of Laplace transforms, Comm. ACM, January, pp. 47-49.

Sternberg, Y.M. (1969): Some approximate solutions of radial flow problems, J. of Hydrology, 7, pp. 158-166.

Streltsova, T.D. (1976): Hydrodynamics of groundwater flow in a fractured formation, Water Resour. Res., 12(3), pp. 405-414.

Streltsova, T.D. (1982): Well hydraulics in vertically heterogeneous formations, J. of Hydraul. Div., ASCE, vol. 108, HY11, November, pp. 1311-1327.

Streltsova, T.D. (1984): Buildup analysis for interference tests in stratified formations, Soc. of Pet. Eng. J., February, pp. 301-310.

Streltsova-Adams, T.D. (1978): Well hydraulics in heterogeneous aquifer formstions, Adv. in Hydrosciences 11, V.T. Chow, editor, Academic Press, New York, pp. 357-423.

Taylor, D.W. and Merchant, W. (1940): A theory of clay consolidation accounting for secondary compression, J. of Math. and Physics, 19(3), pp. 167-185.

Theis, C.V. (1935): The relationship between the lowering of the piezometric surface and the rate and duration of a well using groundwater storage, Trans. Am. Geophys. Union 16, pp. 519-524.

Thirriot, C. (1969): Hydrodynamics of flow through porous media, Proc. 13th IAHR Congress, Kyoto, Japan (in French).

Verruijt, A. (1969): Elastic storage of aquifers, *in* Flow through porous media, R.J.M. de Wiest, editor, Academic Press, New York, pp. 331-376.

Warren, J.E. and Root, P.J. (1963): The behavior of naturally fractured reservoirs, Soc. of Pet. Eng. J., 3(3), p. 245.

Widder, D.V. (1946): The Laplace transform, Princeton University Press, Princeton, N.J.

Wikramaratna, R.S. (1984): An analytical solution for the effects of abstraction from a multiple-layered confined aquifer with no cross-flow, Water Resour. Res., 20(8), pp. 1067-1074.

Wynn, P. (1958): On a device for computing the $e_m(S_n)$ transformation, MTAC 10, pp. 91-96.

APPENDIX A

DERIVATION OF THE DIFFUSION EQUATION

We are seeking a relationship describing the movement of a particle of fluid as a function of its position, of time and of the physical characteristics of both the fluid and the saturated medium in which it is moving. In continuum mechanics, such a problem requires consideration of the equations of state and of the principles of mass and energy conservations. These equations may then be merged in the equation of motion. The main assumptions are underlined in the following development.

(a) Equation of State

Any phase - solid, liquid or gas - can be characterized by different parameters that are either specific or of state. As an example, a fluid may be described by its density:

$$\rho = f(\theta, p) \qquad \text{(A1)}$$

but pressure p and temperature θ are related by the thermodynamic relationship:

$$h(p, \theta, \lambda) \equiv 0 \qquad \text{(A2)}$$

where λ can be the enthalpy, the specific heat, etc.
In practice, for groundwater flow, the temperature gradients are small

enough to permit the hypothesis of isothermal flow. It follows that the specific parameters are only pressure dependent. Muskat (1946) and Scheidegger (1963) write:

$$\rho = \rho_0 \, (p/p_0)^m \, \exp[\beta(p-p_0)] \qquad \text{(A3)}$$

where the subscript 0 refers to the normal conditions of 1 g/cm^3 and 1 atm (101.3 kPa) for the density and pressure, respectively; m is a coefficient that can be neglected for a slightly compressible fluid like water and β is the coefficient of compressibility of the fluid [$M^{-1}LT^2$] that depends both on pressure and temperature (Davis, 1966 and de Wiest, 1966). For incompressible fluids, $\beta = 0$.

For water, assuming low pressure gradients, equation A3 can then be approximated with the first term of the series development of the exponential function as:

$$\rho \simeq \rho_0[1+\beta(p-p_0)] \qquad \text{(A4)}$$

that can be differentiated as:

$$\partial\rho = \beta\rho\partial p \qquad \text{(A5)}$$

For water under isothermal conditions, we may assume that the viscosity is constant. Equation A5 is the same as equation 37 in de Wiest (op.cit.) although not obtained in the same way.

(b) Continuity Equation (Mass Conservation)

Let us consider an elemental representative volume ΔV of the porous medium (a parallelepiped $\Delta x \Delta y \Delta z$ in cartesian coordinates) which is statistically homogeneous (sensu Matheron, 1967). The implications of that assumption are discussed in section 1.2.2 of the main text, together with the various levels of heterogeneity and the changes of scale. The velocity vector U (U_x, U_y and U_z) is reported to the total area through which the fluid circulates; it is the specific discharge or Darcy velocity. The knowledge of U at each time t describes unequivocally the movement. The mass conservation principle states that during a time dt, the fluid mass increase within ΔV is equal to the difference between the mass inflow through some sides of the volume and the mass outflow through the opposite sides.

Performing the mass balance between inflow and outflow through each side of the volume leads to: $-\mathrm{div}(\rho U)\Delta x\ \Delta y\ \Delta z\ dt$ where (div) is the divergence operator $[(\partial/\partial x) + (\partial/\partial y) + (\partial/\partial z)]$.

If the porosity is n, the original mass of fluid in the volume is $n\rho\Delta V$.

During the time dt, its variation is:

$$\frac{\partial(n\rho\Delta x\ \Delta y\ \Delta z)}{\partial t}\ dt$$

If both the fluid and the granular skeleton are compressible, then all the terms in parenthesis are variable.

We next assume that the granular skeleton can only be compressed or decompressed in the vertical direction; this simplification is physically sound in the cases of fluid withdrawal or injection by wells mainly considered in this study. This assumption implies that Δx and Δy are not time-dependent. The quantity to evaluate is thus $[\partial(n\rho\Delta z)]/\partial t$. Using the chain rule of differentiation:

$$\frac{\partial(n\rho\Delta z)}{\partial t} = \rho\Delta z\,\frac{\partial n}{\partial t} + \rho n\,\frac{\partial(\Delta z)}{\partial t} + n\,\Delta z\,\frac{\partial\rho}{\partial t} \qquad \text{(A6)}$$

The third term on the right-hand side of A6 is simply: $n\Delta z\rho\beta(\partial p/\partial t)$ making use of the equation of state A5.

Let c be the one-dimensional vertical compressibility of the granular skeleton of the medium treated as a continuum and σ_z is the vertical effective stress on the intergranular skeleton. By definition:

$$\frac{1}{c} = \frac{-d\sigma_z}{\partial(\Delta z)/\Delta z} \qquad \text{(A7)}$$

If we further assume that the total stress σ on the elemental volume remains constant and is the sum of the pore pressure p and of the intergranular stress, then $\sigma = \sigma_z + p$ = constant or $\partial(\sigma_z) = -\partial p$

$$\rho n\,\frac{\partial(\Delta z)}{\partial t} = -cn\rho\Delta z\,\frac{\partial(\sigma_z)}{\partial t} = +\,cn\rho\Delta z\,\frac{\partial p}{\partial t} \qquad \text{(A8)}$$

Note: Narasimhan and Witherspoon (1977) write:

$$\sigma = \sigma_z + xp \qquad \text{(A9)}$$

and then conclude that $x = 1$ is a valid assumption for the case of drained loading that we consider in this work ($p > p_o$). However, as noted by Narasimhan and Kanehiro (1980), equation A9 assumes a negligible compressibility of the solid grains themselves which is known to be smaller than that of the granular skeleton.

The final assumption to evaluate the first term of the right-hand side of A6 is that the volume of solid grains $\Delta V_s = (1-n)\Delta x\Delta y\Delta z$ remains constant. de Wiest (op.cit.) justifies this assumption by stating that the compressibility of the solid grains is much smaller than c and smaller than β. Physically, it means that the deformation of the medium is mostly by a rearrangement of the solid grains and not by a volume change of the grains themselves.

Because $\partial(\Delta V_s)=0$ and Δx and Δy are supposed constant, we have:

$$\partial(\Delta V_s) = \Delta x\Delta y\partial[\Delta z(1-n)] = \Delta x\Delta y\ [(1-n)\partial(\Delta z)-\Delta z\partial n] = 0$$

yielding:

$$\partial n = (1-n)[\frac{\partial(\Delta z)}{\Delta z}] = -c(1-n)\partial(\sigma_z)$$

and thus:

$$\rho\Delta z\ \frac{\partial n}{\partial t} = -\ c\rho\Delta z(1-n)\ \frac{\partial\sigma_z}{\partial t} = c\rho\Delta z(1-n)\frac{\partial p}{\partial t} \qquad \text{(A10)}$$

Finally, equation A6 becomes:

$$\frac{\partial(n\rho\Delta z)}{dt} = c\rho\Delta z(1-n)\frac{\partial p}{\partial t} + cn\rho\Delta z\ \frac{\partial p}{\partial t} + n\Delta z\rho\beta\ \frac{\partial p}{\partial t}$$

and

$$\frac{\partial(n\rho\Delta x\Delta y\Delta z)dt}{\partial t} = \frac{\partial(n\rho\Delta z)}{\partial t}\ \Delta x\Delta ydt = [\rho\frac{\partial p}{\partial t}\ (c + \beta n)]\ \Delta x\Delta y\Delta z\ dt$$

the mass conservation principle yields the equation of continuity:

$$-\mathrm{div}(\rho\overrightarrow{U}) = n\rho(\beta + \frac{c}{n})\ \frac{\partial p}{\partial t} \qquad \text{(A11)}$$

Note: Although we are apparently using the same approach, the right-hand side of equation A11 is different from equation 40 of de Wiest (op.cit.). Narasimhan and Kanehiro (op.cit.) note that the right-hand side of A11 depends on the volume used for normalization (in our case the bulk volume ΔV). They describe equation 40 of de Wiest as a "combined use" of ΔV_s and ΔV (with our notations) and write de Wiest's result (their equation 43 with our notations) as: $n\rho[\beta + (1-n)/n\, a_v] = n\rho[\beta + c/n]$ since $c = (1-n)\, a_v$. This is the same as in A11 and does not represent the result of de Wiest's equation 40 which is precisely: $n\rho\, [\beta + (1-n/n)c]$, with our notations.

The problem was further investigated and it was found that de Wiest (1966) questioned this derivation on the following grounds: when performing the mass balance through the parallelepiped between mass inflow and outflow, Δz is assumed constant while the variation of mass takes into account the deformation: Δz varies with time.

In his derivation, de Wiest assumes an undeformed elemental volume of the aquifer inside which the porosity changes with time "because of compaction of the medium". Further Cooper (1966) questioned de Wiest's approach that does not "distinguish between the rate of flow relative to the moving grains of the medium and the rate of flow across the fixed boundaries of his control volume while the material is deforming"; using fixed and deforming coordinates, Cooper (op.cit.) showed that equation A11 is essentially correct if one considers the coordinate z as the deforming coordinate.

(c) Fundamental Principle of Mechanics

Let us consider an unitary elemental volume of porous medium; the fluid in movement through it is submitted to the following forces (in vectorial notations):

- gravity forces $\overrightarrow{F_G} = n\rho\vec{g}$ ($\vec{g}$ is for unit mass of fluid)
- pressure forces $\overrightarrow{F_p} = -n\overrightarrow{\mathrm{grad}}\ p$ (similar derivation as for the continuity equation)
- viscosity forces friction fluid/grains $\overrightarrow{F_{v1}} = n\rho\vec{f}$ ($\vec{f}$ for unit mass)

  friction fluid/fluid $\overrightarrow{F_{V2}} = n[\mu\Delta\vec{U}+(\mu+\eta)\overrightarrow{\mathrm{grad}}\ (\mathrm{div}\vec{U})]$

  = tangential components + normal components

  The latter forces are external to the volume, along its sides. μ is the dynamic viscosity and η is the kinematic viscosity.

Fluid acceleration $\vec{\gamma} = (\partial\vec{U}/\partial t)+1/2\overrightarrow{\mathrm{grad}}U^2+\overrightarrow{\mathrm{curl}}(\vec{U}\blacksquare\vec{U})$

This is simply obtained by noting, for example, along Ox where $\vec{\gamma}$ component is (dU_x/dt):

$$dU_x = \frac{\partial U_x}{\partial t}dt+\frac{\partial U_x}{\partial x}dx+\frac{\partial U_x}{\partial y}dy+\frac{\partial U_x}{\partial z}dz$$

$$\frac{dU_x}{dt} = \frac{\partial U_x}{\partial t}+U_x\frac{\partial U_x}{\partial x}+U_y\frac{\partial U_x}{\partial y}+U_z\frac{\partial U_x}{\partial z}$$

$$\frac{dU_x}{dt} = \frac{dU_x}{dt}+U_x\frac{\partial U_x}{\partial x}+U_y\frac{\partial U_y}{\partial x}+U_z\frac{\partial U_z}{dx}+U_y\left[\frac{\partial U_x}{\partial y}-\frac{\partial U_y}{\partial x}\right]+U_z\left[\frac{\partial U_x}{\partial z}-\frac{\partial U_z}{\partial x}\right]$$

Writing the fundamental principle of mechanics and simplifying yields:

$$\overrightarrow{F_g}+\overrightarrow{F_p}+\overrightarrow{F_{V_1}}+\overrightarrow{F_{V2}} = n\rho\vec{\gamma}$$

$$\vec{f}-\frac{1}{\rho}\overrightarrow{\mathrm{grad}p}-\vec{g}+\left[\left(\frac{\mu}{\rho}\Delta\vec{U}+\left(\frac{\mu+\eta}{\rho}\right)\overrightarrow{\mathrm{grad}}(\mathrm{div}\vec{U})\right]=\frac{\partial\vec{U}}{\partial t}+\frac{1}{2}\overrightarrow{\mathrm{grad}}U^2+\overrightarrow{\mathrm{curl}}(\vec{U}\blacksquare\vec{U}) \quad \text{(A12)}$$

This is the macroscopic Navier-Stokes' law derived for the considered volume in vectorial form.

Note: in this equation, one of the dependent variables is Darcy's fictitious velocity U; it is thus different from the classical Navier equations derived for the real and microscopic velocities. This is consistant with our previous assumption of a statistically homogeneous volume of porous medium.

Assume now that $\overline{f}$, $\overline{g}$ and $\overline{U}$ are all deriving from a potential. It implies:

$\overline{f} = \overline{\text{grad}}F$

$\overline{g} = \overline{\text{grad}}(gz)$

$\overline{\text{curl}}(\overline{U}\blacksquare\overline{U}) \equiv 0$

Assume moreover that the velocity is not time-dependent or $\partial\overline{U}/\partial t = 0$ and that the external forces of viscosity $\overline{F_{v2}}$ are negligible compared to the internal ones (friction fluid/grains $\overline{F_{v_1}}$).

Equation A12 reduces to:

$$\overline{\text{grad}}F = 1/\rho\overline{\text{grad}}p + \overline{\text{grad}}\ (gz) + \frac{1}{2}\overline{\text{grad}}\ U^2 \qquad \text{(A13)}$$

which can be integrated between two points 1 and 2 as:

$$W_1^2 = [z + (p/\rho g) + (U^2/2g)]_1^2 \qquad \text{(A14)}$$

This is the generalized Bernouilli equation. It states physically that: the loss of energy of position, pressure and velocity between two points is equal to the dissipated internal energy W between these same points. This is the principle of conservation of energy.

In equation A14, the kinetic term $U^2/2g$ can be neglected in the case of groundwater flow because U is small.

By conducting one-dimensional experiments through sand columns, Darcy (1856) established an empirical relationship that can be expressed in the following vectorial form:

$$\vec{U} = -\bar{\bar{K}}\,\overline{\text{grad}}\,[z+(p/\rho g)] \tag{A15}$$

The quantity $\bar{\bar{K}}$ is the hydraulic conductivity tensor (LT^{-1}) and the quantity $[z+(p/\rho g)]$ is the energy per unit weight of fluid or hydraulic head (L) for water. Darcy's experiment represents an *a posteriori* justification of the fact that U derives from a potential.

The "proof" of equation A15 has been attempted by various researchers starting from the microscopic Navier equations for viscous flow (Hubbert, 1956; de Wiest, 1965 and Matheron, 1967); invariably, these derivations imply "statistical considerations and simplifications of the complicated microscopic flow picture" (de Wiest, 1969).

Assuming that the medium is *isotropic and homogeneous, i.e. K is not dependent on x, y or z*, the components of Darcy's velocity can be written as:

$$\left.\begin{aligned} U_x &= -K[(\partial p/\rho g\partial x)-(p/\rho^2 g)(\partial\rho/\partial x)] \\ U_y &= -K[(\partial p/\rho g\partial y)-(p/\rho^2 g)(\partial\rho/\partial y)] \\ U_z &= -K[(\partial p/\rho g\partial z)-(p/\rho^2 g)(\partial\rho/\partial z)+1] \end{aligned}\right\} \text{(A16)}$$

which from A5 can be written as:

$$\left.\begin{aligned} U_x &= (-K/\rho g)(1-\beta p)(\partial p/\partial x) \\ U_y &= (-K/\rho g)(1-\beta p)(\partial p/\partial y) \\ U_z &= -K[(1/\rho g)(1-\beta p)(\partial p/\partial z)+1] \end{aligned}\right\} \text{(A17)}$$

In this study and for a globally considered phenomenon, we admit that when velocities vary or when the kinetic terms are not negligible or for time-dependent Darcy velocity (Mongan, 1985), equation A15 still applies.

An interesting similitude between A15 and Poiseuille tubes for viscous flow can be developed to show that K may be written as:

$$K = \sum_i K_i s_i / s$$

where K_i and s_i are the hydraulic conductivity and sectional area of the tubes, respectively and s is the total area of the assembled tubes.

From this development, it can be concluded that:

$$\left.\begin{array}{l} \overline{\overline{K}} = \overline{\overline{k}}(\rho g/\mu) \\ U^* = U/n \end{array}\right\} \quad (A18)$$

where $k = (\Sigma s_i k_i)/s$ is the intrinsic permeability (L^2), μ is the fluid dynamic viscosity ($M\ L^{-1}T^{-1}$) and U^* is the real seepage velocity.

(d) Partial Differential Equation

We now combine equations A5, A11 and A15 which represent simplified versions of the equation of state, of mass and energy conservation, respectively. Consider the left-hand side of equation A11, that is $-\mathrm{div}(\rho U)$. Using A5, it can be expressed as:

$$-\mathrm{div}(\rho\vec{U}) = -\rho\,\mathrm{div}(\vec{U}) - \vec{U}\partial\rho = -\rho\,\mathrm{div}\vec{U} - \vec{U}\beta\rho\partial p$$

Replacing $\vec{U}$ by A15 yields:

$$-\mathrm{div}(\rho\vec{U}) = -\rho\,\mathrm{div}\vec{U} + \overline{\overline{K}}\beta\rho\ \overrightarrow{\mathrm{grad}}(z+[p/\rho g]).\overrightarrow{\mathrm{grad}}p$$

In equation A17, we may neglect βp with respect to unity. In these conditions, performing the scalar product of the two vectors on the right-hand side yields:

$$-\mathrm{div}(\rho\vec{U}) = -\rho\,\mathrm{div}\vec{U} + \frac{K\beta}{g}\left[\left(\frac{\partial p}{\partial x}\right)^2 + \left(\frac{\partial p}{\partial y}\right)^2 + \left(\frac{\partial p}{\partial z}\right)^2 + \rho g\left(\frac{\partial p}{\partial z}\right)\right]$$

If the pressure gradient is assumed to be low enough to neglect the terms in $(\ )^2$ and if it is small enough in the vertical direction, then:

$$-\mathrm{div}(\rho\vec{U}) = -\rho\,\mathrm{div}\vec{U} \tag{A19}$$

For a homogeneous and isotropic medium and for a fluid of constant density, defining the hydraulic head by $h = z + (p/\rho g)$ [L], the continuity equation A11 becomes:

$$\rho K\,\mathrm{div}(\overrightarrow{\mathrm{grad}}h) = n\rho^2 g\left(\beta + \frac{c}{n}\right)\frac{\partial h}{\partial t} \tag{A20}$$

since $\frac{\partial h}{\partial t} = \rho g \frac{\partial p}{\partial t}$

$\mathrm{div}(\overrightarrow{\mathrm{grad}}\ h)$ is the Laplacian operator $\Delta = \frac{\partial^2}{\partial x^2} + \frac{\partial^2}{\partial y^2} + \frac{\partial^2}{\partial z^2} \equiv \nabla^2$

Defining the specific storage $S_s = \rho g n[\beta + (c/n)]$ $[L^{-1}]$ as in Jacob (1950), the equation A20 takes the classical and simple form:

$$\Delta h = \frac{S_s}{K}\frac{\partial h}{\partial t} = \frac{1}{\alpha}\frac{\partial h}{\partial t} \tag{A21}$$

where α is the hydraulic diffusivity $[L^2T^{-1}]$.

Equation A21 is a linear parabolic partial differential equation similar to the heat diffusion equation for which solutions have been thoroughly analysed in the classical work of Carslaw and Jaeger (1959).

APPENDIX B

In this appendix, we ~~first present in~~ table form and without demonstration, the main properties of the integral transforms used in the derivation of analytical solutions to IBVPs. Then we will give a simple example to demonstrate their use.

1. One Dimensional Laplace Transformation

The letter "s" is used to represent drawdowns, as commonly done. Therefore, unconventionally, we call the Laplace transform parameter "p".

Original Function(s)	Image Function(s)	
$F(t)$	$f(p)=\int_0^\infty \exp(-pt)F(t)dt$	(B1)
$A\,F(t)+BG(t)$	$Af(p)+Bg(p)$	(B2)
$F'(t)$	$pf(p)-F(0+)$	(B3)
$F''(t)$	$p^2f(p)-pF(0+)-F'(0+)$	(B4)
$\int_0^t F(\tau)d\tau$	$f(p)/p$	(B5)
$\int_0^t F_1(t-\tau)F_2(\tau)d\tau=F_1{*}F_2$	$f_1(p)f_2(p)$	(B6)
$(1/t)F(t)$	$\int_p^\infty f(x)dx$	(B7)
$(1/c)F(t/c)\ c>0$	$f(cp)$	(B8)
1	$1/p$	(B9)

Inversion formula: $L^{-1}[f(p)]=1/(2\pi i)\int_{c+i\infty}^{c+i\infty} \exp(tp)f(p)dp$ (B10)

(Mellin inversion)

2. Infinite Zero Hankel Transform

Original Function(s)	Image Function(s)		
$G(r)$	$g(a)=\int_0^\infty rJo(ar)G(r)dr$		(B11)
$\int_0^\infty aJo(ra)g(a)da$ (inverse)	$g(a)$		(B12)
$\frac{1}{r}\frac{\partial}{\partial r}[r\frac{\partial G(r)}{\partial r}]$	$-a^2g(a) - \lim_{r\to 0}[r\frac{\partial G(r)}{\partial r}]$		(B13)
$(-1)^n\lambda^{2n}K_0(r\lambda)$	$\frac{a^{2n}}{a^2+\lambda^2}$	$n>0$ λ real	(B14)

3. Example: The Theis Solution

3.1 The IBVP

A perfectly confined, homogeneous and isotropic aquifer system of infinite extension, constant thickness H and zero slope whose initial hydraulic head h_0 is constant at all points is being produced (Q positive) or injected (Q negative) at a constant rate Q by a fully penetrating well of negligible radius. Water is released or accepted instantaneously by the aquifer following a pressure drop or increase. Find the transient solution $h(r,t)$ at a radial distance r from the well and after a time t of the described operation on the well?

Let us solve the drawdown case: the well is being pumped. We define the two-dimensional function $s(r,t)=h_0-h(r,t)$. The solution $s(r,t)$ for injection is strictly the same since the build-up is defined by $s(r,t)=h(r,t)-h_0$ and Q is negative. The IBVP for the function $s(r,t)$ in cylindrical polar coordinates can be written as (see equation A21 and the meaning of α and K in Appendix A):

1. $\frac{\partial^2 s}{\partial r^2} + \frac{1}{r}\frac{\partial s}{\partial r} = \frac{1}{\alpha}\frac{\partial s}{\partial t}$

2. $s(r,o+)=0$ (initial condition)

3. $s(\infty,t)=0$ $t>0$ (outer boundary condition) (B15)

4. $\lim_{r\to 0}\left(r\frac{\partial s}{\partial r}\right) = -\frac{Q}{2\pi KH}$ (inner boundary condition = Darcy's law at the well face)

We are going to find the analytical solution of this well-posed problem by three methods.

3.2 Use of Laplace Transform with respect to time

We define: $L[s(r,t)]=\bar{s}(r,p)$

From equation B3 and (2) of equation B15, the right-hand side (RHS) of the governing equation (1) in B15 is:

$$\frac{p\bar{s}}{\alpha}-0 = \frac{p\bar{s}}{\alpha}$$

The RHS of the inner boundary condition (4) is transformed into:

$$-\frac{Q}{2\pi KH} \times \frac{1}{p}$$

Because the transformation operates on the time variable only, both left-hand sides of (1) and (4) are just transformed by changing s into $\bar{s}$ but the partial differential operator becomes a total one. Also, the outer boundary condition (3) is not integrated in the resulting differential equation and we will have to verify that the ~~L~~aplace plane solution satisfies $\bar{s}(\infty,p)=0$ for all p. The transformed problem is thus:

$$\frac{d^2\bar{s}}{dr^2} + \frac{1}{r}\frac{d\bar{s}}{dr} - \frac{p\bar{s}}{\alpha} = 0$$

$$\lim_{r\to 0}\left(r\frac{d\bar{s}}{dr}\right) = -\frac{Q}{2\pi KH}\frac{1}{p} \qquad \text{(B16)}$$

The first equation of B16 is the Bessel differential equation whose solution is:

$\bar{s} = AIo(yr) + C\,K_0(yr)$ with $y^2=p/\alpha$

A = 0 to satisfy $\bar{s}(\infty,p)$ because $I_0(\infty)=\infty$ $(K_0(\infty)=0)$.

hence:

$$\bar{s} = C\,K_0\left[r\left(\frac{p}{\alpha}\right)^{1/2}\right] \qquad \text{(B17)}$$

The coefficient C is found by differentiating B17 with respect to r and using the second equation of B16:

$$r\frac{d\bar{s}}{dr} = -Cr\left(\frac{p}{\alpha}\right)^{1/2} K_1\left[r\left(\frac{p}{\alpha}\right)^{1/2}\right] \qquad \text{(B18)}$$

K_0 and K_1 are the modified Bessel functions of zero and first order, respectively. Noting that:

$\lim_{x\to 0}[xK_1(x)] = \Gamma(1)=1$ where Γ is the gamma function, then:

$C = \frac{Q}{2\pi KH}\frac{1}{p}$ and B17 becomes:

$$\bar{s} = \frac{Q}{2\pi KH}\frac{K_0[r(p/\alpha)^{1/2}]}{p} \qquad \text{(B19)}$$

This result satisfies the transformed outer boundary condition for all p since the function K_0 tends towards zero when its argument is infinite. The equation B19 can be used in further developments to study the asymptotic behaviour of more complex solutions in the Laplace space. To invert B19, we may use the property of equation B5 and obtain from the tables of Abramowitz and Stegun (1972, p. 1028):

$$L^{-1}\,[K_0[r(\frac{p}{\alpha})^{1/2}]]=\frac{1}{2t}\exp(-r^2/4\alpha t) \qquad \text{(B20)}$$

So that, without needing the complex inversion formula:

$$s(r,t)=\frac{Q}{2\pi KH}\int_0^t \frac{1}{2u}\ \exp(-r^2/4\alpha u)du \qquad \text{(B21)}$$

which by change of variable

$$z=\frac{r^2}{4\alpha u}\ ,\ \frac{du}{u}=-\frac{dz}{z}$$

$$s(r,t)=\frac{Q}{4\pi KH}\int_\infty^{r^2/4\alpha t} -\frac{\exp(-z)}{z}\,dz=\frac{Q}{4\pi KH}\int_{r^2/4\alpha t}^\infty \frac{\exp(-z)}{z}\,dz \qquad \text{(B22)}$$

that is:

$$s(r,t)=\frac{Q}{4\pi KH}\ E_1\ (\frac{r^2}{4\alpha t}) \qquad \text{(B23)}$$

where E_1 is the exponential integral function.

Defining the usual dimensionless groups: $s_D=[4\pi KHs(r,t)]/Q$ and $t_D=\alpha t/r^2$, the solution is: $s_D=E_1(1/4t_D)$ (B24)

This function often designed as the "well function" is tabulated and represents the exact solution of the Theis model. A single type-curve evaluated from equation B24 will represent that solution (usually plotted on log-log paper).

3.3 Successive Laplace and Hankel Transforms:

We consider the two successive transformations:

$L[s(r,t)]=\bar{s}(r,p)$

$H[\bar{s}(r,p)]=\bar{\bar{s}}(a,p)$

The first transformation leads to the first equation of B16 in section 3.2. Using equation B13, this equation is further transformed as:

$$-a^2 \bar{\bar{s}}(a,p) - \lim_{r \to 0} [r\frac{d\bar{s}}{dr}] - \frac{p}{\alpha} \bar{\bar{s}}(a,p) = 0 \tag{B25}$$

Since $\lim_{r \to 0} [r\frac{d\bar{s}}{dr}] = - \frac{Q}{2\pi KH} \frac{1}{p}$, the solution after both transformations has the simple algebraic form: $\bar{\bar{s}}(a,p) = \frac{Q}{2\pi KH} \frac{1}{p} \frac{1}{a^2+p/\alpha}$ (B26)

which by using the inverse transform of equation B14 for n=0 leads to the same Laplace space solution as in B19. This solution is then inverted as previously done.

For this simple case, the use of successive transforms was not really necessary but it shows that the expression obtained in B26 has a simple algebraic form. This result will be verified in more complicated cases where the Laplace space solution cannot be directly obtained as in section 3.2.

3.4 Use of Source Function

The exponential integral solution of the Theis model can be obtained even faster by using the line source of equation 6 (text) when $r' \to 0$ that is $I_0(\ ) \to 1$. the drawdown solution for an instantaneous line sink of infinitely small diameter is immediate:

$$s' = \frac{C}{4\pi\alpha t} \exp(-\frac{r^2}{4\alpha t})$$

where $C = Q/S_sH$ for the Theis model. Replacing t by (t-t') and integrating s' with respect to t' between 0 and t yields the exponential integral solution of B23.

APPENDIX C

1. TWO-AQUIFER SYSTEM: REVISED LAPLACE SPACE SOLUTIONS

Neuman and Witherspoon's solutions (1969) in the Laplace space are their equations II36, II37 and II38 that are written as:

$$\left.\begin{aligned}
\bar{s}_1\,(r,p) &= \frac{Q}{2\pi T_1 p}\left[\left(\frac{A_2-\zeta_1^2}{D}\right) K_o(\zeta_1 r) - \left(\frac{A_2-\zeta_2^2}{D}\right) K_o(\zeta_2 r)\right] \\
\bar{s}_2(r,p) &= \frac{Q}{2\pi T_1 p}\,\frac{B_2}{D}\left[K_o(\zeta_1 r) - K_o(\zeta_2 r)\right] \\
\bar{s}'\,(r,z,p) &= \bar{s}_2\, M \sinh(z\sqrt{p/\alpha'}) + \bar{s}_1\, M \sinh[(H'-z)\sqrt{p/\alpha'}]
\end{aligned}\right\} \quad (C1)$$

where:

$A_1(p) = p/\alpha_1 + K'/T_1 \sqrt{p/\alpha'} \coth(H'\sqrt{p/\alpha'})$

$A_2(p) = p/\alpha_2 + K'/T_2 \sqrt{p/\alpha'} \coth(H'\sqrt{p/\alpha'})$

$B_1(p) = K'/T_1 \sqrt{p/\alpha'}\ M$

$B_2(p) = K'/T_2 \sqrt{p/\alpha'}\ M$

$M = 1/\sinh(H'\sqrt{p/\alpha'})$

$D = [4B_1B_2+(A_1-A_2)^2]^{1/2}$

$\zeta_1^2 = \dfrac{A_1+A_2-D}{2}$

$\zeta_2^2 = \dfrac{A_1+A_2+D}{2}$

For the structural flow parameters, subscript 1 refers to the pumped (lower) aquifer, subscript 2 to the unpumped (upper) aquifer and superscript ' to the intervening aquitard. The principal dimensionless quantities are defined by:

- dimensionless drawdowns:

$$s_{D_1} = \frac{4\pi T_1 s_1}{Q},\ s_{D_2} = \frac{4\pi T_1 s_2}{Q},\ s'_D = \frac{4\pi T_1 s'}{Q}$$

where T=KH is the transmissivity $[L^2T^{-1}]$

- dimensionless time:

$$t_{D_1} = \frac{\alpha_1 t}{r^2}$$

Depending dimensionless groups can be defined by:

$$a = (T_1/T_2)^{1/2},\ b = (S'/S_1)^{1/2},\ c = (S_2/S_1)^{1/2},$$

$$r_D = r/H'(T'/T_1)^{1/2} = r/\sqrt{H_1H'}(K'/K_1)^{1/2},\ z_D = z/H'$$

where $S=S_sH$ is the storativity (dimensionless)

The set of equation C1 can be transformed into the dimensionless Laplace space using the property B8 (Appendix B, section 1) as follows:

Considering the principal dimensionless quantities and calling L' the dimensionless Laplace transform and p' the dimensionless Laplace parameter corresponding to t_{D_1}, we have:

$$L'(p') = \alpha_1/r^2\ L(p) \text{ with } p' = r^2/\alpha_1/p \tag{C2}$$

Introducing the dimensionless groups and replacing for p' gives for the subsidiary equations of (C1):

$$\left.\begin{aligned}
A &= a^2c^2p'+abr_D\sqrt{p'}\coth(b\sqrt{p'}/r_D) \equiv r^2A_2(p')\\
B &= p'+br_D\sqrt{p'}\coth(b\sqrt{p'}/r_D) \equiv r^2A_1(p')\\
G_1 &= br_DM'\sqrt{p'} \equiv r^2B_1(p') \text{ with } M' = 1/\sinh(b\sqrt{p'}/r_D)\\
G_2 &= abr_DM'\sqrt{p'} \equiv r^2B_2(p')\\
D^{*} &= [4G_1G_2+(B-A)^2]^{1/2} \equiv r^2D(p')\\
E &= (A+B-D')/2 \equiv r^2\zeta_1{}^2(p')\\
F &= (A+B+D')/2 \equiv r^2\zeta_2{}^2(p')
\end{aligned}\right\} \quad (C3)$$

Applying the relationship between L' and L and using the fact that, for example,

$\overline{s_{D_1}} = \frac{4\pi T_1 \overline{s_1}}{Q}$, we finally arrive at:

$$\left.\begin{aligned} \overline{s_{D_1}} &= \frac{1}{p'}\left[\left(\frac{A-B}{D^*}\right) +1\right) K_o(\sqrt{E}) - \left(\frac{A-B}{D^*}-1\right) K_o(\sqrt{F})\right] \\ \overline{s_{D_2}} &= \frac{2G_2}{p'D^*}\left[K_o(\sqrt{E}) - K_o(\sqrt{F})\right] \\ \overline{s'_D} &= \overline{s_{D_2}}\ M' \sinh\left(\frac{bz_D\sqrt{p'}}{r_D}\right) + \overline{s_{D_1}}\ M' \sinh\left[\frac{(1-z_D)b\sqrt{p'}}{r_D}\right] \end{aligned}\right\} \quad (C4)$$

where the quantities in C4 are defined by C3.

Computational Procedure

The ten equations of C3 and C4 are prepared as input functions for the Stehfest inverter that is applied five times to obtain the real space values of s_{D_1}, of s'_D at z_D=0.2, z_D=0.5 and z_D=0.8 and of s_{D_2} for a given set of numerical values for a, b, c and r_D and for the range of t_{D_1} betweem 0.02 and 100,000. The variable p' and the 10 equations defined by C3 and C4 are treated as real entities.

The code TWOAQ has been written in FORTRAN to perform the calculations of the five sets of values for each value of t_{D_1}; it presents the results in a 6-column table. All the calculations are made in arithmetic double-precision.

Because the calculations are conducted for a wide range of t_{D_1}, potential overflows may occur when the arguments of the hyperbolic functions coth and 1/sinh become too large. We have used the following approximations to avoid these computational problems.

Letting $\phi = \frac{b\sqrt{p'}}{r_D}$ be the argument of these functions, when $\phi > 10$, we use: $\coth \phi \approx 1+2 \exp(-2\phi)$

$$1/\sinh\phi \approx \exp(\ln 2-\phi)$$

When $\max(\phi,\ z_D\phi,\ (1-z_D)\phi)>10$, $M'\sinh(z_D\phi) \approx \exp[(z_D-1)\phi]$ and $M'\sinh[(1-z_D)\phi] \approx \exp(-z_D\phi)$.

For the other values of the arguments of the hyperbolic functions, we used the double-precision functions (tanh) and (sinh) of the VAX system. The values of the Bessel functions are obtained in double-precision by the IMSL subroutine MMBSK0.

Reduction to Theis Solution

Doing $K'=0$ for H' different of zero and $T_2\to\infty$ in the equations C3 and C4 is equivalent to $r_D=0$ and $a=0$. It follows that $A=0$, $B=p'$, $G_1=G_2=0$, $E=0$, $F=D=B$ so that the solution reduces to:

$$\bar{s}_{D_1} = \frac{2K_0(\sqrt{p'})}{p'}$$

which is the dimensionless Laplace transform of the Theis solution (equation 20 of text). The obtention of this result needed two pages of mathematical development with real space solutions in Neuman and Witherspoon (1969).

Reduction to Hantush Solutions

When the drawdown in the upper aquifer is neglected, $T_2\to\infty$ and $a=0$. In that case $A=G_2=0$, $D=B=F$ and $E=0$ yielding:

$$\bar{s}_{D_1} = \frac{2K_0(\sqrt{B})}{p'} = \frac{2}{p'}K_0\left\{\left[p'+br_D\sqrt{p'}\coth\left(\frac{b\sqrt{p'}}{r_D}\right)\right]^{1/2}\right\} \qquad \text{(C5)}$$

This result is the same as Hantush's modified solution that accounts for storage in the aquitard (Hantush, 1960). The asymptotic solutions in that case are:

Early Times:

When t_{D_1} is small, p' is large. In particular, when $\phi > 3$ (of the order $t_{D_1} < (b/3r_D)^2$), $\coth\phi = 1$ and $B = p' + br_D\sqrt{p'}$.

Equation C5 is readily inverted (Hantush, 1964, p. 303) as:

$$s_{D_1} = H(1/4t_{D_1}, br_D/4) \tag{C6}$$

Function H is both defined and tabulated in Hantush (op.cit. p. 312 and 313). The solution C6 is Hantush's "β" solution.

Long Times:

When t_{D_1} is small, p' is small. When $\phi < 0.4$ (of the order $t_{D_1} > (\frac{2.5b}{r_D})^2$), $\phi\coth\phi = 1 + \frac{\phi^2}{3}$, yielding $B = p'(1 + \frac{b^2}{3}) + r_D^2$.

Again, equation C5 can be readily inverted (Hantush, op.cit., p. 303) as:

$$s_{D_1} = W(\frac{\delta_1}{4t_{D_1}}, r_D) \equiv W(\delta_1 u, \frac{r}{B}) \tag{C7}$$

where u and r/B are Hantush's notations, and

$$\delta_1 = 1 + b^2/3 = 1 + S'/3S_1$$

The function W (u,r/B) is known as the "well function for leaky aquifers"; it is defined on p. 321 and tabulated on pp. 322-323 of Hantush (op.cit.).

Asymptotic Behavior of the Two-Aquifer System

Early Times:

When t_{D_1} is small, p' is large. Considering equations C3 and C4, we have:

$$4G_1G_2 = 4ar_D^4(\phi/\sinh\phi)^2 = 4ar_D^4\ \phi^2(\coth^2\phi-1)$$

When $\phi>3$ (of the order $t_{D_1}<(b/3r_D)^2$), $\coth\phi\simeq 1$ and $4G_1G_2\rightarrow 0$. For example, when $\phi=10$, $4G_1G_2=3.3\times10^{-6}\ ar_D^4$. In the usual range of values for r_D ($r_D<10$), $4G_1G_2<<(B-A)^2$, yielding $D^*\simeq B-A, E\simeq A$, $F\simeq B$ and $(A-B)/D^*\simeq -1$, so that:

$$\overline{s_{D_1}} \simeq \frac{2K_0(\sqrt{B})}{p'}$$

which is inverted as equation C6 since $\coth\phi\simeq 1$. At early times, the dimensionless drawdown in the pumped aquifer is independent of a and c, that is of the parameters of the unpumped aquifer. As long as $t_{D_1}<(b/3r_D)^2$, s_{D_1} can be approximated by the Hantush "β solution". Coincidence with the Theis solution only occurs when b=0 (r_D non nil) or when $r_D=0$ (b non nil). The first case neglects storage in the aquitard (S'=0); the second case merely neglects leakage (K'=0).

Long Times:

When t_{D_1} is large and p' small, we do not find in the general case reduced asymptotic solutions for the dimensionless drawdown which have an infinite number of branches depending on the values of a, b, c and r_D. Remembering that when $\phi<0.4$ (of the order $t_{D_1}>(2.5b/r_D)^2$), we have $\phi\coth\phi \approx 1+(\phi^2/3)$, we have:

$$A \approx a^2c^2p' + ar_D{}^2[1+(\phi^2/3)]$$

$$B \approx p' + r_D{}^2[1+(\phi^2/3)]$$

$$4G1G_2 \approx 4ar_D{}^4(1-\frac{\phi^2}{3} + \frac{\phi^4}{9})$$

Even neglecting the term in ϕ^4, the quantities $\frac{A-B}{D^*}$, $\frac{G_2}{D^*}$, E and F remain a function of a, b, c and r_D in the expression of the dimensionless drawdowns of C_4.

A Special Case: The "Equal Two-Aquifer System"

When $T_1=T_2$ and $S_2=S_1$, we have a=c=1. It follows that $A=B=A_o$ and $G_1=G_2=G_o$ in equation C3. Therefore, $D=2G_o$, $E_o=A_o-G_o$ and $F_o=A_o+G_o$, where: $A_o=p'+r_D{}^2\phi\coth\phi$ and $G_o=r_D{}^2\phi/\sinh\phi$. The aquifer dimensionless drawdowns become:

$$\left.\begin{aligned} \overline{s_{D_1}} &= 1/p'[K_o(\sqrt{E_o}) + K_o(\sqrt{F_o})] \\ \overline{s_{D_2}} &= 1/p'[K_o(\sqrt{E_o}) - K_o(\sqrt{F_o})] \end{aligned}\right\} \quad (C8)$$

At early times (ϕ large), $G_o<<A_o$ and $E_o \approx F_o \approx p'+br_D\sqrt{p'}$ so that s_{D_1} is approximated by the same function H of equation C6. Although the unpumped aquifer and consequently the aquitard do not admit an asymptotic solution because $\overline{s_{D_2}} \approx 0$, it can be assumed that both drawdowns are negligibly small.

At large times (ϕ small), $\phi \coth\phi \simeq 1+\phi^2/3$ and $\phi/\sinh\phi \simeq 1-\phi^2/6$. The quantity $E_0 = A_0 - G_0 = p'(1+b^2/2)$ and the quantity $F_0 = p'(1+b^2/6)+2r_D{}^2$. Inversion of equation C8 can be readily obtained (Hantush, op.cit. p. 303) to yield the asymptotic solutions:

$$\left.\begin{aligned} s_{D_1} &= \frac{1}{2} E_1\left(\frac{\gamma_1}{4t_{D_1}}\right) + \frac{1}{2} W\left(\frac{\gamma_2}{4t_{D_1}}, \sqrt{2}r_D\right) \\ s_{D_2} &\simeq \frac{1}{2} E_1\left(\frac{\gamma_1}{4t_{D_1}}\right) - \frac{1}{2} W\left(\frac{\gamma_2}{4t_{D_1}}, \sqrt{2}r_D\right) \end{aligned}\right\} \qquad (C9)$$

where $\gamma_1 = 1 + \frac{b^2}{2} = 1 + \frac{S'}{2S_1}$ and $\gamma_2 = 1 + \frac{b^2}{6} = 1 + \frac{S'}{6S_1}$ and the functions E_1 and W as previously defined.

It is interesting to consider the solution at mid-point in the aquitard ($z_D=0.5$). In the Laplace space, we have:

$$\overline{s'_D}_{z_D=0.5} = \frac{1}{p'} \frac{\sinh(\phi/2)}{\sinh\phi} (\overline{sD_1} + \overline{sD_2}) = \frac{1}{p'} \frac{1}{\cosh(\phi/2)} K_0(\sqrt{E_0})$$

As $\phi<0.4$, $\cosh(\phi/2)<1.02007$ and $1/\cosh(\phi/2) \simeq 1$, so that:

$$\overline{s'_D}_{z_D=0.5} = \frac{1}{p'} K_0\left[\sqrt{(1+\frac{b^2}{2})p'}\right]$$

that is by inversion:

$$s'_{D_{z_D=0.5}} = \frac{1}{2} E_1\left(\frac{\gamma_1}{4t_{D_1}}\right) \qquad (C10)$$

Equation C10 is the first term on the right-hand side of equation C9. To our knowledge, the asymptotic solutions in equations C9 and C10 have never been presented. Because C9 and C10 are long-time asymptotic solutions of the "equal" two-aquifer system, depending on the values of γ_1, $\gamma_2=(\gamma_1+2)/3$ and r_D, the usual approximations for E_1 and W can be used. In any case, both functions are tabulated in Hantush (op.cit.). Equation C9 for s_{D_1} does not reduce to Hantush "r/B" solution even when

$\gamma_1=\gamma_2=1$ or $b=0$. The long-time solutions of the "equal" two-aquifer system are represented by the upper branches of the Figures IV-2 and IV-10 in Neuman and Witherspoon (1969).

Comparing the "shifting" factors δ_1 in equation C7, γ_1 and γ_2, we have $\gamma_2=(\delta_1+1)/2$ and the obvious inequality: $\gamma_2<\delta_1<\gamma_1$

These parameters are called "shifting" factors because they displace the functions of $1/4t_{D_1}$ to the right by a factor of S'/xS_1 with $x=2$ for γ_1, $x=3$ for δ_1, and $x=6$ for γ_2. It is worth noting that:

$$\frac{S'}{xS_1}\cdot\frac{1}{4t_{D_1}}=\frac{1}{x}\frac{S'r^2}{4T_1t}=\frac{1}{x}\frac{1}{4t'_D}$$

where t'_D is a dimensionless time for the aquifer-aquitard system.

2. THREE-AQUIFER SYSTEM - REVISED LAPLACE SPACE SOLUTIONS

Neuman and Witherspoon's solutions in Laplace space when the lower aquifer is mobilized can be written as follows:

$$\overline{s_1} = C[M_1N_1K_o(\zeta_1r) + M_2N_2K_o(\zeta_2r) + M_3N_3K_o(\zeta_3r)]$$

$$\overline{s_2} = CB_2[M_1(A_3-\zeta_1^2)\ K_o(\zeta_1r) + M_2(A_3-\zeta_2^2)\ K_o(\zeta_2r) + M_3(A_3-\zeta_3^2)\ K_o(\zeta_3r)]$$

$$\overline{s_3} = CB_2B_4[M_1K_o(\zeta_1r) + M_2K_o(\zeta_2r) + M_3\ K_o(\zeta_3r)]$$

$$\overline{s'}_1 = P_1\overline{s_2} + P_2\overline{s_1}$$

$$\overline{s'}_2 = Q_1\overline{s_3} + Q_2\overline{s_2}$$

where:

$$M_1 = \frac{-3(U+V)+i\sqrt{3}(V-U)}{3i\sqrt{3}(U^3-V^3)},\ M_2 = \frac{3(U+V)+i\sqrt{3}(V-U)}{3i\sqrt{3}(U^3-V^3)},\ M_3 = \frac{2i\sqrt{3}(U-V)}{3i\sqrt{3}(U^3-V^3)}$$

$$N_1 = A_2A_3-B_3B_4-(A_2+A_3)\zeta_1^2 + \zeta_1^4$$

$$N_2 = A_2A_3-B_3B_4-(A_2+A_3)\zeta_2^2+\zeta_2^4$$

$$N_3 = A_2A_3-B_3B_4-(A_2+A_3)\zeta_3^2+\zeta_3^4$$

$$P_1 = \sinh(z\sqrt{p/\alpha'_1})/R_1 \text{ with } R_1=\sinh(H'_1\sqrt{p/\alpha'_1})$$

$$P_2 = \sinh[(H'_1-z)\sqrt{p/\alpha'_1}]/R_1$$

$$Q_1 = \sinh[(z-z_1)\ \sqrt{p/\alpha'_2}]/R_2 \text{ with } R_2 = \sinh(H'_2\ \sqrt{p/\alpha'_2}) \text{ and } z_1 = H'_1+H_2$$

$$Q_2 = \sinh[(z_2-z)\ \sqrt{p/\alpha'_2}]/R_2 \text{ where } z_2 = z_1+H'_2$$

$$\zeta_1^2 = \frac{m}{3} + \frac{1}{2}[(U+V) + i\ \sqrt{3}(V-U)]$$

$$\zeta_2^2 = \frac{m}{3} + \frac{1}{2}[(U+V) - i\ \sqrt{3}(V-U)]$$

$$\zeta_3^2 = \frac{m}{3} -(U+V)$$

$$U = (-\frac{\delta}{2} +\sqrt{\frac{\delta^2}{4} + \frac{\gamma^3}{27}})^{1/3},\ V = (-\frac{\delta}{2} -\sqrt{\frac{\delta^2}{4} + \frac{\gamma^3}{27}})^{1/3}$$

$$\gamma = q - \frac{m^2}{3}, \quad \delta = \frac{2m^3}{27} - \frac{mq}{3} + n$$

$$m = A_1 + A_2 + A_3, \quad q = A_1A_3 + A_2A_3 + A_1A_2 - B_1B_2 - B_3B_4$$

$$n = A_1A_2A_3 - A_1B_3B_4 - A_3B_1B_2$$

and:

$$A_1 = \frac{p}{\alpha_1} + \frac{K'_1}{T_1}\sqrt{\frac{p}{\alpha'_1}} \coth(\phi_1) \qquad \phi_1 = H'_1 \sqrt{\frac{p}{\alpha'_1}}$$

$$A_2 = \frac{p}{\alpha_2} + \frac{K'_1}{T_2} \sqrt{\frac{p}{\alpha'_1}} \coth(\phi_1) + \frac{K'_2}{T_2} \sqrt{\frac{p}{\alpha'_2}} \coth(\phi_2) \qquad \phi_2 = H'_2 \sqrt{\frac{p}{\alpha'_2}}$$

$$A_3 = \frac{p}{\alpha_3} + \frac{K'_2}{T_3} \sqrt{\frac{p}{\alpha'_2}} \coth(\phi_2)$$

$$B_1 = \frac{K'_1}{T_1} \sqrt{\frac{p}{\alpha'_1}} / \sinh(\phi_1)$$

$$B_2 = \frac{K'_1}{T_2} \sqrt{\frac{p}{\alpha'_1}} / \sinh(\phi_1)$$

$$B_3 = \frac{K'_2}{T_2} \sqrt{\frac{p}{\alpha'_2}} / \sinh(\phi_2)$$

$$B_4 = \frac{K'_2}{T_3} \sqrt{\frac{p}{\alpha'_2}} / \sinh(\phi_2)$$

$$C = \frac{Q}{4\pi T_1 p}$$

For the flow parameters in the definitions of the functions A, B and C, the subscripts 1, 2 and 3 refer to the pumped (lower) aquifer, the intermediate aquifer and the upper aquifer, respectively. The notation ($'_1$) refers to the lower aquitard and the notation ($'_2$) refers to the upper aquitard.

As for the two-aquifer system, we transform these equations into the dimensionless Laplace space defined by:

$$\overline{s_{D_1}} = \frac{4\pi T_1 \overline{s_1}}{Q}, \quad \overline{s_{D_2}} = \frac{4\pi T_1 \overline{s_2}}{Q}, \quad \overline{s_{D_3}} = \frac{4\pi T_1 \overline{s_3}}{Q}, \quad \overline{s'_{D_1}} = \frac{4\pi T_1 \overline{s'_1}}{Q} \text{ and } \overline{s'_{D_2}} = \frac{4\pi T_1 \overline{s'_2}}{Q}$$

and by the Laplace variable p' that corresponds to:

$$t_{D_1} = \frac{\alpha_1 t}{r^2}$$

The hydraulic and geometric parameters of the system are grouped into the following eight dimensionless parameters:

$$a_1 = \frac{T_1}{T_2},\ a_2 = \frac{T_1}{T_3},\ b_1 = \left(\frac{S'_1}{S_1}\right)^{1/2},\ b_2 = \left(\frac{S'_2}{S_1}\right)^{1/2},\ c_1 = \frac{S_2}{S_1},\ c_2 = \frac{S_3}{S_1}$$

$$r_{D_1} = \frac{r}{H'_1}\left(\frac{T'_1}{T_1}\right)^{1/2} \text{ and } r_{D_2} = \frac{r}{H'_2}\left(\frac{T'_2}{T_1}\right)^{1/2}.$$

The correspondence between these groups and the groups θ_{ij} and η_{ij} used by Neuman and Witherspoon to express the real space solutions are easily obtained as:

$$\theta_{11} = \frac{\alpha'_1}{\alpha_1}\frac{r^2}{H'_1} = \left(\frac{r_{D_1}}{b_1}\right)^2 \qquad \theta_{21} = \frac{\alpha'_1}{\alpha_2}\left(\frac{r}{H'_1}\right)^2 = a_1c_1\left(\frac{r_{D_1}}{b_1}\right)^2 \qquad \theta_{22} = \frac{\alpha'_2}{\alpha_2}\left(\frac{r}{H'_2}\right)^2 = a_1c_1\left(\frac{r_{D_2}}{b_2}\right)^2$$

$$\theta_{32} = a_2c_2\left(\frac{r_{D_2}}{b_2}\right)^2 \qquad \eta_{11} = r_{D_1}{}^2 \qquad \eta_{22} = a_1(r_{D_2})^2 \qquad \eta_{32} = a_2(r_{D_2})^2$$

The correspondence between the θ_{ij} and η_{ij} and the r/B_{ij} and β_{ij} are simply: $r/B_{ij} = (\eta_{ij})^{1/2}$ and $4\beta_{ij} = \eta_{ij}(\theta_{ij})^{-1/2}$.

We first transform the functions A_1, A_2, A_3, B_1, B_2, B_3, B_4 and C by changing p into p' ($p = \alpha_1 p'/r^2$). Let the superscript (*) refer to the transformed functions.

The easiest is the function C, we have $C^*(p') = \frac{r^2}{\alpha_1}C(p')$. We notice that C(p) is a common factor to the five Laplace transforms of the drawdowns. Because $L' = \frac{1}{r^2}L$ and for instance $\overline{s_{D_1}} = \frac{4\pi T_1 \overline{s_1}}{Q}$, it follows that the five functions $\overline{s_D}$ will have a multiplying factor of 1/p' instead of C as for the functions $\bar{s}$.

Using the 8 depending dimensionless parameters previously defined, we find for the basic functions:

$$\left.\begin{aligned}
&A_1^* = p'+r_{D_1}^2\,\phi_1^*\coth(\phi_1^*)\equiv r^2A_1(p') \text{ where: } \phi_1^*=b_1\sqrt{p'}/r_{D_1}\equiv\phi_1(p')\\
&A_2^* = a_1c_1p'+a_1r_{D_1}^2\phi_1^*\coth(\phi_1^*)+a_1r_{D_2}^2\phi_2^*\coth(\phi_2^*)\equiv r^2A_2(p')\\
&\text{where: } \phi_2^*=b_2\sqrt{p'}/r_{D_2}\equiv\phi_2(p')\\
&A_3^* = a_2c_2p'+a_2r_{D_2}^2\phi_2^*\coth(\phi_2^*)\equiv r^2A_3(p')\\
&B_1^* = r_{D_1}^2\,\phi_1^*/\sinh(\phi_1^*)\equiv r^2B_1(p')\\
&B_2^* = a_1B_1^*\equiv r^2B_2(p')\\
&B_3^* = a_1r_{D_2}^2\,\phi_2^*/\sinh(\phi_2^*)\equiv r^2B_3(p')\\
&B_4^* = a_2B_3^*\equiv r^2B_4(p')
\end{aligned}\right\}\quad\text{(C11)}$$

To obtain a strict equivalence between the solutions using the basic function (*), we have to show that the factor r^2 is cancelling out when the A and B functions of p' are introduced in the remaining functions. In effect,

we will have $m^* = (A_1 + A_2 + A_3)/r^2$ or $m^*\equiv r^2m$, $q^*\equiv r^4q$, $n^*=r^6n$, $\gamma^*\equiv r^4\gamma$, $\delta^*\equiv r^6\delta$, $U^*\equiv r^2U$, $V^*\equiv r^2V$. It follows that $r\zeta_1=\zeta_1^*$, $r\zeta_2=\zeta_2^*$ and $r\zeta_3=\zeta_3^*$.

Similarly, we then have: $M_1^*\equiv\frac{M_1}{r^4}$, $M_2^*\equiv\frac{M_2}{r^4}$ and $M_3^*\equiv\frac{M_3}{r^4}$ meanwhile $N_1\equiv r^4N_1$, $N_2^*\equiv r^4N_2$ and $N_3^*\equiv r^4N_3$ yielding $M_1^*N_1^*=M_1N_1$, $M_2^*N_2^*=M_2N_2$ and $M_3^*N_3^*=M_3N_3$. The expressions of s_1 and s_1^* are thus strictly equivalent.

The same can be said for s_2 and s_2^* since for example:

$$B_2^*M_1^*(A^*{}_3-\zeta_1^2)\equiv B_2M_1(A_3-\zeta_1^2)$$

and for s_3 and s_3^* since for example $B_2^*B_4^*M_1^*\equiv B_2B_4M_1$. For the solutions in the aquitards, we need to define three additional dimensionless quantities:

$z_{D_1} = \frac{z}{H'_1}$, $h_D = \frac{H'_1+H_2}{H'_2}$, $z_{D_2} = \frac{z}{H'_2}$ from which:

$$\left.\begin{aligned}
P_1^* &= \sinh(z_{D_1}\phi_1^*)/\sinh(\phi_1^*) \equiv P_1(p') \\
P_2^* &= \sinh[(1-z_{D_1})\phi_1^*]/\sinh(\phi_1^*) \equiv P_2(p') \\
Q_1^* &= \sinh[(z_{D_2}-h_D)\phi_2^*]/\sinh(\phi_2^*) \equiv Q_1(p') \\
Q_2^* &= \sinh([(1+h_D-z_{D_2})\phi_2^*]/\sinh(\phi_2^*) \equiv Q_2(p')
\end{aligned}\right\} \quad (C12)$$

Having shown the strict equivalence of the five drawdowns in the Laplace dimensionless space with those of the Laplace space, we may simplify the notations by removing the (*) superscripts.

We consider next the cubic algebraic equation:

$$Z^3 + mZ^2 + qZ + n = 0$$

whose roots are Z_1, Z_2 and Z_3. m, q and n are as previously defined and functions of A_1, A_2, A_3, B_1, B_2, B_3 and B_4. In addition, we have:

$$Z_1 + Z_2 + Z_3 = -m$$

These roots can be real or complex conjugate.

We wish to express the nine functions ζ_1^2, ζ_2^2, ζ_3^2, M_1, M_2, M_3, N_1, N_2 and N_3 as previously defined in terms of Z_1, Z_2 and Z_3. This will greatly simplify the computational procedure since the roots of a cubic equation can be found by computer, using an IMSL subroutine.

We have immediately:

$$\zeta_1^2 \equiv -Z_3,\ \zeta_2^2 \equiv -Z_2,\ \zeta_3^2 \equiv -Z_1 \quad (C13)$$

because, $Z_1 = U+V \frac{-m}{3}$, $Z_2 = \frac{m}{3} - \frac{1}{2}[(U+V)-i\sqrt{3}(U-V)]$ and

$$Z_3 = -\frac{m}{3} - \frac{1}{2}[(U+V)+i\sqrt{3}(U-V)]$$

with U and V as previously defined.

It follows that:

$$\left.\begin{aligned} N_1 &\equiv A_2A_3-B_3B_4+(A_2+A_3)Z_3+Z_3^2 \\ N_2 &\equiv A_2A_3-B_3B_4+(A_2+A_3)Z_2+Z_2^2 \\ N_3 &\equiv A_2A_3-B_3B_4+(A_2+A_3)Z_1+Z_1^2 \end{aligned}\right\} \qquad \text{(C14)}$$

We may rewrite:

$$M_1 = \frac{(V-U)+i\sqrt{3}(U+V)}{3(U^3-V^3)},\ M_2 = \frac{(V-U)-i\sqrt{3}(U+V)}{3(U^3-V^3)},\ \text{and } M_3 = \frac{2(U-V)}{3(U^3-V^3)}$$

We wish to express M_1, M_2 and M_3 solely in terms of Z_1, Z_2 and Z_3 as previously defined. We notice that $M_3 = -(M_1+M_2)$. The numerators of M_1 and M_2 are easily obtained as $2(Z_1-Z_2)$,$-2(Z_1-Z_3)$, respectively. For the denominator (U^3-V^3), we may write it as $(U-V)\ (U^2+UV+V^2)=(U-V)[(U+V)^2-UV]$. Operating the change of variable $W_2=Z_2+m/3$, $W_3=Z_3+m/3$ and $W_1=Z_1+m/3$, we have: $UV=1/3(W_1^2-W_2W_3)$, $(U+V)=W_1$. Backsubstituting for Z, we obtain for the denominator $(Z_2-Z_1)(Z_3-Z_1)$ yielding:

$$\left.\begin{aligned} M_1 &= 2/(Z_1-Z_3)(Z_2-Z_3) \\ M_2 &= 2/(Z_2-Z_3)(Z_2-Z_1) \\ M_3 &= 2/(Z_3-Z_1)(Z_2-Z_1) \end{aligned}\right\} \qquad \text{(C15)}$$

The final dimensionless Laplace space solutions can now be written as equations 39 and others in the main text.

The Program 3AQF

The real space dimensionless solutions are evaluated with the Crump inverter, which exists as an IMSL subroutine. Three major difficulties were encountered in developing this code:

1. the calculations have to be conducted in the complex plane with p' considered as a complex variable;
2. the function $K_o(z)$ where z is a complex variable has to be evaluated;
3. functions of the type zcoth(z) and z/sinh(z) have to be evaluated for a large (and a priori unknown) range of z.

The calculations are performed in arithmetic double precision. The first and part of the third problem can be easily solved using the VAX-11 FORTRAN generic functions for complex variables; useful functions are DREAL, DIMAG, DCMPLX that permit the transformation of complex numbers into real numbers and reverse. The function DCONJG allows the evaluation of z^*, the complex conjugate of z. The roots of the cubic equation 40 (in text) are obtained with the IMSL subroutine ZCPOLY written by Jenkins and Traub (1972) to calculate the zeros of a polynomial with complex coefficients.

The second problem was solved by using the subroutine BESK01 of Burrell (1972) that returns the values of $e^x K_o(z)$ for a given z of real part x. For $|z|$ large, $|K_o(z)| \approx e^{-x}\left(\frac{\pi}{2}\,\frac{1}{|z|}\right)^{1/2}$ is the approximation used. For $|z| < 3$, the subroutine uses the series expansions of the complex function K_o; otherwise, it uses the integral representation of Hunter (1964) that is calculated with the trapezoidal rule.

For the third problem, we take advantage of the following expressions ($z = x + iy$):

$$z\coth z = (x+iy)\frac{\sinh 2x - i\sin 2y}{\cosh 2x-\cos 2y} = \frac{x\sinh 2x + y\sin 2y}{\cosh 2x-\cos 2y} + i\,\frac{y\sinh 2x - x\sin 2y}{\cosh 2x-\cos 2y} \tag{C16}$$

$$z/\sinh z = (x+iy)\frac{1}{\sinh x\cos y + i\cosh x\sin y} = \frac{2(x\sinh x\cos y + y\cosh x\sin y)}{\cosh 2x-\cos 2y}$$

$$+2i\frac{y\sinh x\cos y - x\cosh x\sin y)}{\cosh 2x-\cos 2y}$$

Because the imaginary part y of z is only appearing with the sine and cosine functions that are always defined, it is clear that overflows for zcothz and z/sinhz will occur only when x is large. Specifically, when $x>5$, $z\coth z \sim x+iy=z$ and when $x>10$, $z/\sinh z \sim 2\exp(-x)[(x\cos y+y\sin y)+i(y\cos y-x\sin y)]$. Otherwise, the formulation C16 is used to obtain zcothz and z/sinhz since the functions cothz and sinhz do not exist as VAX-11 FORTRAN generic functions.

Reduction to the Two-Aquifer System

We have simply: $K'_2=0$ and $T_3 \to \infty$, yielding $r_{D_2}=0$ and $a_2=0$ that is $B_3=B_4=0$ and $A_3=0$. It follows that $m=A_1+A_2$, $q=A_1A_2-B_1B_2$ and $n=0$ and equation 40 reduces to:

$$z^2 + mz + q = z^2 + (A_1+A_2)z + (A_1A_2-B_1B_2) = 0$$

with $A_1 = p'+r_{D_1}{}^2\phi_1 \coth\phi_1$, $A_2 = a_1c_1p'+a_1r_{D_1}{}^2\phi_1 \coth\phi_1$.
and $B_1B_2 = a_1B_1{}^2 = a_1r_{D_1}{}^4\phi_1{}^2/\sinh^2\phi_1 = a_1r_{D_1}{}^2b_1{}^2p'/\sinh^2\phi_1$
The discriminant of this quadratic equation is:

$$m^2 - 4q = (A_1-A_2)^2 + 4B_1B_2$$

In previous developments, we have seen that for the two-aquifer system, the Laplace transformation could be considered as a real procedure. Thus p' is a real and positive (because t_{D_1} is positive) variable. It follows that its discriminant being always positive, the two roots of the quadratic equation are real and expressed by:

$$2Z_1 = -(A_1+A_2) + \sqrt{[(A_1-A_2)^2 + 4B_1B_2]} \equiv -2E$$

$$2Z_2 = -(A_1+A_2) - \sqrt{[(A_1-A_2)^2 + 4B_1B_2]} \equiv -2F$$

since $A_2 \equiv A$, $A_1 \equiv B$, $B_1 \equiv G_1$ and $B_2 \equiv G_2$ of equation C3.

Now: $M_1 = \frac{2}{Z_1Z_2}$, $M_2 = \frac{2}{Z_2(Z_2-Z_1)}$ $M_3 = \frac{2}{Z_1(Z_1-Z_2)}$

$N_1 = 0$, $N_2 = A_2Z_2+Z_2^2$, $N_3 = A_2Z_1+Z_1^2$

yielding: $M_1N_1 = 0$, $M_2N_2 = \frac{2(A_2+Z_2)}{(Z_2-Z_1)}$, $M_3N_3 = \frac{2(A_2+Z_1)}{(Z_1-Z_2)}$

We obtain the following identities with the notations of C3:

$$M_2N_2 \equiv \frac{-2(A-F)}{D}, \quad M_3N_3 \equiv \frac{2(A-E)}{D}, \quad M_2Z_2 = \frac{2}{Z_2-Z_1} \equiv \frac{-2}{D} \quad M_3Z_1 \equiv \frac{2}{D}$$

and replacing in equation 39 of the text, we find:

$$\overline{s_{D_1}} = \frac{1}{p'} \left[\frac{2(A-E)}{D} K_0(\sqrt{E}) - \frac{2(A-F)}{D} K_0(\sqrt{F})\right]$$

$$\overline{s_{D_2}} = \frac{2G_2}{Dp'}[K_0(\sqrt{E}) - K_0(\sqrt{F})]$$

which are strictly the same equations as C4, D being the discriminant of the above quadratic equation. It is easy to show that $\frac{2(A-E)}{D} = \frac{A-B}{D} +1$ and $\frac{2(A-F)}{D} = \frac{A-B}{D} -1$

Reduction to Hantush's "Modified Leaky Aquifer System"

Hantush (1960) proposed asymptotic solutions for the case when an aquifer is over and underlain by leaky aquitards. In his case 1, the supply of leakage comes from two source beds over and underlying these aquitards. This case is, in fact, a three-aquifer system where $T_1 \to \infty$, $T_3 \to \infty$ and the intermediate aquifer (T_2, S_2) is pumped. It follows that a_1 and a_2 are infinite.

For a three-aquifer system where aquifer 2 is exploited, Neuman and Witherspoon (1969) give the Laplace space solution for that aquifer as equation II116 (ref.cit.). That solution in the Laplace dimensionless space becomes:

$$\overline{s_{D_2}} = \frac{1}{p'}[M_1N'_1Ko(\sqrt{-Z_3})+M_2N'_2K_o(\sqrt{-Z_2})+M_3N'_3K_o(\sqrt{-Z_1})] \tag{C17}$$

where $N'_1 = A'_1A'_3+(A'_1+A'_3)Z_3+Z_3^2$

$N'_2 = A'_1A'_3+(A'_1+A'_3)Z_2+Z_2^2$

$N'_3 = A'_1A'_3+(A'_1+A'_3)Z_1+Z_1^2$

and p' refers now to the dimensionless time $t_{D_2} = \frac{\alpha_2 t}{r^2}$

The Laplace space functions A_1, A_3, B_1 and B_4 are all zero when T_1 and T_3 are infinite. In the dimensionless Laplace space, their equivalent A'_1, A'_3, B'_1 and B'_4 are thus all zero, yielding $N'_1=Z_3^2$, $N'_2=Z_2^2$, $N'_3=Z_1^2$. To evaluate the roots of the cubic equations, we notice that its coefficients are: $m'=A_2$, $q'=0$ and $n'=0$ and the cubic equation reduces to:

$$Z^3 + A'_2Z^2 = 0 \text{ or } Z^2(Z+A'_2) = 0$$

that is $Z_1 = Z_3 = 0$ and $Z_2 = -A'_2$

Consequently, equation C17 reduces to:

$$\overline{s_{D_2}} = \frac{1}{p'}\left[M_2 N'_2 K_0\left(\sqrt{A'_2}\right)\right]$$

$$\left.\begin{aligned}
&\text{with } M_2 = 2/z_2{}^2 = 2/A'_2{}^2 \text{ and } N'_2 = A'_2{}^2 \\
&\text{Thus: } \overline{s_{D_2}} = \frac{2}{p'} K_0\left(\sqrt{A'_2}\right) \\
&\text{where: } A'_2 = p' + r_{D_1}{}^2\phi_1 \coth\phi_1 + r_{D_2}{}^2\phi_2 \coth\phi_2 \\
&\text{with } \phi_2 = \frac{b_2\sqrt{p'}}{r_{D_2}} \text{ and } \phi_1 = \frac{b_1\sqrt{p'}}{r_{D_1}}
\end{aligned}\right\} \qquad \text{(C18)}$$

Equation C18 is precisely Hantush's Laplace solution expressed in dimensionless terms. The solution C18 for s_{D_2} is easy to evaluate with Stehfest's inverter. Neuman and Witherspoon (op.cit.) have performed the exact inversion of $\overline{s_{D_2}}$ (of C17).

APPENDIX D

1. DERIVATION OF THE GOVERNING EQUATIONS FOR DUAL POROSITY MODELS

A fundamental assumption in the continualized approach is that an elemental volume of aquifer contains a large number of fractures and a large number of blocks. The derivation of the associated continuity equations also postulates that two pore pressures can be defined at any point in the dual porosity medium: an average pore pressure in the fractures in the vicinity of the point and an average pore pressure in the blocks in that same vicinity. Reasoning in a similar fashion as in Appendix A with normalization with respect to the bulk volume of the medium and using subscripts 1 and 2 for characteristics related to fractures and matrix, respectively, we may write the continuity equations for the two overlapping systems as:

$$\begin{aligned} &\rho(\beta\bar{n}_1+c_1)\,\partial p_1/\partial t+\mathrm{div}(\rho\vec{v_1})-\rho q = 0 \\ &\rho(\beta\bar{n}_2+c_2)\,\partial p_2/\partial t + \mathrm{div}(\rho\vec{v_2}) + \rho q = 0 \end{aligned} \qquad \text{(D1)}$$

where:

c_i $(i=1,2)$ is the vertical compressibility of the granular skeleton

$\bar{n}_i$ $(i=1,2) = \delta_i n_i$

δ_i $(i=1,2)$ is the ratio of the volume of medium to the bulk volume

n_i $(i=1,2)$ is the porosity of medium i defined as the ratio of the pore volume to the total volume of the medium

ρ and β are the density and compressibility of water, respectively

$p_i (i=1,2)$ is the pore pressure in medium i

$\vec{v_i} (i=1,2)$ is the velocity vector in medium i q is the volumetric interporosity flow between the two systems $[T^{-1}]$ (per unit bulk volume and per unit time)

Note that in the formulation of D_1, q is negative (water loss in the blocks). This convention of sign will have to be respected. With these notations, it is obvious that if the fractures do not contain any porous material, we may have $n_1=1$ but because usually $\delta_1 \ll 1$, $\bar{n}_1$ remains closer to 0 than to 1. Assuming that the linear law of flow (Darcy's law) is applicable to both media and because $\mathrm{div}(\rho\overrightarrow{v_i})=\rho\,\mathrm{div}(\overrightarrow{v_i})$ (from equation A19) and $\partial h/\partial t=\rho g(\partial p/\partial t)$ from the definition of hydraulic head, we may rewrite D1 as:

$$\begin{aligned} &\rho^2 g(\beta\bar{n}_1+c_1)\ \partial h_1/\partial t + \rho\ \mathrm{div}[-\overline{\overline{K}}_1\ \overrightarrow{\mathrm{grad}}(h_1)] - \rho q = 0 \\ &\rho^2 g(\beta\bar{n}_2+c_2)\ \partial h_2/\partial t + \rho\ \mathrm{div}[-\overline{\overline{K}}_2\ \overrightarrow{\mathrm{grad}}(h_2)] + \rho q = 0 \end{aligned} \qquad \text{(D2)}$$

where $\overline{\overline{K}}_i$ (i=1,2) is the hydraulic conductivity tensor and h_i (i=1,2) is the hydraulic head. $\overrightarrow{\mathrm{grad}}(h_i)$ is a vector of components $\partial h_i/\partial x$, $\partial h_i/\partial y$ and $\partial h_i/\partial z$. If the cartesian coordinate system is chosen to match the principle directions of flow in each medium, the tensors of hydraulic conductivity reduce to their principal components and operating the usual substitution:

$$\bar{x} = \frac{K_i}{\sqrt{K_{i_x}}}\ x \qquad \bar{y} = \frac{K_i}{\sqrt{K_{i_y}}}\ y \quad \text{and} \quad \bar{z} = \frac{K_i}{\sqrt{K_{i_z}}}\ z$$

where $K_i = (K_{i_x}\ K_{i_y}\ K_{i_z})^{1/3}$ is the mean hydraulic conductivity for each medium, we may finally rewrite D_2 as:

$$\begin{aligned} &\rho g(\beta\bar{n}_1+c_1)\ \partial h_1/\partial t - K_1\ \Delta h_1 - q = 0 \\ &\rho g(\beta\bar{n}_2+c_2)\ \partial h_2/\partial t - K_2\ \Delta h_2 + q = 0 \end{aligned} \qquad \text{(D3)}$$

Defining $S_{si} = \rho g(\beta\bar{n}_i + c_i)$ as the specific storage and $\alpha_i = K_i/S_{si}$ as the hydraulic diffusivity for each medium, we have:

$$\begin{aligned} \Delta h_1 + \frac{q}{K_1} &= \frac{1}{\alpha_1}\frac{\partial h_1}{\partial t} \\ \Delta h_2 - \frac{q}{K_2} &= \frac{1}{\alpha_2}\frac{\partial h_2}{\partial t} \end{aligned} \tag{D4}$$

Practical solutions of the system of partial differential equations D4 are difficult to obtain. Simplified forms relying on various assumptions permit easier analytical treatment for a given set of initial and boundary conditions and these consitute the dual porosity models discussed in the text. Note that in D4, the hydraulic parameters are defined in terms of anisotropy for K_i and are spatially averaged with respect to the bulk volume for S_{s_i}.

2. DERIVATION OF THE BARENBLATT ET AL. SOLUTION

With their assumptions, these authors write:

$$K_1 \Delta h_1 + q = 0$$

$$S_{s_2} \, \partial h_2/\partial t + q = 0$$

which in terms of mean drawdowns $s_1 = h_1 - h_o$ and $s_2 = h_2 - h_o$, becomes:

$$K_1 \Delta s_1 + q = 0$$

$$S_{s_2} \, \partial \bar{s}_2/\partial t + q = 0$$

The interporosity flow, that is the source term q, occurs under steady-state conditions; therefore, $q = mK_2(s_2 - s_1)$ where $m[L^{-2}]$ is a block shape parameter. Note that because s_2 is expected to be less than s_1 at all times, q, as expressed, is negative. This respects the sign convention of D_1. Therefore, the constitutive equations may be rewritten as:

$$K_1 \Delta s_1 + mK_2(s_2 - s_1) = 0$$

$$\partial s_2/\partial t + \alpha_2 m(s_2 - s_1) = 0$$

where α_2 is the matrix diffusivity. Solving the first equation for s_2 leads to:

$$s_2 = s_1 - (K_1/mK_2)\Delta s_1 \qquad \text{(D5)}$$

which by substitution in the second equation:

$$\frac{\partial s_1}{\partial t} - \frac{K_1}{mK_2}\frac{\partial \Delta s_1}{\partial t} - \frac{K_1}{S_{s_2}}\Delta s_1 = 0$$

or

$$\Delta s_1 = \frac{S_{s_2}}{K_1}\frac{\partial s_1}{\partial t} - \frac{1}{m\alpha_2}\frac{\partial \Delta s_1}{\partial t} \qquad \text{(D6)}$$

The average thickness of the fracture system is small and s_1 is independent of z. For an axisymmetrical problem in radial coordinates

$$\Delta s_1 = \frac{1}{r}\frac{\partial}{\partial r}\left(r\frac{\partial s_1}{\partial r}\right)$$

The initial boundary conditions are: $s_1(r,0)=s_2(r,0)=0$ (D7)

The outer boundary conditions are: $s_1(\infty,t)=s_2(\infty,t)=0$ (D8)

The problem willbe well-posed, that is susceptible to yield solutions for $s_1(r,t)$ from D6 and for $s_2(r,t)$ from D5 if we add the inner boundary condition for $s_1(r,t)$. Since the fracture has zero specific storage and simply conveys to the well the water released from storage in the blocks, we may write:

$$\lim_{r\to 0}(r\partial s_1/\partial r) = 0 \quad \text{for } t = 0 \qquad \text{(D9)}$$

that states that, initially, all the production comes from the block. As the pumping time evolves, a simple mass balance calculation gives:

$$Q = -2\pi K_1 H \lim_{r\to 0}\left[\left(r\frac{\partial s_1}{\partial r}\right) + \frac{1}{m\alpha_2}\frac{\partial}{\partial t}\left(r\frac{\partial s_1}{\partial r}\right)\right]$$

where H is the aquifer thickness fully tapped by the well. This differential equation can be easily integrated by letting $y = r\partial s_1/\partial r$ and the constant of integration is obtained from D9. The solution is:

$$\lim_{r\to 0}\left(r\frac{\partial s_1}{\partial r}\right) = -\frac{Q}{2\pi K_1 H}[1-\exp(-m\alpha_2 t)] \qquad \text{(D10)}$$

The Laplace transformation with respect to time (transform parameter=p) is then applied successively to D6 and D5 with the help of D7 and to D10. We obtain with our usual notation for Laplace transforms:

$$\Delta\bar{s}_1 = \frac{S_{s_2}}{K_1}p\bar{s}_1 - \frac{p}{m\alpha_2}\Delta\bar{s}_1$$

$$s_2 = \bar{s}_1 - \frac{K_1}{mK_2}\Delta\bar{s}_1$$

$$\lim_{r\to 0}\left(r\frac{\partial\bar{s}_1}{\partial r}\right) = -\frac{Q}{2\pi K_1 H}\left(\frac{1}{p} - \frac{1}{p+m\alpha_2}\right) = -\frac{Q}{2\pi K_1 H}\frac{1}{p}\frac{m\alpha_2}{p+m\alpha_2}$$

Applying the zero Hankel transnsformation H_o for the radial distance r (transform parameter a), we have:

$$s_1^*(a,p) = H_0[\bar{s}(r,p)],\ H_0(\Delta\bar{s}_1) = -a^2 s_1^* - \lim_{r\to 0}\left(r\frac{\partial\bar{s}_1}{\partial r}\right)$$

or

$$H_0(\Delta\bar{s}_1) = -a^2 s_1^* + \frac{Q}{2\pi K_1 H}\frac{1}{p}\frac{m\alpha_2}{p+m\alpha_2}$$

The solutions are expressed in the Laplace-Zero Hankel space after simple algebraic manipulations as:

$$\left.\begin{aligned} \frac{2\pi K_1 H}{Q}s_1^* &= \frac{1}{p}\frac{m\alpha_2}{p+m\alpha_2}\frac{1}{[a^2+mK_2/K_1(p/p+m\alpha_2)]} \\ \frac{2\pi K_1 H}{Q}s_2^* &= \frac{1}{p}\frac{m\alpha_2}{p+m\alpha_2}\left\{\left(1+\frac{p}{p+m\alpha_2}\right)\frac{1}{\left[a^2+\frac{mK_2}{K_1}\left(\frac{p}{p+m\alpha_2}\right)\right]} + \frac{2K_1}{mK_2}\frac{a^2}{\left[a^2+\frac{mK_2}{K_1}\left(\frac{p}{p+m\alpha_2}\right)\right]}\right\} \end{aligned}\right\} \text{(D11)}$$

whereby making use of B14 for the zero Hankel inverse transformation:

$$\frac{2\pi K_1 H}{Q}\bar{s}_1 = \frac{1}{p}\,\frac{m\alpha_2}{p+m\alpha_2}\,K_o\left\{r\left[\frac{mK_2}{K_1}\,\frac{p}{p+m\alpha_2}\right]^{1/2}\right\} \qquad \text{(D12)}$$

$$\frac{2\pi K_1 H}{Q}\bar{s}_2 = \frac{1}{p}\left(\frac{m\alpha_2}{p+m\alpha_2}\right)^2 K_o\left[r\left(\frac{mK_2}{K_1}\,\frac{p}{p+m\alpha_2}\right)^{1/2}\right]$$

Defining our usual dimensionless groups:

$$s_{D_1} = \frac{4\pi K_1 H s_1}{Q},\quad s_{D_2} = \frac{4\pi K_1 H s_2}{Q}$$

and the less conventional dimensionless time

$t_D = \frac{K_1 t}{S_{s_2} r^2}$ (since $S_{s_1} = 0$) and dimensionless radius $r_D = r\sqrt{\frac{mK_2}{K_1}}$ we may express the Laplace solutions of D12 by their equivalent dimensionless forms.

If p' is the Laplace transform of t_D, we have immediately:

$$\bar{s}_{D_1} = \frac{2}{p'}\,\frac{r_D^2}{p'+r_D^2}\,K_o\left[r_D\left(p'/p'+r_D^2\right)^{1/2}\right] \qquad \text{(D13)}$$

$$\bar{s}_{D_2} = \frac{2}{p'}\left(\frac{r_D^2}{p'+r_D^2}\right)^2 K_o\left[r_D\left(\frac{p'}{p'+r_D^2}\right)^{1/2}\right]$$

NOTE: In D12, we have:

$$\bar{s}_2 = \frac{m\alpha_2}{p+m\alpha_2}\bar{s}_1$$

This result can be obtained more quickly by simply inverting q in the Laplace space.

In the real space:

$$q = mK_2(s_2 - s_1) = S_{s_2}\frac{\partial s_2}{\partial t}$$

In the Laplace space:

$$mK_2(\bar{s}_2 - \bar{s}_1) = -pS_{s_2}\bar{s}_2 \qquad \text{(D14)}$$

Solving this equation for $\bar{s}_2$ yields the above relationship between $\bar{s}_2$ and $\bar{s}_1$. This can be used as a control of the validity of the expression of $\bar{s}_2$ in D12 which was obtained using D5 after lengthier developments. The use of D14 is actually a better way to arrive at the Laplace space solution for s_2.

Defining the function $f(p') = \frac{1}{(1+p'/r_D{}^2)}$, we have:

$$s_{D_1} = \frac{2}{p'} f(p')K_0([p'f(p')]^{1/2})$$
$$s_{D_2} = \frac{2}{p'} f^2(p')\ K_0\ ([p'f(p'))]^{1/2}) \tag{D15}$$

The forms of D15 may be useful for direct comparison with other analytical solutions in the Laplace dimensionless space of dual porosity models. When t_D is large (t is large), p' tends toward zero and f(p') tends towards unity; both $\overline{s_{D_1}}$ and $\overline{s_{D_2}}$ tend towards $2/p'[K_0(\sqrt{p'})]$ which, by inversion, gives the Theis solution for the dimensionless time t_D (see Appendix B, equation B19). Both type curves are asymptotic to the Theis type curve. When t and t_D tend towards zero, a similar analytical expression cannot be derived exactly from D13 for $\overline{s_{D_1}}$ and $\overline{s_{D_2}}$ since both s_{D_1} and s_{D_2} tend towards zero (finite argument of the Bessel function) and their inverse Laplace transforms are undefined. Similarly, when r tends towards infinity, t_D tends towards zero and we cannot verify from D13 that $s_1(\infty,t)=s_2(\infty,t)=0$. However, this boundary condition has been applied when deriving $H_0(\Delta\bar{s}_1)$ so that the solutions in the real space certainly verify D8. The same applies to the case when $t \to 0$ since the boundary conditions D7 have been used for applying the Laplace transformation to D5 and D6. So that we certainly have:

$s_1(r,0)=s_2(r,0)=0$. Finally, we may view the Barenblatt et al. model as a limiting case when the fracture specific storage is vanishingly small. Defining $b=S_{s_2}/S_{s_1}$, the solutions in the dimensionless Laplace space given by D15 correspond to b tending towards infinity. If we define as usual:

$$t_{D_1}=\frac{K_1 t}{S_{s_1} r^2}$$

then we have obviously $t_{D_1}=bt_D$. Calling p'' the Laplace transform with respect to t_{D_1} and $\bar{s}'_{D_1}$ and $\bar{s}_{D'_2}$ the corresponding dimensionless drawdowns, we may rewrite D15 using B8 as:

$$\overline{s'}_{D_1} = \frac{2}{p''} f(\frac{p''}{b}) K_0([\frac{p''}{b} f(\frac{p''}{b})]^{1/2})$$

(D16)

$$\overline{s'}_{D_2} = \frac{2}{p'} f^2(\frac{p''}{b}) K_0([\frac{p''}{b} f(\frac{p''}{b})]^{1/2})$$

where $f(p''/b)=(1+p''/r_D^2 b)^{-1}$

These forms rather than D15 should be used to compare analytical solutions of other models (for which b is not nil) to the Barenblatt et al. model. D16 is equivalent to D15 when b tends towards infinity. The computer code DUPBAR computes s_{D_1} and s_{D_2} for the usual range of t_D and various r_D from D13. It uses the Stehfest numerical inverter.

3. A UNIFIED FORMULATION FOR THE LAPLACE SPACE LINE-SOURCE SOLUTIONS

The following developments relate work started in 1982 as an effort to propose a unified "theory" for dual porosity systems. The idea is that the Laplace space solutions can be condensed in a single dimensionless form for easier comparison and evaluation; at the same time, the condensed form facilitates the study of asymptotic solutions. Similar effort has been published since by Moench (1984). Our approach, however, is more complete and uses more appropriate dimensionless time and radius for line source solutions (with r instead of the well radius r_w); therefore, we present here the integrity of these developments and results.

The objective is to find the functions u(p') and v(p') for selected line source solutions and for insertion in the equation 46 of the text. To that end, we define two dimensionless depending parameters:

$$r_D = \frac{r}{\ell}\left(\frac{K_2}{K_1}\right)^{1/2} \qquad \text{and} \qquad b = \frac{S_{s_2}}{S_{s_1}}$$

where ℓ is a characteristic length for the matrix blocks and:

$$s_{D_i} = \frac{4\pi K_1 H s_i}{Q} \quad \text{where } i=1,2 \text{ and } H \text{ is the aquifer thickness}$$

$$t_{D_1} = \frac{K_1 t}{S_{s_1} r^2}$$

are the dimensionless drawdowns and the dimensionless time, respectively.

3.1 Pseudo-Steady-State Interporosity Flow Solutions

With the original definitions and notations, both line-source solutions (fracture and blocks) for the Warren and Root model are presented in Kazemi et al. (1969) in the Laplace space. Again, these are including the well radius r_w that is assumed infinitesimal in line-source solutions (see for example, the inner boundary condition 4 in B15) and should not be present in the definition of the dimensionless groups. For simplicity, we affect the dimensionless groups and symbols of Kazemi et al. (op.cit.) with the superscript (*). The equivalences with our notations are easily established as follows:

$$s_{D_1} \equiv 2\psi^*{}_2, \quad s_{D_2} \equiv 2\psi^*{}_1, \quad t_{D_1} \equiv \frac{t_D{}^*}{(1-w^*)r_D{}^{*2}}, \quad b \equiv \frac{w^*}{1-w^*} \quad \text{and}$$

$$r_D \equiv r_D{}^* \left[\frac{\lambda^*}{n(n+2)}\right]^{1/2} \quad \text{where n is the number of fracture planes.}$$

In the equivalence for r_D, we take advantage of the expression of the interporosity flow parameter given by Warren and Root (op.cit.) as:

$$\alpha^* = 4n(n+2)/\ell^2 \qquad \text{(his equation 1-8 of Appendix A)}$$

Calling s^* the Laplace transform parameter with respect to $t_D{}^*$, Kazemi et al. (1969) give:

$$\psi_2^* = \frac{K_0[r_D{}^*(s^*f(s^*)^{1/2}]}{s^*} \quad \text{and} \quad \psi_1^* = \frac{\lambda^*}{(1-w^*)s^*+\lambda^*}\,\psi_2^*$$

with $f(s^*) = \dfrac{w^*(1-w^*)s^*+\lambda^*}{(1-w^*)s^*+\lambda^*}$

Letting p' be the Laplace transform parameter with respect to t_{D_1}, it is straightforward to establish the following expressions using the above equivalences between dimensionless groups:

$$u(p') = \frac{r_D^2 p'}{p'/N + r_D^2/b} \qquad v(p') = \frac{r_D^2}{p'/N + r_D^2} \qquad \text{(D17)}$$

with N = 4n(n+2) is a number that can easily be determined for each considered block of geometries, N = 12 for horizontal slabs, N = 32 for match-sticks or cylinders and N = 60 for cubes or spheres.

The asymptotic behavior of the line-source solutions for the Warren and Root model are immediate if one considers D17 together with 46 in the text. When p' is small (late time behavior), we may neglect p'/N in both denominators of u(p') and v(p') yielding: $u(p') \sim bp'$ and $v(p') = 1$. Equation 46 in the text becomes unique:

$$\bar{s}_{D_1} = \bar{s}_{D_2} \sim 2K_o\left\{[p'(1+b)]^{1/2}\right\}/p'$$

which in the real space gives $s_{D_1} = s_{D_2} \sim E_1\left(\frac{1+b}{4t_{D_1}}\right)$, the Theis solution shifted by (1+b).

When p' is large (early time behavior), we have, $u(p') \sim Nr_D^2$ and $v(p') \sim Nr_D^2/p'$.

Neglecting Nr_D^2 in front of p' yields $s_{D_1} \sim 2K_o(\sqrt{p'})/p'$ which is inverted as the Theis solution. However, the behavior of s_{D_2} is different from the one of s_{D_1}. In the Laplace space, we have:

$$\bar{s}_{D_2} \sim \frac{2Nr_D^2}{p'^2} K_o(\sqrt{p'})$$

which using B6 is inverted as:

$$\bar{s}_{D_2} \sim Nr_D^2 \int_0^{t_{D_1}} E_1\left(\frac{1}{4z}\right)dz \sim Nr_D^2\left[-E_2\left(\frac{1}{4t_{D_1}}\right)+E_2(0)\right]$$

$$\bar{s}_{D_2} \sim Nr_D^2\left[1 + \frac{1}{4t_{D_1}} E_1\left(\frac{1}{4t_{D_1}}\right) - \exp(-1/4t_{D_1})\right]$$

where we have used classical results for the exponential integral functions (Abramovitz and Stegun, 1972, pp. 229-230).

When $x = 1/4t_{D_1}$ is large, $xE_1(x) - \exp(-x) \sim -\exp(-x)/x$ (p.231 of above reference).

Hence:

$$s_{D_2} \sim Nr_D^2[1 - 4t_{D_1} \exp(-1/4t_{D_1})] \qquad \text{(D18)}$$

which, of course, is different from the Theis solution. It is interesting to note that the limiting slope of the type curves from D18 at early times is independent of t_{D_1}. It is equal to Nr_D^2 since the derivative of $4t_{D_1} \exp(-1/4t_{D_1})$ tends towards zero when $1/4t_{D_1}$ tends towards infinity.

Both asymptotic behaviors for fracture drawdown look similar to those related to the delayed yield concept proposed by Boulton (1963) for unconfined aquifers. This deserves a closer examination. Boulton (op.cit.) solves:

$$\Delta s = \frac{S_s}{K}\frac{\partial s}{\partial t} + \alpha \frac{S'_s}{K}\int_0^t \left.\frac{\partial s}{\partial t}\right|_{t=z} \exp[-\alpha(t-z)]dz$$

where S_s and S'_s are the instantaneous and delayed specific storages, and $1/\alpha[T]$ is the delay index. This PDE is solved with the usual initial and boundary conditions for line-source solutions. In the Laplace space, the above equation becomes:

$$\Delta\bar{s} = \frac{S_s}{K} p\bar{s} + \alpha \frac{S'_s}{K} p\bar{s}/(p+\alpha)$$

Upon zero-Hankel transformation, we find:

$$-a^2 s^* + \frac{Q}{2\pi KHp} = \frac{S_s}{K} ps^* + \alpha \frac{S'_s}{K} p\, s^*/(p+\alpha) \quad \text{with } H = \text{aquifer thickness}$$

Solving for s* yields:

$$s^*[a^2 + \frac{pS_s}{K} + \frac{\alpha S'_s}{K}\,\frac{p}{p+\alpha}] = \frac{Q}{2\pi KHp}$$

immediately inverted as:

$$\frac{2\pi KH}{Q}\bar{s} = \frac{1}{p}K_o[r\sqrt{A(p)}] \quad \text{with } A(p) = p\frac{S_s}{K} + \alpha\frac{S'_s}{K}\,\frac{p}{p+\alpha}$$

Transforming in the dimensionless Laplace space with

$$[L(t_D = \frac{Kt}{S_s r^2})] = p' = \frac{r^2 S_s}{K}p$$

$$\overline{s_D} = \frac{2}{p'}\; K_o\left\{[(p'+A(p')]^{1/2}\right\} \text{with } A(p') = r'_D{}^2\, p'/\left[p' + \frac{r'_D{}^2}{b'}\right] \qquad \text{(D19)}$$

with $r'_D = r(\frac{K}{\alpha S'_s})^{-1/2} = (\frac{r}{B})^* \text{ and } b' = \frac{S'_s}{S_s} = (\eta^*-1)$

where $(\frac{r}{B})^*$ and η^* are Boulton's dimensionless parameters and

$s_D = \frac{4\pi KHs}{Q}$

D19 compared to D17 clearly establishes that type curves for unconfined aquifers with delayed yield are the same over the entire time domain as the type curves for fracture drawdown in a dual porosity confined aquifer with pseudo-steady-state interporosity flow. Evaluation of D19 can be done for the entire time-domain with the Stehfest inverter; the depending parameters obtained when using the same set of type curves for aquifer test analysis will simply have another physical significance. Another theoretical implication is that, in spite of the appearances, the concept of delayed yield of Boulton is, in fact, treated as a pseudo-steady-state physical process for a "dual porosity" (S_s and S'_s) unconfined aquifer. S'_s is commonly called "specific yield".

3.2 Transient Interporosity Flow Solutions

Because the same developments can be applied to all the other solutions, we only present the details of the derivation of the u and v functions for the case of transient interporosity flow in horizontal and infinite slab-shaped blocks. The reader can easily verify the validity of the other expressions starting from the original publications referenced in the text.

- For infinite slabs of thickness ℓ

de Swaan (1976) expresses the interporosity flow as a convolution-type source term:

$$\int_0^t \frac{\partial s_1}{\partial t}\bigg|_{t=\tau} q_u(t-\tau)d\tau$$

where q_u is the flow corresponding to a unit-step head loss at the interface matrix block-fracture.

For obvious symmetry reasons in a series of slab-shaped blocks and fractures, the characteristic length is $\ell/2$ for the blocks, the mean block thickness being ℓ.

Solving the one-dimensional (vertical) flow in the matrix slab (origin of z at the interface matrix-fracture), de Swaan (op.cit.) obtains:

$$\frac{\partial s_2}{\partial z}\bigg|_{z=\ell/2} = \frac{2}{\ell}\,\theta_1\left(\frac{1}{2},\ \exp[\pi^2\alpha_2 t/(\ell/2)^2]\right)$$

where θ_1 is the first order Theta function. In the Laplace space and from tables of Laplace transforms, one can easily evaluate:

$$\left.\frac{\partial \overline{s_2}}{\partial z}\right|_{z=\ell/2} = -\frac{1}{(\alpha_2 p)^{1/2}} \tanh\left(\frac{\ell}{2\sqrt{\alpha_2}}\sqrt{p}\right)^{1/2}$$

and

$$q_u(p) = K_2 A \left.\frac{\partial \overline{s_2}}{\partial z}\right|_{z=\ell/2} = -K_2 A(\alpha_2 p)^{-1/2} \tanh\left[\frac{\ell}{2}\left(\frac{p}{\alpha_2}\right)^{1/2}\right]$$

The governing equation for $\overline{s_1}$ in the Laplace space becomes[1]:

$$\Delta\overline{s_1} = \frac{p}{\alpha_1}\overline{s_1} + \frac{2\overline{s_1}}{\ell} p \frac{K_2}{K_1}(\alpha_2 p)^{-1/2} \tanh\left[\frac{\ell}{2}\left(\frac{p}{\alpha_2}\right)^{1/2}\right]$$

Unfortunately, de Swaan stops at this stage of the derivation because he was only interested in late time asymptotic solutions. A possible continuation is to use the zero-Hankel transformation which yields as before:

$$s_{D_1}^{*} (a^2 + A(p)] = \frac{2}{p}$$

that is inverted into:

$$s_{D_1} = \frac{2}{p} K_0 \left(r[A(p)]^{1/2}\right)$$

with $A(p) = \frac{p}{\alpha_1} + \frac{2p}{\ell}\frac{K_2}{K_1}(\alpha_2 p)^{-1/2} \tanh\left[\frac{\ell}{2}\left(\frac{p}{\alpha_2}\right)^{1/2}\right]$

In the dimensionless Laplace space ($p' = \frac{r^2 S_{s_1}}{K_1} p$) and with $r_D = \frac{2r}{\ell}(K_2/K_1)^{1/2}$ (characteristic length = $\ell/2$).

$$A(p') = p' + r_D(bp')^{1/2} \tanh[(bp')^{1/2}/r_D]$$

The one-dimensional diffusion equation solved for the block in the Laplace space is:

$$\overline{s_{D_2}}(z,p) = \overline{s_{D_1}}(r,p)[\cosh(zy) - \tanh(\ell y/2)\sinh(zy)]$$

---

[1] The source term for slabs is actually: $\bar{q} = -\frac{2}{Ah_1}(p\overline{s_1})$ $\bar{q} = \frac{2K_2}{K_1\ell}\left.\frac{\partial\overline{s_2}}{\partial z}\right|_{z=\ell/2}$

from tables of Laplace transforms, one can easily evaluate:

$$\left.\frac{\partial \bar{s}_2}{\partial z}\right|_{z=\ell/2} = -\frac{1}{(\alpha_2 p)^{1/2}} \tanh\left(\frac{\ell}{2\sqrt{\alpha_2}}\sqrt{p}\right)^{1/2}$$

and

$$q_u(p) = K_2\, A \left.\frac{\partial \bar{s}_2}{\partial z}\right|_{z=\ell/2} = -K_2 A(\alpha_2 p)^{-1/2} \tanh\left[\frac{\ell}{2}\left(\frac{p}{\alpha_2}\right)^{1/2}\right]$$

The governing equation for $\bar{s}_1$ in the Laplace space becomes[1]:

$$\Delta\bar{s}_1 = \frac{p}{\alpha_1}\,\bar{s}_1 + \frac{2\bar{s}_1}{\ell}\, p\,\frac{K_2}{K_1}(\alpha_2 p)^{-1/2} \tanh\left[\frac{\ell}{2}\left(\frac{p}{\alpha_2}\right)^{1/2}\right]$$

Unfortunately, de Swaan stops at this stage of the derivation because he was only interested in late time asymptotic solutions. A possible continuation is to use the zero-Hankel transformation which yields as before:

$$s_{D_1}^{*}\,(a^2 + A(p)] = \frac{2}{p}$$

that is inverted into:

$$\bar{s}_{D_1} = \frac{2}{p}\,K_0\,\left(r[A(p)]^{1/2}\right)$$

with $A(p) = \frac{p}{\alpha_1} + \frac{2p}{\ell}\frac{K_2}{K_1}(\alpha_2 p)^{-1/2} \tanh\left[\frac{\ell}{2}\left(\frac{p}{\alpha_2}\right)^{1/2}\right]$

In the dimensionless Laplace space ($p' = \frac{r^2 S_{s_1}}{K_1}\,p$) and with $r_D = \frac{2r}{\ell}(K_2/K_1)^{1/2}$ (characteristic length = $\ell/2$).

$$A(p') = p' + r_D(bp')^{1/2} \tanh[(bp')^{1/2}/r_D]$$

The one-dimensional diffusion equation solved for the block in the Laplace space is:

$$\bar{s}_{D_2}\,(z,p) = \bar{s}_{D_1}\,(r,p)[\cosh(zy) - \tanh(\ell y/2)\,\sinh(zy)]$$

---

[1] The source term for slabs is actually: $\bar{q} = -\frac{2}{Ah_1}\,(p\bar{s}_1)\;\bar{q} = \frac{2K_2}{K_1\ell}\left.\frac{\partial \bar{s}_2}{\partial z}\right|_{z=\ell/2}$

with $y = (p/\alpha_2)^{1/2}$

Defining $z_D=2z/\ell$ and transforming in the dimensionless Laplace space, we find easily $v(z_D,p')$.

The sought functions are, therefore, simply:

$$\left.\begin{array}{l} v(z_D,p') = \cosh[(1-z_D)\phi]/\cosh\phi \\ \\ u(p') = r_D{}^2\phi\tanh\phi \end{array}\right\} \text{(D20)}$$

with $\phi = (bp')^{1/2}/r_D$ and $z_D = 2z/\ell$

Late time behavior

When $\phi<0.2$ (of the order of $t_{D_1}>25b/r_D{}^2$), $\tanh(\phi)\sim\phi$ (precision 1%):

$u\sim bp'$

$v\sim 1 - 2bz_D p'/r_D{}^2$

yielding for $\overline{s_{D_1}}$ and $\overline{s_{D_2}}$:

$$\overline{s_{D_1}} \sim 2/p' \; K_o \left\{[p'(1+b)]^{1/2}\right\}$$

$$\overline{s_{D_2}} \sim (1-\frac{2bz_Dp'}{r_D{}^2})\overline{s_{D_1}}$$

which are inverted into:

$$\left.\begin{array}{l} s_{D_1} = E_1(\frac{1+b}{4t_{D_1}}) \\ s_{D_2} = E_1(\frac{1+b}{4t_{D_1}}) - \frac{bz_D}{t_{D_1}r_D{}^2}\exp[-\frac{(1+b)}{4t_{D_1}}] \end{array}\right\} \text{(D21)}$$

At usual values of the parameters: b=100, r_D=0.1 and z_D=0.5 and at the lower bound of t_{D_1} from the above condition, the second term in the expression of s_{D_2} is approximately 10^{-2} meanwhile $E_1(1+b/4t_{D_1}) = \ln[4t_{D_1}/1+b] - 0.5772 = 8.6$. The asymptotic solution for s_{D_2} is, therefore, practically confunded with the Theis solution shifted by (1+b). This homogeneous equivalent behavior will not happen, however, before t_{D_1}=250,000; assuming $S_{s_1} = 5\times10^{-5}$ m^{-1}, r=10 m and K_1=0.1 m/s, the late time homogeneous response could be first observed after 3.5 hours of pumping. This time is tenfold if K_1=0.01 m/s. These are reasonable aquifer test durations.

- For spheres of radius ℓ, with the same argument as for horizontal slabs, de Swaan obtains:

$$\left.\frac{\partial s_2}{\partial r}\right|_{r=\ell} = \frac{2}{\ell}\sum_{n=1}^{\infty} \exp(-n^2\pi^2\alpha_2 t/\ell^2)$$

which is a fourth order Theta function transformed in the Laplace space as:

$$\left.\frac{\partial \bar{s}_2}{\partial r}\right|_{r=\ell} = -\frac{1}{\ell p}[\ell y \coth(\ell y)-1] \text{ with } y = (p/\alpha_2)^{1/2}$$

This will yield for A(p):

$$A(p) = \frac{p}{\alpha_1} + \frac{3}{\ell^2}\frac{K_2}{K_1}[\ell y \coth(\ell y)-1]$$

After the necessary transformations, we obtain u(p') of equation D22 below.

The matrix block drawdown is obtained in a straightforward fashion considering spherical flow with the interface boundary at the contact matrix block-fracture; we obtain:

$$\left.\begin{aligned} v(\rho_D,p') &= \frac{1}{\rho_D}\left[\frac{\sinh(\rho_D\phi)}{\sinh\phi}\right] \\ u(p') &= 3r_D^2(\phi\coth\phi-1) \end{aligned}\right\} \quad (D22)$$

with $\phi = (bp')^{1/2}/r_D$ and $\rho_D = r/\ell$ with $r<\ell$

At late times when $\phi<0.5$ (of the order of $t_{D_1}>b/4r_D^2$) $\phi\coth\phi\sim\phi^2/3+1$ (precision 10^{-3}) and again $u(p')\sim bp'$.

We may also approximate:

$$\sinh(\phi\rho_D)/\sinh\phi\sim\rho_D(1-\phi^2/6) \quad \text{(maximum error < 1\%)}$$

Therefore, $v(p')\sim(1-\phi^2/6)$ is independent of ρ_D. The fracture drawdown type curve will be confunded again with the shifted Theis solution at values of t_{D_1} 25 times smaller than for slab-shaped blocks. For the real space drawdowns as before we obtain:

$$\begin{aligned} s_{D_2} &= E_1\left(\frac{1+b}{4t_{D_1}}\right) - \frac{3}{2}\,\frac{b}{r_D^2}\,\frac{1}{t_{D_1}}\,\exp\left[-\left(\frac{1+b}{4t_{D_1}}\right)\right] \\ s_{D_1} &= E_1\left(\frac{1+b}{4t_{D_1}}\right) \end{aligned} \qquad (D23)$$

The difference $(s_{D_1}-s_{D_2})$ at late times is practically independent of the position within the sphere (of ρ_D). For the same usual set: $b=100$ and $r_D=0.1$, this difference has a maximum of about 6 at the time when the type curve for s_{D_1} starts to merge with the shifted Theis solution; this happens for $t_{D_1}=2500$ and $s_{D_1}=4$.

At $t_{D_1}=10^5$, $(s_{D_1}-s_{D_2})$ is 0.15. Therefore, the same conclusion for the duration of aquifer tests holds as in the case of slab-shaped blocks: the equivalent homogeneous behavior may even require a slightly smaller pumping time to be observed.

- For the case of cylinders of radius ℓ, the reader is referred to the derivation of Kucuk and Sawyer (1980). These authors found (after transformation and with our notations):

$$\begin{aligned} u(p') &= 2r_D^2\phi\ I_1(\phi)/I_0(\phi) \\ v(p') &= I_0(\rho_D\phi)/I_0(\phi) \end{aligned} \qquad (D24)$$

where I_1 and I_0 are the modified Bessel functions of order one and zero, respectively.

At late times, when $\phi<0.3$ (of the order of $t_{D_1}>100b/9r_D^2$),

$I_1(\phi)/I_0(\phi)\sim\phi/2$ (precision 1%)

$$\begin{aligned} u(p') &\sim bp' & & & s_{D_1} &= E_1\left(\frac{1+b}{4t_{D_1}}\right) \\ & & &\text{yielding} & & \\ v(p') &\sim 1-\frac{bp'}{4r_D^2} & & & s_{D_2} &= E_1\left(\frac{1+b}{4t_{D_1}}\right)-\frac{b}{8r_D^2 t_{D_1}}\exp\left(-\frac{1+b}{4t_{D_1}}\right) \end{aligned} \qquad (D25)$$

Hence, both s_{D_1} and s_{D_2} behave in an analogous manner as in the case of slabs and spheres.

- For the cases with fracture skin fs_D, the reader is referred to Moench (1984) for slab-shaped blocks:

$$\begin{aligned} u(p') &= u_0(p')/(1+fs_D\phi\tanh\phi) \\ v(p') &= v_0(p')/(1+fs_D\phi\tanh\phi) \end{aligned} \qquad (D26)$$

where u_0 and v_0 are given by D20, i.e. the case without fracture skin ($f_{s_D}=0$).

- for sphere-shaped blocks:

$$u(p') = u_o(p')/(1+fs_D[\phi\coth\phi-1])$$

(D27)

$$v(p') = v_o(p')/1+fs_D[\phi\coth\phi-1])$$

where u_o and v_o are given by D22.

- for cylindrical blocks (not considered by Moench (op.cit.)), we find:

$$u(p') = u_o(p')/[1+fs_D\phi I_1(\phi)/Io(\phi)]$$

(D28)

$$v(p') = v_o(p')/[1+fs_D\phi I_1(\phi)/Io(\phi)]$$

with u_o and v_o as in D24.

For convenience, these results have been condensed into Table D1.

3.3 Early Time Behavior of the Line-Source Solutions with Transient Interporosity Flow

Asymptotic solutions are less obvious at early times and deserve special attention. When t_{D_1} is small, p' and ϕ are large.

For pseudo-steady-state interporosity flow we have established that:

- the fracture drawdown is asymptotic to the Theis solution since $u(p')\sim Nr_D^2$ negligible when compared to p',

Table D1
Dimensionless Laplace space solutions (together with equation in text) and late asymptotic real space solutions for dual porosity systems.

Interporosity flow regime	Block Geometry	$u(p')$	$v(p')$	Late s_{D_1}	Late $(s_{D_1}-s_{D_2})$
Pseudo-steady-state	function of $N=4n(n+2)$	$\frac{r_D\, p'}{p'/N+r^2_D/b}$	$\frac{r_D^2}{p'/N+r_D^2}$	Theis shifted by (1+b)	0
Transient No skin	slabs*	$r_D^2\phi\tan\phi$	$\cosh[(1-z_D)\phi]/\cosh\phi$	Theis shifted by (1+b)	$\frac{bz_D}{8r_D^2 t_{D_1}}\exp[-\frac{(1+b)}{4t_{D_1}}]$
Transient No skin	spheres*	$3r_D^2(\phi\coth\phi-1)$	$\frac{1}{\rho_D}\frac{\sinh(\rho_D\phi)}{\sinh\phi}$	Theis shifted by (1+b)	$\frac{3}{2}\frac{b}{r_D^2}\frac{1}{t_{D_1}}\exp[-\frac{(1+b)}{4t_{D_1}}]$
Transient No skin	cylinders*	$2r_D^2\phi I_1(\phi)/Id(\phi)$	$I_o(\rho_D\phi)/I_o(\phi)$	Theis shifted by (1+b)	$\frac{b}{8r_D^2}\frac{1}{t_{D_1}}\exp[-\frac{(1+b)}{4t_{D_1}}]$
Transient with pseudo-steady-state flow in fracture skin (f_{s_D})**	slabs spheres cylinders	no skin/$1+f_{s_D}\phi\tanh\phi$ no skin/$1+f_{s_D}(\phi\coth\phi-1)$ no skin/$1+f_{s_D}\phi I_1(\phi)/I_o(\phi)$		Same as pseudo-steady-state with $f_{s_D}\equiv 1/N$	-

* $r_D = 2r/\ell(K_2/K_1)^{1/2}$

** $f_{s_D} = K_2b'/K'\ell$ where b' is the average thickness of the fracture skin [L] of hydraulic conductivity $K'[LT^{-1}]$

- the block drawdown can be approximated by D18, different from the Theis type curve.

a) Slabs with no fracture skin (equation D20):

When $\phi>4$ (i.e. $t_{D_1}<b/16r_D^2$), $\tanh\phi \approx 1$ (precision 10^{-3}) and:

$u(p') \sim r_D(bp')^{1/2}$, therefore, for s_{D_1}:

$$s_{D_1} = 2/p' \; K_o \left\{[p'+r_D(bp')^{1/2}]^{1/2}\right\}$$

which is immediately inverted as $s_{D_1} = H[1/4t_{D_1}, (r_D\sqrt{b}/4)]$ where the function H is tabulated by Hantush (1960) and described by Hantush (1964). At low dimensionless time, when:

$$t_{D_1} < \frac{4\times10^{-4}}{br_D^2} \quad s_{D_1} = E_1(\frac{1}{4t_{D_1}}) - \frac{r_D}{\sqrt{\pi}}\sqrt{4bt}_{D_1}[0.258+0.693 \; \overline{\exp}(-\frac{1}{8t_{D_1}}]$$

which is close to, but not exactly a Theis solution; for example, when $r_D=0.1$ and $b=100$, the condition on t_{D_1} is $t_{D_1}<4\times10^{-4}$. The function $H(1/4t_{D_1}, r_D\sqrt{b}/4)$ is a valid approximation of s_{D_1} over a large early time interval: with the same realistic values of b and r_D, it is valid up to $t_{D_1}=625$.

For $\phi>>10$ ($t_{D_1}<b/100r_D^2$), we have:

$$v(p') \sim \exp[-z_D(bp')^{1/2}/r_D]$$

We may rewrite the argument of K_o in $\overline{s_{D_1}}$ as:

$$p'(1+\frac{r_D\sqrt{b}}{p'})]^{1/2} = \sqrt{p'}$$

and for $\overline{s_{D_2}}$ since now $1/\sqrt{p'} = \sqrt{b}/r_D\ 1/\phi$ is much smaller because of the new condition on ϕ. For s_{D_2} (equation 46 of text), using B6 and this simplified expression for $\overline{s_{D_1}}$, we have:

$$s_{D_2} = \int_0^{t_{D_1}} \mathrm{erfc}[a/\sqrt{4(t_{D_1}-\tau)}]\exp(-1/4\tau)\,\frac{d\tau}{4\tau} \quad \text{where } a=z_D\sqrt{b}/r_D$$

Upon the change of variable $y=1/4\tau$, the integral becomes:

$$s_{D_2} = \int_{1/4t_{D_1}}^{\infty} \mathrm{erfc}[a(4t_{D_1}-\frac{1}{y})^{-1/2}]e^{-y}\,\frac{dy}{y}$$

From erfc(-x)=1+erf(x), we have:

$$\mathrm{erfc}[a(4t_{D_1}-\frac{1}{y})^{-1/2}] = 1+\mathrm{erf}[a\sqrt{y}(1-4t_{D_1}/y)^{-1/2}]=1+\mathrm{erf}(a\sqrt{y})$$

Hence:

$$s_{D_2} = \int_{1/4t_{D_1}}^{\infty} e^{-y}\,\frac{dy}{y} + \int_{1/4t_{D_1}}^{\infty} \mathrm{erf}(a\sqrt{y})e^{-y}\,\frac{dy}{y} = E_1(\frac{1}{4t_{D_1}}) + M(\frac{1}{4t_{D_1}}, \frac{z_D\sqrt{b}}{r_D})$$

where M is again an extensively tabulated function (Hantush, 1964).

In summary, for the horizontal slab configuration:

$$t_{D_1} < b/16r_D^2 \qquad s_{D_1} = H[1/4t_{D_1}, r_D(b/16)^{1/2}]$$

$$t_{D_1} < b/100r_D^2 \qquad s_{D_2} = E_1(1/4t_{D_1}) + M[1/4t_{D_1}, (z_D\sqrt{b}/r_D)] \qquad \text{(D29)}$$

When b=100 and $r_D=0.1$, the asymptotic expression for s_{D_1} is valid up to $t_{D_1}=625$. The time domain of validity for s_{D_2} is up to $t_{D_1}=100$; at that time the "distance" for $z_D=0.5$ between s_{D_2} and the Theis solution is about 5.2; when $t_{D_1}=5$, it is still 3.3 (see tables of the function M in Hantush, op.cit.).

b) spheres with no fracture skin (equation D22)

When $\phi>3$, $\coth\phi\approx1$ (0.5% error). However, within 1% error, we have $\phi\coth\phi-1\approx\phi$ only when ~~$\phi>100$ (of the~~ order of $t_{D_1} < b/100r_D^2$) and we have:

$$u(p')\sim3r_D^2\phi \text{ or } \overline{s_{D_1}} \approx 2/p'\, K_o[(p'+3r_D\sqrt{b}\sqrt{p'})^{1/2}]$$

or

$$s_{D_1} \approx H(\frac{1}{4t_{D_1}}, \frac{3r_D\sqrt{b}}{4})$$

$$v(p') \sim \frac{1}{\rho_D}\exp[-(1-\rho_D)\phi] \text{ when } \phi\rho_D>>10 \text{ (of the order of } t_{D_1}<<\frac{b}{100}(\frac{\rho_D}{r_D})^2 \text{)}$$

With the same argument as for the case of slabs, we find:

$$\text{for } t_{D_1} < \frac{b}{100r_D^2} \quad s_{D_1} \approx H(\frac{1}{4t_{D_1}}, \frac{3r_D\sqrt{b}}{4})$$

$$\text{for } t_{D_1} << \frac{b}{100}(\frac{\rho_D}{r_D})^2 \quad s_{D_2} \approx E_1(\frac{1}{4t_{D_1}}) + M(\frac{1}{4t_{D_1}}, \frac{(1-\rho_D)\sqrt{b}}{r_D}) \tag{D30}$$

c) cylinders with no fracture skin (equation D24)

When $\phi>10(t_{D_1} > \frac{b}{100r_D^2})$, $I_1(\phi)/I_o(\phi) \approx (1-\frac{3}{8\phi})(1-\frac{1}{8\phi}) \approx 1-\frac{1}{2\phi}$ when neglecting the terms with $1/\phi^2$.

$$u(p') \approx 2r_D^2\phi - r_D^2 \approx 2r_D^2\phi \approx 2r_D(bp')^{1/2}$$

$$s_{D_1} \approx H(\frac{1}{4t_{D_1}}, \frac{r_D\sqrt{b}}{2})$$

In the same conditions, $v(p') \sim (1+\frac{\rho_D-1}{8\phi}) \sim 1$ since $0<\rho_D<1$

$$\text{Therefore, when } t_{D_1} > \frac{b}{100r_D^2} \quad s_{D_1} \approx s_{D_2} \approx H(\frac{1}{4t_{D_1}}, \frac{r_D\sqrt{b}}{2}) \tag{D31}$$

d) configurations with fracture skin

If both f_{s_D} and ϕ are such that $(\phi\tanh\phi)^{-1}$, $(\phi\coth\phi-1)^{-1}$ and $[\phi I_1(\phi)/I_0(\phi)]^{-1}$ can be neglected with regard to f_{s_D}, $u(p')\sim r_D^2/f_{s_D}$ which can be neglected when compared to p' ($0<f_{s_D}<10$, usually). The Theis solutions are, therefore, obtained as asymptotic solutions for s_{D_1} for all the configurations, as in the case of pseudo-steady-state interporosity flow. Asymptotic solutions for s_{D_2}, however, will not be Theis curves and are depending on f_{s_D}, ρ_D and z_D values.

4. COMPARISON WITH LINE-SOURCE SOLUTIONS FOR LEAKY AQUIFER SYSTEMS

Consider the two-aquifer system described mathematically in Appendix C.

- Equation C5 is a limiting case when $T_2 \to \infty$ (a=0) which corresponds to no drawdown in the upper aquifer ($s_{D_2}=0$) or to the case of an aquifer overlain by an aquitard with a "source bed" on top. We found:

$$\begin{aligned} \overline{s_{D_1}} &= 2/p' \; K_0 \; [p' + r_D^2 \phi \coth\phi]^{1/2} \\ \overline{s'_D} &= \frac{1}{s_{D_1}} \, \frac{\sinh[(1-z_D)\phi]}{\sinh\phi} \end{aligned} \qquad \text{(D32)}$$

Comparing these results with D22, where ϕ is the same if r_D is the same, we see that the argument of K_0 in $\overline{s_{D_1}}$ will be the same if $\ell \equiv (3H_1H')^{1/2}$ where H_1 and H' are the aquifer and aquitard thickness and if $K_2 \equiv K'$ and finally in D22, if $\phi\coth\phi$ is much greater than 1. For $\overline{s_{D_2}}$ to be equivalent to $\rho_D \overline{s'_D}$, it suffices that $1-z_D \equiv \rho_D$.

Consequently, both solutions D22 and D32 are practically identical; although corresponding to different physical realities, the resulting type-curves will be very similar. This means that practically errors can be done in aquifer test analysis of observation well responses that should look alike.

- The same parallel established for sphere-shaped blocks can be done for the slabs with the aquitard-aquifer system that has no source bed on top of the aquitard (upper unit impermeable $T_2=0$, $a\to\infty$). In this case, the identity of the solutions is even perfect. For such a leaky system, Streltsova (1984) obtains:

$$\overline{s_{D_1}} = 2/p' \; K_0 \, [(p' + r_D{}^2\phi\tan\phi)^{1/2}]$$

$$\overline{s'_D} = \overline{s_{D_1}} \cosh[(1-z_D)\phi]/\cosh\phi \qquad \text{(D33)}$$

This is exactly the same as D20 with $H'\equiv 2\ell$ in the expressions of r_D and z_D.

The reasons of these striking similarities are mathematically obvious: similar IBVP are being solved in both models. The practical implications are discussed in the text.

APPENDIX E

TWO-LAYERED AQUIFER

1. MATHEMATICAL MODELS

Let us consider the transient flow to a well that fully penetrates a two-layer aquifer system and is produced at a constant rate Q. The well has a finite radius r_w and the system is bounded laterally (no flow at a radial distance R) and vertically (no flow at top and base of the system). Both aquifers are homogeneous, isotropic, horizontal and of constant thickness. The lower aquifer (subscript 1) has a thickness H_1 and flow properties K_1, S_{s_1}, α_1; the upper aquifer (subscript 2) is characterized by H_2, K_2, S_{s_2} and α_2. We seek solutions for the drawdowns $s_1(r,z,t)$ and $s_2(r,z,t)$ in the general case with cross-flow occurring at the interface $z=H_1$ and when the system is initially at rest: $s_1(r,z,o)=s_2(r,z,o)=0$. The interface $z=H_1$ has a perfect hydraulic contact. The origin $z=0$ is the base of the system. Using the initial conditions and performing a Laplace transform with respect to time, $s_i(r,z,t)$ becomes $\overline{s_i}(r,z,p)$ with $i=1,2$, the IBVP is completely described by the following set of equations:

- Governing equations in both aquifers:

$$\Delta\overline{s_1} = (p/\alpha_1)\overline{s_1} \qquad \text{(E1)}$$

$$\Delta\overline{s_2} = (p/\alpha_2)\overline{s_2} \qquad \text{(E2)}$$

where, as usual

$$\Delta = \partial^2/\partial r^2 + (1/r)(\partial/\partial r) + \partial^2/\partial z^2$$

- No flow at top and base of the system:

$$\frac{\partial \overline{s_1}}{\partial z}(r,0,p) = 0 \qquad \text{(E3)}$$

$$\frac{\partial \overline{s_2}}{\partial z}(r,H_1+H_2,p) = 0 \qquad \text{(E4)}$$

- Continuity of heads at the interface $z=H_1$:

$$\overline{s_1}(r,H_1,p) = \overline{s_2}(r,H_1,p) \qquad \text{(E5)}$$

- Continuity of fluxes at the interface $z=H_1$:

$$K_1 \frac{\partial \overline{s_1}}{\partial z}(r,H_1,p) = K_2 \frac{\partial \overline{s_2}}{\partial z}(r,H_1,p) \qquad \text{(E6)}$$

- Outer boundary conditions: no flow at $r=R$

$$\frac{\partial \overline{s_1}}{\partial r}(R,z,p) = 0 \qquad \text{(E7)}$$

$$\frac{\partial \overline{s_2}}{\partial r}(R,z,p) = 0 \qquad \text{(E8)}$$

- Inner boundary conditions: Darcy's law at $r=r_w$:

$$\int_0^{H_1} K_1 \frac{\partial \overline{s_1}}{\partial r}(r_w,z,p)\, d_z + \int_{H_1}^{H_1+H_2} K_2 \frac{\partial \overline{s_2}}{\partial r}(r_w,z,p)dz = -\frac{Q}{2\pi r_w p} \qquad \text{(E9)}$$

$$\overline{s_1}(r_w,z,p) = \overline{s_2}(r_w,z,p) = \overline{s_w}(p) \qquad \text{(E10)}$$

Equation E9 states that, at the well face, the total flow rate Q is the sum of both aquifer contributions; wellbore storage and skin effect are neglected. Equation E10 assumes that well loss and gravity effects are neglected at the well rendering the drawdowns independent of z.

Although physically simple and of important practical interest, the IBVP as formulated by equations E1 to E10 does not lead mathematically to analytical solutions that are easy to evaluate, even in the Laplace space. This will be further illustrated. Special cases of this mathematical model are obtained when the following assumptions are made:

1. assuming that the well radius is negligible with respect to r, H_i and R; the inner boundary conditions ($r_w \to 0$) become:

   $$\lim_{r\to 0} \left(r\frac{\partial \bar{s}_1}{\partial r}\right) + \lim_{r\to 0} \left(r\frac{\partial \bar{s}_2}{\partial r}\right) = -\frac{Q}{2\pi(T_1+T_2)p} \qquad \text{(E11)}$$

   $$\lim_{r\to 0} [\bar{s}_1(r,z,p)] = \lim_{r\to 0} [\bar{s}_2(r,z,p)] = \bar{s}_w(p) \qquad \text{(E12)}$$

   this assumption is generally applicable to aquifer (or interference) tests;

2. assuming that the system is laterally infinite ($R\to\infty$) changes the equations E7 and E8 to:

   $$\lim_{r\to\infty} [\bar{s}_1(r,z,p)] = \lim_{r\to\infty} [\bar{s}_2(r,z,p)] = 0 \qquad \text{(E13)}$$

   the validity of this assumption is problem-specific and depends on the information available to describe the system geometry.

3. assuming that $H_1 \ll H_2$ renders s_1 independent of z so that we may reduce equations E1, E4 and E5 to the two equations:

   $$\frac{\partial^2 \bar{s}_1}{\partial r^2} + \frac{1}{r}\frac{\partial \bar{s}_1}{\partial r} = \frac{p}{\alpha_1}\bar{s}_1 + \frac{1}{T_1}\left(-K_2 \frac{\partial \bar{s}_2}{\partial z}\bigg|_{z=H_1}\right) \qquad \text{(E14)}$$

   $$\bar{s}_1(r,p) = \bar{s}_2(r,H_2,p) \qquad \text{(E15)}$$

this case with assumptions 1 and 2 has been fully treated by Boulton and Streltsova (1977b) and will not be considered here;

4. assuming no cross-flow at the interface renders both drawdowns independent of z so that $\Delta = \partial^2/\partial r^2 + (1/r)(\partial/\partial r)$ in E1 and E2; E3, E4, E5 and E6 disappear; E7, E8, E9 and E10 are rewritten, respectively, as:

$$\lim_{r\to\infty}[\overline{s_1}(r,p)]=0 \tag{E16}$$

$$\lim_{r\to\infty}[\overline{s_2}(r,p)]=0 \tag{E17}$$

$$T_1\frac{\partial\overline{s_1}}{\partial r}(r_w,p) + T_2\frac{\partial\overline{s_2}}{\partial r}(r_w,p) = -\frac{Q}{2\pi r_w p} \tag{E18}$$

$$\overline{s_1}(r_w,p) = \overline{s_2}(r_w,p) = \overline{s_w}(p) \tag{E19}$$

Depending on the flow problem, further simplification of the mathematical model E1 to E10 can be imagined by combining these four series of assumptions. For example, grouping assumptions 1 and 2 describes the IBVP of an infinite two-layer system with cross-flow fully penetrated by a well of negligible radius with the additional assumption 3 on the aquifer thicknesses.

2. THE GENERAL SOLUTIONS IN THE LAPLACE SPACE

Solving the system of equations E1 to E10, Jacquard (1960) proposes the following (general) solutions in the Laplace space (with our usual notations):

$$\overline{s_1}(r,z,p) = \overline{s_w}(p) \sum_{n=0}^{\infty} A_n \frac{Un,r}{Un,r_w} \frac{\cos(x_n \; z/H_1)}{\cos(x_n)} \qquad \text{(E20)}$$

$$\overline{s_2}r,z,p) = \overline{s_w}(p) \sum_{n=0}^{\infty} A_n \frac{Un,r}{Un,r_w} \frac{\cos[y_n(H_1 + H_2 - z)/H_2]}{\cos(y_n)} \qquad \text{(E21)}$$

where:

$$\overline{s_w}(p) = \frac{Q}{2\pi p} \left[\sum_{n=0}^{\infty} A_n \frac{Wn,r_w}{U_n,r_w} (T_1\tan(x_n)/x_n + T_2\tan(y_n)/y_n)\right]^{-1}$$

$A_n = 2N/D$ with $N = T_1\tan(x_n)/x_n + T_2 \tan(y_n)/y_n$

and $D = T_1/\cos^2(x_n) + T_2/\cos^2(y_n) + T_1\tan(x_n)/x_n + T_2\tan(y_n)/y_n$

$$Un,r = I_1(Rq_n)\, K_o(rq_n) + K_1(Rq_n)\, I_o(rq_n)$$

$$Un,r_w = I_1(Rq_n)\, K_o(r_w q_n) + K_1(Rq_n)\, I_o(r_w q_n)$$

$$Wn,r_w = r_w q_n[I_1(Rq_n)\, K_1(r_w q_n) - K_1(Rq_n)\, I_1(r_w q_n)]$$

$$q_n = \left[\frac{p}{\alpha_1} + \left(\frac{x_n}{H_1}\right)^2\right]^{1/2} = \left[\frac{p}{\alpha_2} + \left(\frac{y_n}{H_2}\right)^2\right]^{1/2}$$

and (x_n,y_n) are the n roots of the system of equations:

$$\left.\begin{aligned} &x\tan(x) + \lambda\, y\tan(y) = 0 \\ &\left(\frac{x}{H_1}\right)^2 - \left(\frac{y}{H_2}\right)^2 = \frac{p}{\alpha^*} \end{aligned}\right\} \text{(E22)}$$

with $\lambda = \frac{K_2H_1}{H_2K_1}$ and $\frac{1}{\alpha^*} = \frac{1}{\alpha_2} - \frac{1}{\alpha_1} = \frac{\alpha_1-\alpha_2}{\alpha_1\alpha_2}$

In the expressions of Un,r, Un,r_w and Wn,r_w, the functions K_0 K_1, I_0 and I_1, are the modified Bessel functions of order zero (subscript 0) and one (subscript 1). Investigating the nature of the roots x_n and y_n, Jacquard (op.cit.) concludes that when $\alpha_1 > \alpha_2$, x_n is always real but, for a given n, y_n may become imaginary beyond $p_0 = n^2\pi^2/(H_1)^2\alpha^*$. To maintain real solutions in the Laplace space (for example to permit the use of the Stehfest inverter). it suffices to change ytan(y) into ytanh(y) and $-(y/H_2)^2$ by $+(y/H_2)^2$ in the system of equations that give the roots x_n and y_n when $p > p_0$. Obviously, when $\alpha_1 < \alpha_2$, then xtan(x) has to be changed into xtanh(x) to obtain the same real result.

3. THE GENERAL SOLUTIONS IN THE DIMENSIONLESS LAPLACE SPACE

Following the same idea of Appendix C, that is to obtain directly type curve solutions of E20 and E21, and depending expressions, we transform these equations in the dimensionless Laplace space defined by $L'(p')=(\alpha_1/r^2)L(p)$ where $p'=pr^2/\alpha_1$ is the Laplace dimensionless variable corresponding to the dimensionless time $t_{D_1}=\alpha_1 t/r^2$. For simplicity, we will only perform this transformation to the case $\alpha_1>\alpha_2$ and normalize the dimensionless groups to the lower aquifer 1 (of greater diffusivity). The opposite case $\alpha_2>\alpha_1$ can be easily treated with adequate changes of the subscripts in the derived equations.

We thus define the dimensionless drawdowns as:

$$s_{D_1} = \frac{4\pi T_1 s_1}{Q} \text{ and } s_{D_2} = \frac{4\pi T_1 s_2}{Q}$$

In the following, the superscript (') refers to dimensionless Laplace space. Examination of E20, E21 and depending equations suggest that the sought solutions will be simplified by defining the following set of reduced parameters:

$$r_D = \frac{r}{H_1},\quad R_D = \frac{r}{R},\quad r_{D_w} = \frac{r_w}{r},\quad a = \frac{T_1}{T_2},\quad b = \frac{S_2}{S_1},\quad h_D = \frac{H_1}{H_2} \text{ and } z_D = \frac{z}{H_1}$$

With these definitions, we have the following relationships:

$ab = \frac{\alpha_1}{\alpha_2}$, $\frac{a}{h_D} = \frac{K_1}{K_2}$, $h_D z_D = \frac{z}{H_2}$ that are useful in the following developments.

Multiplying the second equation of E22 by r^2, changing p into p' and making sure that the transforms are always real implies:

$$\left.\begin{array}{ll} \text{when } p' < \dfrac{(n\pi r_D)^2}{(ab-1)} & x'\tan(x') + \dfrac{h_D^2}{a}\, y'\tan(y') = 0 \\[2ex] & (r_D x')^2 - (r_D h_D y')^2 = p'(ab-1) \\[2ex] \text{when } p' > \dfrac{(n\pi r_D)^2}{(ab-1)} & x'\tan(x') - \dfrac{h_D^2}{a}\, y'\tanh(y') = 0 \\[2ex] & (r_D x')^2 + (r_D h_D y')^2 = p'(ab-1) \end{array}\right\} \quad \text{(E23)}$$

Calling x'_n and y'_n the n roots of the systems E23, the transformed solutions are:

$$\overline{s_{D_1}} = \overline{s_{D_w}}(p') \sum_{n=0}^{\infty} A'_n \frac{U'_n r_D}{U'n,r_{D_w}} \frac{\cos(z_D x'_n)}{\cos(x'_n)} \qquad \text{(E24)}$$

$$\overline{s_{D_2}} = \overline{s_{D_w}}(p') \sum_{n=0}^{\infty} A'_n \frac{U'_{n,}r_D}{U'_{n,}r_{D_w}} \frac{\cos[(1+h_D-z_D h_D)y'_n]}{\cos(y'_n)} \qquad \text{(E25)}$$

$$A'_n = \frac{N'}{D'} \qquad N' = \frac{a\tan(x'_n)}{x'_n} + \frac{\tan(y'_n)}{y'_n}$$

$$D' = \frac{a}{\cos^2(x'_n)} + \frac{1}{\cos^2(x'_n)} + \frac{a\tan(x'_n)}{x'_n} + \frac{\tan(y'_n)}{y'_n}$$

$$U_{n,r_D} = I_1\left(\frac{q'_n}{R_D}\right) K_o(q'_n) + K_1\left(\frac{q'_n}{R_D}\right) I_o(q'_n)$$

$$\text{(E26)}$$

$$U_{n,r_{D_w}} = I_1\left(\frac{q'_n}{R_D}\right) K_o(q'_n r_{D_w}) + K_1\left(\frac{q'_n}{r_D}\right) I_o(q'_n r_{D_w})$$

$$W_{n,r_{D_w}} = q'_n r_{D_w} \left[I_1\left(\frac{q'_n}{R_D}\right) K_1(q'_n r_{D_w}) - K_1\left(\frac{q'_n}{R_D}\right) I_1(q'_n r_{D_w})\right]$$

$$q'_n = [p' + (r_D x'_n)^2]^{1/2} = [abp' + (r_D h_D y'_n)^2]^{1/2}$$

and $$\overline{s_{D_w}} = \left\{ \sum_{n=0}^{\infty} A'_n \frac{W'_{n,r_{D_w}}}{U'_{n,r_{D_w}}} \left[\frac{\tan(x'_n)}{x'_n} + \frac{\tan(y'_n)}{a y'_n} \right] \right\}^{-1}$$

The complete dimensionless Laplace space solutions are thus given by E24 and E25 and the depending expressions E26 and E23. One may notice that E23 can be rearranged with the change of variable $X = r_D x'$ and $y = r_D h_D y'$.

4. SPECIAL CASES AND THEIR SOLUTIONS IN THE DIMENSIONLESS LAPLACE SPACE

Consider the first two sets of assumptions of section 1 of this appendix.

(1) Bounded two-layer aquifer with cross-flow fully penetrated by a well of negligible radius:

When $r_w \to 0$,

$$\frac{U'_{n,r_D}}{U'_{n,r_{D_w}}} \times \frac{U'_{n,r_{D_w}}}{W'_{n,r_{D_w}}} = \frac{U'_{n}r_D}{I_1(q'_n/R_D)} \qquad \text{in E26.}$$

Accounting for the boundary conditions E11 and E12 and defining now the dimensionless drawdowns by:

$s_{D_1} = \frac{4\pi(T_1+T_2)s_1}{Q}$ and $s_{D_2} = \frac{4\pi(T_1+T_2)s_2}{Q}$, the solutions are immediately obtained[1]:

$$\left.\begin{aligned}
\overline{s_{D_1}} &= \frac{1}{p} \sum_{n=0}^{\infty} A'_n \frac{U'_{n,r_D}}{I_1(q'_n/R_D)} \cos(z_D x'_n)/\cos(x'_n) \\
\overline{s_{D_2}} &= \frac{1}{p} \sum_{n=0}^{\infty} A'_n \frac{U'_{n,r_D}}{I_1(q'_n/R_D)} \cos[1+h_D-z_D h_D)y'_n]/\cos(y'_n)
\end{aligned}\right\} \text{(E27)}$$

where x'_n and y'_n are defined by E23 and A'_n and U'_{n},r_D are the same as in E26.

(2) Infinite two-layer aquifer with cross-flow and well of negligible radius:

It corresponds to the combined assumptions (1) and (2) of section 1.

When $R \to \infty$, $(\frac{q'_n}{R_D}) \to \infty$ and $\frac{U'_{n,r_D}}{I_1(q'_n/R_D)} = K_o(q'_n)$.

We thus have from E27[1].

$$\left.\begin{aligned}\overline{s_{D_1}} &= \frac{1}{p} \sum_{n=0}^{\infty} A'_n\, K_0(q'_n)\, \cos(z_D x'_n)/\cos(x'_n)\\ \overline{s_{D_2}} &= \frac{1}{p} \sum_{n=0}^{\infty} A'_n\, K_0(q'_n)\, \cos[(1+h_D-z_D h_D) y'_n]/\cos(y'_n)\end{aligned}\right\} \quad (E28)$$

where x'_n and y'_n are defined by E23 and A'_n is given by E26. E28 are the same dimensionless expressions of the Laplace transforms obtained by Jacquard (op.cit.) when he integrates along O_z a distribution of point sources of density $Q/(T_1+T_2)$. Also, E28 depends only on r_D, a, b, h_D and z_D; if the series can be evaluated, the type curves $s_{D_1}(t_{D_1})$ and $s_{D_2}(t_{D_2})$ may be obtained for example as functions of r_D, giving fixed numerical values to the set (a,b,h_D,z_D).

---

[1] To obtain E27 and E28, we use the following asymptotic properties of the Bessel functions:

$x \to 0$ $xK_1(x) \to 1$, $I_1(x) \to 0$; $x \to \infty$, $K_1(x) \to 0$.

Neglecting cross-flow, the Laplace space IBVP is in the general case of a laterally bounded system fully penetrated by a well of finite radius:

$$\left.\begin{aligned}
&\frac{d^2\overline{s_1}}{dr^2} + \frac{1}{r}\frac{d\overline{s_1}}{dr} = \frac{p}{\alpha_1}\overline{s_1}\\
&\frac{d^2\overline{s_2}}{dr^2} + \frac{1}{r}\frac{d\overline{s_2}}{dr} = \frac{p}{\alpha_2}\overline{s_2}\\
&\frac{\partial\overline{s_1}}{\partial r}(R,p) = \frac{\partial\overline{s_2}}{\partial r}(R,p) = 0\\
&\overline{s_1}(r_w,p) = \overline{s_2}(r_w,p) = \overline{s_w}(p)\\
&T_1\frac{\partial\overline{s_1}}{\partial r}(r_w,p) + T_2\frac{\partial\overline{s_2}}{\partial r}(r_w,p) = -\frac{Q}{2\pi r_w p}
\end{aligned}\right\} \quad \text{(E29)}$$

The solution to this problem does not require the use of further integral tranform because the governing equations are the Bessel differential equations[2]. We thus have:

$$\overline{s_1}(r,p) = A_1K_0\left(r\sqrt{\frac{p}{\alpha_1}}\right) + B_1I_0\left(r\sqrt{\frac{p}{\alpha_1}}\right)$$

$$\overline{s_2}(r,p) = A_2K_0\left(r\sqrt{\frac{p}{\alpha_2}}\right) + B_2I_0\left(r\sqrt{\frac{p}{\alpha_2}}\right)$$

---

[2] Consequently, there is no difficulty in finding the Laplace solutions for the multilayered aquifer system (Duvaut, 1961).

where $A_1(p)$, $B_1(p)$, $A_2(p)$ and $B_2(p)$ are uniquely and easily defined by the four boundary conditions. If we normalize as before with respect to aquifer 1 with the dimensionless groups:

$$s_{D_1} = \frac{4\pi T_1 s_1}{Q}, \quad s_{D_2} = \frac{4\pi T_1 s_2}{Q}, \quad t_{D_1} = \frac{\alpha_1 t}{r^2}, \quad a = \frac{T_1}{T_2}, \quad b = \frac{S_2}{S_1},$$

$$r_{D_w} = \frac{r_w}{r} \text{ and } R_D = \frac{r}{R}$$

the solutions in the dimensionless Laplace space are easily obtained as:

$$\overline{s_{D_1}} = \overline{s_{D_w}} \quad \frac{K_o(\sqrt{p'})I_1(\sqrt{p'}/R_D) + K_1(\sqrt{p'}/R_D)\ I_o(\sqrt{p'})}{K_o(r_{D_w}\sqrt{p'})I_1(\sqrt{p'}/R_D)+K_1(\sqrt{p'}/R_D)\ I_o(r_{D_w}\sqrt{p'})} = \overline{s_{D_w}}\ \frac{N_1}{D_1}$$

$$\overline{s_{D_2}} = \frac{K_o(\phi)I_1(\phi/R_D)+K_1(\phi/R_D)I_o(\phi)}{K_o(r_{D_w}\phi)I_1(\phi/R_D)+K_1(\phi/R_D)I_o(r_{D_w}\phi)} = \overline{s_{D_w}}\ \frac{N_2}{D_2}$$

with $\phi = (p'/ab)^{1/2}$

$$\overline{s_{D_w}} = \frac{2}{p'}\ [r_{D_w}\sqrt{p'}(\frac{W_1}{D_1} + \quad \frac{b}{a}\frac{W_2}{D_2})]^{-1}$$

$$W_1 = I_1\ (\frac{\sqrt{p'}}{R_D})\ K_1(r_{D_w}\sqrt{p'})\ -I_1(r_{D_w}\sqrt{p'})\ K_1(\frac{\sqrt{p'}}{R_D})$$

W_2 is the same as W_1 but with ϕ instead of $(p')^{1/2}$.

Modifying the dimensionless drawdowns as $sD_1 = \dfrac{4\pi(T_1+T_2)s_1}{Q}$ and $s_{D_2} = \dfrac{4\pi(T_1+T_2)s_2}{Q}$, the solutions for the infinite ($R\to\infty$) two-layer aquifer and a finite well radius are:

$$\overline{s_{D_1}} = \overline{s_{D_w}}\ \frac{K_o(\sqrt{p'})}{K_o(r_{D_w}\sqrt{p'})} \qquad \overline{s_{D_2}} = \overline{s_{D_w}}\ \frac{K_o(\phi)}{K_o(r_{D_w}\phi)} \tag{E31}$$

$$\text{with } \overline{s_{D_w}} = \frac{2}{p'}\left\{r_{D_w}\sqrt{p'}\left[\frac{K_1(r_{D_w}\sqrt{p'})}{K_o(r_{D_w}\sqrt{p'})} + \sqrt{\frac{b}{a}}\ \frac{K_1(r_{D_w}\phi)}{K_o(r_{D_w}\phi)}\right]\right\}^{-1}$$

And finally, letting $r_w \to 0$, we find simply:

$$\overline{s_{D_1}} = 2K_0(\sqrt{p'})/p'$$
$$\overline{s_{D_2}} = 2K_0(\phi)/p' \qquad \text{(E32)}$$

that are immediately inverted as:

$$s_{D_1} = E_1(1/4t_{D_1}) \text{ and } s_{D_2} = E_1(ab/4t_{D_1}) \qquad \text{(E33)}$$

Defining the "homogeneous equivalent" aquifer as an aquifer of characteristics $T=T_1+T_2$ and $S=S_1+S_2$ with $s_D=4\pi Ts/Q$ and $t_D=Tt/Sr^2$, it is obvious that $s=s_1$ when $t_{D_1}=t_D$, since $s_D=s_{D_1}$. We have $t_D=t_{D_1}(a+1)/[a(1+b)]$. Hence the condition $t_{D_1}=t_D$ implies that $(a+1)/[a(1+b)]=1$ or $ab=1$, that is $\alpha_1=\alpha_2$. The same reasoning shows that $s=s_2$ for the same condition.

It is also interesting to evaluate the departures at late times between the "homogeneous equivalent" and the two-layer system without cross-flow of E33. We find simply:

$$s_D-s_{D_1} = -\gamma + \ln(1/4t_D) + \gamma-\ln(1/4t_{D_1}) = \ln[a(1+b)/(a+1)] \qquad \text{(E34)}$$

Calling $t_{D_2} = \alpha_2 t/r^2$, since $ab=\alpha_1/\alpha_2$, we have $s_{D_2}=E_1(1/4t_{D_2})$.

Then, $t_D = t_{D_2}[b(1+a)/1+b]$, implying:

$$s_D-s_{D_2} = \ln[b(1+a)/(1+b)] \qquad \text{(E35)}$$

Therefore, the long-time departures with the "homogeneous equivalent" aquifer given by E34 and E35 will only be equal when $a=b$ that is when $T_1S_1=T_2S_2$. These departures become equal to $\ln a$ (or $\ln b$).

6. COMPARISON BETWEEN CROSS-FLOW AND NO-CROSS-FLOW CONDITIONS

Let us consider the case of an infinite two-layered aquifer with cross-flow and well of negligible radius. The general dimensionless Laplace solutions in that case are given by equations E28 which are not particularly suitable to study asymptotic behaviours. Integrating along Oz a distribution of point sources of density $Q/(t_1+T_2)$ in the Laplace space, Jacquard (op.cit.) finds:

$$\frac{2\pi(T_1+T_2)\overline{s_1}}{Q} = \int_0^\infty \left[\frac{1}{pw_1^2} + \frac{A_1}{p}\right] J_0(ur)udu$$
$$\frac{2\pi(T_1+T_2)\overline{s_2}}{Q} = \int_0^\infty \left[\frac{1}{pw_2^2} + \frac{A_2}{p}\right] J_0(ur)udu \qquad \text{(E36)}$$

where:

$$\frac{A_1(a,z,p)}{p} = \frac{K_2\cosh(w_1z)}{\alpha w_1^2w_2\sinh(w_1H_1)D}$$

$$\frac{A_2(a,z,p)}{p} = \frac{K_1\cosh\left[w_2(H_1+H_2-z)\right]}{\alpha w_1^2w_2\sinh(w_2H_2)D}$$

$$D = K_2w_2\coth(w_1H_1) + K_1w_1\coth(w_2H_2)$$

$$\frac{1}{\alpha} = \frac{1}{\alpha_1} - \frac{1}{\alpha_2}$$

$$w_i = \left(\frac{p}{\alpha_i} + u^2\right)^{1/2} \qquad \text{with } i = 1,2$$

The equations E36 mean that the bracketed functions are the zero-Hankel infinite transforms of $\overline{s_1}$ and s_2 with the transform parameter u. This same result can in fact be obtained by solving the Laplace space problem with a zero-Hankel infinite transform of parameter u. Jacquard (op.cit.) shows that the integration of E35 yields E28.

At early times when p is large enough so that w_i is large, we have:

$$\frac{A_1(u,z,p)}{p} = \frac{K_2\exp[w_1(z-H_1)]}{\alpha w^2{}_1 w_2(K_2w_2+K_1w_1)} \to 0 \quad \text{since } (z-H_1) < 0 \text{ for aquifer 1}$$

$$\frac{A_2(u,z,p)}{p} = \frac{K_1\exp[w_2(H_1-z)]}{\alpha w^2{}_1 w_2(K_2w_2+K_1w_1)} \to 0 \quad \text{since } (H_1-z) < 0 \text{ for aquifer 2}$$

Hence, for E36, using the property B14:

$$\frac{4\pi(T_1+T_2)\overline{s_2}}{Q} = \frac{2}{p}K_0(r\sqrt{p}/\alpha_2)$$

$$\frac{4\pi(T_1+T_2)\overline{s_1}}{Q} = \frac{2}{p}K_0(r\sqrt{p}/\alpha_1) \qquad \text{(E37)}$$

E 37 can be immediately inverted (section 3.2 of Appendix B).

We have, in dimensionless form:

$$s_{D_1} = E_1\left(\frac{1}{4t_{D_1}}\right)$$

$$s_{D_2} = E_1\left(\frac{ab}{4t_{D_1}}\right) \qquad \text{(E38)}$$

where $sD_i = \dfrac{4\pi(T_1+T_2)s_i}{Q}$ (i=1,2)

$$t_{D1} = \frac{\alpha_1 t}{r^2} \text{ and } ab = \frac{\alpha_1}{\alpha_2}$$

E38 is obviously the same as E33. This leads to the interesting conclusion:

At early-times, the infinite two-layered aquifer system with cross-flow and for a well of negligible radius behaves as the corresponding no-cross-flow case; in other words, cross-flow can be neglected. The drawdowns are independent of z and the flow is radial in each aquifer.

When $\alpha_1 > \alpha_2$ and $H_1 < H_2$, we have $w_1 H_1 < w_2 H_2$. Rewriting w_1 as $(p/\alpha_1)^{1/2} [1+(u^2\alpha_1/p)]^{1/2} \sim (p/\alpha_1)^{1/2}$ and noticing that $\coth(w_1 H_1)$ is practically 1 when $w_1 H_1 > \sqrt{10}$, we deduce an approximate time range of validity for E38:

$$t_{D_1} < 0.1\left(\frac{H_1}{r}\right)^2 = \frac{0.1}{r_D^{\,2}} \qquad \text{(E39)}$$

At late times, when p is small, we may write $w_i = u(1+\varepsilon)$ where $\varepsilon = p/(2\alpha_i u^2)$ is a quantity that tends towards zero with p (a small quantity). However, the integrals in E36 do not yield a simple close form expression in the Laplace space as for the early times: the drawdowns are depending on z (cross flow is not negligible) and the Laplace space expressions contain infinite series. Although we are not fully treating this case, it is expected that these series are easier to evaluate because they do not depend on the roots of a transcendental system of equations as in E28.

APPENDIX F

LINE-SOURCE SOLUTIONS FOR RADIALLY COMPOSITE AND INFINITE AQUIFERS

With the text assumptions and the usual notations, the IBVP can be written as follows:

$$\Delta s_1 = \frac{1}{\alpha_1} \frac{\partial s_1}{\partial t}$$

$$s_1(r,0) = 0$$

$$\lim_{r \to 0} \left(r \frac{\partial s_1}{\partial r}\right) = - \frac{Q}{2\pi K_1 H} = q \text{ (H=aquifer thickness)}$$

For region 2 (outer region):

$$\Delta s_2 = \frac{1}{\alpha_2} \frac{\partial s_2}{\partial t}$$

$$s_2(r,0) = 0$$

$$s_2(\infty,t) = 0$$

At the interface $r=R$ between the two regions:

$$s_1(R,t) = s_2(R,t)$$

$$K_1 \left.\frac{\partial s_1}{\partial r}\right|_{r=R} = K_2 \left.\frac{\partial s_2}{\partial r}\right|_{r=R}$$

We have neglected the gravitational effects: s_1 and s_2 are independent of the vertical position in the aquifer. In the Laplace space, the IBVP becomes [$L(t)=p$]:

$$\Delta \bar{s}_1 - p/\alpha_1 \, \bar{s}_1 = 0 \qquad \Delta \bar{s}_2 - p/\alpha_2 \, \bar{s}_2 = 0$$

$$\lim_{r\to 0} \left(r\frac{d\bar{s}_1}{dr}\right) = -\frac{q}{p} \qquad \bar{s}_2(\infty,p) = 0$$

$$K_1 \left.\frac{d\bar{s}_1}{dr}\right|_{r=R} = K_2 \left.\frac{d\bar{s}_2}{dr}\right|_{r=R}$$

$$\bar{s}_1(R,p) = \bar{s}_2(R,p)$$

Recognizing Bessel differential equations, the problem can be solved without further transformation and the zero-Hankel infinite transform is not suited because of the last two conditions.

The general solutions are:

$$\bar{s}_1 = A\, I_0(y_1 r) + BK_0(y_1 r) \text{ with } y_1^2 = p/\alpha_1$$

$$\bar{s}_2 = C\, I_0(y_2 r) + D\, K_0(y_2 r) \text{ with } y_2^2 = p/\alpha_2$$

The coefficients A, B, C and D are functions of p that have to be determined from the boundary conditions. K_0 and I_0 are the modified Bessel functions of zero order.

When r is infinite, $I_0(y_2 r)$ is infinite and the condition $s_2(\infty,p)=0$ imposes: C=0. Hence:

$$\bar{s}_2 = DK_0(y_2 r) \tag{F1}$$

We must also have:

$$\lim_{r\to 0} [r\, Ay_1 I_1(y,r) - Bry_1 K_1(y,r)] = -\frac{q}{p}$$

When r tends towards zero: $ry_1 I_o(y_1 r) \sim (1/2)(ry_1)^2 \to 0$ and $ry_1 K_1(y_1 r)$ tends towards unity. Therefore $B=q/p$ and:

$$\overline{s_1} = A\ I_o(y_1 r) + q/p\ K_o(y_1 r) \qquad \text{(F2)}$$

The continuity of flux at the interface with $a^2=K_1/K_2$ may be written as:

$$Aa^2 y_1 I_1(y_1 R) + Dy_2 K_1(y_2 R) = q/p\ a^2\ y_1 K_1(y_1 R)$$

Dividing throughout by y_1 and noticing that $y_2/y_1 = (\alpha_1/\alpha_2)^{1/2} = (ab)$ where $b = (S_{s_2}/S_{s_1})^{1/2}$:

$$A\ I_1(y_1 R) + D(b/a)\ K_1(y_2 R) = q/p\ K_1\ (y_1 R) \qquad \text{(F3)}$$

The continuity of hydraulic heads at the interface implies:

$$A\ I_o(y_1 R) - D\ K_o(y_2 R) = -q/p\ K_o(y_1 R) \qquad \text{(F4)}$$

Defining: $\ell=I_1(y_1 R)$, $m=(b/a)\ K_1(y_2 R)$, $n=q/p\ K_1(y_1 R)$ and

$u=I_o(y_1 R)$, $v=K_o(y_2 R)$, $w=-q/p\ K_o(y_1 R)$

The system of equations F3 and F4 becomes:

$$\ell A + mD = n$$

$$uA - vD = w$$

yielding:

$$A = \frac{nv+mw}{\ell v+mu} = \frac{q}{p}\,\frac{U}{W} \qquad D = \frac{nu-w\ell}{\ell v+mu} = \frac{q}{p}\,\frac{V}{W}$$

where:

$$U = K_1(y_1R)K_o(y_2R) - (b/a)K_1(y_2R)K_o(y_1R)$$

$$V = K_1(y_1R)I_o(y_1R) + (K_o(y_1R)I_1(y_1R) = 1/y_1R$$

$$W = K_o(y_2R)I_1(y_1R) + (b/a)K_1(y_2R)I_o(y_1R)$$

The simple expression for V is directly deduced from the wronskian of the modified Bessel function of zero order (Abramovitz and Stegun, op.cit., p. 375). The Laplace space solutions are immediately deduced as:

$$\overline{s_1} = \frac{q}{p} K_o(y_1r) \left[1 + \frac{U}{W}\,\frac{I_o(y_1r)}{K_o(y_1r)}\right] \qquad \text{(F5)}$$

$$\overline{s_2} = \frac{q}{p}\,\frac{V}{W} K_o(y_2r) = \frac{q}{p}\,\frac{K_o(y_2r)}{y_1R}\,\frac{1}{W} \qquad \text{(F6)}$$

It can be noticed that s_1 is not finite when $r \to 0[K_0(0)=\infty]$ and F5 is only valid in the interval $0<r<R$. This means that the drawdown at the well cannot be described by F5 with the IBVP considered. Imposing the extra condition for s_1 that $s_1(o,t)$ remains finite would lead to undetermined solutions (B=0 in F2 and A=D=0 as a result of F3 and F4).

Making use of the important relationship $y_2/y_1 = ab$, one can think of various transformations of F5 and F6 in dimensionless Laplace space. For example, one may choose to normalize with respect to the flow properties of a single region (either 1 or 2). However, acknowledging the fact that the distance R to the radial discontinuity is generally unknown for aquifer tests and that, a priori, one does not know if the observation well response will refer to a location in region 1 or in region 2, it is found more useful to generate two families of type curves $s_{D_1}(t_{D_1})$ and $s_{D_2}(t_{D_2})$ for a given set of the depending parameters a, b and $r_D=r/R$.

Dimensionless drawdowns in region 1

We wish to transform F5 in the dimensionless Laplace space defined by:

$$\overline{s_{D_1}} = \frac{4\pi K_1 H \overline{s_1}}{Q},\ r_D = \frac{r}{R}\ (0<r_D<1),\ L(t_{D_1} = \frac{\alpha_1 t}{r^2}) = p'_1 = \frac{r^2 p}{\alpha_1}$$

We notice that $\frac{\overline{s_1}}{q} = \frac{\overline{s_{D_1}}}{2}$, $y_1 r = \sqrt{p'_1}$, $y_2 R = \sqrt{p'_1}/r_D$, $y_2 R = \frac{ab\sqrt{p'_1}}{r_D}$

The notations are simplified by introducing $\phi_1 = \sqrt{p'_1}/r_D$. With this convention and after application of B8, we find for F5:

$$\overline{s_{D_1}} = \frac{2K_o(\phi_1 r_D)}{\phi^2{}_1 r_D{}^2} \left[1+ \frac{U(\phi_1)}{W(\phi_1)} \frac{I_o(\phi_1 r_D)}{K_o(\phi_1 r_D)}\right] \tag{F7}$$

$$U(\phi_1) = K_1(\phi_1) K_o(ab\phi_1) - b/a\ K_1(ab\phi_1)(K_o(\phi_1)$$

$$W(\phi_1) = K_o(ab\phi_1)\ I_1(\phi_1) + b/a\ K_1(ab\phi_1) I_o(\phi_1)$$

In order to ensure numerical stability over a wide range of ϕ_1(of t_{D_1}), it is convenient to express this solution in a more useful form:

$$\overline{s_{D_1}} = \frac{2K_o(\phi_1 r_D)}{\phi_1{}^2 r_D{}^2} \left[1 + \frac{1}{M(\phi_1)} - \frac{1}{N(\phi_1)}\right] \tag{F8}$$

$$M(\phi_1) = \frac{K_o(\phi_1 r_D)\ I_1(\phi_1)}{K_1(\phi_1)\ \ I_o(\phi_1 r_D)} + \frac{b}{a}\ \frac{K_1(ab\phi_1)\ K_o(\phi_1 r_D)\ I_o(\phi_1)}{K_1(\phi_1)\ \ K_o(ab\phi_1)\ I_o(\phi_1 r_D)}$$

$$N(\phi_1) = \frac{a}{b}\ \frac{K_o(ab\phi_1)\ K_o(\phi_1 r_D)\ I_1(\phi_1)}{K_1(ab\phi_1)\ \ K_o(\phi_1)\ \ I_o(\phi_1 r_D)} + \frac{K_o(\phi_1 r_D)\ \ I_o(\phi_1)}{K_o(\phi_1)\ \ I_o(\phi_1 r_D)}$$

Although less compact, this formulation permits the calculation of the Bessel functions using IMSL subroutines for $e^z K_o(z)$, $e^z K_1(z)$, $e^{-z} I_o(z)$ and $e^{-z} I_1(z)$ which remain reasonable quantities for any real z. The necessary "balance" for $1/M(\phi_1)$ and $1/N(\phi_1)$ is easily shown to be $\exp[-2\phi_1(1-r_D)]$ which remains also a reasonable quantity for any ϕ_1. Unpredictable overflows can then be avoided when evaluating $\overline{s_{D_1}}$.

Dimensionless drawdown in region 2

The dimensionless Laplace space groups are now:

$$\overline{s_{D_2}} = \frac{4\pi K_2 H \overline{s_2}}{Q},\ r_D = \frac{r}{R}\ (r_D > 1),\ L[t_{D_2} = \alpha_2\, t/r^2] = p'_2 = r^2 p/\alpha_2$$

and we have:

$$\overline{s_2}/q = a^2\, \overline{s_{D_2}}/2,\ y_2 r = \sqrt{p'_2},\quad y_1 R = \sqrt{p'_2}/r_D ab,\ y_2 R = \sqrt{p'_2}/r_D$$

Defining $\phi_2 = \sqrt{p'_2}/r_D$ and applying B8 to F6 yields:

$$\overline{s_{D_2}} = \frac{2K_0(\sqrt{p'_2})}{p'_2}\,\frac{1}{\phi_2 W(\phi_2)} \tag{F9}$$

$$W = a/b\ K_0(\phi_2) I_1(\phi_2/ab) + K_1(\phi_2)\ I_0(\phi_2/ab)$$

Using the "stable" calculations of the Bessel functions, the overall multiplying factor for $\overline{s_{D_2}}$ is $\exp[-\phi_2(r_D-1+1/ab)]$ that should be a reasonable quantity since the term between parenthesis is positive ($r_D > 1$).

Asymptotic behaviors

We make use of the asymptotic expressions for the Bessel functions (Hantush, 1964).

For region 1 at early times, there is no simple asymptotic solution that can be easily derived from F7 or F8. It is found that the limiting function for s_{D_1} will depend on a, b and r_D.

At late times for region 1, it can be shown that $1/M-1/N$ tends towards zero in F8, yielding approximately a Theis solution for s_{D_1}. The condition on t_{D_1} is:

$$t_{D_1} > \left(\frac{20ab}{r_D}\right)^2$$

For region 2, an interesting case is when $ab=1$ and $b^2=1$, then we find the Theis solution at all times, as it should be since $K_1=K_2$ and $S_{s_2}=S_{s_1}$. At early times there is no simple asymptotic solution. At late times, when $t_{D_2}>(20ab/r_D)^2$, we have:

$$\phi_2 W(\phi_2) = 1 + \frac{\phi_2^2}{b^2}\ln\left(\frac{2}{\phi_2 e^{\gamma}}\right) = 1 + \frac{\phi_2^2}{b^2}[\ln 2-\ln(\phi_2 e^{\gamma})]$$

where $b^2 > 1$, $S_{s_2} > S_{s_1}$, the second term is negligible when compared to unity: at most when $\phi_2=0.05$, it is $3.09\times10^{-3}/b^2$ and s_{D_2} is following a Theis solution. This approximation is still valid within 1% error when $b^2=0.25$, i.e. when $S_{s_2}=S_{s_1}/4$ and within 3% when $b^2=0.1$ ($S_{s_2}=S_{s_1}/10$). It thus covers most of the field situations.

Comparison with previous solutions

- The solutions presented by William Hurst (1981) - which are strictly the same as the one he published in 1960 - for the so-called "sand in series" model neglect the difference of specific storage between region 1 and region 2. His solutions obviously reduce to F7 and F9 doing $b=1$ ($S_{s_2}=S_{s_1}$). Hence, F7 and F9 are more general because there is no physical reason to assume $b=1$.

- Satman (1985) proposes a solution for s_{D_2} when wellbore storage and skin effect are not neglected (cylindrical-source solution). In most field situations of aquifer testing, it is legitimate to neglect these nearby well effects to interpret observation well responses (i.e. the s_{D_2} type curves). In addition, there is an error in Satman's derivation that makes the comparison useless. He defines $\eta=\alpha_1/\alpha_2$ as the ratio of diffusivities between region 1 and region 2. With this notation, his governing equation for region 1 should read:

$$\Delta p_{1_D} = \frac{1}{\eta}\frac{\partial p_{1_D}}{\partial t_{2_D}}$$

and not as written in his equation A1 of the appendix:

$$\Delta p_{1_D} = \eta\frac{\partial p_{1_D}}{\partial t_{2_D}}$$

where $p_{1_D} = \frac{2\pi x 10^{-6} K_2 H}{qB\mu_1}(pi-p_1)$ and $t_{2_D} = \frac{3.6x10^{-6} K_2 t}{(\phi\mu c_t)_2 r_w{}^2}$ are the usual dimensionless groups in reservoir engineering. Unfortunately, this error persists in his final expression for s_{D_2}.

Reduction to useful line-source solutions for cylindrical aquifers

- Bounded system

For a well at the centre of a cylindrical aquifer with no flux at distance R from the well we have $K_2=0$ while b remains finite. Doing $a\to\infty$ in F8 yields:

$$\overline{s_{D_1}} = \frac{2K_0(\sqrt{p'_1})}{p'_1} + 2A\,\frac{I_0(\sqrt{p'_1})}{p'_1} \qquad \text{(F10)}$$

$A = K_1(\sqrt{p'_1}/r_D)/I_1(\sqrt{p'_1}/r_D)$ with $r_D = r/R<1$

since $1/N(\phi_1) \rightarrow 0$ and $M(\phi_1)$ is equivalent to its first term.

This solution (F10) is easily inverted with the Stehfest inverter.

- "Island" aquifer

When a constant head boundary exists at distance R from a well at the centre of a cylindrical aquifer, $s_1(R,t)=0$ and $a=0$ since K_2 is infinite. In that case, $M(\phi_1)$ is infinite and $1/M(\phi_1) \rightarrow 0$ in F8, meanwhile $N(\phi_1)$ reduces to its second term and:

$$s_{D_1} = \frac{2K_0(\sqrt{p'_1})}{p'_1} - 2B\,\frac{I_0(\sqrt{p'_1})}{p'_1} \qquad \text{(F11)}$$

with $B = K_0(\sqrt{p'_1}/r_D)/I_0(\sqrt{p'_1}/r_D)$ with $r_D = r/R < 1$

Again this solution (F11) is easily inverted with the Stehfest inverter. However, this case is less frequent in nature than the previous case with solution F10.

APPENDIX G

COMBINED FLOW REGIME IN CONFINED AQUIFERS

The considered IBVP with the assumptions exposed in section 4.5 of the text can be mathematically transcribed as follows (with our usual notations):

Continuity equation:

Writing the mass balance for an annulus of radius Δr during a time Δt and letting Δr→dr and Δt→dt yields:

$$\frac{\partial Q}{\partial r} = -2\pi r S_s H \frac{\partial s}{\partial t} \tag{G1}$$

with $Q = 2\pi H r v$. Deriving Q with respect to r and using G_1, we obtain:

$$2\pi H \frac{\partial (rv)}{\partial r} = -2\pi r S_s H \frac{\partial s}{\partial t}$$

that can be rearranged as:

$$\frac{\partial v}{\partial r} + \frac{v}{r} = -S_s \frac{\partial s}{\partial t} \tag{G2}$$

Forchheimer equation:

$$-\frac{\partial s}{\partial r} = av + bv^2 \tag{G3}$$

Initial and boundary conditions:

$$s(r,0) = 0 \qquad r>0 \tag{G4}$$

$$s(\infty,t) = 0 \qquad t>0 \tag{G5}$$

$$\lim_{r\to 0} (rv) = \frac{Q}{2\pi H} \tag{G6}$$

Solution

Defining the Boltzmann variable $x=r/2\sqrt{t}$, we transform the equations G2 and G3 as follows:

$$\frac{\partial v}{\partial r} = \frac{1}{2\sqrt{t}}\frac{dv}{dx} \qquad \frac{\partial s}{\partial t} = \frac{-x}{2t}\frac{ds}{dx} \qquad \frac{\partial s}{\partial r} = \frac{1}{2\sqrt{t}}\frac{ds}{dx}$$

Substitution in G2 and G3 gives:

$$\frac{x}{2t}\frac{ds}{dx} = \frac{1}{S_s}\left(\frac{1}{2\sqrt{t}}\frac{dv}{dx} + \frac{v}{2\sqrt{t}x}\right)$$

$$-\frac{1}{2\sqrt{t}}\frac{ds}{dx} = av + bv^2$$

Eliminating ds/dx and rearranging yields:

$$\frac{1}{x}\frac{dv}{dx} + \left(\frac{1}{x^2} + 2aS_s\right)v = -2bS_s v^2 \qquad \text{(G7)}$$

This is a Bernouilli ordinary differential equation for which the solution v(x) is immediate:

$$v(x) = \frac{1}{x}\exp(-aS_s x^2)\left[A + 2bS_s\int_0^x \exp(-aS_s z^2)dz\right]^{-1} \qquad \text{(G8)}$$

Consider the integral I in the denominator of v(x) and operate the change of variable: $y=Bz=(aS_s)^{1/2}z$, $dz=dy/B$. We have:

$$I = \frac{1}{B}\int_0^{Bx} \exp(-y^2)dy = \frac{\sqrt{\pi}}{2B}\operatorname{erf}(Bx)$$

where erf is the error function. And G8 becomes:

$$v(x) = 1/x\ \exp(-aS_s x^2)(A + b(\pi S_s/a)^{1/2}\ \operatorname{erf}[(aS_s)^{1/2}x])^{-1} \qquad \text{(G9)}$$

The constant of integration A is easily obtained after substitution of x by its expression in terms of r and t and application of G6:

$$A = \frac{4\pi H\sqrt{t}}{Q}$$

We have $(rv)_{r\to 0} = \frac{2\sqrt{t}}{A}$ since erf(0)=0 and exp(0)=1

We define the following dimensionless groups:

$$v_D = \frac{2\pi H r v(r,t)}{Q} \qquad t_D = \frac{4t}{aS_s r^2} \qquad b_D = \frac{bQ}{\sqrt{\pi} aHr}$$

we obtain:

$$v_D(t_D,b_D) = \exp(-1/t_D)/[1+\frac{b_D}{2\sqrt{t_D}}\,\mathrm{erf}(\frac{1}{\sqrt{t_D}})] \qquad \text{(G10)}$$

G10 is the dimensionless form of the solution for the velocity. It is easy to verify that $v(r,0)=v(\infty,t)=0$ when doing $t=0$ and $r\to\infty$, that is $t_D=0$ in G10. The coefficient a is equivalent to 1/K for Darcy linear flow that is of dimension $(L^{-1}T]$. From G3, b has dimension $[L^{-2}T^2]$ or the inverse of a squared velocity. Therefore b_D is dimensionless.

When $b=0$, $b_D=0$ and from G10, $v_D=\exp(-1t_D)$. In that case when $t\to\infty$, $v_D\to 1$ and $v=Q/2\pi rH$ which is independent of time (pseudo-steady-state regime).

Defining $s'_D = \frac{\pi r^2 S_s H}{Q}\frac{\partial s}{\partial t}$, we may use the continuity equation G2 and G10 to obtain an expression for $s'_D(t_D,b_D)$. After some lengthy algebra, we find:

$$s'_D(t_D,b_D) = \frac{e^{-1/t_D}}{t_D}\frac{N}{D} \qquad \text{(G11)}$$

$$N = 1 + \frac{b_D}{2}[\frac{1}{\sqrt{\pi}}\exp(-1/t_D) + \frac{1}{\sqrt{t_D}}\,\mathrm{erf}(1/\sqrt{t_D})]$$

$$D = [1 + \frac{b_D}{2}\frac{1}{\sqrt{t_D}}\,\mathrm{erf}(1/\sqrt{t_D})]^2$$

G11 is interesting because:

1. it can be verified that $s'_D(t_D,0)$ is the same as with the Theis solution for linear flow regime and $a \equiv 1/K$;
2. it permits the obtaining of the dimensionless drawdowns upon integration between 0 and t_D. In effect if we define

$$s_D = \frac{4\pi H s(\bar{r},\bar{t})}{aQ}, \text{ then } \frac{\partial s_D}{\partial t_D} = s'_D$$

A single FORTRAN code NONDARC computes v_D from G10, s'_D from G11 and s_D after integration of G11 for the usual range of dimensionless time and various values of b_D. The integration of G11 is performed with the IMSL subroutine DCADRE. All the calculations are in arithmetic double-precision. DCADRE uses an algorithm for numerical quadrature proposed by de Boor (1971). The resulting type curves are presented and analysed in section 3.5 of the text. Numerical values of v_D, s'_D and s_D are also presented in Table G1 attached for the range t_D=0.1-100,000 and for b_D=0 (Theis solution), b_D=1, 3, 5, 7 and 10.

Asymptotic behaviours

Early time

- When $t_D \to 0$, if $z=1/t_D$, $z \to \infty$ and $b_D/2\sqrt{z}\ \mathrm{erf}(\sqrt{z}) \sim b_D/2\sqrt{\pi}\exp(-z) \to 0$

Then from G11,

$$N/D \sim \left[1+\frac{b_D}{\sqrt{\pi}}\exp(-z)\right]\left[1-\frac{b_D}{\sqrt{\pi}}\exp(-z)\right] \text{ and:}$$

$$s'_D \sim z\exp(-z)\ [1-\frac{b_D^2}{\pi}\exp(-2z)] \sim z\exp(-z) \sim \exp(-1/t_D)/t_D$$

which is the same as s'_D for the Theis solution where $a \equiv 1/K$.

- When $t_D \to \infty$, $z = 1/t_D \to 0$, $N_D \sim 1 + b_D/2\sqrt{\pi}$

$$s'_D \sim \frac{1}{t_D}\ (1 + \frac{b_D}{2\sqrt{\pi}})$$

which depends on b_D. Therefore, s_D will depend on b_D.

Table G1.
Values of dimensionless groups for combined flow regime in confined aquifers.

BD=0			
TD	VD	S'D	SD
0.100000	0.453999E-04	0.453999E-03	0.415697E-05
0.200000	0.673795E-02	0.336897E-01	0.114830E-02
0.500000	0.135335	0.270671	0.489005E-01
0.600000	0.188876	0.314793	0.783334E-01
0.700000	0.239651	0.342359	0.111308
0.800000	0.286505	0.358131	0.146413
0.900000	0.329193	0.365770	0.182664
1.00000	0.367879	0.367879	0.219384
1.10000	0.402890	0.366264	0.256116
1.20000	0.434598	0.362165	0.292554
1.30000	0.463369	0.356438	0.328495
1.40000	0.489542	0.349673	0.363808
1.50000	0.513417	0.342278	0.398409
1.60000	0.535261	0.334538	0.432252
1.75000	0.564718	0.322696	0.481546
2.00000	0.606531	0.303265	0.559774
5.00000	0.818731	0.163746	1.22265
10.0000	0.904837	0.904837E-01	1.82292
20.0000	0.951229	0.475615E-01	2.46790
50.0000	0.980199	0.196040E-01	3.35471
100.000	0.990050	0.990050E-02	4.03793
200.000	0.995012	0.497506E-02	4.72610
500.000	0.998002	0.199600E-02	5.63939
1000.00	0.999000	0.999000E-03	6.33154
2000.00	0.999500	0.499750E-03	7.02419
5000.00	0.999800	0.199960E-03	7.94018
10000.0	0.999900	0.999900E-04	8.63322
20000.0	0.999950	0.499975E-04	9.32632
50000.0	0.999980	0.199996E-04	10.2426
100000.	0.999990	0.999990E-05	10.9357

Table G1 continued

BD=1			
TD	VD	S'D	SD
0.100000	0.175892E-04	0.175895E-03	0.156907E-05
0.200000	0.318386E-02	0.159642E-01	0.521784E-03
0.500000	0.808004E-01	0.173173	0.282802E-01
1.00000	0.258824	0.318192	0.158265
2.00000	0.488599	0.350083	0.505267
2.50000	0.559123	0.334470	0.676677
3.00000	0.612891	0.315263	0.839165
3.50000	0.655124	0.295852	0.991916
4.00000	0.689128	0.277499	1.13520
4.50000	0.717072	0.260614	1.26966
5.00000	0.740433	0.245260	1.39607
10.0000	0.857996	0.151040	2.35145
20.0000	0.925549	0.842363E-01	3.46431
50.0000	0.969333	0.360408E-01	5.06909
100.000	0.984514	0.184350E-01	6.33411
200.000	0.992218	0.932353E-02	7.62010
500.000	0.996878	0.375516E-02	9.33549
1000.00	0.998437	0.188190E-02	10.6386
2000.00	0.999218	0.942030E-03	11.9439
5000.00	0.999687	0.377072E-03	13.6709
10000.0	0.999844	0.188579E-03	14.9779
20000.0	0.999922	0.943005E-04	16.2851
50000.0	0.999969	0.377228E-04	18.0133
100000.	0.999984	0.188618E-04	19.3207

Table G1 continued

BD=3			
TD	VD	S'D	SD
0.100000	0.790474E-05	0.790491E-04	0.699076E-06
0.200000	0.154936E-02	0.777872E-02	0.249727E-03
0.500000	0.447419E-01	0.100128	0.154020E-01
1.00000	0.162487	0.232682	0.101558
2.00000	0.351795	0.340417	0.400361
3.00000	0.475373	0.358727	0.753826
3.50000	0.521415	0.355497	0.932584
4.00000	0.560137	0.348577	1.10872
4.50000	0.593126	0.339655	1.28083
5.00000	0.621551	0.329734	1.44821
5.50000	0.646288	0.319416	1.61050
10.0000	0.777498	0.238468	2.85409
20.0000	0.878134	0.146415	4.70827
50.0000	0.948310	0.667848E-01	7.60251
100.000	0.973625	0.349391E-01	9.97630
200.000	0.986676	0.178749E-01	12.4293
500.000	0.994637	0.724976E-02	15.7312
1000.00	0.997313	0.364173E-02	18.2503
2000.00	0.998655	0.182509E-02	20.7778
5000.00	0.999462	0.731056E-03	24.1251
10000.0	0.999731	0.365698E-03	26.6594
20000.0	0.999865	0.182892E-03	29.1946
50000.0	0.999946	0.731668E-04	32.5465
100000.	0.999973	0.365851E-04	35.0823

Table G1 continued

BD=5			
TD	VD	S'D	SD
0.100000	0.509789E-05	0.509800E-04	0.449732E-06
0.200000	0.102378E-02	0.514214E-02	0.16416[illegible]E-03
0.500000	0.309361E-01	0.703539E-01	0.105894E-01
1.00000	0.118413	0.180545	0.747194E-01
2.00000	0.274842	0.304780	0.326453
3.00000	0.388257	0.352074	0.659049
3.50000	0.433033	0.361128	0.837632
4.00000	0.471822	0.364566	1.01925
4.50000	0.505714	0.364213	1.20157
5.00000	0.535563	0.361307	1.38304
5.50000	0.562040	0.356689	1.56259
10.0000	0.710810	0.294964	3.03221
20.0000	0.835341	0.196368	5.43201
50.0000	0.928179	0.949134E-01	9.44569
100.000	0.962975	0.507206E-01	12.8595
200.000	0.981196	0.262363E-01	16.4424
500.000	0.992407	0.107130E-01	21.3077
1000.00	0.996191	0.539364E-02	25.0349
2000.00	0.998093	0.270617E-02	28.7807
5000.00	0.999236	0.108472E-02	33.7459
10000.0	0.999618	0.542737E-03	37.5067
20000.0	0.999809	0.271463E-03	41.2694
50000.0	0.999924	0.108608E-03	46.2448
100000.	0.999962	0.543076E-04	50.0090

Table G1 continued

BD=7			
TD	VD	S'D	SD
0.100000	0.376204E-05	0.376213E-04	0.331496E-06
0.200000	0.764461E-03	0.384043E-02	0.122268E-03
0.500000	0.236413E-01	0.542171E-01	0.806932E-02
1.00000	0.931469E-01	0.146971	0.590889E-01
2.00000	0.225512	0.270500	0.274454
3.00000	0.328126	0.332015	0.579500
3.50000	0.370271	0.348796	0.749997
4.00000	0.407562	0.359506	0.927289
4.50000	0.440757	0.365757	1.10876
5.00000	0.470475	0.368724	1.29250
5.50000	0.497224	0.369263	1.47708
10.0000	0.654657	0.331337	3.06889
20.0000	0.796525	0.236620	5.87269
50.0000	0.908885	0.120670	10.8611
100.000	0.952555	0.658145E-01	15.2510
200.000	0.975776	0.344123E-01	19.9281
500.000	0.990186	0.141452E-01	26.3341
1000.00	0.995072	0.713767E-02	31.2616
2000.00	0.997531	0.358526E-02	36.2217
5000.00	0.999011	0.143807E-02	42.8024
10000.0	0.999505	0.719696E-03	47.7889
20000.0	0.999753	0.360014E-03	52.7788
50000.0	0.999901	0.144045E-03	59.3774
100000.	0.999951	0.720292E-04	64.3698

Table G1 continued

BD=10			
TD	VD	S'D	SD
0.100000	0.270057E-05	0.270063E-04	0.237742E-06
0.200000	0.553978E-03	0.278349E-02	0.884224E-04
0.500000	0.174641E-01	0.403341E-01	0.594692E-02
0.600000	0.269178E-01	0.555652E-01	0.107406E-01
0.700000	0.372563E-01	0.707963E-01	0.170598E-01
0.800000	0.481217E-01	0.858051E-01	0.248923E-01
0.900000	0.592768E-01	0.100463	0.342090E-01
1.00000	0.705628E-01	0.114689	0.449705E-01
2.00000	0.177677	0.228725	0.220972
3.00000	0.266268	0.298198	0.487477
4.00000	0.338425	0.338359	0.807660
5.00000	0.397933	0.360255	1.15815
5.50000	0.423896	0.366608	1.33997
6.00000	0.447735	0.370720	1.52439
7.00000	0.489984	0.373954	1.89720
8.00000	0.526260	0.372583	2.27077
9.00000	0.557736	0.368280	2.64139
10.0000	0.585301	0.362132	3.00672
15.0000	0.683884	0.321916	4.71958
20.0000	0.744624	0.282922	6.22925
50.0000	0.881402	0.155325	12.4532
100.000	0.937342	0.872382E-01	18.1970
200.000	0.967758	0.463388E-01	24.4513
500.000	0.986874	0.192360E-01	33.1265
1000.00	0.993398	0.973903E-02	39.8399
2000.00	0.996689	0.490018E-02	46.6141
5000.00	0.998673	0.196749E-02	55.6136
10000.0	0.999336	0.984984E-03	62.4372
20000.0	0.999668	0.492803E-03	69.2670
50000.0	0.999867	0.197196E-03	78.3000
100000.	0.999934	0.986103E-04	85.1347